We thank Dr. Pugh for providing constructive and insightful comments on our manuscript. Below, we provide a point-by-point response to each comment, together with a new marked-up version of our manuscript.

Thomas Pugh: I presume the LPJ-GUESS simulations used to calibrate the BME model were potential natural vegetation (would help if this was explicitly stated)? In which case I wonder how effectively NPP of natural ecosystems can be used as a proxy for NPP of agricultural ones. NPP is not independent of plant type, and the distinction between natural vegetation, which may well be woody, and cereal and pasture vegetation may be particularly relevant in the Sahel, where the deeper roots of trees may have access to water resources that herbaceous plants cannot use. Can the authors demonstrate that such effects are not large, both in the LPJ-GUESS model and also based on any observations in the Sahel or analogous ecosystems?

Authors' Response: Page 4, lines 13- 14 of our revised manuscript now reads "LPJ-GUESS is a state-of-the-art dynamic global potential natural vegetation model that incorporates carbon and nitrogen interactions (Smith et al., 2014)."

In order to test how effectively the NPP of natural ecosystems can be can be used as a proxy for the NPP of agricultural ones we ran LPJ-GUESS managed land (C-N version) for the period 1970 to 2010 and compared this to LPJ-GUESS (C-N, and used to develop BME), for the greater Sahel region defined in our manuscript (note that for comparison purposes, we also provide runs of LPJ-GUESS, BME and MOD-17 and LPJ-GUESS C only). Accordingly, we provide some new discussion in Appendix A of our revised manuscript, to take into consideration these aspects (see new Section A.2.2, p. 30, lines 12-16 and p. 31, lines 1-6.

"In order to test how effectively the NPP of natural ecosystems can be can be used as a proxy for the NPP of agricultural ones we ran LPJ-GUESS managed land (Olin et al., 2015) for the period 1970 to 2006 and compared this to LPJ-GUESS (used to develop BME) for the entire Sahel region. The results (see Fig. A5) of this experiment show that mean NPP derived from LPJ-GUESS ml over the region underestimates mean NPP derived from BME by 0.7% (0.006 dry-weight m^{-2} yr^{-1}) and LPJ-GUESS by 2.4% (0.020 kg dry-weight m^{-2} yr^{-1}), though all models show similar levels of interannual variability and trend (see Fig. A5). The implication of this experiment is that there is a demonstrable reduction in NPP when land management is taken into consideration, but the effect is relatively minor. Lindeskog et al. (2013) show that LPJ-GUESS managed land (C-version) overestimated actual yield derived from FAO country-level crop statistics and Smith et al. (2014b) also report that natural systems are more productive than agricultural systems in sub-Saharan Africa. We conclude with that possibility that our results are in the upper range for NPP found in the Sahel."

Note that we do not use the 'C-N' designation for specifying LPJ-GUESS version in the manuscript, as it is stated from the beginning that this is the version we use to develop the BME, based on Smith et al. (2014).

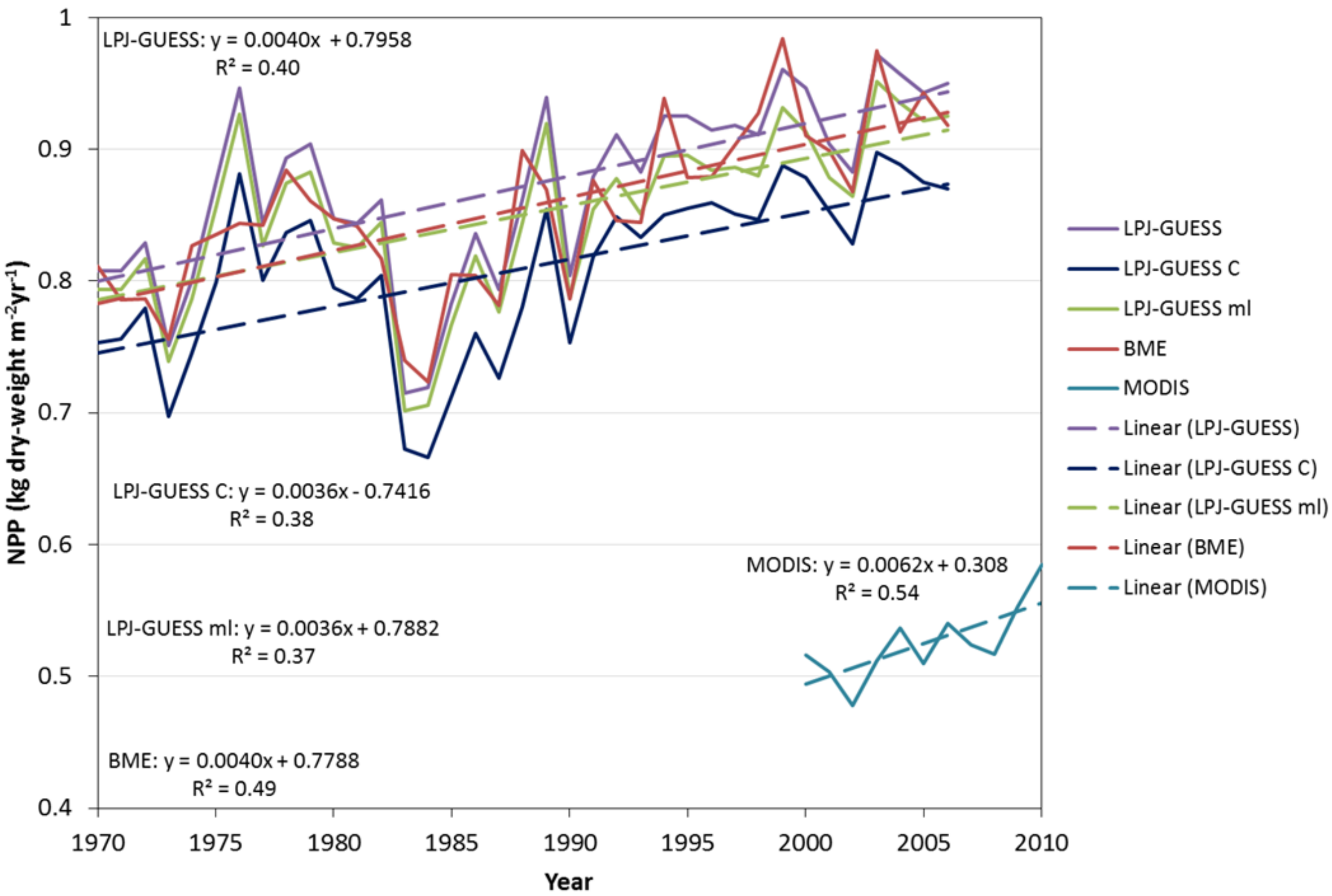

Fig. A5. Regional annual NPP Annual means of NPP for BME, LPJ-GUESS, LPJ-GUESS C (carbon only) and LPJ-GUESS ml (managed land) (1970 to 2006) and MODIS (2000-2010) for the greater Sahel region.

Thomas Pugh: Whilst the BME model is evaluated against LPJ-GUESS, any evaluation of the extent to which LPJ-GUESS can accurately represent actual NPP in the Sahel region is lacking. The references given (pg. 4 l. 14) did not address this ecosystem and also used a version of the model lacking carbon-nitrogen interactions, which leads to quite different vegetation simulations for the Sahel (Smith et al., 2014). Evaluation of the model response for the Sahel is necessary to give credence to the comparisons of supply and demand, which strongly depend on simulated absolute values for NPP. Whilst there is no gold-standard NPP (or GPP) dataset to compare against, comparison against NPP from the ESMs used to assess uncertainty, along with comparison of GPP against the alternative approaches of Jung et al. (2011) and Zhao et al. (2005) could go a long way towards increasing confidence. Alternatively (or additionally), FAO yield statistics could be used to evaluate the "yields" calculated here. Although none of these sources of comparison are likely to be low in uncertainty in the Sahel region, as it stands we have no idea how well LPJ-GUESS performs in this region - and current DGVMs cover a wide range of possibilities at regional scales (Sitch et al., 2015).

Authors' Response: Firstly, thank-you very much for highlighting these validation issues. In a revamped and much extended version of Appendix A.2.1 (pp. 24 – 29), we now include a global-level biome-by-biome validation of both LPJ-GUESS (C-N) and BME where we highlight the results for Sahel biomes):

"A.2.1 Biome Level Model Validation

We validate biome-level LPJ-GUESS and BME performance for estimating NPP of natural vegetation with NPP field-measurements from Michaletz et al. (2016) and Luyssaert et al. (2009) (see Sallaba et al., 2015) for the Major Biome Classification of Reich and Eswaran (2002) including the biomes found in the Sahel (desert temperate, tropical semi-arid and tropical humid – no observations were available for desert tropical). Note that since only two observations were available for our study area (see Fig. A1) this evaluation demonstrates the ability of both LPJ-GUESS and BME to replicate NPP for Sahel biomes found elsewhere in the world.

Before we combined the Michaletz et al. (2016) and Luyssaert et al. (2009) datasets, we removed sites with no records of combined above- and below-ground NPP measurements. After we merged the data, we checked the final assembly of NPP measurements for duplicates and removed them. The final dataset consists of 1561 samples (i.e. 1247 samples from Michaletz et al. (2016) and 314 samples from Luyssaert et al. (2009)) representing total NPP measurements across the terrestrial biosphere (sample sizes are 18, 6, and 12 for Sahel biomes of desert temperate, tropical semi-arid and tropical humid, respectively) from 1959-2006. Both LPJ-GUESS and BME were driven with CRU TS 3.21 climate data (Harris et al. 2014, Trenberth et al. 2014) that has global coverage across the time period.

We calculated mean values of the NPP field-measurements and the modelled NPP estimates located in the respective biomes, following Smith et al. (2014b). We aggregated to the biome-level to account for the difference in scale between in situ NPP measurements and modelled grid cell NPP estimates (being grid cell averages).

Finally, we determined the overall model performance, biome-by-biome, with the coefficient of determination (R^2 value) and the root mean square error (RMSE). Additionally, we investigated model agreement with performance ratios (hereafter referred to as 'Q') by dividing mean biome NPP estimates (for both models) with mean biome NPP observations. Model overestimation in comparison to in situ NPP measurements is indicated by Q > 1 and underestimation by Q < 1. Good model performance is classified with a Q range between 0.9-1.1 assuming an error of ± 10% following Sallaba et al. (2015). However, we further defined an acceptable model performance error range of ±20% (i.e. Q = 0.8-1.25) given the limitations of using LPJ-GUESS standard modelling protocol, PNV and CRU climate observations, and especially the simplicity of BME.

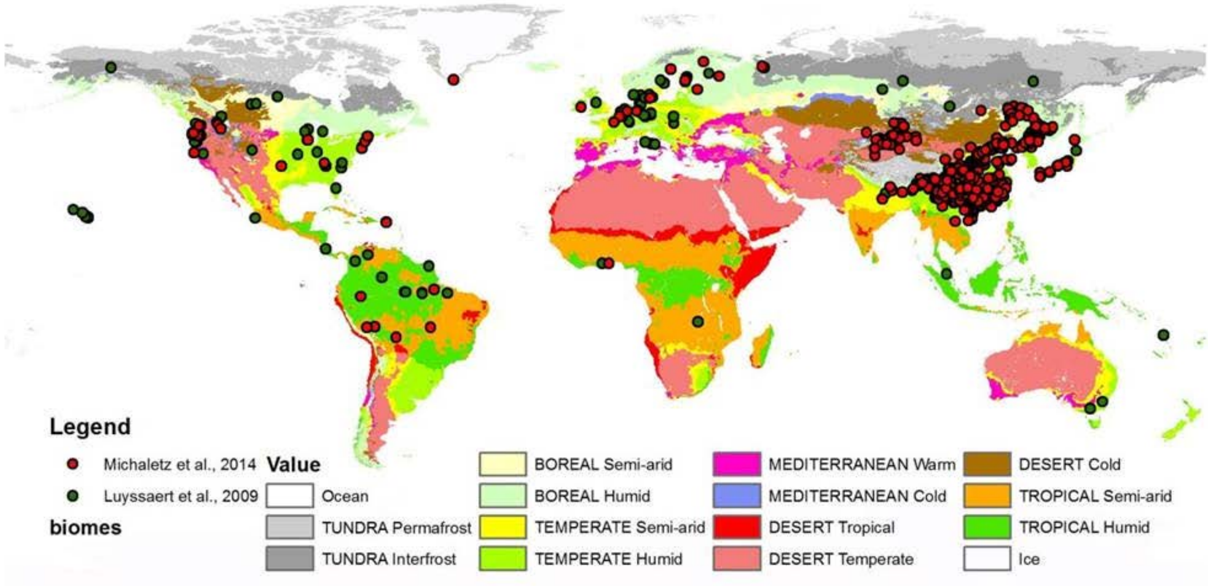

Fig. A1 Map of the Major Biome Classification based on Reich and Eswaran (2002). The red and green points are the locations of the NPP field-data from Michaletz et al. (2016) and Luyssaert et al. (2009).

LPJ-GUESS performs reasonably well in simulating NPP at the overall biome level (R^2 = 0.71 and RMSE = 0.16) but the model performance varies notably across the biomes (see Fig. A2 and Table A6). In general, LPJ-GUESS yields acceptable model agreement in seven (with good performance in four biomes) out of thirteen biomes. At the same time, the model underestimates NPP in three biomes while it overestimates NPP in two biomes (Fig. A2).

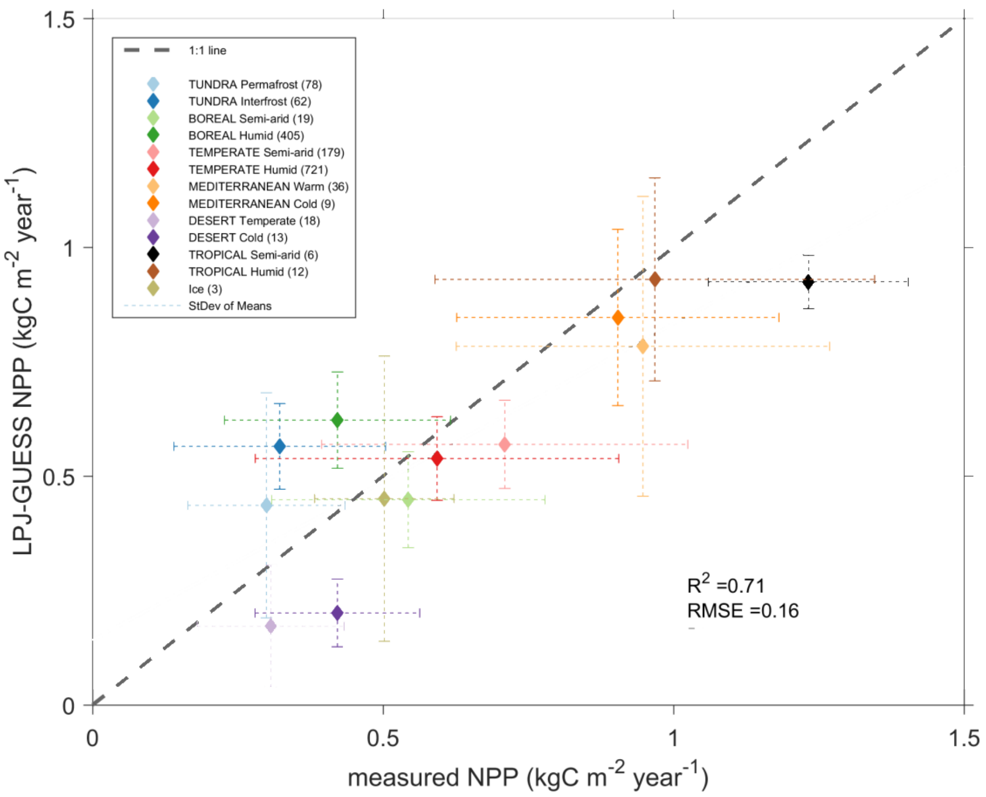

Fig. A2 Comparison of LPJ-GUESS through NPP estimates and NPP field-measurements at the biome level using biome mean NPP values and their standard deviation. The different colours represent

MBC biomes based on (Reich and Eswaran 2002). The number of NPP observations in each biome is given in the legend. Note that Sahel biomes Desert temperate, Tropical Semi-arid, and Tropical Humid.

Table A6 Comparison between mean biome NPP field-measurements, LPJ-GUESS, BME NPP estimates; and their Q as model performance measure. Sahel biomes are underlined.

Biome (sample size)	Field-data mean NPP [kg C m^{-2} yr^{-1}]	LPJ-GUESS mean NPP [kgC m^{-2} yr^{-1}]	LPJ-GUESS Q	BME mean NPP [kgC m^{-2} yr^{-1}]	BME Q
TUNDRA Permafrost (78)	0.30	0.44	1.46	0.24	0.79
TUNDRA Interfrost (62)	0.32	0.56	1.75	0.44	1.36
BOREAL Semi-arid (19)	0.54	0.45	0.83	0.49	0.91
BOREAL Humid (405)	0.42	0.62	1.48	0.56	1.32
TEMPERATE Semi-arid (179)	0.71	0.57	0.80	0.45	0.63
TEMPERATE Humid (729)	0.59	0.54	0.91	0.56	0.95
MEDITERRANEAN Warm (36)	0.95	0.78	0.83	0.52	0.55
MEDITERRANEAN Cold (9)	0.90	0.85	0.94	0.41	0.45
DESERT Temperate (18)	0.31	0.17	0.56	0.09	0.28
DESERT Cold (13)	0.42	0.20	0.48	0.24	0.57
TROPICAL Semi-arid (6)	1.23	0.92	0.75	0.84	0.68
TROPICAL Humid (12)	0.97	0.93	0.96	0.81	0.84
Ice (3)	0.50	0.45	0.90	-	-

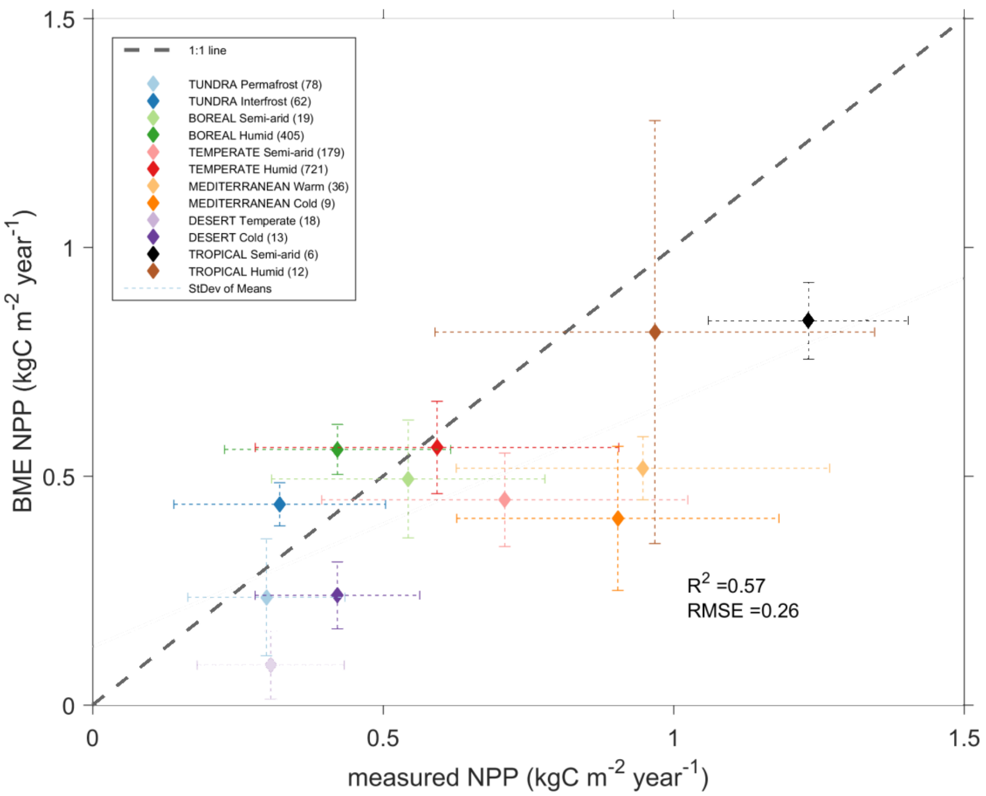

Fig. A3 Comparison of BME NPP estimates and NPP field-measurements on biome level using biome mean values as well as biome standard deviation of the means. The different colours represent MBC biomes based on (Reich and Eswaran 2002). The number of NPP observations in each biome is given in the legend. Note that Greter Sahel biomes Desert temperate, Tropical Semi-arid, and Tropical Humid.

For Greater Sahel biomes: LPJ-GUESS exhibits good skill in simulating NPP in the Tropical humid (Q = 0.96, see Table A6) where it also captures satisfactorily the variability of the NPP measurements. LPJ-GUESS underestimates NPP for the tropical semi-arid biome (Q = 0.75) showing reduced NPP variation compared to the observations. Performance is reduced for Desert temperate (Q =0.56).

BME performance is acceptable at the overall biome level (R^2 = 0.57 and RMSE = 0.26) but varies substantially for individual biomes (see Fig. A3). Overall, BME model agreement is reasonable in four biomes (with good performance in two biomes). At the same time, BME overestimates NPP in two biomes while it underestimates plant growth in six biomes. The variability in in- situ NPP measurements cannot be captured by BME in the majority of biomes except in the tropical humid and tundra permafrost biomes (see vertical and horizontal lines connected to the diamonds in Fig. A3).

For Greater Sahel biomes: BME yields acceptable agreement in estimating NPP in the tropical semi-arid and tropical humid biomes (Q = 0.84, 0.81 respectively) but accuracy drops more water limited biomes of desert temperate (Q = 0.28).

Overall, BME mimics the behavior of LPJ-GUESS shown by a good model agreement of R^2 = 0.71 and moderate RMSE = 0.12 kg C m^{-2} yr^{-1} between the average biome NPP estimates of BME and LPJ-GUESS. Notable is that BME yields, on average, less NPP in the majority of biomes compared to the observations.”

We also include the comparison with the results of the MODIS processing stream p. 31 lines 7 – 18:

"We also compare total yearly means of NPP from BME and LPJ-GUESS to NPP derived from the MOD17A3 processing stream (using MOD17A3 data obtained from the NASA Earth Observation System repository at the University of Montana at www.ntsg.umt.edu) for the period 2000 to 2006 for the greater Sahel region (Running, 2004). We averaged resampled MODIS NPP from 1km to the spatial resolution of the BME estimates (0.5 x 0.5 degrees) and excluded urban areas. We removed below-ground NPP and plant parts unable to be consumed by applying the same R:S and harvest index as described in Section 2.1.1. Lastly, we calculated mean values of MODIS NPP estimates from 2000 to 2010 for each grid cell covering the study area. Our results show that between 2000 and 2006 MODIS-derived NPP underestimate BME-derived NPP by 42% (difference of 0.38 kg dry-weight m^{-2} yr^{-1}), on average (Figure A5). Ardö (2015) also reports that that average annual MODIS NPP underestimates LPJ-GUESS (C version only) for Africa for 2000-2010 and attributes this to the fact that autotrophic respiration is considerably higher for MODIS NPP compared to LPJ-GUESS, due to large temperature sensitivity in the MODIS algorithm, differences in the biome-specific parameterizations for MODIS as well as specification of plant functional types in LPJ-GUESS."

Thomas Pugh: On the theme of evaluation. I'm not clear from the manuscript if PLUM land-use simulations are normalised in some way to the dataset of Hurtt et al. (2011) in 2000, or if they represent a purely "PLUM version" of the Sahel land-use in 2000. The former would raise the question of how much the model drifts from the observed towards its preferred state at the start of the simulations. The latter suggests the need for a comparison of the PLUM initial state with current observation-based estimates (such as Hurtt et al., 2011). I realise there are significant difficulties in modelling actual land-use, but surely the size of any discrepancies and the resulting implications should be discussed?

Authors' Response: The Hurtt et al. (2011) data for the year 2000 is used as basis, as stated on p. 5 lines 12-15:

"We estimated crop- and grassland scaling factors for each country by dividing the PLUM-predicted land-use area with the total land-use area provided by the Hurtt et al. (2011) dataset (Table C1). We then applied the scaling factors to the Hurtt et al. (2011) land-use data and multiplied the resulting crop- and grassland areas with the NPP estimates to obtain annual NPP_{cereal_supply} and $NPP_{grazing\_supply}$ (kg DW $cell^{-1}$ yr^{-1})."

We have also added the country specific factors (along with country-specific land area from FAO) to Table C1 of the appendix:

Table C1 Per capita NPP supply and demand of countries in the greater Sahel region for 2000 and 2050. Portions of food and feed (including grazing) in per capita NPP demand for SSP2-RCP6.0. All NPP is given in dry-weight (DW). Hurtt:PLUM scaling factors and land areas (from FAO) are also included.

Hurtt:PLUM scaling factors 2000	Land area from FAOSTAT 1000 ha
0.89	11062
0.90	27360
1.04	47271
1.00	125920
0.00	2318
1.10	10100
0.98	1000000
1.58	1000
1.03	22754
1.73	24572
1.25	2812
0.98	31800
0.91	9632
0.97	122019
0.97	103070
1.01	126670
1.04	91077
0.74	19253
0.99	7162
0.98	237600
1.10	5439
-	-

We have also added the following discussion, p. 17, lines 32-33 and p. 18, lines 1-3.

"Finally, we note that country-specific scaling factors used to convert PLUM output to per pixel changes using the Hurtt et al. (2011) data set for the year 2000 did not depart substantially from 1 (scaling factors for the larger countries were all within 10%, and the area weighted mean of the scaling factors was 0.95), but a few smaller countries in West Africa diverge by more than 25% (<0.80 or > 1.25) (see Table C1). We expect these to have only marginal influence on the results at the regional level, but could have a larger impact on localities along the West African coast (Fig. 4 and Fig. B1)."

Thomas Pugh: pg. 2 l. 31. Why does a 31% population increase lead to a 100% increase in NPP requirement? What information is missing here?

Authors' Response: p2 lines 31-33 now read:

"Since the NPP demand increased at an annual rate of 2.2% over the period while the supply was near constant, the near doubling in NPP demand implies, in relative terms, that there was less NPP supply to service the increase in population."

Thomas Pugh: pg. 6 l. 16. I'm confused about the cropland cover, I thought it was taken from PLUM? How is Hurtt being used here?

Authors' Response: Please refer the previous response.

Thomas Pugh: pg. 6 l. 23. Surely the total amount of NPP for human appropriation must be the sum of NPP_{cereal_demand} and $NPP_{grazing\_demand}$, not just NPP_{cereal_demand} alone? As parts of both cereal and grazing demand contribute to animal raising, the current definition is inconsistent. Was it meant to be something like "total amount of annual NPP for human appropriation via cropland"?

Authors' Response: this clause, on p. 7, line 4 now reads

"total amount of annual NPP for human appropriation via cropland."

Indeed, we explicitly distinguish between the demand of cereal and pasture products. Cereal demand is given in Equation 1 of the manuscript, while grazing demand is given in Equation 9 (not Equation 8 as stated in the first version, Appendix A3 – we have changed this too). Cereal-based and grazing-based supply-demand balances are then computed separately. They are then summed according to Table 1 in the manuscript in order to determine final balances of supply and demand of NPP.

Thomas Pugh: The SSP-RCP scenario likelihoods seem rather important. Rather than referring the reader to another paper, maybe you could include them in this analysis? For instance along the right y-axis of Fig. 3b?

Authors' Response: -We now provided Table 1 in our revised manuscript, referred to on p. 7 line 17. Table 1 shows the scenario likelihoods, and is the same as Table 4 found in Engström et al. (2016b). Note that these likelihoods refer to the most consistent SSP-RCP combinations (e.g. it is more likely that the sustainability assumptions for SSP1 would yield greenhouse gas concentrations in line with RCP4.5/6 rather than RCP2.6/8.5).

Table 1 Scenario matrix translated into quantitative probabilities (see also Engström et al. (2016b).

	RCP 2.6	RCP 4.5	RCP 6	RCP 8.5	Sum
SSP1	0.0909	0.4545	0.4545	0.0000	1
SSP2	0.0000	0.0909	0.6818	0.2273	1
SSP3	0.0000	0.1667	0.5000	0.3333	1
SSP4	0.0000	0.3704	0.5556	0.0741	1
SSP5	0.0000	0.0741	0.3704	0.5556	1

Thomas Pugh: pg. 7 l. 29-33. This text reads as if it was originally located before the first paragraph of 2.1.3, and some of the text would seem to be more logically located there, where this likelihood matrix is first mentioned.

Authors' Response: This information is now moved to the suggested location, p. 7 lines 18-21.

Thomas Pugh: pg. 9 l. 11. I would say that the shortfalls in SSP5-RCP6.0 and SSP5-RCP8.5 are pretty sustained. They just don't run to the end of the century. Consider rephrasing? More generally, regarding the discussion of "shortfalls", it seems strange that you only consider shortfalls to occur when the 95% confidence limits do not overlap (and demand is higher of course). To my mind this lack of overlap of the confidence limits suggests very high likelihood of shortfalls, but the best guess result shows shortfalls occurring for a larger number of scenarios. For instance, on pg. 11, l. 26 it is stated that "statistically significant shortages never develop" in the context of SSP1, but that doesn't seem quite right. Assuming non-skewed distributions of uncertainty (big assumption, I know), then when the best estimate of demand exceeds the best estimate of supply there is a more than even chance of shortages occurring, but it's not possible to say with high certainty that a shortage will occur until the 95% limits no longer overlap. Consider rephrasing also?

Authors' Response: These items have been rephrased and here we produce a rewritten portion of the results, found on p. 10, lines 6-19:

"Per capita demand exceeds supply in the early 2040s for SSP2-RCP6.0 after which a very high likelihood for shortfalls begins in 2070 (see black dots in Fig. 3a showing non-overlapping 95% confidence limits). By 2050, per capita demand almost doubles while per capita supply drops by almost 30% for the same scenario. Across the scenarios, differences in the timing of the start of persistent supply shortfalls with high statistical certainty are observed (see black dots in Fig. 3b). Three of these high likelihood shortfalls begin at 2050 or before (SSP5 scenarios – see black dots in Fig. 3b) while an additional six display shortfalls with high certainty by the end of the 21st century (black dots in Fig. 3a, b). Out of these nine, two scenarios never achieve a sustained run of shortfalls (SSP2-RCP6.0, SPP2-RCP8.5). In total, there is better than an even chance for shortfalls before 2050 for 9 scenarios (exceptions are SSP1-RCP2.6, SSP1-RCP6.0, and all SSP4 scenarios.

Variations in the timing of onset and end of supply shortfalls are generally greater between the SSPs than between the RCPs (Fig. 3b). For SSP2 and SSP3 scenarios, onsets of high likelihood supply shortfall range from the early 2050s to the mid-2070s (even chance from late 2030s to early 2050s). The SSP5 family shows the largest deficits of high likelihood shortfalls beginning in the 2040s-2050s (even chance from the early 2030s), and after several decades of deepening begin to diminish in the

2080s. Shortfalls with high certainty never emerge for SSP1 (even chance from the early 2050s) while the SSP4 scenarios show sustained but diminishing surplus throughout."

Thomas Pugh: pg. 9 l. 22. Reference to Table 3 here?

Authors' Response: We now reference this table on p. 11 line 6 of our revised manuscript. Note that a new Table 1 means that Table 3 of the original manuscript is now Table 4 in the revised manuscript.

Thomas Pugh: pg. 12 l. 3. Regarding, "so strong efforts should be made to reduce these gaps", this is too simplistic. Efforts to close yield gaps have other environmental and socio-economic consequences which are not addressed here, meaning that this statement cannot be supported by the presented evidence. I suggest to remove this recommendation. Going beyond this however, can you say anything about the potential additional yield by closing yield gaps in this region, and whether such efforts could alleviate the shortages simulated? Maybe PLUM can provide the necessary data?

Authors' Response: The recommendation has now been removed. We have now added the following information on p. 14, lines 3-5 of our revised manuscript:

"The closure of yield gaps by 2050 (for scenario SSP2-6.0) would result in a change in mean per capita NPP balance from -107 kg DW yr-1 (see Table 3) to 9 kg DW yr-1. Though the balance for many countries will still be negative, the magnitudes of shortfalls could be reduced. Thus, closing yield gaps in the region could indeed alleviate the simulated shortages."

Thomas Pugh: pg. 12 l. 24. Where is the attribution of supply increases to additional rainfall and CO2 fertilisation shown in the results?

Authors' Response: We have conducted this experiment and added the following to p. 15, lines 14-17 of our revised manuscript:

"In order to isolate the CO_2 (rainfall) effect on NPP increase for RCP6.0, we compared a simulation where rainfall (CO_2) was held constant with a simulation where both were held constant for the period 2000-2050 for all GCMs. We found that supply increases mostly due to CO_2 fertilization (see Fig. B2), with very little attributed to rainfall. However, yield gap closure from SSP2 contributes most to NPP increase (Fig. B2)."

The CO_2 fertilization effect increases with the magnitude of climate change and explains the smaller shortages in SSP-RCP8.5 scenarios compared to SSP-RCP4.5 scenarios (Fig. 3b)."

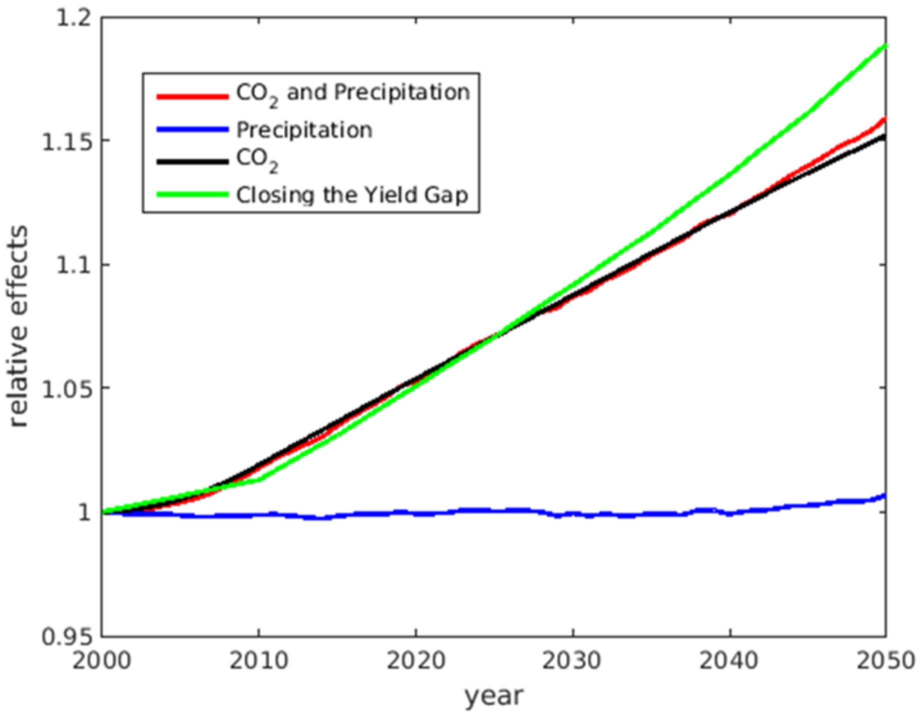

Fig. B2. The relative contributions of CO_2, precipitation and yield gap closure to the increase in NPP over the greater Sahel region, 2000-2050. Results for CO2 and precipitation are from RCP 6.0 and yield gap is from SSP2. Simulated climate and CO_2 effects shown here are mean effects over the five GCMs (GFDL,MIROC,Hadley,NorESM, IPSL).

We have now removed the original statement alluding to the fact that NPP increases are attributed to CO2 fertilization and rainfall from this section entirely.

Thomas Pugh: pg. 13 l. 7. The relative attribution of supply growth to climate/co2 and closure of yield gaps would be very informative, allowing the results to be interpreted more subtly. Your approach seems to be suitable to make this isolation.

Authors' Response: See previous comment.

Thomas Pugh: pg. 13 l. 12. I would take the opposite view. The extent to which models appropriately represent CO2 fertilisation is not clear, and the difference in NPP trends between models is very large (e.g. Friend et al., 2014; Körner, 2006; Pugh et al., 2016; Rosenzweig et al., 2014). Therefore, I think it is fair to say that we have no more confidence in the trends than we do in the absolute levels. Moreover, the reference here to Fig. A2 does nothing to support the point, as the point of comparison is an LPJ-GUESS simulation, not observations.

Authors' Response: Thanks very much for highlighting issues with the trends. Please see our response to RC3 for a broader discussion of the trends (e.g. responses to comments #3 and #6). We have now removed this sentence entirely from this section and have modified Fig. A2 (now Fig. A5 in the revised manuscript (see a previous comment), and in order to meet this critique (and that of RC3), we have added the following to Section 4.6 (Uncertainties), p. 17, lines 13-31. This section also refers to our new Fig. B7 where we rerun supply-demand scenarios with CO2 turned off:

“Additional uncertainty exists with respect to the total magnitude and trends of simulated NPP supply, given the lack of ground truth for the region, and that differences in NPP trends between other models is very large (e.g. Friend et al., 2014; Körner et al., 2006; Pugh et al., 2016; Rosenzweig et al., 2014). Indeed, recent observational evidence suggests that the effect of CO_2 fertilization on plant growth may be constrained by counteracting feedbacks associated with increasing atmospheric moisture demand and nutrient availability (e.g. Smith et al., 2016; Wieder et al. 2015). For example, NPP is reduced under warmer and dryer conditions due to moisture stress, particularly in temperate and arid ecosystems. Future trends NPP trends in the Sahel could therefore be strongly determined by changes in the frequencies of wet years versus dry years, with the dry years counteracting the CO_2 fertilization effect. Furthermore, nutrient supply rates may not be able to keep up with extra demand associated with CO_2 fertilization, and leading to a depletion of soil nutrients, as current evidence suggests. This could also curtail the CO_2 fertilization effect, particularly in the more southerly parts of our study area, where nutrients tend to become a limiting factor. We performed a simple experiment negating the CO_2 fertilization effect in order to gauge its impact on supply-demand balance on all scenarios. For the SSP2-RCP6.0, per capita demand has an equal chance of exceeding per capita supply in 2036 for the SSP2-6.0 scenario as opposed to 2043 if CO_2 fertilization in included (Fig. B7), with a very high likelihood of continuous supply shortfall beginning in 2056, as opposed to 2073 with CO_2 fertilization. The effect on all other scenarios is an earlier shift to the onset of supply shortfalls, by about 10 years, compared to Fig. 3b (see Fig. B7). Supply shortfalls with high likelihood of occurrence (black dots showing non-overlapping 95% confidence intervals) are similarly shifted, and occur with greater consistency and frequency. All of this suggests that the NPP increases found in our current analysis are likely optimistic, due the potential overestimation of the CO_2 fertilization effect, as well as the fact that BME is based on potential natural vegetation.”

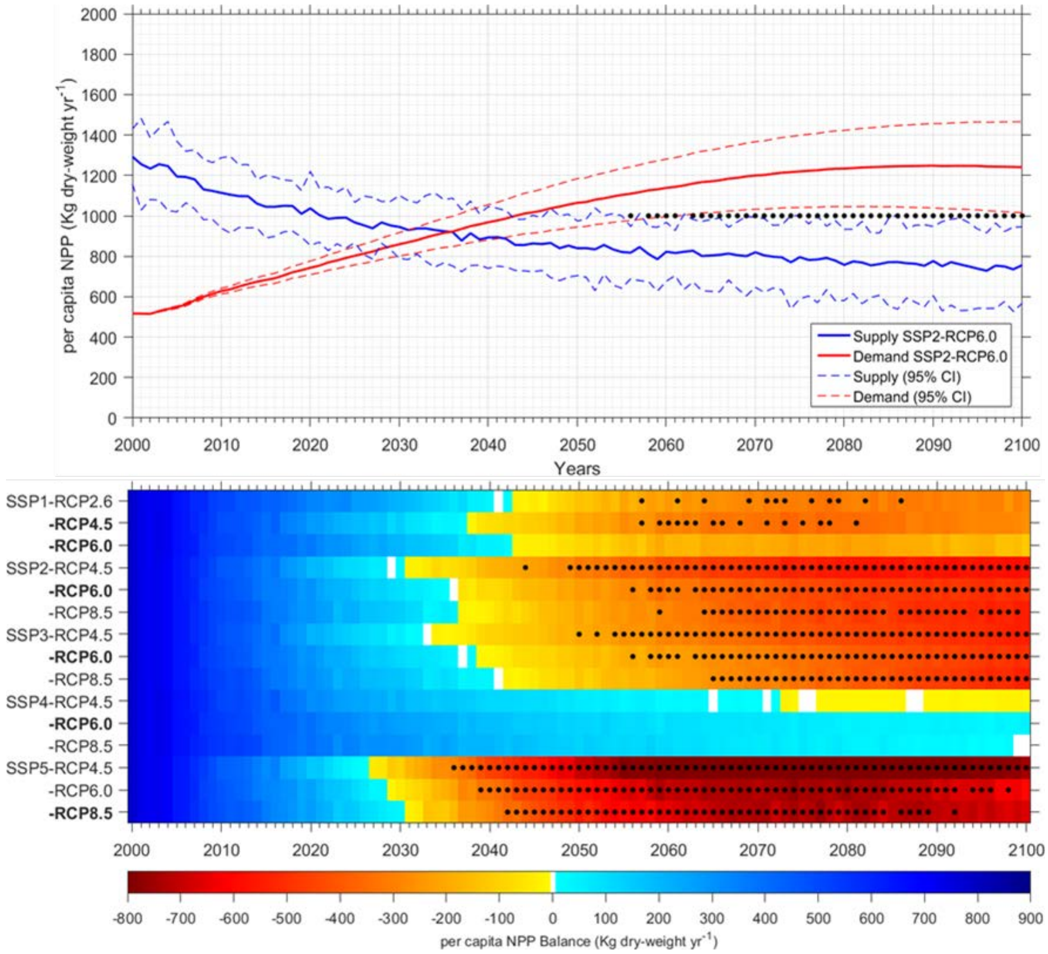

Fig. B7 Per capita NPP supply, demand and balance for the greater Sahel (2000-2100) without CO_2 fertilization. **B7a)** shows NPP supply (red) and demand (blue). The solid curves illustrate the mean of the SSP2-RCP6.0 combination. The dashed blue curves show supply uncertainty (95% confidence interval around the mean) based on the five GCMs NPP results. The dashed red curves show demand uncertainty (95% confidence interval around the mean) based on the uncertainty related to the interpretation and quantification of SSP2. **B7b)** shows the different magnitudes of the NPP balance and the varying onsets of shortage across all SSP-RCP combinations. Black dots illustrate years with a shortage outside of the 95% confidence intervals. Combinations are grouped according to the socio-economic scenarios (y-axis). The RCPs are ordered from low to high radiative forcing in each SSP group. The temporal trajectory is shown along the x-axis and the colouring indicates the sign of the annual NPP balance. Blues show a surplus of the NPP supply while yellow to red represent small to very large the gaps between supply and demand). SSP-RCP combinations in bold indicate the most likely SSP-RCP pairs based on Table 1.

<u>**Thomas Pugh:**</u> pg. 13 l. 22. You could also briefly mention irrigation water availability projections here (Elliott et al., 2014).

Authors' Response: We have now appended our manuscript with the following, found on p. 16 lines 3-6:

"However, Elliott et al. (2014) underscore that freshwater limitations in the dryer regions of the globe could limit agricultural production, and even lead to the reversion of irrigated farmland to rainfed farmland thereby negatively affecting food production."

Thomas Pugh: pg. 1, l. 20. "surplus, while" pg. 1 l. 23. "diet" pg. 2 l. 13. "global food security is not ensured" pg. 2 l. 16. "world, where" pg. 2 l. 19. "own land, where", also full stop missing after "pastoralism" pg. 4 l 32. Should "estimates to the total area", read " estimates to sum over the total area"? I don't think you translated NPP to total area literally? pg. 5 l. 22. Replace "Furthermore" with "Therefore" pg. 5 l. 32. "choice, and the" pg. 6 l. 13, 14, 20. "Fig. 2" should be "Fig. 1"? Also there are several boxes in red in Fig. 1 so "box outlined in red" is of limited use, and the distinction between cereal and pasture products can't be seen in the picture. pg. 8 l. 4. "Hence, one" pg. 10 l. 2. Only two countries are listed. pg. 12 l. 26. "mobilization is one method local" pg. 12 l. 31. "increase" pg. 14 l. 2. I think this would read better as "the Sahel is likely to experience NPP shortages in most SSP scenarios due to" pg. 14 l. 7. Reference formatting. pg. 14 l. 25. "show" rather than "assume"? pg. 15 l. 2. "will outstrip supply during the 21st century". pg. 15 l.12. "unfolds, a relatively"

Authors Response: These typos have been fixed.

References in our responses

Abdi, A. M., Seaquist, J., Tenenbaum, D. E., Eklundh, L., and Ardö, J.: The supply and demand of net primary production in the Sahel, Environmental Research Letters, 9, 094003, 2014.

Ardö, J. Comparison between remote sensing and a dynamic vegetation model for estimating terrestrial primary production of Africa. Carbon Balance and Management, 10(8), 2015.

Ceccato, P., Cressman, K., Giannini, A., and Trzaska, S.: The desert locust upsurge in West Africa (2003-2005): Information on the desert locust early warning system and the prospects for seasonal climate forecasting, International Journal of Pest Management, 53, 7-13, 2007.

Elliott, J., Deryng, D., Müller, C., Frieler, K., Konzmann, M., Gerten, D., Glotter, M., Flörke, M., Wada, Y., Best, N., Eisner, S., Fekete, B.M., Folberth, C., Foster, I., Gosling, S.N., Haddeland, I., Khabarov, N., Ludwig, F., Masaki, Y., Olin, S., Rosenzweig, C., Ruane, A.C., Satoh, Y., Schmid, E., Stacke, T., Tang, Q., Wisser, D., 2014. Constraints and potentials of future irrigation water availability on agricultural production under climate change. Proc. Natl. Acad. Sci. U. S. A. 111, 3239–44. doi:10.1073/pnas.1222474110

Engström, K., Olin, S., Rounsevell, M. D. A., Brogaard, S., van Vuuren, D. P., Alexander, P., Murray-Rust, D., and Arneth, A.: Assessing uncertainties in global cropland futures using a conditional probabilistic modelling framework, Earth System Dynamics, 7, 893–915, 2016.

Foley, J. A., Defries, R., Asner, G. P., Barford, C., Bonan, G., Carpenter, S. R., Chapin, F. S., Coe, M. T., Daily, G. C., Gibbs, H. K., Helkowski, J. H., Holloway, T., Howard, E. A., Kucharik, C. J., Monfreda, C., Patz, J. A., Prentice, I. C., Ramankutty, N., and Snyder, P. K.: Global consequences of land use, Science, 309, 570-574, 2005.

Friend, A.D., Lucht, W., Rademacher, T.T., Keribin, R., Betts, R., Cadule, P., Ciais, P., Clark, D.B., Dankers, R., Falloon, P.D., Ito, A., Kahana, R., Kleidon, A., Lomas, M.R., Nishina, K., Ostberg, S., Pavlick, R., Peylin, P., Schaphoff, S., Vuichard, N., Warszawski, L., Wiltshire, A., Woodward, F.I., 2014. Carbon residence time dominates uncertainty in terrestrial vegetation responses to future climate and atmospheric CO2. Proc. Natl. Acad. Sci. U. S. A. 111, 3280–3285. doi:10.1073/pnas.1222477110

Harris, I., P. D. Jones, T. J. Osborn, and D. H. Lister. 2014. Updated high-resolution grids of monthly climatic observations – the CRU TS3.10 Dataset. International Journal of Climatology 34:623-642.

Hurtt, G. C., Chini, L. P., Frolking, S., Betts, R. A., Feddema, J., Fischer, G., Fisk, J. P., Hibbard, K., Houghton, R. A., Janetos, A., Jones, C. D., Kindermann, G., Kinoshita, T., Goldewijk, K. K., Riahi, K., Shevliakova, E., Smith, S., Stehfest, E., Thomson, A., Thornton, P., van Vuuren, D. P., and Wang, Y. P.: Harmonization of land-use scenarios for the period 1500-2100: 600 years of global gridded annual land-use transitions, wood harvest, and resulting secondary lands, Climatic Change, 109, 117-161, 2011.

Körner, C., 2006. Plant CO2 responses: an issue of definition, time and resource supply. New Phytol. 172, 393–411. Pugh, T.A.M., Müller, C., Arneth, A., Haverd, V., Smith, B., 2016. Key knowledge and data gaps in modelling the influence of CO2 concentration on the terrestrial carbon sink. J. Plant Physiol. 203, 3–15. doi:10.1016/j.jplph.2016.05.001

Lindeskog, M., Arneth, A., Bondeau, A., Waha, K., Seaquist, J., Olin, S., and Smith, B.: Implications of accounting for land use in simulations of ecosystem carbon cycling in Africa, Earth Syst. Dynam., 4, 385-407, doi:10.5194/esd-4-385-2013, 2013.

Luyssaert, S., I. Inglima, and M. Jung. 2009. Global Forest Ecosystem Structure and Function Data for Carbon Balance Research. Global Forest Ecosystem Structure and Function Data for Carbon Balance Research. Data set. Available on-line [http://daac.ornl.gov/] from Oak Ridge National Laboratory Distributed Active Archive Center, Oak Ridge, Tennessee, U.S.A. doi:10.3334/ORNLDAAC/949.

Michaletz, S. T., D. Cheng, A. J. Kerkhoff, and B. J. Enquist. 2014. Convergence of terrestrial plant production across global climate gradients. Nature 512:39-43

Pugh, T.A.M., Müller, C., Arneth, A., Haverd, V., Smith, B., 2016. Key knowledge and data gaps in modelling the influence of CO2 concentration on the terrestrial carbon sink. J. Plant Physiol. 203, 3–15. doi:10.1016/j.jplph.2016.05.001

Reich, P. F., and H. Eswaran. 2002. Global resources. In: Lal, R. (ed.). Encyclopedia of Soil Science, pp. 607-611. Marcel Dekker, New York.

Rosenzweig, C., Elliott, J., Deryng, D., Ruane, A.C., Müller, C., Arneth, A., Boote, K.J., Folberth, C., Glotter, M., Khabarov, N., Neumann, K., Piontek, F., Pugh, T. a M., Schmid, E., Stehfest, E., Yang, H., Jones, J.W., 2014. Assessing agricultural risks of climate change in the 21st century in a global gridded crop model intercomparison. Proc. Natl. Acad. Sci. U. S. A. 111, 3268–73. doi:10.1073/pnas.1222463110

Sallaba, F., D. Lehsten, J. Seaquist, and M. T. Sykes. 2015. A rapid NPP meta-model for current and future climate and CO2 scenarios in Europe. Ecological Modelling 302:29-41.

Smith, W., Cleveland, C.C., Reed, S.C. & Running, S.W. (2014a). Agricultural conversion without external water and nutrient inputs reduces terrestrial vegetation productivity. Geophys. Res. Lett., 41, 449–455.

Smith, B., Wårlind, D., Arneth, a., Hickler, T., Leadley, P., Siltberg, J., Zaehle, S., 2014b. Implications of incorporating N cycling and N limitations on primary production in an individual-based dynamic vegetation model. Biogeosciences 11, 2027–2054. doi:10.5194/bg-11-2027-2014

Trenberth, K. E., A. Dai, G. van der Schrier, P. D. Jones, J. Barichivich, K. R. Briffa, and J. Sheffield. 2014. Global warming and changes in drought. Nature Clim. Change 4:17-22.

We thank RC2 for challenging us with some thought-provoking critique. What follows is a point-by-point response to these comments, together with a new marked-up version of our manuscript.

RC2: This manuscript does NOT satisfies your editorial criteria as described at http://www.earth-system-dynamics.net/peer_review/review_criteria.html This manuscript perhaps intends to make contributions to regional studies of the socioeconomic implications of global change, particularly about the Sahel and its delicate balance between supply and demand of natural resources, with a focus on its implications for food production; however some of its methods are flawed and the use of information weak. This paper deals with very delicate topics that deserve honour and credit, but using the wrong tools to address them, for which the authors deserve no mercy. Therefore I recommend the rejection of this manuscript.

Authors' Response: Thanks very much for your general opinion. Please read through our responses below and our responses to the first and third reviewers which we hope will allay some of your concerns.

RC2: LPJ and the like models are normally very rough on their predictions, if you simplify them more, then your results might be useless.

Authors' Response: We concur that 'LPJ and the like models' can be 'very rough on their predictions,' which is the reason for taking an exploratory approach (rather than a predictive one) in this study. We emphasize a structural analysis of NPP supply-demand outcomes across a range of scenarios, using simplified models that can easily be coupled across sectors. One of the purposes of the manuscript is to demonstrate such a framework. We re-iterate our rationale, taken from p. 3 lines 3-12 of our original manuscript, and p. 3 lines 5-14 of our revised manuscript:

"Developing such tools requires coupling of specific models that address different sectors, such as a model for supply and a model for demand that can be run across multiple future climate, socio-economic and CO2 concentration scenarios. However, the supply-demand system in the Sahel is complex and the future cannot be precisely evaluated. This is because there are many uncertainties associated with the assumptions that underpin the natural and socioeconomic drivers that lead to particular supply-demand balances. As such, an exploratory modelling approach is required, where an emphasis is placed on a structured analysis across a range of outcomes. This approach capitalizes on future indeterminacy for developing adaptive policy insights (e.g. Kwakkel and Pruyt (2013)). As the goal of exploratory frameworks is not prediction, they often employ parsimonious or simplified versions of more complex models (often referred to as meta-models in the latter case) that run across a range of scenarios (e.g. Harrison et al. (2016)). Another benefit of using such simplified models lies in the ease to which they can be coupled to other sectoral models (e.g. Kebede et al. (2015))."

RC2: Pg. 4 line 25, you evaluate the performance of your model against another model (LPJ)? Why this is good science deserving publication? This is bad science. Have you thought about doing it against data?

Authors' Response: The rationale for evaluating the performance of BME against LPJ-GUESS is to verify that BME (a meta-model based on LPJ-GUESS) captures the magnitude, interannual variation and trends in LPJ-GUESS across the historical climate record. In accordance with specific requests by

Thomas Pugh (RC1) and RC3, we have also compared our LPJ-GUESS and BME NPP with MOD-17 (absolute values, interannual variability, and trends) for the years 2000-2006, as well as against trends in crop yields found in the literature. We have also performed a validation of LPJ-GUESS and BME for all biomes used to develop BME. Please see our responses to R#1 and AR#3 for details, and our revised Appendix A2 (pp. 24-33).

RC2: You do a regional level study using GCM data? Not good practice. See what other Swedish colleagues do with regional data there: http://www.smhi.se/en/research/research-departments/climate-research-rossbycentre2-552/an-ensemble-of-cordex-africa-climate-projections-simulated-by-rca4- 1.25312

Authors' Response: PLUM is a global scale model (see Engström et al. 2016a, 2016b) that links all countries via international trade to help regulate the balance of feed and food. The implication is that the supply and demand generated in any one country or world region (e.g. the greater Sahel) is a function of supply-demand dynamics across the globe. GCM output is therefore consistent with the level of organization at which PLUM operates (global) and requires global level climate projections. Spatial resolution may certainly be a factor but as the Sahel does not exhibit large topographical variation we hypothesize that the effect of downscaling will not be large. Indeed, Blanke et al. (2016) also conclude that there is no large gain in LPJ-GUESS simulations of C and N stocks when using regionally downscaled, bias corrected climate products compared to GCM simulations, at least for Europe.

RC2: What you intend to argue, deriving insights from NPP into food production related arguments, is very weak in methodological terms, and although your rationale and arguments are sensible, the methods you use disqualify the support you use for the argumentation. Then you use a convenient "technology improvement factor"? and close the yield gap with it? I am sorry, again, this is bad science, and it should not be published.

Authors' Response: Please see our responses to your previous comments, as well as our responses to the other two reviewers that deal with various methodological issues. We now clarify on p. 5, lines 17-22:

"The technology improvement factor is the aggregate result of parameterizing three technology related parameters (trends in technology, change in yield with GDP per capita, as well as how agricultural management practices are transferred both within and between countries) that are consistent with the scenario storyline of each SSP. Parameter ranges have been empirically determined based on analysis of data between the years 1995 and 2005. Yield gaps are not necessarily closed, but are decreased (see Engström et al. 2016b for more detail)."

References in our responses

Blanke, J.H., Lindeskog, M., Lindström, J., and Lehsten, V. Effect of climate data on simulated carbonand nitrogen balances for Europe, Journal of Geophysical Research: Biogeosciences, 121, 1352-1371, 2016.

Engström, K., Olin, S., Rounsevell, M. D. A., Brogaard, S., van Vuuren, D. P., Alexander, P., Murray-Rust, D., and Arneth, A.: Assessing uncertainties in global cropland futures using a conditional probabilistic modelling framework, Earth System Dynamics, 7, 893–915, 2016b.

Engström, K., Rounsevell, M. D. A., Murray-Rust, D., Hardacre, C., Alexander, P., Cui, X. F., Palmer, P. I., and Arneth, A.: Applying Occam's razor to global agricultural land use change, Environmental Modelling & Software, 75, 212-229, 2016a.

Harrison, P. A., Dunford, R. W., Holman, I. P., and Rounsevell, M. D. A.: Climate change impact modelling needs to include cross-sectoral interactions, Nature Clim. Change, advance online publication, 2016.

Kebede, A. S., Dunford, R., Mokrech, M., Audsley, E., Harrison, P. A., Holman, I. P., Nicholls, R. J., Rickebusch, S., Rounsevell, M. D. A., Sabaté, S., Sallaba, F., Sanchez, A., Savin, C., Trnka, M., and Wimmer, F.: Direct and indirect impacts of climate and socio-economic change in Europe: a sensitivity analysis for key land- and water-based sectors, Climatic Change, 128, 261-277, 2015.

Kwakkel, J. H. and Pruyt, E.: Exploratory Modeling and Analysis, an approach for model-based foresight under deep uncertainty, Technological Forecasting and Social Change, 80, 419-431, 2013.

We also thank RC3 for their insightful and constructive comments. What follows is a point-by-point treatment of these comments. We respond to each comment in turn, while at the same time provide a marked up manuscript with changes.

RC3: 1. The introduction is very well-written and does an excellent job of framing the question and establishing the importance of the work.

Authors' Response: Thank-you very much. It is good to know that the effort we made crafting the introduction does not go unnoticed.

RC3: 2. Page 4, line 27: It is stated that the authors used 0.5 degree climate data from five GCMs, and [CO2] based on four RCPs (Representative Concentration Pathways). The way it is phased it is unclear which RCPs were used to generate the climate projections for each GCM. The authors should have used climate data derived from runs across the 4 RCPs for each of the 5 models. Please clarify the text if this is the case. If not, please explain more fully why the climate data were not derived for all RCPs.

Authors' Response: This section in our revised manuscript now reads (p. 5, lines 3-6):

"We forced BME with climate data (spatial resolution 0.5 x 0.5 degrees) from five GCMs (General Circulation Models, including HADLEY, GFDL, IPSL, MIROC and NorESM), and [CO_2] based on four RCPs (Representative Concentration Pathways, including 2.6, 4.5, 6.0 and 8.5) to estimate annual total NPP in kg dry-weight m^{-2} yr^{-1}. (DW, dry-weight). We used climate data derived from runs across the 4 RCPs for each of the 5 models."

RC 3: Robustly representing future NPP trajectories is challenging due to the many potential counteracting feedbacks. The authors show a good fit with LPJ NPP simulations, but do not consider observational data or alternative runs of the LPJ model itself. I recommend further comparison against both census derived yield trends (Rey et al. 2013) and satellite-derived yield trends (Running et al. 2004). For instance, the authors could consider runs in which the CO2 fertilization effect is turned off. Currently all the NPP trends considered in the paper are increasing due to CO2 fertilization (page 9, line 24). This is an area of debate and may be counter to observational data (see Smith et al. 2016, Oberneier et al. 2016, and Ort & Long et al. 2014). Thus, I wonder if a scenario in which CO2 fertilization effects are isolated and removed would be a more realistic lower boundary on what to expect for the region? I would imagine very large increases in the NPP debt (without large irrigation efforts), much larger than what is currently considered in the paper.

Authors' Response: We thank this reviewer for underscoring these issues with the trends, and for suggesting some ways forward. In order to address these comments, we compare BME simulations with MODIS data for the period 2000-2006 (see new section, Appendix 2.2, p. 31, lines 7-18):

"We also compare total yearly means of NPP from BME and LPJ-GUESS to NPP derived from the MOD17A3 processing stream (using MOD17A3 data obtained from the NASA Earth Observation System repository at the University of Montana at www.ntsg.umt.edu) for the period 2000 to 2006 for the greater Sahel region (Running, 2004). We averaged resampled MODIS NPP from 1km to the spatial resolution of the BME estimates (0.5 x 0.5 degrees) and excluded urban areas. We removed below-ground NPP and plant parts unable to be consumed by applying the same R:S and harvest index as described in Section 2.1.1. Lastly, we calculated mean values of MODIS NPP estimates from

2000 to 2010 for each grid cell covering the study area. Our results show that between 2000 and 2006 MODIS-derived NPP underestimate BME-derived NPP by 42% (difference of 0.38 kg dry-weight m^{-2} yr^{-1}), on average (Figure A5). Ardö (2015) also reports that that average annual MODIS NPP underestimates LPJ-GUESS (C version only) for Africa for 2000-2010 and attributes this to the fact that autotrophic respiration is considerably higher for MODIS NPP compared to LPJ-GUESS, due to large temperature sensitivity in the MODIS algorithm, differences in the biome-specific parameterizations for MODIS as well as specification of plant functional types in LPJ-GUESS."

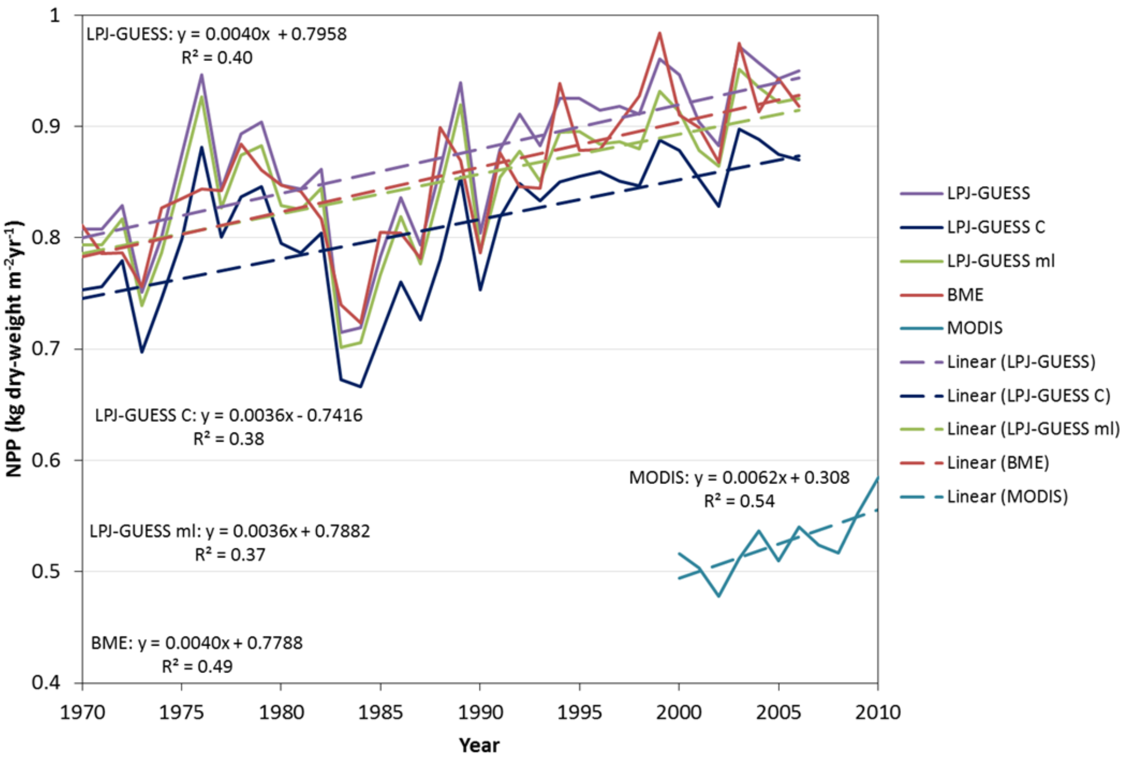

Fig A5 Regional annual NPP Annual means of NPP for BME, LPJ-GUESS, LPJ-GUESS C (carbon only) and LPJ-GUESS ml (managed land) (1970 to 2006) and MODIS (2000-2010) for the greater Sahel region.

We also compare these results with country level census yield trends (1989-2008) for 4 major crops (rice, maize, wheat, and soybean) from appendix Data S1 of Ray et al. (2013), for some countries found in our study area (see Appendix 2.2, p. 31, lines 19-29):

"Country-level census yield trends (1989-2008) for 4 major crops from appendix Data S1 of Ray et al. (2013) for rice (Benin, Burkina Faso, Chad, Ghana, Guinea, Guinea-Bissau, Ivory Coast, Liberia, Mali, Nigeria, Senegal, Sierra Leone, Togo), maize (Benin, Burkina Faso, Cameroon, Chad, Ethiopia, Ghana, Guinea, Ivory Coast, Mali, Nigeria, Senegal, Togo), wheat (Cameroon, Chad, Eritrea, Ethiopia, Mali, Mauritania, Niger, Nigeria, Sudan) and soybean (Benin, Burkina Faso, and Nigeria) range from -5.98 to 2.80 (mean of -0.002), -0.94 to 4.08 (mean of 1.400), -2.58 to 3.1 (mean of 1.280) and 1.15 to 3.98 (mean of 2.280) respectively. Trends for BME, LPJ-GUESS and MODIS NPP fall within most of the ranges for crop yield trends, showing yearly increases of 0.55% (BME), 0.58% (LPJ-GUESS) and 0.51% (MODIS), for the 7 year period of overlap. For the entire length of each series (1970-2006 for BME and LPJ-GUESS, and 2000-2010 for MODIS), slopes indicate yearly increases of 0.40%, 0.40%, and 0.62% respectively. We note the number of uncertainties involved in this comparison (e.g.

spatial/temporal sampling, and the fact that BME and MODIS represent natural vegetation and a mix of natural vegetation and crops, respectively).”

Finally, we compare BME trajectories of NPP with and without CO2 fertilization for all scenarios for the period 2000-2100 in order to account for the fertilization effect and deal with this in an expanded uncertainty section in the manuscript (p. 17, lines 13-31, and a new Fig. B7 in the appendix):

“Additional uncertainty exists with respect to the total magnitude and trends of simulated NPP supply, given the lack of ground truth for the region, and that differences in NPP trends between other models is very large (e.g. Friend et al., 2014; Körner et al., 2006; Pugh et al., 2016; Rosenzweig et al., 2014). Indeed, recent observational evidence suggests that the effect of CO_2 fertilization on plant growth may be constrained by counteracting feedbacks associated with increasing atmospheric moisture demand and nutrient availability (e.g. Smith et al., 2016; Wieder et al. 2015). For example, NPP is reduced under warmer and dryer conditions due to moisture stress, particularly in temperate and arid ecosystems. Future trends NPP trends in the Sahel could therefore be strongly determined by changes in the frequencies of wet years versus dry years, with the dry years counteracting the CO_2 fertilization effect. Furthermore, nutrient supply rates may not be able to keep up with extra demand associated with CO_2 fertilization, and leading to a depletion of soil nutrients, as current evidence suggests. This could also curtail the CO_2 fertilization effect, particularly in the more southerly parts of our study area, where nutrients tend to become a limiting factor. We performed a simple experiment negating the CO_2 fertilization effect in order to gauge its impact on supply-demand balance on all scenarios. For the SSP2-RCP6.0, per capita demand has an equal chance of exceeding per capita supply in 2036 for the SSP2-6.0 scenario as opposed to 2043 if CO_2 fertilization in included (Fig. B7), with a very high likelihood of continuous supply shortfall beginning in 2056, as opposed to 2073 with CO_2 fertilization. The effect on all other scenarios is an earlier shift to the onset of supply shortfalls, by about 10 years, compared to Fig. 3b (see Fig. B7). Supply shortfalls with high likelihood of occurrence (black dots showing non-overlapping 95% confidence intervals) are similarly shifted, and occur with greater consistency and frequency. All of this suggests that the NPP increases found in our current analysis are likely optimistic, due the potential overestimation of the CO_2 fertilization effect, as well as the fact that BME is based on potential natural vegetation.”

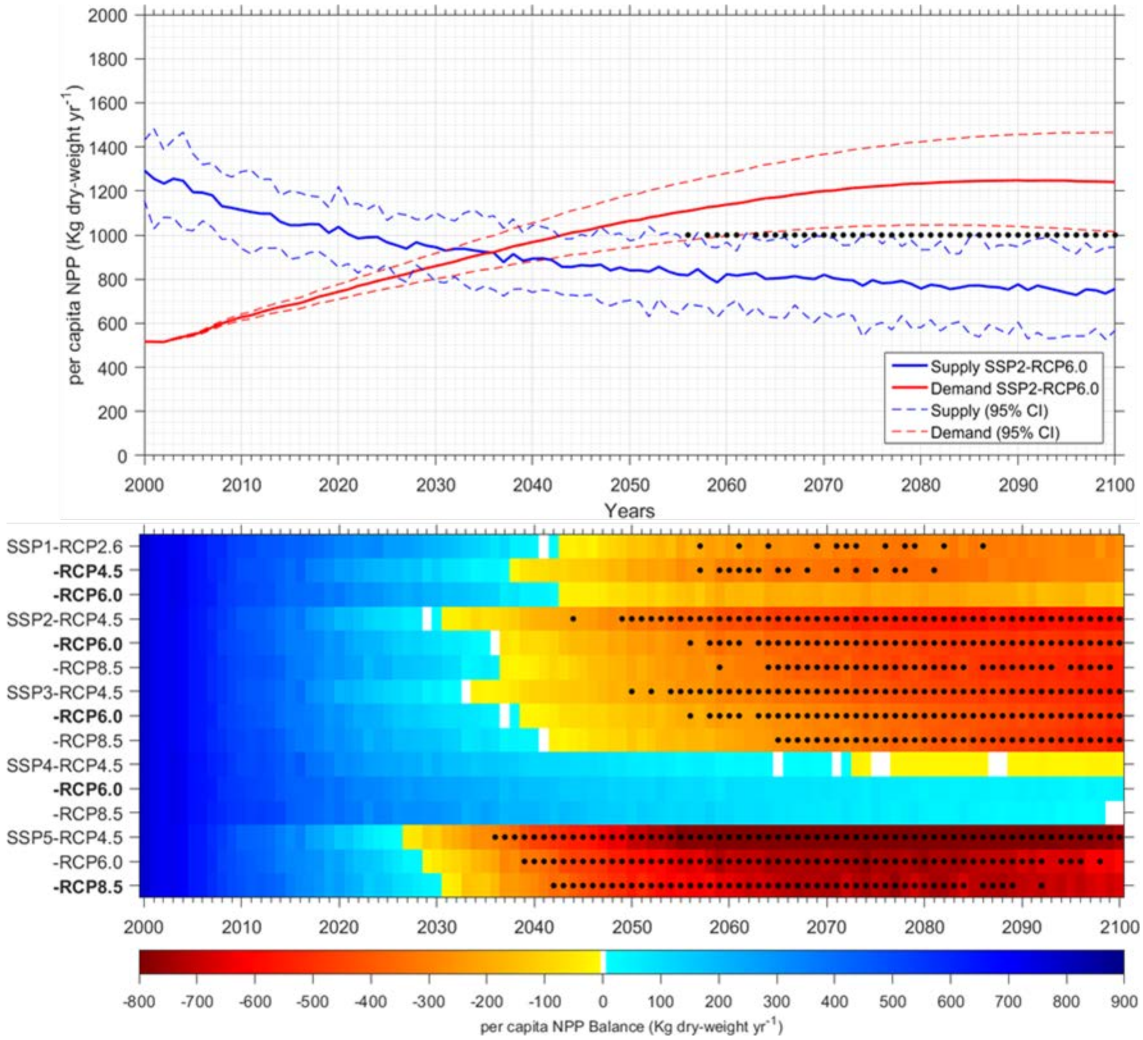

Fig. B7 Per capita NPP supply, demand and balance for the greater Sahel (2000-2100) without CO_2 fertilization. **B7a)** shows NPP supply (red) and demand (blue). The solid curves illustrate the mean of the SSP2-RCP6.0 combination. The dashed blue curves show supply uncertainty (95% confidence interval around the mean) based on the five GCMs NPP results. The dashed red curves show demand uncertainty (95% confidence interval around the mean) based on the uncertainty related to the interpretation and quantification of SSP2. **B7b)** shows the different magnitudes of the NPP balance and the varying onsets of shortage across all SSP-RCP combinations. Black dots illustrate years with a shortage outside of the 95% confidence intervals. Combinations are grouped according to the socio-economic scenarios (y-axis). The RCPs are ordered from low to high radiative forcing in each SSP group. The temporal trajectory is shown along the x-axis and the colouring indicates the sign of the annual NPP balance. Blues show a surplus of the NPP supply while yellow to red represent small to very large the gaps between supply and demand). SSP-RCP combinations in bold indicate the most likely SSP-RCP pairs based on Table 1.

RC3: 4. Page 5, line 4: When the fractional agricultural landcover estimates from Hurtt et al (2011) were applied, was it assumed that natural and agricultural NPP were similar? If so, this assumption should be revisited after considering differences between agricultural vs. natural NPP for the region. For instance, the authors could compare census based estimates of crop productivity with their estimates as a reality check. Smith et al. 2014 (see reference below), found that agricultural productivity for the region is significantly lower than natural productivity. If this potential reality is not considered, then the scenarios in this manuscript may be overly optimistic.

Authors' Response: Yes, it is true that we considered the NPP to be equal for all land covers. However, by using a relatively low (0.235) harvest index, we have implicitly accounted for at least some of that lower productivity.

In several sections, we have now pointed out that that our estimates of NPP are optimistic (eg. p. 17, lines 29-31):

"All of this suggests that the NPP increases found in our current analysis are likely optimistic, due the potential overestimation of the CO_2 fertilization effect, as well as the fact that BME is based on potential natural vegetation. "

Appendix A, p. 31 lines 2-6:

"The implication of this experiment is that there is a demonstrable reduction in NPP when land management is taken into consideration, but the effect is relatively minor. Lindeskog et al. (2013) show that LPJ-GUESS managed land (C-version) overestimated actual yield derived from FAO country-level crop statistics and Smith et al. (2014b) also report that natural systems are more productive than agricultural systems in sub-Saharan Africa. We conclude with that possibility that our results are in the upper range for NPP found in the Sahel."

Appendix A, p. 32, lines 7-9:

"We therefore conclude that BME and LPJ-GUESS replicate ground observations of NPP at similar orders of magnitude at the biome level, but may be overestimated due to the fact that natural systems are usually more productive than agricultural ones."

RC3: 5. I would recommend revisiting all crop allocation parameters based on those reported by Monfreda et al. (2008). Given the high variability in crop specific harvest fractions, it seems it may be necessary to parameterize the model for each individual crop grown in the region.

Authors' Response: It is true that the representation of crop allometry in the current setup is simplistic and cannot likely capture all the variability present in agricultural landscapes in the region. But the approach taken here, by having one root-to-shoot ratio and harvest index for all crops in the region is consistent with the underlying theme of the study, e.g. have a simplistic modelling framework to be able to explore supply-demand outcomes with a minimum of input data. Furthermore, as we do not know how these cropping systems would develop in the future across the scenarios, we think a simple approach is the safest bet.

RC3: 6. Page 12 line 24-26: This statement is not representative of the literature (see below references). I would suggest more nuanced discussion of the potential limitations of the supply approach used in this analysis. For instances, how much did CO2 fertilization drive increases? How uncertain are the precipitation estimates? Were nutrient constraints considered and if so what are the management implications? If not, how might nutrient constraints limit NPP? How will increases in atmospheric water demand (Vapor pressure deficit) affect yields and productivity? Could increased drought and desertification also represent a potential scenario had the CO2 sensitivity been adjusted? The way that this section is currently written is a gross over extension of the simplified NPP modeling that the paper is based on.

<u>Authors' Response</u>: Thank-you very much for directing us to the salient literature. In response to this, we have removed these statements from Section 4.4 (Additional Perspectives) and treat these issues in an expanded Section 4.6 (Uncertainties). Please see p. 17, lines 13-31:

"Additional uncertainty exists with respect to the total magnitude and trends of simulated NPP supply, given the lack of ground truth for the region, and that differences in NPP trends between other models is very large (e.g. Friend et al., 2014; Körner et al., 2006; Pugh et al., 2016; Rosenzweig et al., 2014). Indeed, recent observational evidence suggests that the effect of CO_2 fertilization on plant growth may be constrained by counteracting feedbacks associated with increasing atmospheric moisture demand and nutrient availability (e.g. Smith et al., 2016; Wieder et al. 2015). For example, NPP is reduced under warmer and dryer conditions due to moisture stress, particularly in temperate and arid ecosystems. Future trends NPP trends in the Sahel could therefore be strongly determined by changes in the frequencies of wet years versus dry years, with the dry years counteracting the CO_2 fertilization effect. Furthermore, nutrient supply rates may not be able to keep up with extra demand associated with CO_2 fertilization, and leading to a depletion of soil nutrients, as current evidence suggests. This could also curtail the CO_2 fertilization effect, particularly in the more southerly parts of our study area, where nutrients tend to become a limiting factor. We performed a simple experiment negating the CO_2 fertilization effect in order to gauge its impact on supply-demand balance on all scenarios. For the SSP2-RCP6.0, per capita demand has an equal chance of exceeding per capita supply in 2036 for the SSP2-6.0 scenario as opposed to 2043 if CO_2 fertilization in included (Fig. B7), with a very high likelihood of continuous supply shortfall beginning in 2056, as opposed to 2073 with CO_2 fertilization. The effect on all other scenarios is an earlier shift to the onset of supply shortfalls, by about 10 years, compared to Fig. 3b (see Fig. B7). Supply shortfalls with high likelihood of occurrence (black dots showing non-overlapping 95% confidence intervals) are similarly shifted, and occur with greater consistency and frequency. All of this suggests that the NPP increases found in our current analysis are likely optimistic, due the potential overestimation of the CO_2 fertilization effect, as well as the fact that BME is based on potential natural vegetation."

<u>RC3:</u> Minor Comments: 1. Page 3, Line 17: "Three different aggregation levels are considered, including Sahel, the country, and the local". Please define what is meant by local level. Pixel level? What resolution? 2. Page 12 line 12: missing end of parentheses.

<u>Authors' Response:</u> We clarify this on p. 3, lines 19-20 of our marked up manuscript:

"Three different aggregation levels are considered, including Sahel, the country, and the local (cell level with a spatial resolution of 0.5^{o} x 0.5^{o})."

We have also fixed the typos.

<u>References in our responses</u>

Brandt, M., Mbow, C., Diouf, A. A., Verger, A., Samimi, C., and Fensholt, R.: Ground- and satellite-based evidence of the biophysical mechanisms behind the greening Sahel, Global Change Biology, 21, 1610-1620, 2015.

Eklundh, L. and Olsson, L.: Vegetation index trends for the African Sahel 1982–1999, Geophysical Research Letters, 30, 8, 1430, 2003.

Herrmann, S. M., Sall, I., and Sy, O.: People and pixels in the Sahel: a study linking coarse-resolution remote sensing observations to land users' perceptions of their changing environment in Senegal, Ecology and Society, 19, 2014.

Hickler, T., Eklundh, L., Seaquist, J. W., Smith, B., Ardo, J., Olsson, L., Sykes, M. T., and Sjostrom, M.: Precipitation controls Sahel greening trend, Geophysical Research Letters, 32, L21415, 2005.

Obermeier, W.A., Lehnert, L.W., Kammann, C.I., Müller, C., Grünhage, L., Luterbacher, J., Erbs, M., Moser, G., Seibert, R., Yuan, N. & Bendix, J. (2016). Reduced CO2 fertilization effect in temperate C3 grasslands under more extreme weather conditions. Nat. Clim. Chang., 7, 137–142.

Ray, D.K., Mueller, N.D., West, P.C. & Foley, J.A. (2013). Yield Trends Are Insufficient to Double Global Crop Production by 2050. PLoS One, 8, e66428.

Seaquist, J. W., Hickler, T., Eklundh, L., Ardo, J., and Heumann, B. W.: Disentangling the effects of climate and people on Sahel vegetation dynamics, Biogeosciences, 6, 469-477, 2009.

Smith, W.K., Reed, S.C., Cleveland, C.C., Ballantyne, A.P., Anderegg, W.R.L., Wieder, W.R., Liu, Y.Y. & Running, S.W. (2016). Large divergence of satellite and Earth system model estimates of global terrestrial CO2 fertilization. Nat. Clim. Chang., 6, 306–310

Wieder, W.R., Cleveland, C.C., Smith, W.K. & Todd-Brown, K. (2015). Future productivity and carbon storage limited by terrestrial nutrient availability. Nat. Geosci., 1–5.

Future supply and demand of net primary production in the Sahel

Florian Sallaba[1], Stefan Olin[1], Kerstin Engström[1], Abdulhakim M. Abdi[1], Niklas Boke-Olén[1], Veiko Lehsten[1], Jonas Ardö[1], Jonathan W. Seaquist[1]

[1]Department of Physical Geography and Ecosystem Science, Lund University, Lund, 22362, Sweden

Correspondence to: J.W. Seaquist~~F. Sallaba~~ (jonathan.seaquist~~florian.sallaba~~@nateko.lu.se~~gmail.com~~)

Abstract

In the 21st century, climate change in combination with increasing demand, mainly from population growth, will exert greater pressure on the ecosystems of the Sahel to supply food and feed resources. The balance between supply and demand, defined as the ~~(~~annual biomass required for human consumption,~~)~~ serves as a key metric for quantifying basic resource shortfalls over broad regions.

Here we apply an exploratory modelling framework to analyze the variations in the timing and geography of different NPP (net primary production) supply-demand scenarios,~~ (~~with distinct assumptions determining supply and demand,~~)~~ for the 21st century Sahel. We achieve this by coupling a simple NPP supply model,~~ (~~forced with projections from four representative concentration pathways,~~)~~, with a global, reduced-complexity demand model ~~(~~driven by socio-economic data and assumptions derived from five shared socio-economic pathways~~)~~.

For the scenario that deviates least from current socio-economic and climate trends, we find that per capita NPP begins to outstrip~~s its~~ supply in the 204~~7~~0s, while by 2050, half the countries in the Sahel experience NPP shortfalls. We also find that despite variations in the timing of the onset of NPP shortfalls, demand cannot consistently be met across the majority of scenarios. Moreover, large between-country variations are shown across the scenarios where by the year 2050, some countries consistently experience shortage or~~, others~~ surplus, while~~ yet~~ others shift from surplus to shortage. At the local level (i.e. grid cell) hotspots of total NPP shortfall consistently occur in the same locations across all scenarios, but vary in size and magnitude. These hotspots are linked to population density and high demand. For all scenarios, total simulated NPP supply doubles by 2050 but is outpaced by increasing demand due to a combination of population growth and adoption of ~~a~~ diets rich in animal products. Finally, variations in the timing of onset and end of supply shortfalls stem from the assumptions that underpin the shared socio-economic pathways rather than the representative concentration pathways.

Our results suggest that the UN sustainable development goals for eradicating hunger are at high risk for failure. This emphasizes the importance of policy interventions such as the implementation of sustainable and healthy diets, family planning, reducing yield gaps, and encouraging transfer of resources to impoverished areas via trade relations.

1 Introduction

The global demand for food is projected to increase by up to double by 2050 (compared to the year 2005) due to rapid population growth and changes in dietary preferences (Hertel, 2015; Tilman et al., 2011). As a consequence, global agricultural supply needs to increase substantially in order to satisfy this demand (Ray et al., 2013). Agricultural practices can be intensified with technological investments (i.e. mechanization, irrigation and fertilization) to increase yields but these are costly and often lead to environmental degradation (Foley et al., 2005). As opposed to agricultural intensification, the amount of agricultural land can be expanded in order to meet future demand. This results in changing land use and land cover (LULCC), for example from natural vegetation to cropland. Approximately 35% of the total ice-free land surface is used for agriculture (Ramankutty et al., 2008). Agricultural land (grassland and cropland) expanded by 3% globally between 1985 and 2005 and is expected to further increase, especially in the tropics (Foley et al., 2011). The production of the most common crops (e.g. cereals, oil crops, and vegetables) increased by nearly 80% over the past four decades (FAOSTAT, 2015; Foley et al., 2011), mostly due to increases in yield (Kastner et al., 2012) and to a smaller extent by LULCC (Foley et al., 2011). Despite the large increase in agricultural production, global food security is~~cannot be~~ not ensured (due to access and distribution challenges~~ e.g.~~ (e.g. Brown, 2016; Pinstrup-Andersen, 2009)), as there are presently 792 million people chronically undernourished across the planet, a third of which are in Africa (FAOSTAT, 2015).

The Sahel region of sub-Saharan Africa is one of the most technologically underdeveloped regions in the world, where yield gaps are explained by low and variable rainfall combined with low soil fertility (Yengoh and Ardö, 2014). The population by-and-large relies on rain-fed farming practices including subsistence agriculture, cash crops, pastoralism and agro-pastoralism. The population has a high reliance on their own land, where 95% of food produce is for domestic consumption, (Abdi et al., 2014; Running, 2014). The vulnerability of the population to variations in agricultural supply due to frequent drought undermines wealth accumulation, which would otherwise provide a buffer in drought years (Barbier et al., 2009). Additionally, poor transportation infrastructure inhibit the trade and distribution of food resources (Olsson, 1993). Between the late-1960s to the early 1990s, the Sahel experienced a protracted dry period in which severe droughts caused fluctuating levels of food supply leading, in some cases, to severe humanitarian crises. The devastating droughts in 1972/73 and 1983/84 induced complete crop failure leading to the largest famines in the recent history of the Sahel (Ibrahim, 1988). The latest major drought to hit the region was in 2002. As of 2013, over 11 million people across the region were considered to be food insecure (United Nations, 2013).

NPP estimates from the MODIS (Moderate Resolution Imaging Spectroradiometer (MODIS) suggest that t~~T~~he Sahel region experienced a near-constant rate of crop productivity between 2000 and 2010, while population grew at a rate of 3.1% over the same period (Abdi et al., 2014). Abdi et al. (2014) also showed that 19% of the NPP supply in the Sahel was able to satisfy demand for the year 2000 but this increased to 41% in 2010 due to a 31% increase in the population. Since the NPP demand increased at an annual rate of 2.2% over the period while the supply was near constant, the near doubling in NPP demand implies, in relative terms, that there was less NPP supply to service the increase in population. This raises the question of whether demand could consistently outstrip supply in the future and underscores the importance for developing tools for analyzing potential future supply and demand that could be of use for policy makers. Indeed, the balance between supply and demand (annual biomass required for human consumption) serves as a key metric for quantifying basic resource shortfalls over broad regions (Abdi et al., 2014; Running, 2014).

Developing such tools requires coupling of specific models that address different sectors, such as a model for supply and a model for demand that can be run across multiple future climate, socio-economic and CO_2 concentration scenarios. However, the supply-demand system in the Sahel is complex and the future cannot be precisely evaluated. This is because there are many uncertainties associated with the assumptions that underpin the natural and socioeconomic drivers that lead to particular supply-demand balances. As such, an exploratory modelling approach is required, where an emphasis is placed on a structured analysis across a range of outcomes. This approach capitalizes on future indeterminacy for developing adaptive policy insights (e.g. Kwakkel and Pruyt (2013)). As the goal of exploratory frameworks is not prediction, they often employ parsimonious or simplified versions of more complex models (often referred to as meta-models in the latter case) that run across a range of scenarios (e.g. Harrison et al. (2016)). Another benefit of using such simplified models lies in the ease to which they can be coupled to other sectoral models (e.g. Kebede et al. (2015)).

In this study we couple a simple supply model (Biome-based Meta-model Ensemble - BME) with a demand model (Parsimonious Land Use Model - PLUM) to compute NPP supply-demand balance for a set of 21st century Sahel scenarios covering different climate, [CO_2] and socio-economic trajectories in an exploratory modelling framework. Our overall aim is to quantify variations in the timing and geography of NPP supply and demand in the Sahel in association with these trajectories. Three different aggregation levels are considered, including Sahel, the national~~country~~, and ~~the~~ local (cell level with a spatial resolution of 0.5^{o} x 0.5^{o}). Thereafter we discuss those natural and socio-economic factors that lead to changes in the balance between supply and demand throughout the 21^{st} century, as accounted for by the coupled models. The Sahel-level analysis focuses on the total impact of the different future climatic and socio-economic pathways and its timing on supply and demand and asks the fundamental question of whether the Sahel as a whole, could potentially be self-sufficient. By contrast, the country-level analysis focusses on a level relevant for policy, international relations, and aid agencies. Finally, the local-level analysis identifies potential hotspots of supply shortage occurring at sub-national levels. We restrict our analyses to localized supply-demand only in order to flag those areas that would require the lateral transfer of supply from elsewhere via trade or aid. This would provide a first order boundary condition for further studies or for use by policy makers. As a consequence, specifically accounting for the myriad of political, social and cultural factors that affect lateral transfer, access to, and distribution of supply is beyond the scope of this study.

2 Materials and Methods

2.1 Modelling framework

In the current study, we couple two sectoral models to assess the future supply and demand trajectories for the Sahel region. We divided the modelling framework into three parts (Fig. 1), where the first part describes NPP supply; the second encapsulates NPP demand, while the third combines the two.

2.1.1 NPP supply

Supply is dependent on vegetation growth, and can be quantified as net primary production (NPP), which is defined as the difference in gross photosynthetic assimilation of carbon and carbon loss due to autotrophic respiration, per area per unit time (Foley, 1994). NPP is an established measure of ecosystem productivity indicating how much energy is available for all life on Earth. We estimated future plant productivity of the Sahel with the BME (Biome-based NPP meta-models). The BME is a rapid biome-based NPP meta-model that emulates the performance of the more complex model LPJ-GUESS (Lund-Potsdam-Jena General Ecosystem Simulator, Smith et al., 2014), but in a simplified, and more time-efficient manner. LPJ-GUESS is a state-of-the-art dynamic global potential natural vegetation model that incorporates carbon and nitrogen interactions (Smith et al., 2014). LPJ-GUESS (carbon cycling only) ~~that~~ shows good skill in predicting NPP at regional and global scales (Hickler et al., 2008; Tang et al., 2010). We developed the BME using LPJ-GUESS NPP simulations driven by several climate and CO_2 concentration perturbations (see Table A1). The biome definition in BME is taken from the Major Biome classification (MBC) (Reich and Eswaran, 2002), which stratifies the terrestrial biosphere into 13 biomes based on soil moisture and temperature regimes. We chose this biome definition because it represents a trade-off between global biosphere classifications that either have too many biomes or too few, compared to other stratifications (Kottek et al., 2006; Metzger et al., 2013; Olson et al., 2001). The trade-off also allowed for a reasonably accurate reproduction of vegetation dynamics, compared with LPJ-GUESS. For our study, we parameterized BME for the four major biomes of the Sahel: a) desert tropical, b) desert temperate, c) tropical semi-arid and d) tropical humid (~~see~~ Fig. 2). A recent study by Gonzalez et al. (2010) shows that climate change has the potential to shift biomes by the end 21st century. For simplicity, we therefore assumed static biomes that persist during climatic changes encountered during the modelling period (year 2000-2100). A detailed description of the BME implementation is provided in Appendix A.1.

We also evaluated LPJ-GUESS (e.g. Olin et al., 2015) and BME performance (magnitudes, trends and interannual variability) by first implementing a global biome-by-biome-level validation, where results from the Sahel are highlighted. We then ~~by~~ compar~~eing~~e BME estimates with LPJ-GUESS NPP simulations (including LPJ-GUESS managed land, in order to gauge the effect of agriculture on NPP, keeping in mind that BME is based on a model of potential natural vegetation) that were excluded from BME parameterization. Finally, we compare BME estimates against MODIS-derived NPP (2000-2006) (Running, 2004), as well as country-level censuses of crop yield trends from Rey et al. (2013). We also include a comparison with LPJ-GUESS C (carbon cycling only), a version that has been previously validated at the global scale (e.g. Hickler et al., 2008).~~.~~The evaluation covered the entire Sahel region and was run from 1970 to 2006 (see Appendix A.2).

We forced BME with climate data (spatial resolution 0.5 x 0.5 degrees) from five GCMs (General Circulation Models, including HADLEY, GFDL, IPSL, MIROC and NorESM), and [CO_2] based on four RCPs (Representative Concentration Pathways, including 2.6, 4.5, 6.0 and 8.5) to estimate annual total NPP in kg dry-weight m^{-2} yr^{-1}~~.~~ (DW, dry-weight). We used climate data derived from runs across the 4 RCPs for each of the 5 models. We then calculated annual means of the five GCM NPP yields, resulting in four NPP time-series (covering each RCP) each spanning from 2000 to 2100. By averaging the GCM based NPP estimates we decreased the data amount while reducing spatial and temporal variability stemming from individual GCMs. In the next step, we summed ~~translated~~ the annual NPP estimates over the grid cell area~~to the total area of each grid cell~~ in m^2 using the latitude of each grid cell centre. Additionally, we used annual land use projections from Hurtt et al. (2011) to calculate the total area of pasture and cropland in each grid cell. This allowed us to estimate annual total NPP_{supply} (kg $cell^{-1}$ yr^{-1}) for pasture and cropland separately. We estimated crop- and grassland scaling factors for each country by dividing the PLUM-predicted land-use area with the total land-use area provided by the Hurtt et al. (2011) dataset (Table C1). We then applied the scaling factors to the Hurtt et al. (2011) land-use data and multiplied the resulting crop- and grassland areas with the NPP estimates to obtain annual NPP_{cereal_supply} and $NPP_{grazing\_supply}$ (kg DW $cell^{-1}$ yr^{-1}). We addressed potential developments in the wider use of existing agricultural technology that result in higher plant productivity with a technology improvement factor, where this factor is used to decrease~~close~~ the yield gap. The technology improvement factor is the aggregate result of parameterizing three technology related parameters (trends in technology, change in yield with GDP per capita, as well as how agricultural management practices are transferred both within and between countries) that are consistent with the scenario storyline of each SSP. Parameter ranges have been empirically determined based on analysis of data between the years 1995 and 2005. Yield gaps are not necessarily closed, but are decreased (see Engström eta al., 2016 for more detail).~~.~~We then used country-wide yield gap fractions provided by PLUM spanning from 2000 to 2100 (Engström et al., 2016b; Licker et al., 2010). The yield gap fractions are country-specific and dependent on technological development in each scenario, and are thus consistent with the SSP storylines (Engström et al., 2016b). For example, a scenario with strong technological change has large decreasing yield gaps while a scenario with slow technological change has slowly, or stagnating (or even increasing) yield gaps. Here, we calculated yearly technology improvement factors by dividing the inverse yield gap fraction (i.e. 1-yield gap fraction) of the respective year with the inverse yield gap of the starting year (i.e. 2000). Thereafter, we applied the annual technology improvement factors to the NPP_{cereal_supply} (kg $cell^{-1}$ yr^{-1}) of the respective year and country.

Finally, we used root-to-shoot ratio (R:S) to remove below ground biomass NPP of croplands (we exclude tubers and groundnuts) and pasture from our NPP estimates, since this component cannot generally be appropriated by humans or by the majority of animals. For croplands, we assumed common agricultural practice across the Sahel region and therefore applied a region-wide R:S=0.1 (Jackson et al., 1996). This a reasonable R:S since crops produce low root biomass compared to the above ground biomass. Moreover, we extracted the consumable parts of the above ground NPP by using a region-wide crop harvest index of 0.235, which is the average of reported harvest indices for maize, millet, sorghum and wheat (Haberl et al., 2007; Wirsenius, 2000). In contrast to crops, grasslands produce more below ground NPP in relation to above ground NPP (R:S >1) (Jackson et al., 1996). Therefore~~Furthermore~~ we considered the climatic limitations of individual biomes by extracting above ground NPP (for grasslands): a) desert tropical R:S=2.8; b) desert temperate R:S=1.1; c) tropical semi-arid R:S=2.8; and d) tropical humid R:S=1.6 (IPCC, 2006; Mokany et al., 2006).

2.1.2 NPP demand

For the calculation of NPP demand only, the parts of NPP that are available for direct consumption (excluding e.g. NPP preserved in e.g. national parks) are here considered. Future NPP demand can be projected applying a set of consistent assumptions for future societal and economic developments, described in socio-economic scenarios. We simulated future NPP demand for each country of the greater Sahel with PLUM, which is based on a conceptual model of socio-economic processes that determine global agricultural land-use change (Engström et al., 2016c). These processes include population and economic development, the consumption of cereal, milk and meat dependent on economic development and lifestyle/diet choice~~s~~ and the development of cereal yields dependent on technological change. PLUM is driven by country-level population and gross domestic product (GDP) data, and a range of parameters that characterize the development of the socio-economic processes mentioned above. PLUM was evaluated against historic (1991-2010) consumption and land-use data at the country scale and was shown to reproduce land-use change and consumption patterns at the global aggregated scale (Engström et al., 2016c). Due to the model’s relative simplicity and the limited number of scenario parameters it is suited for scenario studies and was used to quantify uncertainty ranges for global cropland scenarios based on the Shared Socio-economic Pathways (SSPs) (Engström et al., 2016b). Mean cropland change for the five scenarios resulted in 963-2280 Mha cropland by 2100 compared to 1503 Mha cropland in 2000. The parameter-settings resulting in the uncertainty ranges for each scenario are described in Engström et al. (2016b) and the reported mean values were used in the current study. For more details see Engström et al. (2016b). In the version of PLUM applied in our study, we introduced an additional parameter which characterizes the increasing intensification of the livestock production systems in scenarios with strong increase in milk and meat consumption (Engström et al., 2016a). This process was previously not included in PLUM, but it was later identified to lead to an underestimation of land requirements for scenarios with strong increases in milk and meat consumption (Engström et al., 2016b).

We forced PLUM with the five socio-economic scenarios from 2000-2100 (see box outlined in red in Part 2 of Fig. 1~~2~~) taken from the SSPs, but it is important to remember that is it also coupled to the BME (see dashed arrow in Fig. 1~~2~~) through annual country-level total NPP estimates for cropland. Aggregation of BME NPP estimates was implemented as described in Engström et al. (2016b), except that cropland fractions in 2000 from MIRCA dataset were replaced with Hurtt et al. (2011) cropland fractions from 2000-2100.

Finally, we defined the demand of NPP as compounds that are necessary for human livelihood in the Sahel region, following the NPP_{demand} approach of Abdi et al. (2014). However, our approach differs from Abdi et al. (2014) by distinguishing between the demand of cereal- and pasture products~~ (see red box Fig. 2)~~. PLUM outputs were combined to determine NPP_{cereal_demand} as given in Eq. (1) and $NPP_{grazing\_demand}$ (see Eq. A9~~8~~ in the Appendix A.3).

$$NPP_{cereal\_demand} = NPP_{food} + NPP_{feed} \qquad (1)$$

where NPP_{cereal_demand} is the total amount of annual NPP needed for human appropriation via cropland; NPP_{food} (ton country^{-1}) is the NPP needed for consumed cereals; and NPP_{feed} (ton country^{-1}) is the amount of cereal based fodder to support the region's livestock population. $NPP_{grazing\_demand}$ is the NPP needed for sustaining the livestock by grazing (ton country^{-1}). Furthermore, we converted NPP_{cereal_demand} and $NPP_{grazing\_demand}$ to per capita demand (kg person^{-1}) using country population projections of the corresponding year in the SSP. A detailed methodology of the PLUM output combinations to satisfy Eq. (1) is given in Appendix A.

In the following step, we disaggregated the annual per capita NPP_{cereal_demand} and $NPP_{grazing\_demand}$ from country to 0.5 degree grid cell resolution in order to facilitate the spatial analysis of NPP supply and demand at the grid cell level. For that we multiplied annual per capita demands with gridded population data (0.5 x 0.5 degree resolution) of the corresponding years. The disaggregated annual NPP_{cereal_demand} and $NPP_{grazing\_demand}$ (kg cell^{-1} yr^{-1}) are therefore weighted by population density (i.e. population centers achieve high demand).

2.1.3 NPP Supply-Demand Balance

In the next step, we combined the NPP_{supply} (i.e. RCP based) with the NPP_{demand} (i.e. SSP driven) using a~~the~~ SSP-RCP likelihood matrix (Engström et al. (2016b), see Table 1~~4 therein~~) in order to facilitate the analysis of the NPP supply~~demand~~ and demand~~supply~~ balance.~~ The SSPs and RCPs were matched in a ~~To create the likelihood matrix, a~~likelihood matrix where~~ ~~a~~ qualitative probability was~~is~~ assigned to describe the likelihood of a SSP resulting in a RCP (Engström et al., 2016b). The qualitative likelihood estimates are based on experts' judgements, ranging from "very low" to "very high" and were translated to quantitative probabilities (Engström et al., 2016b). For the analysis, we considered SPP-RCP combinations with likelihoods above > 0.05 (> very low likelihood).

Next, we computed cereal-based (i.e. $NPP_{cereal\_balance}$=NPP_{cereal_supply}-NPP_{cereal_demand}) and grazing (i.e. $NPP_{grazing\_balance}$=$NPP_{grazing\_supply}$-$NPP_{grazing\_demand}$) balances. In order to combine the balances meaningfully we defined four rules as outlined in Table 2~~1~~. Rule no. 1 states that a deficit of cereal products ($NPP_{cereal\_balance}$<0) cannot be balanced with surplus of plant growth on grassland ($NPP_{grazing\_balance}$ ≥0) because grassland products are inappropriate for direct human consumption, resulting in all grazing surplus being disregarded. Rule no. 2 regulates the treatment of cereal and grazing surplus occurring simultaneously, where pasture NPP surplus ($NPP_{grazing\_balance}$ ≥0) is ignored but the cereal-based NPP surplus ($NPP_{cereal\_balance}$≥0) is retained. This surplus is of interest because it can potentially balance NPP shortages in adjacent grid cells as well as on the country level. Rule no. 3 permits the combination of cereal ($NPP_{cereal\_balance}$<0) and grazing ($NPP_{grazing\_balance}$<0) deficits in order to quantify the total NPP shortage of the grid cell. The last rule allows supplementation of grazing-based shortages ($NPP_{grazing\_balance}$<0) with cereal surplus ($NPP_{cereal\_balance}$≥0).

2.2 Scenarios

In the current study, we combine four Representative Concentration Pathways (RCPs) with five SSPs which are the latest future climate, [CO_2] and socio-economic projections (O'Neill et al., 2014; van Vuuren et al., 2011; van Vuuren et al., 2013) from the Intergovernmental Panel on Climate Change (IPCC) Fifth Assessment Report (AR5) framework. Each RCP represents a different cumulative measure of future human greenhouse gases (GHG) emissions and is defined by their radiative forcing targets for the year 2100, and which range from 2.6 to 8.5 W m^{-2} (van Vuuren et al., 2011). For each RCP, we obtained climate data from the Inter-Sectoral Impact Model Intercomparison project (ISI-MIP), containing climate simulations of five General Circulation Models (GCMs) for each RCP (Hempel et al., 2013). (GCMs : (Collins et al., 2013; Dufresne et al., 2013; Dunne et al., 2013; Iversen et al., 2013; Watanabe et al., 2011)). The climate data (0.5 x 0.5 degrees resolution) was bias corrected by the ISI-MIP approach that preserves trends in absolute changes in monthly temperature, and relative changes in monthly precipitation amounts (Hempel et al., 2013). For future socio-economic developments, the SSPs consider different narratives of future population levels, urbanization scenarios and economic development (O'Neill et al., 2017~~*in press*~~; van Vuuren et al., 2013) as summarized in Table 3 ~~2~~.

~~The SSPs and RCPs were matched in a likelihood matrix where a qualitative probability is assigned to describe the likelihood of a SSP resulting in a RCP (Engström et al., 2016b). The qualitative likelihood estimates are based on experts' judgements, ranging from "very low" to "very high" and were translated to quantitative probabilities (Engström et al., 2016b).~~ No mitigation strategies are assumed and resulting scenarios are thus reference scenarios. Furthermore, ~~we used~~ for each of the considered SSP and RCP combinations, we used a distributed population projection dataset at 1 km^2 from Boke-Olén et al. (~~*in review at Nature Scientific Data, submitted july*~~ *2017*~~*6*~~). The ~~used~~ population dataset was created by Boke-Olén et al. (~~*in review at Nature Scientific Data, submitted july*~~ *2017*~~*6*~~) to match both the RCP specific urban fractions from Hurtt et al. (2011) and SSP country urban and rural population counts. Hence, one population dataset exists for each SSP and RCP combination used in this study. We resampled (summed) the population dataset to the same spatial resolution as the climate data (0.5 x 0.5 degrees) and grid cells with population count below 3000 people per grid cell (~ one person per 1km^2) were excluded following Abdi et al. (2014).

Additionally, variation in NPP supply estimates originating from the five GCMs was retained for an estimate of supply uncertainty to be included in the analysis. Uncertainty estimates for NPP demand associated with each SSP were derived from the results of Engström et al. (2016b) and applied here. In their study, conditional probability ranges were defined for twelve PLUM input parameters (reflecting uncertainties in SSP interpretation and quantification) in order to estimate uncertainty in a range of PLUM outputs.

2.3 Study area

The study area covers the African continent between roughly 5° and 25° northern latitude and stretches from the Red Sea to the Atlantic Ocean, hereafter referred to as the greater Sahel. Following Abdi et al. (2014), the area also includes the neighbouring countries of the Sahel belt (encompassing 21 countries see Table 4~~3~~). Note that this study uses the African country definition for the year 2000 where South Sudan was a part of Sudan. The actual Sahel belt is described by an annual rainfall range between 100mm and 600mm (hatched area in Fig. 2). The Sahel is an arid and semi-arid region that separates the Sahara desert from the humid and tropical regions to the south. The northern parts of the region border the Sahara Desert with low mean annual precipitation (<100mm) while the southern parts of the Sahel belt border the savannas of the tropical semi-arid biome, permitting increased plant productivity due to higher mean annual rainfall (~600mm). The southern parts of the study area cover the tropical semi-arid and tropical humid biomes with much higher mean annual precipitation amounts ranging from 600 to 1000 mm enabling larger vegetation growth. The study area is one of the poorest as well as most technologically underdeveloped regions on the African continent (Chidumayo and Gumbo, 2010).

3 Results

In the following the results are presented at Sahel, country and local (grid cell) level. Results for the different scenario combinations are reported, but emphasis is given to the SSP2-RCP6.0 scenario, as this scenario deviates least from current socio-economic and climate trends at the global level. Additionally, Fig. 3a also provides a basis for interpreting Fig. 3b.

3.1 Sahel

Per capita demand exceeds supply in the early 2040s for SSP2-RCP6.0 after which a very high likelihood for shortfalls begins in 2070 (see black dots in Fig. 3a showing non-overlapping 95% confidence limits). By 2050, per capita demand almost doubles while per capita supply drops by almost 30% for the same scenario. Across the scenarios, differences in the timing of the start of persistent supply shortfalls with high statistical certainty are observed (see black dots in Fig. 3b). Three of these high likelihood shortfalls begin at 2050 or before (SSP5 scenarios – see black dots in Fig. 3b) while an additional six display shortfalls with high certainty by the end of the 21st century (black dots in Fig. 3a, b). Out of these nine, two scenarios never achieve a sustained run of shortfalls (SSP2-RCP6.0, SPP2-RCP8.5). In total, there is better than an even chance for shortfalls before 2050 for 9 scenarios (exceptions are SSP1-RCP2.6, SSP1-RCP6.0, and all SSP4 scenarios.

Variations in the timing of onset and end of supply shortfalls are generally greater between the SSPs than between the RCPs (Fig. 3b). For SSP2 and SSP3 scenarios, onsets of high likelihood supply shortfall range from the early 2050s to the mid-2070s (even chance from late 2030s to early 2050s). The SSP5 family shows the largest deficits of high likelihood shortfalls beginning in the 2040s-2050s (even chance from the early 2030s), and after several decades of deepening begin to diminish in the 2080s. Shortfalls with high certainty never emerge for SSP1 (even chance from the early 2050s) while the SSP4 scenarios show sustained but diminishing surplus throughout.

~~Per capita demand exceeds supply in the 2070s for SSP2-RCP6.0 after which shortfalls occur discontinuously (Fig. 3a). By 2050, per capita demand almost doubles while per capita supply drops by almost 30% for the same scenario. Across the scenarios, differences in the timing of the start of persistent supply shortfalls are observed. Three of these show shortfalls at 2050 or before (SSP5 scenarios – see black dots in Fig. 3b) while an additional six display shortfalls by the end of the 21st century (black dots in Fig. 3a, b). Out of these nine, four scenarios never achieve a sustained run of shortfalls (SSP2-RCP6.0, SPP2-RCP8.5, SSP5-RCP6.0 and SSP5-RCP 8.5).~~

~~Variations in the timing of onset and end of supply shortfalls are generally greater between the SSPs than between the RCPs (Fig. 3b). For SSP2 and SSP3 scenarios, onsets of supply shortfall range from the early 2050s to the mid-2070s. The SSP5 family shows the largest deficits beginning in the 2040s-2050s, and after several decades of deepening begin to diminish in the 2080s. Shortfalls never emerge for the SSP1 and SSP4 scenario groups, with SSP4 scenarios showing diminishing surplus throughout.~~

3.2 Country-level

For scenario SSP2-RCP6.0, per capita NPP balances generally show a decrease for all countries. Eleven countries (out of twenty-two) experience per capita shortages by 2050, up from two countries (Djibouti and Mauritania) in 2000. Ethiopia shows the most extreme shortfall while Togo the greatest surplus. The largest change amongst all countries (is exemplified by Niger which starts with a surplus in 2000 but ends up with a deficit by 2050. Conversely, Djibouti shows a small decrease in deficit over the period (Table 4).

Large changes in per capita NPP balance are caused by contrasting development of NPP supply and demand, as analyzed in the following two paragraphs. Despite large total NPP increases between 2000 and 2050 (SSP2-RCP6.0), per capita NPP supply decreases for almost all countries, the largest decreases being for Niger and Sudan while an increase is noted for Liberia.

Since all countries double or even triple their population counts from 2000 to 2050 (Table 4~~3~~), large increases in demand occur over the 50 year period, while even per capita demand increases. By 2050, the largest increases in demand per capita are projected for Liberia, Ethiopia and Ghana by 2050 respectively (Table 4~~3~~).

Generally, the differences in NPP balances across scenarios are high, with the largest variations attributed to the SSPs as opposed to the RCPs (Table C2), with two~~three~~ countries (Sierra Leone and Liberia) showing considerable variation across the scenarios (coefficients of variation > 2.0).

3.3 Local level

For SSP2-RCP6.0, the localities experiencing negative NPP balance expand and become more connected between 2000 and 2050. By 2050, a semi continuous band of low magnitude NPP shortage emerges (generally > -0.2 Mt dry weight yr^{-1} per grid cell), stretching from the Atlantic Ocean to the Red Sea, between 15^o and 20^o N (Fig. 4b). In the east, this band extends down along the coast and wraps around the horn of Africa. A separate band of similar magnitude emerges toward the south, from just above 10^o N, and stretching toward the east-southeast into Cameroon. Additionally, four separate locations of large magnitude shortfalls (> 1.5 Mt dry weight yr^{-1} per grid cell) of varying extents emerge. The first hotspot (relatively small cluster of large magnitude shortfall) is located along the Nigerian coast, stretching from the metropolitan areas of Lagos to the densely populated area of the Niger delta (Fig. 4a, h1). The second hotspot is located in northern Nigeria, close to the city Kano (Fig. 4a, h2) while the third is located in the Ethiopian highlands of Eastern Africa (Fig. 4a, h3). Finally, the fourth covers the area of around Khartoum in the Sudan (Fig. 4a, h4). Elsewhere, very small pockets (e.g. 1 grid cell in size) of large magnitude NPP shortages (<-1.0 Mt DW yr^{-1} per grid cell) are distributed unevenly across the region.

Both supply and demand increase over most localities for the SSP2-6.0 scenario from 2000 to 2050 (Fig. 4 c-d). For supply, largest increases (up to, and exceeding 1 Mt dry weight yr^{-1} per grid cell) occur in those areas that already see large supply in 2000, including the southern parts of Ivory Coast and Ghana, and most of Nigeria and the southern part of Niger (Fig. 4c,d). Smaller increases occur throughout central Sudan and Ethiopia. Large magnitude increases (between 1 and > 2 Mt dry weight per year^{-1} per grid cell) in demand are seen for distinct geographic regions, the largest patches covering coastal Nigeria, northern Nigeria-southern Niger, north-central Sudan around Khartoum, and Ethiopia (Fig. 4f). By-and-large, these correspond to the hotspots of supply shortfall identified in Fig. 4b. Smaller areas, sometimes no larger than one grid cell, are seen scattered across Sudan, Chad, the west coast, and south Sudan.

The general geographical patterns of NPP shortage remain persistent across all scenarios, including the four hotspots identified for SSP2-RCP6.0. The largest magnitude shortages are indicated for SSP5-RCP8.5 (Fig. B1).

4 Discussion

4.1 Sahel-level

World-wide cereal production in 2010 amounted to 2400 Mt and current food aid shipments to countries in the Sahel are below 1 Mt yr^{-1} (FAOSTAT, 2016). At present about 260 million people are chronically undernourished in Africa (FAOSTAT, 2015) and this is despite the fact that we also estimate a per capita NPP surplus of 860 (±144) kg DW yr^{-1} (corresponding to 309 (±52) Mt DW yr^{-1}) in the Sahel for the year 2000. This implies that current challenges are associated with other determinants such as access to and distribution of resources (Brown, 2016; Olsson, 1993; Pinstrup-Andersen, 2009). These challenges are set to increase in the future, particularly for scenarios with high social and economic inequalities (SSP4). Furthermore, the majority of all other scenarios show that by mid-century, the NPP surplus will be much reduced compared to the year 2000. According to the sustainable development goals, hunger and all forms of malnutrition should be eradicated by the year 2030 (UN, 2016), but under the current trend given by the SSP2-RCP scenarios, there is a risk that 15-25% (160 to 270 million people) of the population would not be able to be supported with NPP supply (on the basis of assumed adoption of diets rich in animal products, consistent with the SSP2 storyline) and are therefore at high risk for malnutrition by 2050.

Presently, the Sahel has a high reliance on their own land by producing 90% of domestic food consumption resulting in very little import or export of crops (Abdi et al., 2014~~; Running, 2014~~). This implies that agricultural resources from global trade will need to increase considerably in order to reduce the future food shortages across the region. Participation in global markets and investments in infrastructure that enable trade of food commodities to ensure food security via trade will therefore be important (D'Odorico et al., 2014). However, it needs to be kept in mind that the simulated shortages partly occur due to steep increases in per capita consumption. For example, while reducing social inequities is clearly desirable (as embraced by the SSP5 RCP scenarios), from a sustainability perspective, it is questionable if this should mean that developing countries follow the development path of economically developed countries and adopt diets with very high consumption levels of animal products (O'Neill et al., 2017~~*in press*~~). The adoption of sustainable diets (i.e. reduced contribution of animal products to diets) has to be envisaged as a strategy consistent with efforts to reduce food demand to healthy and sustainable levels (Smith, 2013). This would be consistent with the SSP1 ('taking the green road' scenarios) where sustainable diets are adopted statistically significant shortages never develop (e.g. Fig. 3b).

4.2 Country-level

Beyond the import of agricultural products to the Sahel, inter-country trade of such resources will also need to become more important later in the 21st century. Trade relations between productive and high-demand countries should be encouraged (Ahmed et al., 2012). For instance, Cameroon, Ivory Coast, Chad and Togo produce NPP surplus for SSP2-RCP6.0 by 2050 which could be traded to neighbouring countries with NPP shortages (e.g. Nigeria). Across the scenarios, some countries showed continuous NPP shortfalls (e.g. Mauritania), while Ivory Coast and Guinea consistently produce NPP surplus (Table

C2). The large range of different climate conditions in the Sahel region implies that those countries within the tropical humid (and partly in tropical semi-arid) biome have larger potential NPP compared to countries in the desert temperate biome. We note that the closure of yield gaps by 2050 (for scenario SSP2-RCP6.0) would result in a change in mean per capita NPP balance from -107 kg DW yr-1 (see Table 3) to 9 kg DW yr^{-1}. Though the balance for many countries will still be negative, the shortfall magnitudes would be reduced. ~~Closing yield gaps is an important goal for all countries so strong efforts should be made to reduce these gaps~~. ~~As well as reducing yield gaps, d~~Decreased supply due to losses of food during harvest, transport and storage (i.e. household level) should be reduced through improvements of agricultural management, infrastructure and educational development (Godfray et al., 2010). For most countries however, the different socio-economic development pathways prescribed by the SSPs lead to high inter-scenario variability (having positive or negative balances depending on the scenario) and will determine if countries have the potential be a net exporter or importer of resources.

4.3 Local-level

At the local-level, robust NPP shortages across scenarios were found to be strongly linked to densely populated areas. For the example of SSP2-RCP6.0, by 2050, the number of grid cells with high population density (i.e. > 1 million population per 25 km x 25 km increased substantially compared to 2000 (see Fig. B4~~3~~)). For instance, > 1 million people per grid cell trigger NPP shortages in Ethiopia while > 2 million people per grid cell induce NPP shortfalls in Nigeria for SSP2-RCP6.0 by 2050. The NPP shortage hotspots in Nigeria and Ethiopia agree geographically with reported considerable NPP demand expansions in the 2000s (Abdi et al., 2014) indicating a combination of population growth and increased consumption as explanatory factors. Furthermore, the projected deepening and persistent shortages in urban areas underscore the hypothesis that the urban poor are especially at risk for food insecurity since they neither have the means to purchase food on the markets, nor the means to be self-sufficient due to limited land in densely populated areas (Lynch et al., 2001). Thus, connecting productive hinterlands with metropolitan areas will need to be achieved (Owuor, 2007).

That the locations of the hotspots and the overall patterning of NPP shortfalls remain consistent across all scenarios narrows the number of future policy choices in the region for alleviating environmental insecurity despite the very different assumptions and uncertainties embedded in the scenarios and models (Kwakkel and Pruyt, 2013).

4.4 Additional Perspectives

~~Our finding that supply increases for all SSP-RCP scenarios, partly due to increasing rainfall and CO_2 fertilization suggests that the current trend of Sahel greening identified from satellite sensor-based mapping studies (e.g. (Eklundh and Olsson, 2003; Hickler et al., 2005; Seaquist et al., 2009) may continue into the future. Livestock mobilization is one way local populations generally employ to manage risk (e.g. Herrmann et al. (2014). In a greening Sahel, this strategy may help regulate supply shortfalls locally, and over the short term. We also note that greener Sahel (increase in NPP supply) does not necessarily imply an increase in the amount of usable NPP or an enhancement in health and well-being. Recent studies in the Sahel show that much of the greening, at least in some regions, is due to undesirable shifts in species composition (e.g.~~

~~Herrmann et al. (2014)), reductions in biodiversity and an increases in woody biomass (e.g. Brandt et al. (2015)).~~ Livestock mobilization is one way local populations generally employ to manage risk (e.g. Herrmann et al. (2014). ~~In a greening Sahel, t~~This strategy may help regulate supply shortfalls locally, and over the short term. ~~We also note that greener Sahel~~Even if the Sahel were to continue to green up (increase in NPP supply) this would ~~does~~ not necessarily imply an increase in the amount of usable NPP or an enhancement in health and well-being. Recent studies in the Sahel show that much of the recent greening, at least in some regions, is due to undesirable shifts in species composition (e.g. Herrmann et al. (2014)), reductions in biodiversity and an increases in woody biomass (e.g. Brandt et al. (2015)).

Campbell et al. (2014) underscore the importance of family planning and education in the Sahel in order to curb population growth. Generating demand for various forms of birth control and gender empowerment would be two key interventions that would work towards slowing population growth, improving health and facilitating income generation. These interventions would act to curtail supply shortfalls in the future.

4.5 Mechanisms of changes in future NPP supply and demand

4.5.1 NPP supply

In order to isolate the CO_2 (rainfall) effect on NPP increase for RCP6.0, we compared a simulation where rainfall (CO_2) was held constant with a simulation where both were held constant for the period 2000-2050 for all GCMs. We found that supply increases mostly due to CO_2 fertilization (see Fig. B2), with very little attributed to rainfall. However, yield gap closure from SSP2 contributes most to the increase in simulated NPP supply (Fig. B2).

The CO_2 fertilization effect increases with the magnitude of climate change and explains the smaller shortages in SSP-RCP8.5 scenarios compared to SSP-RCP4.5 scenarios (Fig. 3b). ~~Generally, NPP supply increases for all SSP-RCP scenarios due to climate change-induced plant growth and due to decreasing yield gaps. Climate-change induced plant growth (mainly due to increases in rainfall combined with the CO_2 fertilization effect) was shown to increase with the magnitude of climate change, and explains the smaller shortages in SSP-RCP8.5 scenarios compared to SSP-RCP4.5 scenarios (Fig. 3b). Although uncertainty with respect to the total magnitude of simulated NPP supply exists (due to lack of ground truth for the region), greater confidence can be placed in the long-term trends in simulated vegetation growth (e.g. Seaquist et al. (2009) and Fig. A2).~~

The decreases in yield gap (applied to the NPP supply and demand balance through the technological improvement factor) are simulated with PLUM and are strongly dependent on scenario-driven assumptions for technological change. High rates of technological change explain the decreasing shortages at the end of the 21^{st} century for SSP1-RCPs and SSP5-RCPs scenarios. For example, in the SSP1-RCP scenarios, the yield gap decreased from 0.55 in 2000 to 0.43 by 2050 in Nigeria and from 0.69 in 2000 to 0.56 by 2050 in Ethiopia. By contrast, slow technological change in SSP3-RCP scenarios leads to very small decreases in yield gaps, e.g. for Nigeria to 0.54 by 2050 while no improvement at all was simulated for Ethiopia. Uncertainties in yield improvements driven by technological development are very large and critically dependent on investments as well as on infrastructural and political development in developing countries (Engström et al., 2016b; Licker et al., 2010; Mueller et al., 2012). Reducing yield gaps to 0.5 in Sub-Saharan countries can be achieved by intensified nutrient management, while decreases down to 0.25 require increased irrigation and fertilization (Mueller et al., 2012). However, Elliott et al. (2014) underscore that freshwater limitations in the dryer regions of the globe could limit agricultural production, and even lead to the reversion of irrigated farmland to rainfed farmland, thereby negatively affecting food production. Conventional agricultural intensification, however, can result in environmental degradation, vulnerability to pests, and depletion of aquifers (Ceccato et al., 2007; Foley et al., 2005). Agricultural management should consider strategies of sustainable intensification while simultaneously considering adaptation of agriculture to changing climates (Dile et al., 2013; Pretty, 2008, 2011).

An additional driver of NPP supply is the simulated increase in agricultural land area provided by PLUM (i.e. grass- and cropland – Fig. B5). However, the simplified representation of grassland in PLUM potentially underestimates the expansion of agricultural land into naturally vegetated areas, and thus the magnitude of total NPP supply. As with agricultural intensification, the expansion of agricultural land into natural forests and grasslands has the potential to produce negative impacts on the environment and on climate (Canadell and Schulze, 2014; Foley et al., 2005; Pugh et al., 2015).

4.5.2 NPP demand

Despite increases in future NPP supply, according to our results, the Sahel is likely to~~will~~ experience NPP shortages for most NPP scenarios due to strong increases in demand. Generally, the increasing NPP demand in the Sahel region can be explained by doubling to tripling population in the period 2000-2050 across the scenarios (Fig. B3~~2~~a). However, changes in economy, lifestyle and consumption patterns as simulated with PLUM were shown to be the important drivers for large total NPP demand. For example, in the SSP5-RCP scenarios, per capita NPP demand almost triples (2000-2050, Fig. B3~~2~~b), driven by the adoption of meat- and milk-rich diets and processed food as previously pointed out by (Kearney, 2010; Tschirley et al., 2015). Increased per capita NPP demand coupled with the doubling in population (2000-2050) leads to almost seven-fold increases in total NPP demand during the period 2000-2100 for SSP5-RCP scenarios. By contrast, for SSP4-RCP scenarios population triples (2000-2050), but widening income gaps and no improvements in diets in the poor population lead to declining per capita NPP demand (Fig. B3~~2~~b) with a low increase (compared to other scenarios) in total NPP demand (doubling between 2000 and 2050, Fig. B3~~2~~b). The relatively weak increase of total NPP demand in the SSP4-RCP scenarios is the underlying reason for a sustained NPP surplus in the scenarios. The NPP surplus per se is not an indicator for achieved food security, as suggested by the decreasing per capita demand (described above). By contrast, food insecurity will be likely more wide-spread than today according to the SSP4-RCP scenarios, aggravated by strong inequalities within the population that are likely to worsen food distribution and food access for the poor (Pinstrup-Andersen, 2009).

The uneven projected changes in per capita NPP demand across countries (Table C1) are partly due to contrasts in the evolution of drivers (e.g. income) for different countries, but also due to differing initial conditions for the different countries. In countries with initially higher per capita demand (e.g. Sudan) the potential to increase per capita demand is limited, while for countries with lower initial per capita demands (e.g. Ethiopia) the potential to increase demands is comparatively higher. Finally, the NPP demand estimates are limited by the assumption of cereals, meat and milk being proxies for food supply, which for countries with high shares of pulses and tubers in their average diet in particular, underestimates the NPP demand.

4.6 Uncertainties

~~In this work we~~We show~~assume~~ that the deep uncertainties represented by the scenarios i.e. not knowing how drivers (e.g., population, technological change) will develop in the future (van Vuuren et al., 2008) are ~~the~~ major sources of uncertainty leading to variations in our results (Fig. 3b). T~~Additionally, t~~he variability in NPP supply and demand, originating from the five GCMs and uncertainties in SSP interpretation and quantification (see Engström et al. (2016b) and Table 1 and Table B1 ~~therein~~), respectively, allows us to ~~confidently~~ assess, with high statistical confidence, when the onset of supply shortfalls begin and are sustained.

Additional uncertainty exists with respect to the total magnitude and trends of simulated NPP supply, given the lack of ground truth for the region, and that differences in NPP trends between other models is very large (e.g. Friend et al., 2014; Körner et al., 2006; Pugh et al., 2016; Rosenzweig et al., 2014). Indeed, recent observational evidence suggests that the effect of CO_2 fertilization on plant growth may be constrained by counteracting feedbacks associated with increasing atmospheric moisture demand and nutrient availability (e.g. Smith et al., 2016; Wieder et al. 2015). For example, NPP is reduced under warmer and dryer conditions due to moisture stress, particularly in temperate and arid ecosystems. Future trends NPP trends in the Sahel could therefore be strongly determined by changes in the frequencies of wet years versus dry years, with the dry years counteracting the CO_2 fertilization effect. Furthermore, nutrient supply rates may not be able to keep up with extra demand associated with CO_2 fertilization, and leading to a depletion of soil nutrients, as current evidence suggests. This could also curtail the CO_2 fertilization effect, particularly in the more southerly parts of our study area, where nutrients tend to become a limiting factor. We performed a simple experiment negating the CO_2 fertilization effect in order to gauge its impact on supply-demand balance on all scenarios. For the SSP2-RCP6.0, per capita demand has an equal chance of exceeding per capita supply in 2036 for the SSP2-6.0 scenario as opposed to 2043 if CO_2 fertilization in included (Fig. B7), with a very high likelihood of continuous supply shortfall beginning in 2056, as opposed to 2073 with CO_2 fertilization. The effect on all other scenarios is an earlier shift to the onset of supply shortfalls, by about 10 years, compared to Fig. 3b (see Fig. B7). Supply shortfalls with high likelihood of occurrence (black dots showing non-overlapping 95% confidence intervals) are similarly shifted, and occur with greater consistency and frequency. All of this suggests that the NPP increases found in our current analysis are likely optimistic, due the potential overestimation of the CO_2 fertilization effect, as well as the fact that BME is based on potential natural vegetation.

Finally, we note that country-specific scaling factors used to convert PLUM output to per pixel changes using the Hurtt et al. (2011) data set for the year 2000 did not depart substantially from 1 (scaling factors for the larger countries were all within

10%, and the area weighted mean of the scaling factors was 0.95), but a few smaller countries in West Africa diverge by more than 25% (<0.80 or > 1.25) (see Table C1). We expect these to have only marginal influence on the results at the regional level, but could have a larger impact on localities along the West African coast (Fig. 4 and Fig. B1).

Other sources of uncertainty, such as model uncertainty stemming from the supply and demand models (Alexander et al., 2016) are not presently taken into account.

5 Conclusions

In the Sahel, population growth and climate change raise the question of whether the demand for NPP will outstrip supply during the 21st century. In order to address this question, we developed a reduced-complexity framework capable of generating a range of NPP supply-demand trajectories for different Sahel futures at the regional, country, and local levels of aggregation. These results are based on differing climate, [CO_2], and socio-economic scenarios supplied by different SSP and RCP combinations.

We conclude that the potential for NPP self-sufficiency in the Sahel will not likely be attainable later in the 21st century. The most likely consequence will be that hunger and malnutrition will become more widespread than it is currently, undermining the UN sustainable development goals. This highlights the importance of establishing strategies that address the reduction of NPP demand, increasing its supply as well as facilitating its access, particularly for the urban poor. The consistency of geographical shortfall patterns across all scenarios also suggests that, despite deep uncertainties associated with assumptions about how the future unfolds and uncertainties associated with NPP supply magnitudes and trends, a relatively narrow range of policy interventions can be crafted.

Finally, we advance previous research by showing how NPP supply-demand balance (a key metric for quantifying resource shortfalls over large regions, but applied retrospectively in previous studies) can also be used to explore the impact of changing socio-economic and climate assumptions in the Sahel to support policy.

Acknowledgements

FS acknowledges support from the Helge Ax:son Johnsons Stiftelse. SO, KE, and JWS acknowledge support from the FORMAS Strong Research Environment project Land use today and tomorrow (LUsTT; dnr: 211-2009-1682), while JWS also acknowledges partial support from LUCID (www.lucid.lu.se), a FORMAS-funded Linnaeus Centre of Excellence at Lund University (dnr: 259-2008-1718). AMA and JA acknowledge funding provided by Swedish National Space Board (Rymdstyrelsen). Finally, VL acknowledges support from the BIODIVERSA project CONNECT via FORMAS.

Appendices

Appendix A Methods

A.1 Biome based Meta-model Ensemble

In this section, we describe the development of the biome based meta-model ensemble (BME) for the Sahel region. BME consists of rapid NPP meta-models tailored for the desert temperate, desert tropical, tropical semi-arid and tropical humid biome. The BME is based on the dynamic vegetation model LPJ-GUESS (Smith et al., 2014) and NPP simulations following the methodology of Sallaba et al. (2015).

A.1.1 LPJ-GUESS

LPJ-GUESS (Smith et al., 2014) is a mechanistic model of plant physiological and biogeochemical processes that incorporate ecosystem carbon and nitrogen cycles as well as water fluxes. The model uses a detailed individual- and patch-based representation of vegetation structure where individual plants differ in growth form, phenology, life history strategy and photosynthetic pathway, demography and resource competition. LPJ-GUESS is forced by various climate (i.e. solar radiation, temperature and precipitation), atmospheric [CO_2], soil characteristics and nitrogen deposition. Vegetation is represented as plant functional types (PFTs) with different age cohorts interacting on patch level. Ten generalized trees and two generalized grass functional types (i.e. C3 and C4 grass) following Smith et al. (2014) were used for global potential natural vegetation (PNV). Several patches (here 25) are applied in parallel within a grid cell with distinguished establishment of vegetation, fire impacts, random disturbance and mortality rate of different age cohorts (Sitch et al., 2003; Smith et al., 2001; Smith et al., 2014). We applied the LPJ-GUESS in cohort mode which represents individual PFTs in different age classes competing for resources (light, water and space) in a patch. We defined disturbance events with an expected return interval of 100 years following Ahlström et al. (2015). We spun up each LPJ-GUESS simulations with a 500 years long phase of de-trended climate data and a particular [CO_2] (unique for each simulation as outlined in Input data) in order to run the model from bare soil to a vegetation equilibrium state.

A.1.2 Input Data

We collected our BME development dataset with a random stratified selection of climate data using the Major Biome classification (BMC) (Reich and Eswaran, 2002) on a 0.5°x0.5° spatial resolution. The BMC characterizes four biomes in the greater Sahel region based on soil moisture and soil temperature regimes (see Fig. 1). We chose randomly 2-5% of the total cells in each biome.

We overlaid the sampled cells with CRU TS. 3.0 climate data (Harris et al., 2014; Mitchell and Jones, 2005), which have the same spatial resolution. CRU data span from 1901 to 2006 providing monthly data of temperature, precipitation and cloudiness. Soil texture characteristics were taken from the FAO global soil dataset (FAO, 1991) as described in Sitch et al.

(2003). Historical monthly nitrogen deposition rates were achieved from the Atmospheric Chemistry and Climate Model Intercomparison Project (ACCMIP) database of Lamarque et al. (2010) and processed as described by Smith et al. (2014). We developed climate and [CO_2] scenarios based on a factorial approach where increasing monthly temperature, [CO_2] and changing monthly precipitation amounts are varied multiple variables -at-a-time (i.e. MAT) (Smith and Smith, 2007). We set maximum changes for each variable (see Table A1) in order to design reasonable climate and [CO_2] scenario limits as described by Sallaba et al. (2015). We used CRU TS 3.0 climate data as the baseline time-series and superimposed the climate and [CO_2] scenarios upon the baseline data while we held the nitrogen deposition rates according to the ACCMIP records. In total, we developed 100 scenarios (including baseline) for each CRU grid cell, which were then applied to simulate NPP in LPJ-GUESS. We assumed that grid cells maintain the biome membership even though the climate conditions change during the LPJ-GUESS simulations since we consider transitions of vegetation biomes to be long-termed, 100 years.

Table A1 Minimum and maximum stepwise changes of the climate variables and [CO_2]. The magnitudes of increases are related to how much a variable could be adjusted. Temperature was increased in four steps and the other variables in five steps resulting in 100 different climate change scenarios.

Change attributes	**Temperature change [°C]**	**Precipitation [% of baseline]**	**Atmospheric CO_2 [ppm]**
Minimum Value	0	50	350
Maximum Value	6	150	670
Magnitude of increase	2	25	80
No. of steps	4	5	5

A.1.3 Biome meta-models

We followed the assumption that plant growth is controlled by climate conditions (Sallaba et al., 2015) and defined biome specific assumptions of ecosystem-climate interactions. As Sallaba et al. (2015) we assume that vegetation growth is controlled synergistically by temperature and precipitation. Under optimal climate conditions maximum plant growth can be reached but decreases when temperature and/or precipitation are not at the optimum. In order to keep the meta-modelling framework as simple but efficient as possible, we limited the meta-model to three input climate surrogates that control plant growth: (1) annual precipitation (P_{cum}), (2) maximum temperature (T_{max}) and (3) minimum temperature (T_{min}) temperature. We followed the methodology of Sallaba et al. (2015) by defining functions of the climate surrogates that yield maximum NPP at baseline [CO_2], combining these in a synergistic function and then adding the CO_2 fertilization effect.

For the meta-model development at baseline [CO_2], we scaled the LPJ-GUESS NPP estimates between 0-1 (i.e. NPP_{min} =0 and NPP_{max} =1) using the highest NPP yield of each biome and combined them with the climate surrogates. The highest NPP yields of the biomes Max_{biome} at baseline [CO_2] are given in Table A3. We then extracted the climate surrogate - NPP value combinations that yield highest NPP, assuming that maximum NPP yields can only be reached under optimal climate conditions (Sallaba et al., 2015).

For NPP as a function of temperature we assumed a hump-shaped curve relationship, which is based on the temperature-photosynthesis relationship (Sallaba et al., 2015). For T_{max} we developed a function that is built upon the *beta*-distribution as given in Eq. (A1).

$$f(T_{max}) = \frac{\left(\frac{T-Lim_{min}}{Lim_{max}-Lim_{min}}\right)^{\partial-1}\left(1-\left(\frac{T-Lim_{min}}{Lim_{max}-Lim_{min}}\right)\right)^{\beta-1}}{\left(\frac{\Gamma(\partial)\Gamma(\partial\beta)}{\Gamma(\partial+\beta)}\right)} a \qquad \text{(A1)}$$

where $f(T_{max})$ calculates the NPP yield (relative) of the given temperature surrogate; T is the value (°C) of T_{max}; Lim_{min} and Lim_{max} are the minimum and maximum temperature limits of the biome normalizing T between 0 and 1; Γ is the gamma function ; ∂ and β describe the shape of the function and a stretches the function along the ordinate (the amplitude).

For T_{min} we developed a function that is identical to T_{max} as given in Eq. (A2).

$$f(T_{min}) = \frac{\left(\frac{T-Lim_{min}}{Lim_{max}-Lim_{min}}\right)^{\partial-1}\left(1-\left(\frac{T-Lim_{min}}{Lim_{max}-Lim_{min}}\right)\right)^{\beta-1}}{\left(\frac{\Gamma(\partial)\Gamma(\partial\beta)}{\Gamma(\partial+\beta)}\right)} a \qquad \text{(A2)}$$

where$f(T_{min})$ estimates relative NPP and T is the value (°C) of T_{min}. The function parameters of Eq. (A1) and (A2) are provided in Table A2.

For NPP as a function of precipitation we applied two function types because the dataset shows saturation as well as linear NPP growth with increasing precipitation amounts in the Sahelian biomes. Both function types let NPP increase with increasing precipitation amounts until NPP_{max} is reached. Further increasing precipitation levels only yield NPP_{max} because precipitation surplus is assigned as run-off and percolation, following the treatment of high precipitation levels in LPJ-GUESS (Gerten et al., 2004; Smith et al., 2014).

Table A2 Parameter values for maximum temperature $\boldsymbol{f(T_{max})}$ in Eq. (A1) and minimum temperature $\boldsymbol{f(T_{min})}$ in Eq. (A2).

Biomes	**Temperature function in $\boldsymbol{f(T_{lim})}$**	$\boldsymbol{Lim_{min}}$	$\boldsymbol{Lim_{max}}$	$\boldsymbol{\partial}$	$\boldsymbol{\beta}$	$\boldsymbol{a}$
Desert tropical	$f(T_{min})$	9.00	33.00	2.12	1.22	0.46
Desert temperate	$f(T_{min})$	-14.00	28.00	2.06	1.33	0.52
Tropical semi-arid	$f(T_{min})$	4.00	33.00	2.27	1.57	0.52
Tropical humid	$f(T_{max})$	13.00	36	1.47	1.49	0.68

In the tropical humid and tropical semi-arid biomes, we applied a saturation function where NPP grows rapidly with increasing precipitation until NPP_{max} is reached, as given in Eq. (A3),

$$g(P_{cum}) = min\left(1, k - \frac{o}{P_{cum}{}^{l}}\right) \qquad \text{(A3)}$$

where $g(P_{cum})$ estimates the cumulative precipitation NPP (relative); P_{cum} is the annual cumulative precipitation; k is the maximum relative NPP (here NPP_{max}=1) that limits the growth of the function; o is a constant; l determines the slope of the function and min() limits the linear function to NPP_{max}=1. If P_{cum} is 0 mm than $g(P_{cum})$ is set to 0.

In the desert tropical and desert temperate biomes we defined NPP as a simple linear function of precipitation (see Eq. (A4)), which is limited to NPP_{max}=1 in order to consider the treatment of precipitation surplus in LPJ-GUESS (Gerten et al., 2004; Smith et al., 2014).

$$g(P_{cum}) = \min(1, mP_{cum}) \quad \text{(A4)}$$

where $g(P_{npp})$ calculates the cumulative precipitation NPP (relative); P is the annual cumulative precipitation; m is the slope of the linear function; and min() limits the linear function to NPP_{max}=1. All parameter values of Eq. (A3) and (A4) are presented in Table A3. For the parameter values determination of the temperature and precipitation functions we randomly halved the biome training subsets (at [CO_2] = 350 ppm) in analysis and validation parts, and then applied nonlinear least-squares model fit in MATLAB® (2015b). We chose the parameter values that yield the lowest root mean square error (RMSE) in the validation part following (Del Grosso et al., 2008).

Table A3 Parameter values for cumulative precipitation functions in Eq. (A2) for the tropical biomes and Eq. (A3) for the desert biomes.

Biomes	*k*	*o*	*l*	*m*
Desert tropical*	-	-	-	0.0009
Desert temperate*	-	-	-	0.0014
Tropical semi-arid	1.84	4.29	0.18	-
Tropical humid	1.24	19.69	0.51	-

* The asterisk indicates linear precipitation functions

We then combined the climate variable functions and investigated model complexity. We combined $f(T_{min}), f(T_{max})$ and $g(P_{cum})$ in seven groupings ranging from one function to multiplying all three climate functions to calculate NPP in each biome. We assessed model complexity with the Bayesian information criterion (BIC) (Burnham and Anderson, 2002; Schwarz, 1978) and model agreement with RMSE and the Wilmott index (DR) (Smith and Smith, 2007; Smith et al., 1997; Willmott et al., 2012). We chose the combinations with lowest BIC and best model agreement. In all biomes the best results were obtained by a combination of precipitation with either one temperature function (because T_{max} and T_{min} are potentially auto-correlated). The combination of $g(P_{cum})$ with $f(T_{max})$gave the best results in the tropical humid biome while $g(P_{cum})$ combined with $f(T_{min})$ yielded the best results in the remaining biomes (see applied temperature function in Table A2).

In the next step, we combined the selected functions, converted the synergistic function from relative to absolute NPP (kg C m^{-2} yr^{-1}) and rescaled the function to independent LPJ-GUESS NPP simulations in order to correct for differences in NPP magnitudes as given in Eq. (A4).

$$NPP_{base} = NPP_{scale}\left(\left(f(T_{lim})\, g(P_{cum})\right) Max_{biome}\right),\ f(T_{lim}) \in [f(T_{max}), f(T_{min})] \quad \text{(A4)}$$

where NPP_{base} is the estimate (kg C m^{-2} yr^{-1}) at baseline [CO_2]; $f(T_{lim})$ is the temperature function used for the specific biome (either $f(T_{max})$ or $f(T_{min})$ - see Table A2); Max_{biome} is maximum NPP yield of the biome at baseline [CO_2] for converting NPP from relative to absolute units; and NPP_{scale} is the scaling factor to minimize the magnitude difference between LPJ-GUESS and BME estimates. The scaling factor is a ratio based on the mean of LPJ-GUESS NPP and the mean of biome meta-model NPP estimates from 1985-2006. In the tropical humid biome $f(T_{min})$ is set to 1 and in the remaining biomes $f(T_{max})$ is set to 1 based on the model complexity analysis. The parameter values are given in Table A4.

Table A4 Parameter values of the synergistic function in Eq. (A4).

Biomes	$\boldsymbol{Max_{biome}}$	$\boldsymbol{NPP_{scale}}$
Desert tropical	1.25	1.46
Desert temperate	0.86	1.05
Tropical semi-arid	1.46	1.04
Tropical humid	1.56	0.97

We implemented the CO_2 fertilization effect on plant growth in the final meta-model function (see Eq. (A5)) by applying the same methodology as described in Sallaba et al. (2015) (assuming saturating NPP enhancement with increasing [CO_2]) but determined new parameters for each biome using linear fitting in MATLAB® (R2015b). We chose the parameters that yielded lowest RMSE are shown in Table A5.

$$NPP_{scenario} = \left(NPP_{baseline} \left(c \left(1 - \frac{CO_{2\_baseline}}{CO_{2\_scenario}} \right) + 1 \right) \right) \qquad \text{(A5)}$$

Where $NPP_{scenario}$ is NPP (kg C m^{-2} yr^{-1}) under elevated [CO_2] (ppm); $NPP_{baseline}$ is modelled NPP at baseline [CO_2]; c is the slope; $CO_{2\_baseline}$ is the baseline [CO_2] of 350 ppm and $CO_{2\_scenario}$ is an [CO_2] > 350 ppm.

Table A5 Parameter values of the CO_2 function in Sallaba et al. (2015) Eq. (5) therein.

Biomes	$\boldsymbol{c}$
Desert tropical	-0.19
Desert temperate	-0.63
Tropical semi-arid	-0.70
Tropical humid	-1.03

For each biome, we determined CO_2 fertilization function parameter values with a nonlinear least-squares model fit in MATLAB® (R2015b) choosing values yielding the lowest root mean square error (RMSE).

A.2 Model Evaluation

A.2.1 Biome Level Model Validation

We validate biome-level LPJ-GUESS and BME performance for estimating NPP of natural vegetation with NPP field-measurements from Michaletz et al. (2016) and Luyssaert et al. (2009) (see Sallaba et al., 2015) for the Major Biome Classification of Reich and Eswaran (2002) including the biomes found in the Sahel (desert temperate, tropical semi-arid and tropical humid – no observations were available for desert tropical). Note that since only two observations were available for our study area (see Fig. A1) this evaluation demonstrates the ability of both LPJ-GUESS and BME to replicate NPP for Sahel biomes found elsewhere in the world.

Before we combined the Michaletz et al. (2016) and Luyssaert et al. (2009) datasets, we removed sites with no records of combined above- and below-ground NPP measurements. After we merged the data, we checked the final assembly of NPP measurements for duplicates and removed them. The final dataset consists of 1561 samples (i.e. 1247 samples from Michaletz et al. (2016) and 314 samples from Luyssaert et al. (2009)) representing total NPP measurements across the terrestrial biosphere (sample sizes are 18, 6, and 12 for Sahel biomes of desert temperate, tropical semi-arid and tropical humid, respectively) from 1959-2006. Both LPJ-GUESS and BME were driven with CRU TS 3.21 climate data (Harris et al. 2014, Trenberth et al. 2014) that has global coverage across the time period.

We calculated mean values of the NPP field-measurements and the modelled NPP estimates located in the respective biomes, following Smith et al. (2014b). We aggregated to the biome-level to account for the difference in scale between in situ NPP measurements and modelled grid cell NPP estimates (being grid cell averages).

Finally, we determined the overall model performance, biome-by-biome, with the coefficient of determination (R^2 value) and the root mean square error (RMSE). Additionally, we investigated model agreement with performance ratios (hereafter referred to as ‘Q’) by dividing mean biome NPP estimates (for both models) with mean biome NPP observations. Model overestimation in comparison to in situ NPP measurements is indicated by $Q > 1$ and underestimation by $Q < 1$. Good model performance is classified with a Q range between 0.9-1.1 assuming an error of ± 10% following Sallaba et al. (2015). However, we further defined an acceptable model performance error range of ±20% (i.e. Q = 0.8-1.25) given the limitations of using LPJ-GUESS standard modelling protocol, PNV and CRU climate observations, and especially the simplicity of BME.

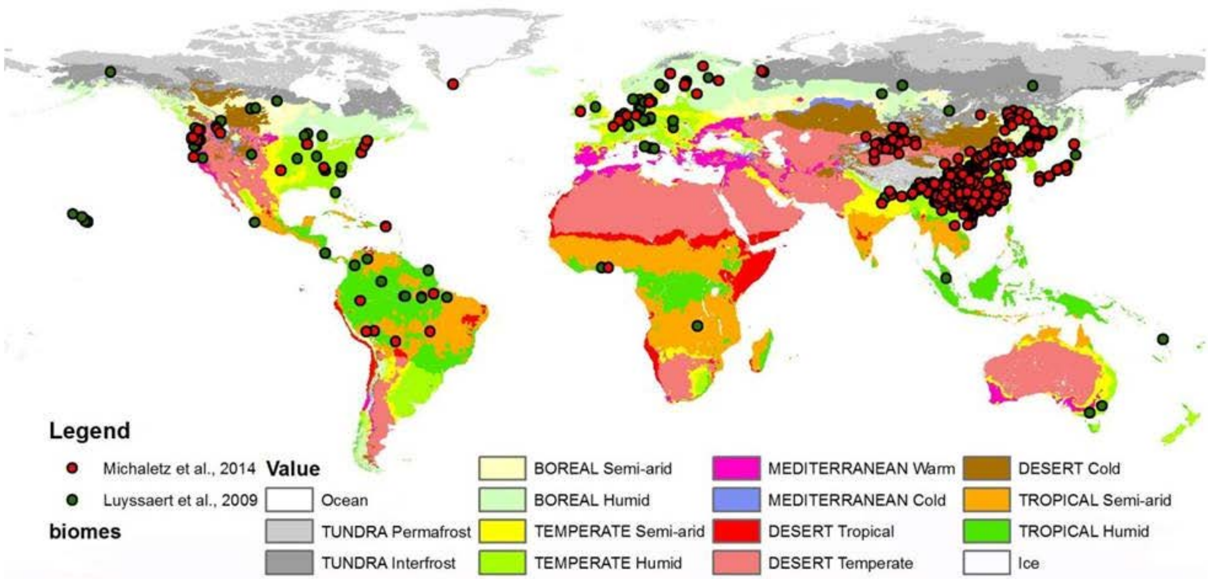

Fig. A1 Map of the Major Biome Classification based on Reich and Eswaran (2002). The red and green points are the locations of the NPP field-data from Michaletz et al. (2016) and Luyssaert et al. (2009).

LPJ-GUESS performs reasonably well in simulating NPP at the overall biome level (R^2 = 0.71 and RMSE = 0.16) but the model performance varies notably across the biomes (see Fig. A2 and Table A6). In general, LPJ-GUESS yields acceptable model agreement in seven (with good performance in four biomes) out of thirteen biomes. At the same time, the model underestimates NPP in three biomes while it overestimates NPP in two biomes (Fig. A2).

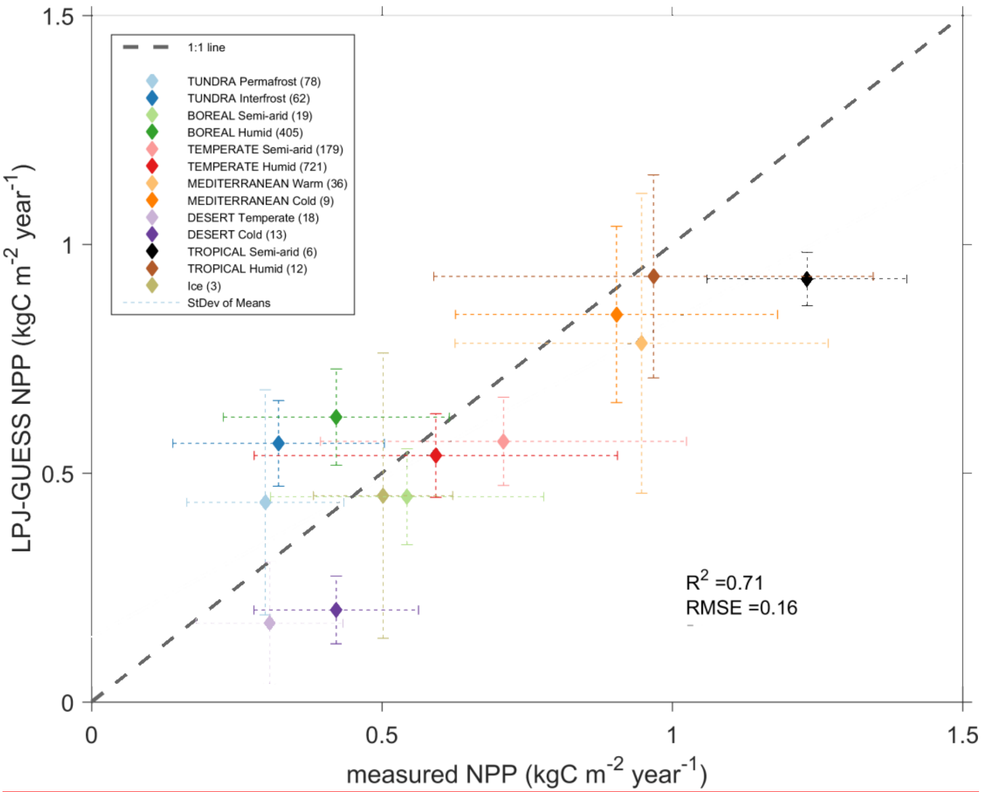

Fig. A2 Comparison of LPJ-GUESS through NPP estimates and NPP field-measurements at the biome level using biome mean NPP values and their standard deviation. The different colours represent MBC biomes based on (Reich and Eswaran 2002). The number of NPP observations in each biome is given in the legend. Note that Sahel biomes Desert temperate, Tropical Semi-arid, and Tropical Humid.

Table A6 Comparison between mean biome NPP field-measurements, LPJ-GUESS, BME NPP estimates; and their Q as model performance measure. Sahel biomes are underlined.

Biome (sample size)	**Field-data mean NPP [kg C m^{-2} yr^{-1}]**	**LPJ-GUESS mean NPP [kgC m^{-2} yr^{-1}]**	**LPJ-GUESS Q**	**BME mean NPP [kgC m^{-2} yr^{-1}]**	**BME Q**
TUNDRA Permafrost (78)	0.30	0.44	1.46	0.24	0.79
TUNDRA Interfrost (62)	0.32	0.56	1.75	0.44	1.36
BOREAL Semi-arid (19)	0.54	0.45	0.83	0.49	0.91
BOREAL Humid (405)	0.42	0.62	1.48	0.56	1.32
TEMPERATE Semi-arid (179)	0.71	0.57	0.80	0.45	0.63
TEMPERATE Humid (729)	0.59	0.54	0.91	0.56	0.95
MEDITERRANEAN Warm (36)	0.95	0.78	0.83	0.52	0.55
MEDITERRANEAN Cold (9)	0.90	0.85	0.94	0.41	0.45
DESERT Temperate (18)	0.31	0.17	0.56	0.09	0.28
DESERT Cold (13)	0.42	0.20	0.48	0.24	0.57
TROPICAL Semi-arid (6)	1.23	0.92	0.75	0.84	0.68
TROPICAL Humid (12)	0.97	0.93	0.96	0.81	0.84
Ice (3)	0.50	0.45	0.90	-	-

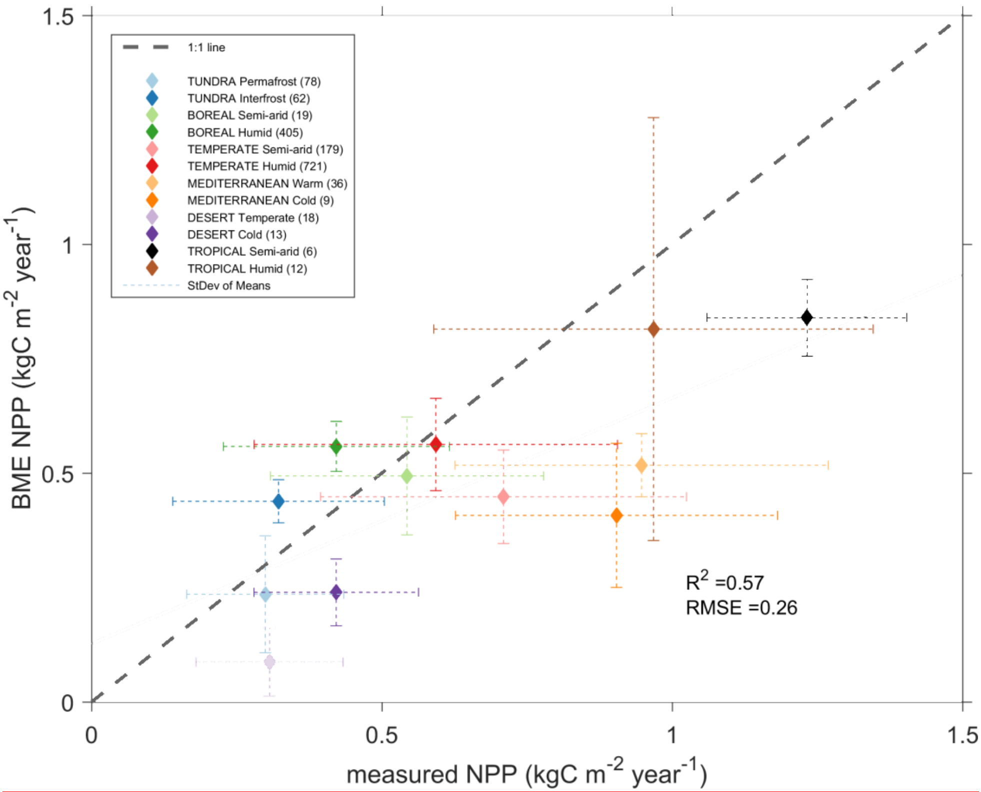

Fig. A3 Comparison of BME NPP estimates and NPP field-measurements on biome level using biome mean values as well as biome standard deviation of the means. The different colours represent MBC biomes based on (Reich and Eswaran 2002). The number of NPP observations in each biome is given in the legend. Note that Greter Sahel biomes Desert temperate, Tropical Semi-arid, and Tropical Humid.

For Greater Sahel biomes: LPJ-GUESS exhibits good skill in simulating NPP in the Tropical humid (Q = 0.96, see Table A6) where it also captures satisfactorily the variability of the NPP measurements. LPJ-GUESS underestimates NPP for the tropical semi-arid biome (Q = 0.75) showing reduced NPP variation compared to the observations. Performance is reduced for Desert temperate (Q =0.56).

BME performance is acceptable at the overall biome level (R^2 = 0.57 and RMSE = 0.26) but varies substantially for individual biomes (see Fig. A3). Overall, BME model agreement is reasonable in four biomes (with good performance in two biomes). At the same time, BME overestimates NPP in two biomes while it underestimates plant growth in six biomes. The variability in in- situ NPP measurements cannot be captured by BME in the majority of biomes except in the tropical humid and tundra permafrost biomes (see vertical and horizontal lines connected to the diamonds in Fig. A3).

For Greater Sahel biomes: BME yields acceptable agreement in estimating NPP in the tropical semi-arid and tropical humid biomes (Q = 0.84, 0.81 respectively) but accuracy drops more water limited biomes of desert temperate (Q = 0.28).

Overall, BME mimics the behavior of LPJ-GUESS shown by a good model agreement of R^2 = 0.71 and moderate RMSE = 0.12 kg C m^{-2} yr^{-1} between the average biome NPP estimates of BME and LPJ-GUESS. Notable is that BME yields, on average, less NPP in the majority of biomes compared to the observations.

A.2.2 BME Performance in the Sahel

For the assessment of BME performance in the Sahel, we chose approximately 4000 CRU TS 3.0 grid cells that cover evenly distributed the Sahel region. We forced LPJ-GUESS with the CRU climate data and measured [CO_2] spanning from 1970-2006 and measured [CO_2] using the same modeling protocol as described in section A.1). The climate data were post-processed as in section A.1 and then applied to BME in order to estimate NPP. We employed several measures to gauge BME performance against LPJ-GUESS simulations. We calculated the BME's agreement (i.e. precision) with LPJ-GUESS simulations with the coefficient of determination (R^2 value) measuring the strength of linear association between the models; the root mean squared error (RMSE) gives the total difference between the models in NPP units (NPP kg C m^{-2} $year^{-1}$) and the Wilmott index (DR) determines how well the plot of LPJ-GUESS simulations and BME NPP fit to a perfect agreement line ranging from -1 to 1 (1 = optimal value) (Smith and Smith, 2007; Smith et al., 1997; Willmott et al., 2012).

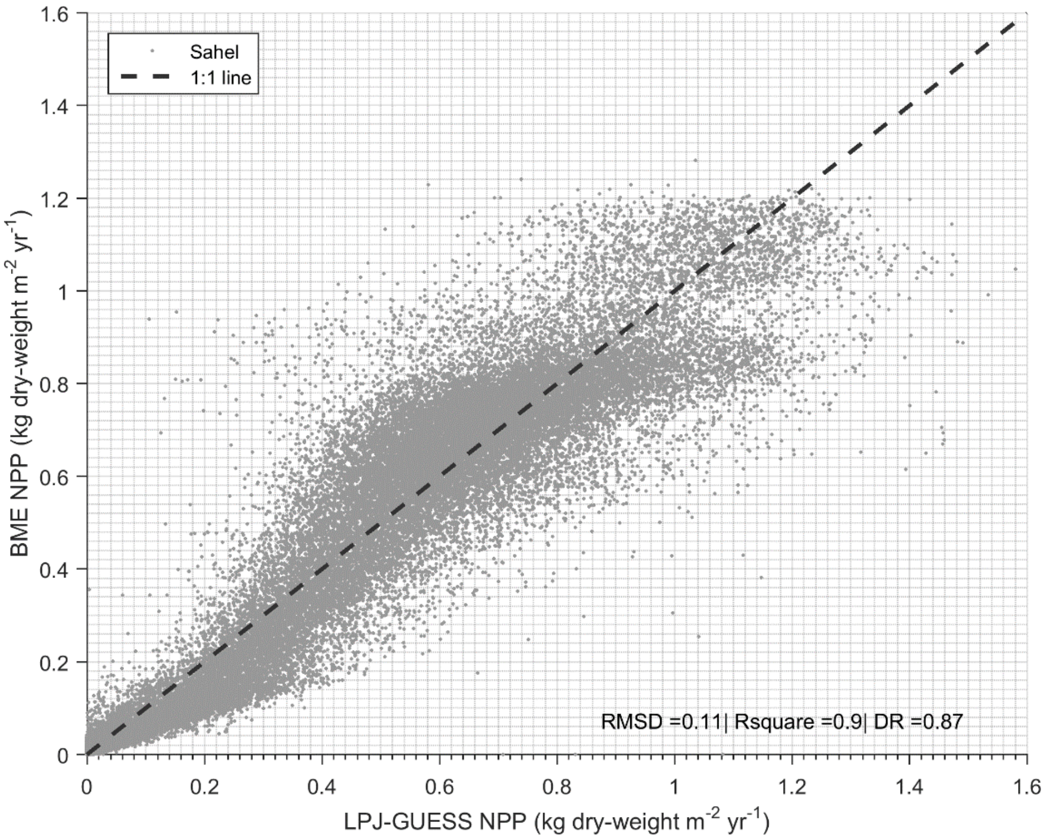

Fig A4~~1~~ Comparison between BME and LPJ-GUESS NPP estimates covering the Sahel region.

The comparison between BME and LPJ-GUESS NPP estimates (see Fig. A1) shows a good agreement R^2=0.9 and DR=0.87 while the RMSE=0.1 NPP kg DW m^{-2} year^{-1} shows notable total differences between the models.

We then calculate annual means of BME and LPJ-GUESS NPP (i.e. aggregating the entire Sahel region) for the time period in order to investigate whether BME follows the inter-annual variation of LPJ-GUESS NPP. As shown in Fig A5~~2~~., BME NPP follows the inter-annual variation of LPJ-GUESS NPP. Both models yield depleted NPP in 1972/73 and 1983/84 showing the impact of devastating droughts that occurred in these years resulting in complete crop failure (Ibrahim, 1988). Furthermore, both models yield a dip in NPP in 2002 when the latest major drought befell the region (see Fig. A5~~2~~) (Balogun et al., 2013). In Fig. A5, we also include runs from LPJ-GUESS C (carbon cycling only), LPJ-GUESS ml (managed land) and MODIS derived NPP for comparison purposes.

In order to test how effectively the NPP of natural ecosystems can be can be used as a proxy for the NPP of agricultural ones we ran LPJ-GUESS managed land (Olin et al., 2015) for the period 1970 to 2006 and compared this to LPJ-GUESS (used to develop BME) for the entire Sahel region. The results (see Fig. A5) of this experiment show that mean NPP derived from LPJ-GUESS ml over the region underestimates mean NPP derived from BME by 0.7% (0.006 dry-weight m^{-2} yr^{-1}) and LPJ-

GUESS by 2.4% (0.020 kg dry-weight m^{-2} yr^{-1}), though all models show similar levels of interannual variability and trend (see Fig. A5). The implication of this experiment is that there is a demonstrable reduction in NPP when land management is taken into consideration, but the effect is relatively minor. Lindeskog et al. (2013) show that LPJ-GUESS managed land (C-version) overestimated actual yield derived from FAO country-level crop statistics and Smith et al. (2014b) also report that natural systems are more productive than agricultural systems in sub-Saharan Africa. We conclude with that possibility that our results are in the upper range for NPP found in the Sahel.

We also compare total yearly means of NPP from BME and LPJ-GUESS to NPP derived from the MOD17A3 processing stream (using MOD17A3 data obtained from the NASA Earth Observation System repository at the University of Montana at www.ntsg.umt.edu) for the period 2000 to 2006 for the greater Sahel region (Running, 2004). We averaged resampled MODIS NPP from 1km to the spatial resolution of the BME estimates (0.5 x 0.5 degrees) and excluded urban areas. We removed below-ground NPP and plant parts unable to be consumed by applying the same R:S and harvest index as described in Section 2.1.1. Lastly, we calculated mean values of MODIS NPP estimates from 2000 to 2010 for each grid cell covering the study area. Our results show that between 2000 and 2006 MODIS-derived NPP underestimate BME-derived NPP by 42% (difference of 0.38 kg dry-weight m^{-2} yr^{-1}), on average (Figure A5). Ardö (2015) also reports that that average annual MODIS NPP underestimates LPJ-GUESS (C version only, Fig. A5) for Africa for 2000-2010 and attributes this to the fact that autotrophic respiration is considerably higher for MODIS NPP compared to LPJ-GUESS, due to large temperature sensitivity in the MODIS algorithm, differences in the biome-specific parameterizations for MODIS as well as specification of plant functional types in LPJ-GUESS.

Country-level census yield trends (1989-2008) for 4 major crops from appendix Data S1 of Ray et al. (2013) for rice (Benin, Burkina Faso, Chad, Ghana, Guinea, Guinea-Bissau, Ivory Coast, Liberia, Mali, Nigeria, Senegal, Sierra Leone, Togo), maize (Benin, Burkina Faso, Cameroon, Chad, Ethiopia, Ghana, Guinea, Ivory Coast, Mali, Nigeria, Senegal, Togo), wheat (Cameroon, Chad, Eritrea, Ethiopia, Mali, Mauritania, Niger, Nigeria, Sudan) and soybean (Benin, Burkina Faso, and Nigeria) range from -5.98 to 2.80 (mean of -0.002), -0.94 to 4.08 (mean of 1.400), -2.58 to 3.1 (mean of 1.280) and 1.15 to 3.98 (mean of 2.280) respectively. Trends for BME, LPJ-GUESS, and MODIS NPP fall within most of the ranges for crop yield trends, showing yearly increases of 0.55% (BME), 0.58% (LPJ-GUESS), and 0.51% (MODIS) for the 7 year period of overlap. For the entire length of each series (1970-2006 for BME and LPJ-GUESS and 2000-2010 for MODIS), slopes indicate yearly increases of 0.40%, 0.40%, and 0.62% respectively. We note the number of uncertainties involved in this comparison (e.g. spatial/temporal sampling, and the fact that BME and MODIS represent natural vegetation and a mix of natural vegetation and crops, respectively).

A.2.3 Concluding Remarks for Model Validation and Evaluation

In sum, a validation involving ground measurements for the same biomes found in the Sahel (but observations mostly from other locations) show that LPJ-GUESS and BME underestimate NPP, while a comparison with MODIS shows that LPJ-GUESS (and BME) overestimate total mean annual NPP in the greater Sahel region (2000-2006). Yet is widely acknowledged, natural systems are likely more productive than agricultural systems. But we also show that trends for BME, LPJ-GUESS, and MODIS mostly fall within trend ranges for country-level yield statistics (though sample size is low). We acknowledge that the uncertainties are significant. Differences in estimates between methods are due to a combination of spatial aggregation/sampling issues (e.g. low sample sizes for biomes typically found in the Sahel, that CRU data do not necessarily represent site-level climate, and the uncertain assessment below-ground and short-lived above-ground plant matter at the site level) as well differing assumptions between the MODIS processing stream and LPJ-GUESS (particularly respiration). We therefore conclude that BME and LPJ-GUESS replicate ground observations of NPP at similar orders of magnitude at the biome level, but may be overestimated due to the fact that natural systems are usually more productive than agricultural ones. This underscores the fact that BME and LPJ-GUESS should be restricted to biome-level applications (or coarser) while applications on the grid cell level should be limited to explorations of patterns and trends, which is the reason why we emphasize an aggregated level of analysis.

~~This favors the application of BME since it mimics reasonably well the behavior of LPJ-GUESS, which exhibits good skills in reproducing vegetation dynamics of the Sahel region (Seaquist et al., 2009). Seaquist et al. (2009) demonstrate that LPJ-GUESS replicates reasonably well satellite-observed greening trend of the Sahel vegetation and its inter-annual variability from 1982 to 2002.~~

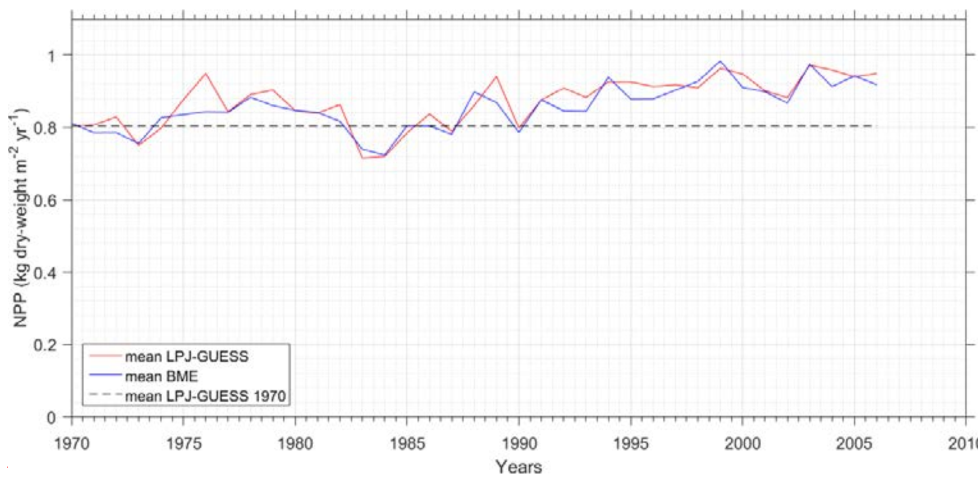

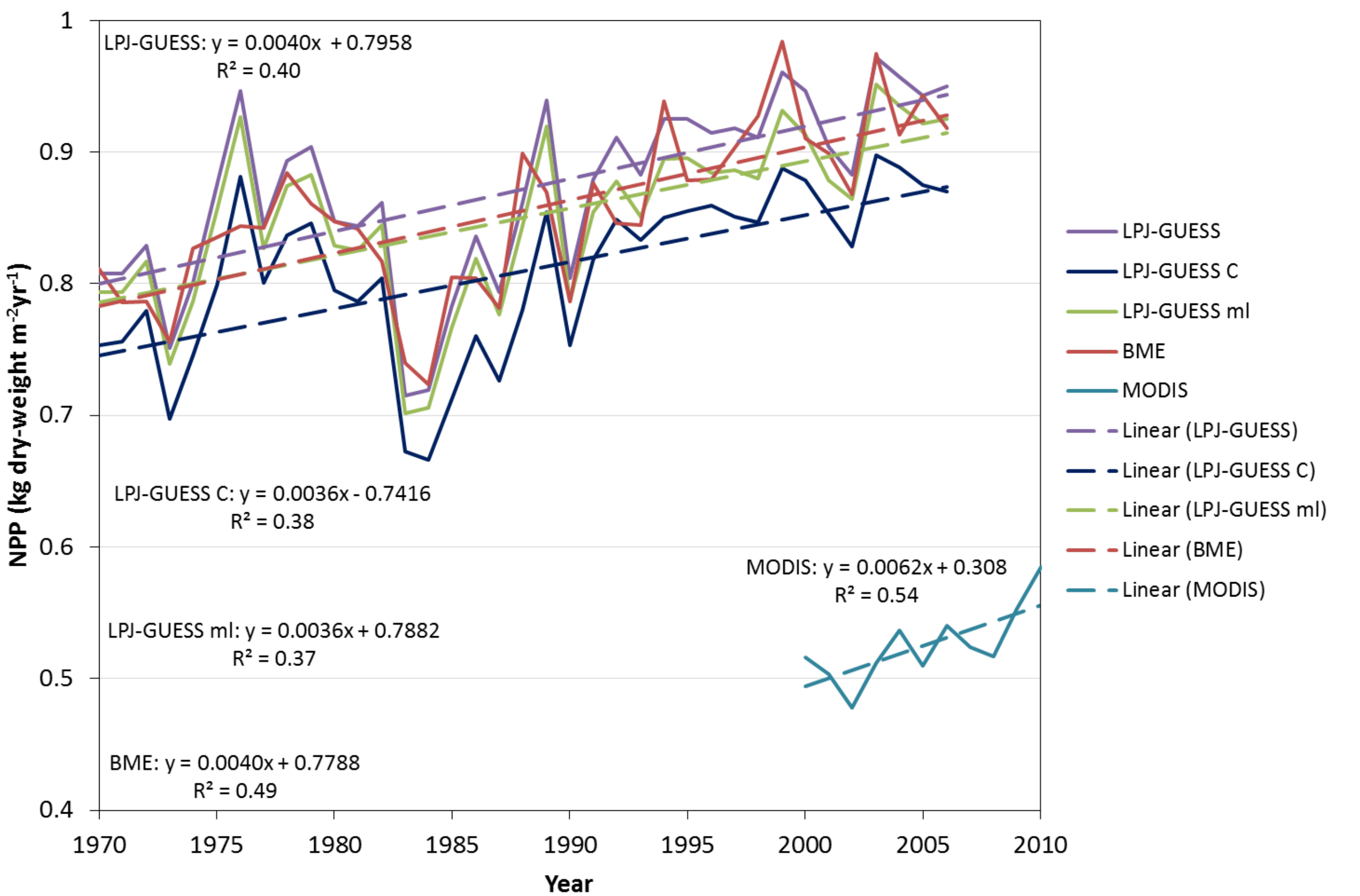

Fig A5~~2~~ Regional annual NPP Annual means of NPP for~~of~~ BME, ~~and~~ LPJ-GUESS, LPJ-GUESS C (carbon only) and LPJ-GUESS ml (managed land) (~~from~~ 1970 to 2006) and MODIS (2000-2010) for the greater Sahel region. ~~LPJ-GUESS NPP estimates are visualized in red and BME in blue.~~

A.3 Estimation of NPP supply and demand

In this modelling framework, we followed the NPP_{demand} definition Abdi et al. (2014) as given in Eq. (A6).

$$NPP_{demand} = NPP_{food} + NPP_{feed} + NPP_{residues} + NPP_{fuel} + NPP_{burned} \qquad \text{(A6)}$$

Where NPP_{demand} is the actual amount of annual NPP needed for human survival; NPP_{food} is the NPP needed for consumed cereals, meat and milk production; NPP_{feed} is the total amount of fodder to support the livestock population and $NPP_{residues}$ are agricultural by-products (after harvesting); NPP_{fuel} describes fuelwood and charcoal from the region's dry woodlands and NPP_{burned} represents the human-driven NPP loss from biomass burning of forest resources for land clearing due to land use change (Abdi et al., 2014).

We adapted Eq. (A6) to the current study's framework by dividing the demand into cereal (Eq. A7) and grazing (Eq. A8) based NPP, and PLUM outputs.

$$NPP_{cereal\_demand} = NPP_{food} + NPP_{feed} \qquad \text{(A7)}$$

where $NPP_{food} = cereal_{total} - cereal_{feed}$ (ton country^{-1}); $cereal_{total}$ (ton country^{-1}) is the total cereal consumption of human and livestock population provided by PLUM; $cereal_{feed}$ (ton country^{-1}) is the total cereal demand to sustain the livestock population (a direct PLUM ouput); NPP_{feed} (ton country^{-1}) is equal with $cereal_{feed}$; We then converted then NPP_{cereal_demand} to per capita (kg person^{-1}) using country population of the corresponding year in the SSP.

The amount of NPP needed to sustain the livestock by grazing that cannot be covered with $cereal_{feed}$ we applied Eq. (A7).

$$NPP_{grazing\_demand} = (1 - feed_{ratio}) * cereal_{feed}/feed_{ratio} \qquad \text{(A8)}$$

Where $NPP_{grazing\_demand}$ (ton country^{-1}) is the NPP obtained from grasslands for sustaining the livestock; $feed_{ratio}$ ranges between 0-1 (given by PLUM) and provides the proportion of how much $cereal_{feed}$ can meet the livestock demand of energy needed to sustain the livestock. Furthermore, we assumed that the Sahelian livestock is kept close to human populated areas and we therefore we converted $NPP_{grazing\_demand}$ to per capita (kg person^{-1}) using country population of the corresponding year in the SSP.

Furthermore, we eliminated NPP_{fuel} in Eq. (A6) because we assumed that fuelwood doesn't directly contribute to the availability of food resources. Fuelwood is a vital variable since it is a necessity for processing cereals and meat but it cannot provide information about food resource availability. Moreover, we eliminated NPP_{burned} in Eq. (A6) since it cannot be counted as an actual food resource in the particular year where the land-clearances occurs but it is an important indirect factor, determining how much food can be produced in the following years.

Appendix B Figures

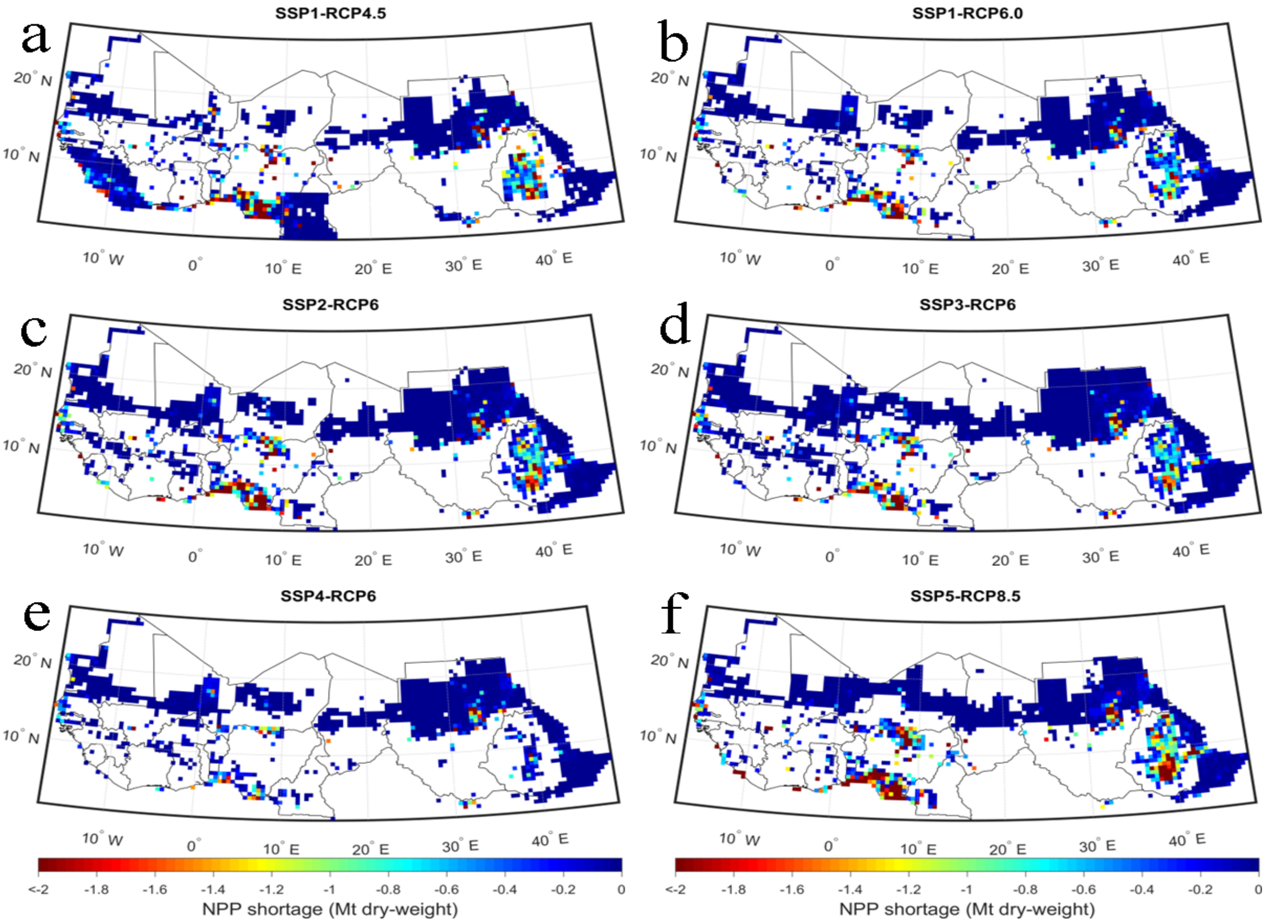

Fig. B1 Spatial distribution of NPP shortage in 2050 for the six most likely SSP-RCP combinations.

The future socio-economic and climatic scenarios are ordered in the panels as following: a) SSP1-RCP4.5, b) SSP1-RCP6.0, c) SSP2-RCP6.0, d) SSP3-RCP6.0, e) SSP4-RCP6.0 and f) SSP5-RCP8.5.

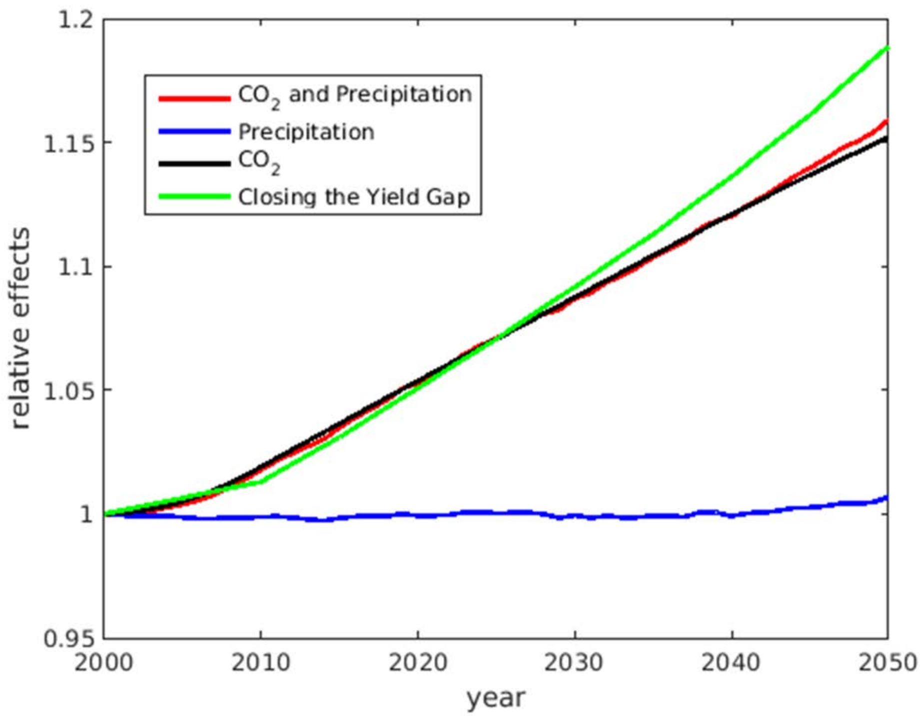

Fig. B2. The relative contributions of CO_2, precipitation and yield gap closure to the increase in NPP over the greater Sahel region, 2000-2050. Results for CO_2 and precipitation are from RCP 6.0 and yield gap is from SSP2. Simulated climate and CO_2 effects shown here are mean effects over the five GCMs (GFDL,MIROC,Hadley,NorESM, IPSL).

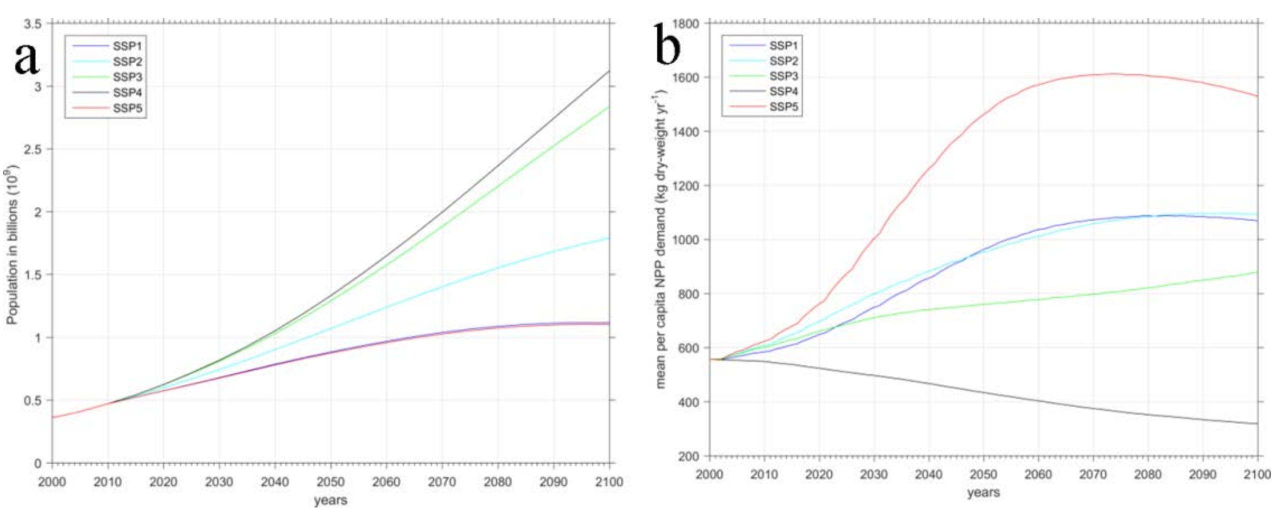

Fig. B3~~2~~ a) population growth scenarios of the greater Sahel region and b) mean per capita demand of Sahelian countries

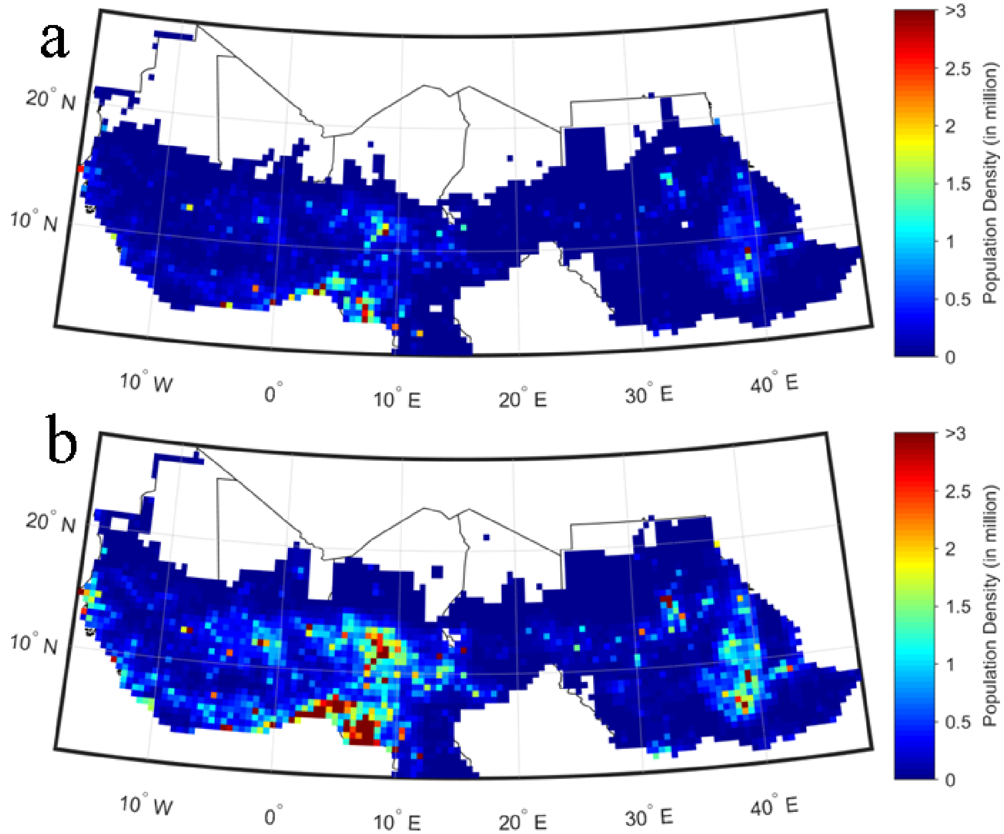

Fig. B4~~3~~ Distribution of population for SSP2-RCP6.0 for the years a) 2000 and b) 2050. Grid cells with less than one person per km^2 are excluded.

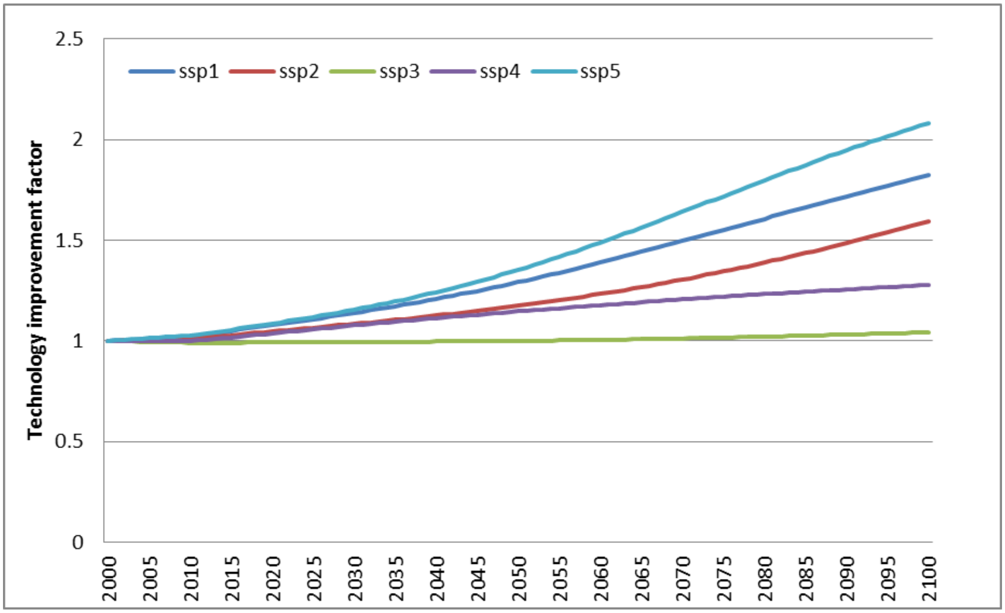

Fig. B5~~4~~ Development of mean technology improvement factor for all countries for the socio-economic pathways.

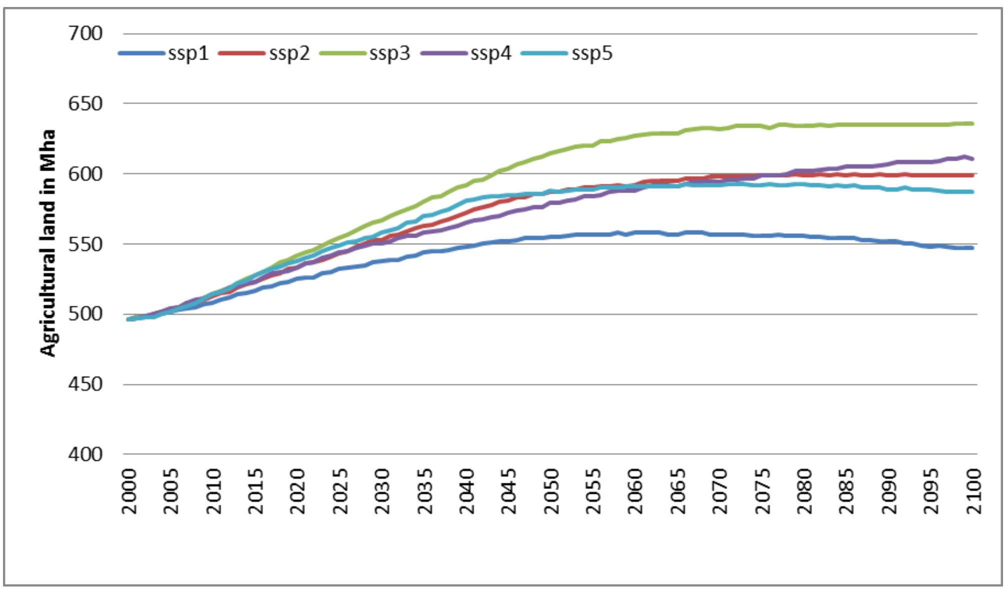

Fig. B6~~5~~ Expansion of total agricultural land, including grass- and cropland, in the Sahel for the socio-economic pathways

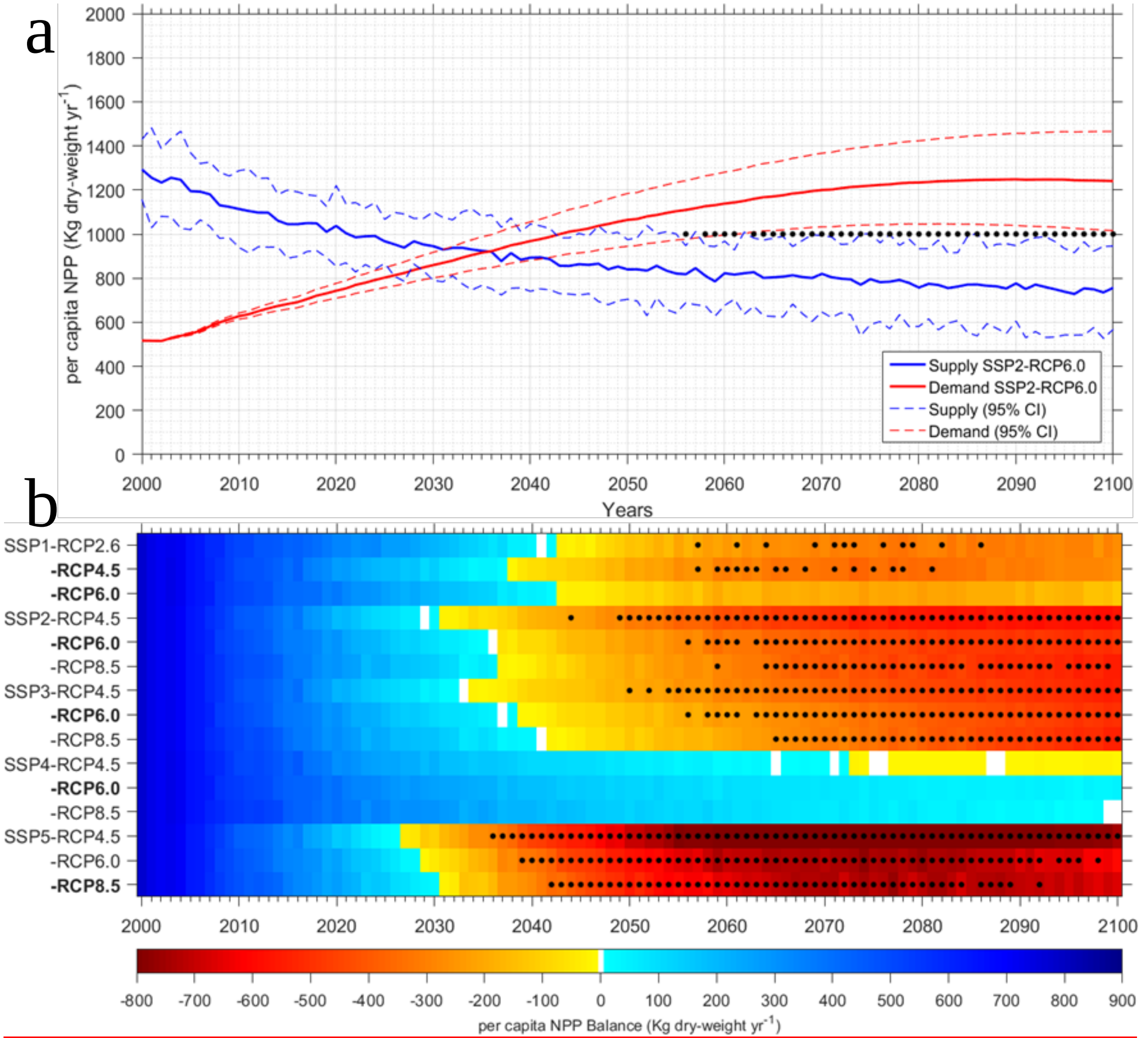

Fig. B7 Per capita NPP supply, demand and balance for the greater Sahel (2000-2100) without CO_2 fertilization. **B7a)** shows NPP supply (red) and demand (blue). The solid curves illustrate the mean of the SSP2-RCP6.0 combination. The dashed blue curves show supply uncertainty (95% confidence interval around the mean) based on the five GCMs NPP results. The dashed red curves show demand uncertainty (95% confidence interval around the mean) based on the uncertainty related to the interpretation and quantification of SSP2. **B7b)** shows the different magnitudes of the NPP balance and the varying onsets of shortage across all SSP-RCP combinations. Black dots illustrate years with a shortage outside of the 95% confidence intervals. Combinations are grouped according to the socio-economic scenarios (y-axis). The RCPs are ordered from low to high radiative forcing in each SSP group. The temporal trajectory is shown along the x-axis and the colouring indicates the sign of the annual NPP balance. Blues show a surplus of the NPP supply while yellow to red represent small to very large the gaps between supply and demand). SSP-RCP combinations in bold indicate the most likely SSP-RCP pairs based on Table 1.

Appendix C Tables

Table C1 Per capita NPP supply and demand of countries in the greater Sahel region for~~between~~ 2000 and 2050. Portions of food and feed (including grazing) in per capita NPP demand for SSP2-RCP6.0. All NPP is given in dry-weight (DW). Hurtt:PLUM scaling factors and land areas (from FAO) are also included.

Country	Per capita NPP supply [kg DW yr^{-1}]		Per capita NPP demand [kg DW yr^{-1}]		Food portions in per capita NPP demand [kg DW yr^{-1}]		Feed portions in per capita NPP demand[kg DW yr^{-1}]		Hurtt:PLUM scaling factors	Land Area from FAOSTAT
	2000	2050	2000	2050	2000	2050	2000	2050	2000	1000 ha
Benin	1341	607	474	874	99	92	375	782	0.89	11062
Burkina Faso	933	316	196	169	196	169	0	0	0.90	27360
Cameroon	2127	1173	387	717	90	82	297	635	1.04	47271
Chad	1878	1484	658	1157	120	116	538	1041	1.00	125920
Djibouti	0	0	134	120	134	120	0	0	0.00	2318
Eritrea	333	221	124	130	124	130	0	0	1.10	10100
Ethiopia	825	779	459	1439	135	157	323	1283	0.98	1000000
Gambia	1137	632	706	1082	168	142	539	940	1.58	1000
Ghana	1490	1291	274	1080	68	67	207	1013	1.03	22754
Guinea	1773	1697	402	1066	123	87	279	979	1.73	24572
Guinea Bissau	2319	1648	599	934	144	118	455	816	1.25	2812
Ivory Coast	1795	1549	282	811	95	75	188	736	0.98	31800
Liberia	1186	1312	212	1273	91	109	121	1164	0.91	9632
Mali	1929	1191	1111	1272	191	170	920	1102	0.97	122019
Mauritania	1129	1043	1530	1555	151	140	1379	1415	0.97	103070
Niger	3437	1426	1274	1540	210	202	1064	1338	1.01	126670
Nigeria	1059	719	321	923	139	139	182	784	1.04	91077
Senegal	925	539	556	837	155	137	401	699	0.74	19253
Sierra Leone	759	949	194	767	117	125	77	642	0.99	7162
Sudan	2517	1512	1530	1609	126	118	1404	1491	0.98	237600
Togo	2171	1491	271	653	127	124	144	529	1.10	5439
Mean[1]	1377	957	517	1064	-	-	-	-	-	-

[1] Weighted mean of per capita NPP measure using total population.

Table C2 Per capita NPP balances, mean, standard deviation and coefficient of variation for all SSP-RCP combinations for the year 2050. All values are given in Kg NPP dry-weight yr^{-1} except the dimensionless coefficient of variation.

2050	SSP1-RCP26	SSP1-RCP45	SSP1-RCP6	SSP2-RCP45	SSP2-RCP6	SSP2-RCP85	SSP3-RCP45	SSP3-RCP6	SSP3-RCP85	SSP4-RCP45	SSP4-RCP6	SSP4-RCP85	SSP5-RCP45	SSP5-RCP6	SSP5-RCP85	Mean	Standard deviation	Co-efficient of Variation
Benin	-288	-264	-290	-256	-267	-247	-95	-97	-84	148	118	150	-945	-968	-939	-288	364	1.3
Burkina Faso	261	257	258	147	147	152	78	78	82	93	95	98	244	244	251	166	75	0.5
Cameroon	604	134	627	47	456	526	91	439	500	258	621	679	-180	285	365	363	244	0.7
Chad	327	311	442	239	326	367	283	312	336	369	423	430	-13	205	314	311	108	0.3
Djibouti	-117	-117	-117	-120	-119	-120	-119	-119	-119	-101	-101	-101	-128	-128	-128	-117	9	0.1
Eritrea	113	142	138	94	91	87	69	67	64	75	73	69	121	117	111	95	26	0.3
Ethiopia	-498	-642	-444	-804	-660	-616	-560	-443	-410	-33	90	98	-1493	-1300	-1229	-596	455	0.8
Gambia	-464	-439	-424	-465	-449	-472	-328	-309	-328	-75	-57	-69	-842	-829	-851	-427	251	0.6
Ghana	289	362	437	151	211	226	253	297	302	488	513	506	-202	-122	-89	241	218	0.9
Guinea	915	675	968	403	631	644	395	603	611	584	808	754	347	633	646	641	170	0.3
Guinea Bissau	910	993	913	801	714	811	700	679	734	708	688	711	822	580	742	767	104	0.1
Ivory Coast	947	873	1044	586	737	773	513	645	680	700	780	785	546	734	780	742	138	0.2
Liberia	52	-1336	211	-1273	39	32	-686	292	290	-204	358	387	-2774	-934	-942	-433	859	2.0
Mali	-113	-123	-24	-147	-81	27	-103	-80	4	-48	12	83	-451	-305	-124	-98	129	1.3
Mauritania	-474	-475	-505	-502	-512	-527	-454	-449	-453	-382	-406	-424	-640	-663	-696	-504	90	0.2
Niger	117	183	247	-151	-114	-148	-290	-271	-303	-7	58	42	-315	-246	-265	-98	184	1.9
Nigeria	-95	-150	-77	-267	-204	-165	-132	-84	-52	135	162	184	-663	-581	-535	-168	248	1.5
Senegal	-119	-134	-202	-240	-297	-238	-205	-249	-193	-25	-51	-26	-421	-508	-429	-222	141	0.6
Sierra Leone	277	-728	334	-767	183	176	-493	217	215	-173	252	260	-1376	-115	-95	-122	487	4.0
Sudan	-44	-49	10	-144	-97	-91	-177	-139	-108	-30	14	-7	-281	-211	-227	-105	87	0.8
Togo	916	998	1022	827	838	842	794	788	789	870	887	894	547	568	581	811	139	0.2
Mean[1]	1	-84	47	-212	-107	-76	-119	-39	-12	131	200	213	-570	-428	-384	-96	217	2.3

[1]Weighted mean using national population data as weight.

References

Abdi, A. M., Seaquist, J., Tenenbaum, D. E., Eklundh, L., and Ardo, J.: The supply and demand of net primary production in the Sahel, Environmental Research Letters, 9, 094003, 2014.

Ahlström, A., Xia, J. Y., Arneth, A., Luo, Y., and Smith, B.: Importance of vegetation dynamics for future terrestrial carbon cycling, Environmental Research Letters, 10, 054019, 2015.

Ahmed, S. A., Diffenbaugh, N. S., Hertel, T. W., and Martin, W. J.: Agriculture and Trade Opportunities for Tanzania: Past Volatility and Future Climate Change, Review of Development Economics, 16, 429-447, 2012.

Alexander, P., Prestele, R., Verburg, P. H., Arneth, A., Baranzelli, C., Batista, E. S. F., Brown, C., Butler, A., Calvin, K., Dendoncker, N., Doelman, J. C., Dunford, R., Engstrom, K., Eitelberg, D., Fujimori, S., Harrison, P. A., Hasegawa, T., Havlik, P., Holzhauer, S., Humpenoder, F., Jacobs-Crisioni, C., Jain, A. K., Krisztin, T., Kyle, P., Lavalle, C., Lenton, T., Liu, J., Meiyappan, P., Popp, A., Powell, T., Sands, R. D., Schaldach, R., Stehfest, E., Steinbuks, J., Tabeau, A., van Meijl, H., Wise, M. A., and Rounsevell, M. D.: Assessing uncertainties in land cover projections, Glob Chang Biol, doi: 10.1111/gcb.13447, 2016. n/a-n/a, 2016.

Ardö, J. Comparison between remote sensing and a dynamic vegetation model for estimating terrestrial primary production of Africa. Carbon Balance and Management, 10(8), 2015.

Balogun, O., Yusuf, S., and Ayantoye, K.: The threats of climate change: implication for food crisis in sub-sahara Africa. In: Sustainable Food Security in the Era of Local and Global Environmental Change, Behnassi, M., Pollmann, O., and Kissinger, G. (Eds.), Springer, Dordrecht, 2013.

Barbier, B., Yacouba, H., Karambiri, H., Zoromé, M., and Somé, B.: Human Vulnerability to Climate Variability in the Sahel: Farmers' Adaptation Strategies in Northern Burkina Faso, Environmental Management, 43, 790-803, 2009.

Boke-Olén, N., Abdi, A. M., Hall, O., and Lehsten, V.: H~~A h~~igh resolution population projections ~~dataset for~~ ~~African future population developed with RCP and SSP scenarios for 2000 – 2100~~from radiative forcing and socio-economic models, 2000-2100,, ~~Nature~~ Scientific Data, ~~*in review at Nature Scientific Data, submitted july 2016. in review at Nature Scientific Data, submitted july 2016.*~~*4,160130, 2017.*

Brandt, M., Mbow, C., Diouf, A. A., Verger, A., Samimi, C., and Fensholt, R.: Ground- and satellite-based evidence of the biophysical mechanisms behind the greening Sahel, Global Change Biology, 21, 1610-1620, 2015.

Brown, M. E.: Remote sensing technology and land use analysis in food security assessment, Journal of Land Use Science, 11, 623-641, 2016.

Burnham, K. P. and Anderson, D. R.: Model Selection and Multimodal Inference. A Practical Information-Theoretic Approach, Springer, New York, 2002.

Campbell, M. M., Casterline, J., Castillo, F., Graves, A., Hall, T. L., May, J. F., Perlman, D., Potts, M., Speidel, J. J., Walsh, J., Wehner, M. F., and Zulu, E. M.: Population and climate change: who will the grand convergence leave behind?, The Lancet Global Health, 2, e253-e254, 2014.

Canadell, J. G. and Schulze, E. D.: Global potential of biospheric carbon management for climate mitigation, Nat Commun, 5, 5282, 2014.

Ceccato, P., Cressman, K., Giannini, A., and Trzaska, S.: The desert locust upsurge in West Africa (2003-2005): Information on the desert locust early warning system and the prospects for seasonal climate forecasting, International Journal of Pest Management, 53, 7-13, 2007.

Chidumayo, E. N. and Gumbo, D. J.: The dry forests and woodlands of Africa : managing for products and services, Routledge, London, 2010.

Collins, M., Knutti, R., Arblaster, J., Dufresne, J.-L., Fichefet, T., Friedlingstein, P., Gao, X., Gutowski, W. J., Johns, T., Krinner, G., Shongwe, M., Tebaldi, C., Weaver, A. J., and Wehner, M.: Long-term Climate Change: Projections, Commitments and Irreversibility. In: Climate Change 2013: The Physical Science Basis. Contribution of Working Group I to the Fifth Assessment Report of the Intergovernmental Panel on Climate Change, Stocker, T. F., Qin, D., Plattner, G.-K., Tignor, M., Allen, S. K., Boschung, J., Nauels, A., Xia, Y., Bex, V., and Midgley, P. M. (Eds.), Cambridge University Press, Cambridge, United Kingdom and New York, NY, USA, 2013.

D'Odorico, P., Carr, J. A., Laio, F., Ridolfi, L., and Vandoni, S.: Feeding humanity through global food trade, Earths Future, 2, 458-469, 2014.

Del Grosso, S., Parton, W., Stohlgren, T., Zheng, D., Bachelet, D., Prince, S., Hibbard, K., and Olson, R.: Global potential net primary production predicted from vegetation class, precipitation, and temperature, Ecology, 89, 2117-2126, 2008.

Dile, Y. T., Karlberg, L., Temesgen, M., and Rockstrom, J.: The role of water harvesting to achieve sustainable agricultural intensification and resilience against water related shocks in sub-Saharan Africa, Agr Ecosyst Environ, 181, 69-79, 2013.

Dufresne, J. L., Foujols, M. A., Denvil, S., Caubel, A., Marti, O., Aumont, O., Balkanski, Y., Bekki, S., Bellenger, H., Benshila, R., Bony, S., Bopp, L., Braconnot, P., Brockmann, P., Cadule, P., Cheruy, F., Codron, F., Cozic, A., Cugnet, D., de Noblet, N., Duvel, J. P., Ethe, C., Fairhead, L., Fichefet, T., Flavoni, S., Friedlingstein, P., Grandpeix, J. Y., Guez, L., Guilyardi, E., Hauglustaine, D., Hourdin, F., Idelkadi, A., Ghattas, J., Joussaume, S., Kageyama, M., Krinner, G., Labetoulle, S., Lahellec, A., Lefebvre, M. P., Lefevre, F., Levy, C., Li, Z. X., Lloyd, J., Lott, F., Madec, G., Mancip, M., Marchand, M., Masson, S., Meurdesoif, Y., Mignot, J., Musat, I., Parouty, S., Polcher, J., Rio, C., Schulz, M., Swingedouw, D., Szopa, S., Talandier, C., Terray, P., Viovy, N., and Vuichard, N.: Climate change projections using the IPSL-CM5 Earth System Model: from CMIP3 to CMIP5, Climate Dynamics, 40, 2123-2165, 2013.

Dunne, J. P., John, J. G., Shevliakova, E., Stouffer, R. J., Krasting, J. P., Malyshev, S. L., Milly, P. C. D., Sentman, L. T., Adcroft, A. J., Cooke, W., Dunne, K. A., Griffies, S. M., Hallberg, R. W., Harrison, M. J., Levy, H., Wittenberg, A. T., Phillips, P. J., and Zadeh, N.: GFDL's ESM2 Global Coupled Climate-Carbon Earth System Models. Part II: Carbon System Formulation and Baseline Simulation Characteristics, Journal of Climate, 26, 2247-2267, 2013.

Eklundh, L. and Olsson, L.: Vegetation index trends for the African Sahel 1982–1999, Geophysical Research Letters, 30, n/a-n/a, 2003.

Elliott, J., Deryng, D., Müller, C., Frieler, K., Konzmann, M., Gerten, D., Glotter, M., Flörke, M., Wada, Y., Best, N., Eisner, S., Fekete, B.M., Folberth, C., Foster, I., Gosling, S.N., Haddeland, I., Khabarov, N., Ludwig, F., Masaki, Y., Olin, S., Rosenzweig, C., Ruane, A.C., Satoh, Y., Schmid, E., Stacke, T., Tang, Q., Wisser, D. Constraints and potentials of future irrigation water availability on agricultural production under climate change. Proc. Natl. Acad. Sci. U.S.A. 111, 3239–44. doi:10.1073/pnas.1222474110, 2014

Engström, K., Lindeskog, M., Olin, S., Hassler, J., and Smith, B.: Impacts of climate mitigation strategies in the energy sector on global land use and carbon balance, Earth System Dynamics Discussions, 2016, 1-43, 2016a.

Engström, K., Olin, S., Rounsevell, M. D. A., Brogaard, S., van Vuuren, D. P., Alexander, P., Murray-Rust, D., and Arneth, A.: Assessing uncertainties in global cropland futures using a conditional probabilistic modelling framework, Earth System Dynamics Discussions, 2016, 1-33, 2016b.

Engström, K., Rounsevell, M. D. A., Murray-Rust, D., Hardacre, C., Alexander, P., Cui, X. F., Palmer, P. I., and Arneth, A.: Applying Occam's razor to global agricultural land use change, Environmental Modelling & Software, 75, 212-229, 2016c.

FAO: The Digitized Soil Map of the World (Release 1.0). World Soil Resources Report 67/1., Food and Agriculture Organization of the United Nations, Rome., 1991. 1991.

FAOSTAT: FAO Statistical Databases. Food and Agriculture Organization of the United Nations, Rome, Italy., 2015.

FAOSTAT: Food Aid Shipments (WFP), last access 2016/08/16. http://faostat3.fao.org/download/X/FA/E, 2016.

Foley, J. A.: Net Primary Productivity in the Terrestrial Biosphere - the Application of a Global-Model, J Geophys Res-Atmos, 99, 20773-20783, 1994.

Foley, J. A., Defries, R., Asner, G. P., Barford, C., Bonan, G., Carpenter, S. R., Chapin, F. S., Coe, M. T., Daily, G. C., Gibbs, H. K., Helkowski, J. H., Holloway, T., Howard, E. A., Kucharik, C. J., Monfreda, C., Patz, J. A., Prentice, I. C., Ramankutty, N., and Snyder, P. K.: Global consequences of land use, Science, 309, 570-574, 2005.

Foley, J. A., Ramankutty, N., Brauman, K. A., Cassidy, E. S., Gerber, J. S., Johnston, M., Mueller, N. D., O'Connell, C., Ray, D. K., West, P. C., Balzer, C., Bennett, E. M., Carpenter, S. R., Hill, J., Monfreda, C., Polasky, S., Rockstrom, J., Sheehan, J., Siebert, S., Tilman, D., and Zaks, D. P.: Solutions for a cultivated planet, Nature, 478, 337-342, 2011.

Friend, A.D., Lucht, W., Rademacher, T.T., Keribin, R., Betts, R., Cadule, P., Ciais, P., Clark, D.B., Dankers, R., Falloon, P.D., Ito, A., Kahana, R., Kleidon, A., Lomas, M.R., Nishina, K., Ostberg, S., Pavlick, R., Peylin, P., Schaphoff, S., Vuichard, N., Warszawski, L., Wiltshire, A., Woodward, F.I., 2014. Carbon residence time dominates uncertainty in terrestrial vegetation responses to future climate and atmospheric CO_2. Proc. Natl. Acad. Sci. U. S. A. 111, 3280–3285. doi:10.1073/pnas.1222477110

Gerten, D., Schaphoff, S., Haberlandt, U., Lucht, W., and Sitch, S.: Terrestrial vegetation and water balance - hydrological evaluation of a dynamic global vegetation model, J Hydrol, 286, 249-270, 2004.

Godfray, H. C., Beddington, J. R., Crute, I. R., Haddad, L., Lawrence, D., Muir, J. F., Pretty, J., Robinson, S., Thomas, S. M., and Toulmin, C.: Food security: the challenge of feeding 9 billion people, Science, 327, 812-818, 2010.

Gonzalez, P., Neilson, R. P., Lenihan, J. M., and Drapek, R. J.: Global patterns in the vulnerability of ecosystems to vegetation shifts due to climate change, Global Ecology and Biogeography, 19, 755-768, 2010.

Haberl, H., Erb, K. H., Krausmann, F., Gaube, V., Bondeau, A., Plutzar, C., Gingrich, S., Lucht, W., and Fischer-Kowalski, M.: Quantifying and mapping the human appropriation of net primary production in earth's terrestrial ecosystems, Proc Natl Acad Sci U S A, 104, 12942-12947, 2007.

Harris, I., Jones, P. D., Osborn, T. J., and Lister, D. H.: Updated high-resolution grids of monthly climatic observations - the CRU TS3.10 Dataset, International Journal of Climatology, 34, 623-642, 2014.

Harrison, P. A., Dunford, R. W., Holman, I. P., and Rounsevell, M. D. A.: Climate change impact modelling needs to include cross-sectoral interactions, Nature Clim. Change, advance online publication, 2016.

Hempel, S., Frieler, K., Warszawski, L., Schewe, J., and Piontek, F.: A trend-preserving bias correction; the ISI-MIP approach, Earth Syst. Dynam., 4, 219-236, 2013.

Herrmann, S. M., Sall, I., and Sy, O.: People and pixels in the Sahel: a study linking coarse-resolution remote sensing observations to land users' perceptions of their changing environment in Senegal, Ecology and Society, 19, 2014.

Hertel, T. W.: The challenges of sustainably feeding a growing planet, Food Security, 7, 185-198, 2015.

Hickler, T., Eklundh, L., Seaquist, J. W., Smith, B., Ardo, J., Olsson, L., Sykes, M. T., and Sjostrom, M.: Precipitation controls Sahel greening trend, Geophysical Research Letters, 32, L21415, 2005.

Hickler, T., Smith, B., Prentice, I. C., Mjöfors, K., Miller, P., Arneth, A., and Sykes, M. T.: CO_2fertilization in temperate FACE experiments not representative of boreal and tropical forests, Global Change Biology, 14, 1531-1542, 2008.

Hurtt, G. C., Chini, L. P., Frolking, S., Betts, R. A., Feddema, J., Fischer, G., Fisk, J. P., Hibbard, K., Houghton, R. A., Janetos, A., Jones, C. D., Kindermann, G., Kinoshita, T., Goldewijk, K. K., Riahi, K., Shevliakova, E., Smith, S., Stehfest, E., Thomson, A., Thornton, P., van Vuuren, D. P., and Wang, Y. P.: Harmonization of land-use scenarios for the period 1500-2100: 600 years of global gridded annual land-use transitions, wood harvest, and resulting secondary lands, Climatic Change, 109, 117-161, 2011.

Ibrahim, F. N.: Causes of the Famine among the Rural Population of the Sahelian Zone of the Sudan, GeoJournal, 17, 133-141, 1988.

IPCC: 2006 IPCC Guidelines for National Greenhouse Gas Inventories. Volume 4: Agriculture, Forestry, and Other Land Use., IGES, 2006.

Iversen, T., Bentsen, M., Bethke, I., Debernard, J. B., Kirkevåg, A., Seland, Ø., Drange, H., Kristjansson, J. E., Medhaug, I., Sand, M., and Seierstad, I. A.: The Norwegian Earth System Model, NorESM1-M – Part 2: Climate response and scenario projections, Geosci. Model Dev., 6, 389-415, 2013.

Jackson, R. B., Canadell, J., Ehleringer, J. R., Mooney, H. A., Sala, O. E., and Schulze, E. D.: A global analysis of root distributions for terrestrial biomes, Oecologia, 108, 389-411, 1996.

Kastner, T., Rivas, M. J., Koch, W., and Nonhebel, S.: Global changes in diets and the consequences for land requirements for food, Proc Natl Acad Sci U S A, 109, 6868-6872, 2012.

Kearney, J.: Food consumption trends and drivers, Philos Trans R Soc Lond B Biol Sci, 365, 2793-2807, 2010.

Kebede, A. S., Dunford, R., Mokrech, M., Audsley, E., Harrison, P. A., Holman, I. P., Nicholls, R. J., Rickebusch, S., Rounsevell, M. D. A., Sabaté, S., Sallaba, F., Sanchez, A., Savin, C., Trnka, M., and Wimmer, F.: Direct and indirect impacts of climate and socio-economic change in Europe: a sensitivity analysis for key land- and water-based sectors, Climatic Change, 128, 261-277, 2015.

Kottek, M., Grieser, J., Beck, C., Rudolf, B., and Rubel, F.: World map of the Koppen-Geiger climate classification updated, Meteorologische Zeitschrift, 15, 259-263, 2006.

Körner, C. Plant CO_2 responses: an issue of definition, time and resource supply. New Phytol. 172, 393–411. Pugh, T.A.M., Müller, C., Arneth, A., Haverd, V., Smith, B., 2016. Key knowledge and data gaps in modelling the influence of CO2 concentration on the terrestrial carbon sink. J. Plant Physiol. 203, 3–15. doi:10.1016/j.jplph.2016.05.001, 2006.

Kwakkel, J. H. and Pruyt, E.: Exploratory Modeling and Analysis, an approach for model-based foresight under deep uncertainty, Technological Forecasting and Social Change, 80, 419-431, 2013.

Lamarque, J. F., Bond, T. C., Eyring, V., Granier, C., Heil, A., Klimont, Z., Lee, D., Liousse, C., Mieville, A., Owen, B., Schultz, M. G., Shindell, D., Smith, S. J., Stehfest, E., Van Aardenne, J., Cooper, O. R., Kainuma, M., Mahowald, N., McConnell, J. R., Naik, V., Riahi, K., and van Vuuren, D. P.: Historical (1850-2000) gridded anthropogenic and biomass burning emissions of reactive gases and aerosols: methodology and application, Atmos Chem Phys, 10, 7017-7039, 2010.

Licker, R., Johnston, M., Foley, J. A., Barford, C., Kucharik, C. J., Monfreda, C., and Ramankutty, N.: Mind the gap: how do climate and agricultural management explain the ‘yield gap’ of croplands around the world?, Global Ecology and Biogeography, 19, 769-782, 2010.

Lindeskog, M., Arneth, A., Bondeau, A., Waha, K., Seaquist, J., Olin, S., and Smith, B.: Implications of accounting for land use in simulations of ecosystem carbon cycling in Africa, Earth Syst. Dynam., 4, 385-407, doi:10.5194/esd-4-385-2013, 2013.

Luyssaert, S., Inglima, I., and Jung, M. Global Forest Ecosystem Structure and Function Data for Carbon Balance Research. Global Forest Ecosystem Structure and Function Data for Carbon Balance Research. Data set. Available on-line [http://daac.ornl.gov/] from Oak Ridge National Laboratory Distributed Active Archive Center, Oak Ridge, Tennessee, U.S.A. doi:10.3334/ORNLDAAC/949, 2009.

Lynch, K., Binns, T., and Olofin, E.: Urban agriculture under threat - The land security question in Kano, Nigeria, Cities, 18, 159-171, 2001.

Metzger, M. J., Bunce, R. G. H., Jongman, R. H. G., Sayre, R., Trabucco, A., and Zomer, R.: A high-resolution bioclimate map of the world: a unifying framework for global biodiversity research and monitoring, Global Ecology and Biogeography, 22, 630-638, 2013.

Michaletz, S. T., Cheng, D., Kerkhoff, A.J., and Enquist, B.J.. Convergence of terrestrial plant production across global climate gradients. Nature 512:39-43, 2014.

Mitchell, T. D. and Jones, P. D.: An improved method of constructing a database of monthly climate observations and associated high-resolution grids, International Journal of Climatology, 25, 693-712, 2005.

Mokany, K., Raison, R. J., and Prokushkin, A. S.: Critical analysis of root : shoot ratios in terrestrial biomes, Global Change Biology, 12, 84-96, 2006.

Mueller, N. D., Gerber, J. S., Johnston, M., Ray, D. K., Ramankutty, N., and Foley, J. A.: Closing yield gaps through nutrient and water management, Nature, 490, 254-257, 2012.

Olin, S., Lindeskog, M., Pugh, T.A.M., Schurgers, G., Wårlind, D., Mishurov, M., Zaehle, S., Stocker, B.D., Smith, B., and Arneth, A..: Soil carbon management in large-scale Earth system modelling: implications for crop yields and nitrogen leaching, Earth System Dynamics, 6, 745-768, 2015.

O'Neill, B. C., Kriegler, E., Riahi, K., Ebi, K. L., Hallegatte, S., Carter, T. R., Mathur, R., and van Vuuren, D. P.: A new scenario framework for climate change research: the concept of shared socioeconomic pathways, Climatic Change, 122, 387-400, 2014.

O’Neill, B. C., Kriegler, E., Ebi, K. L., Kemp-Benedict, E., Riahi, K., Rothman, D. S., van Ruijven, B. J., van Vuuren, D. P., Birkmann, J., Kok, K., Levy, M., and Solecki, W.: The roads ahead: Narratives for shared socioeconomic pathways describing world futures in the 21st century, Global Environmental Change, ~~—~~42, 169-180, 2017.~~doi: 10.1016/j.gloenvcha.2015.01.004, *in press*. *in press*~~.

Olson, D. M., Dinerstein, E., Wikramanayake, E. D., Burgess, N. D., Powell, G. V. N., Underwood, E. C., D'amico, J. A., Itoua, I., Strand, H. E., Morrison, J. C., Loucks, C. J., Allnutt, T. F., Ricketts, T. H., Kura, Y., Lamoreux, J. F., Wettengel, W. W., Hedao, P., and Kassem, K. R.: Terrestrial Ecoregions of the World: A New Map of Life on Earth: A new global map of terrestrial ecoregions provides an innovative tool for conserving biodiversity, BioScience, 51, 933-938, 2001.

Olsson, L.: On the Causes of Famine Drought, Desertification and Market Failure in the Sudan, Ambio, 22, 395-403, 1993.

Owuor, S.: Migrants, urban poverty and the changing nature of urban-rural linkages in Kenya, Development Southern Africa, 24, 109-122, 2007.

Pinstrup-Andersen, P.: Food security: definition and measurement, Food Security, 1, 5-7, 2009.

Pretty, J.: Agricultural sustainability: concepts, principles and evidence, Philos Trans R Soc Lond B Biol Sci, 363, 447-465, 2008.

Pretty, J.: Sustainable intensification in Africa, International Journal of Agricultural Sustainability, 9, 3-4, 2011.

Pugh, T. A. M., Arneth, A., Olin, S., Ahlström, A., Bayer, A. D., Goldewijk, K. K., Lindeskog, M., and Schurgers, G.: Simulated carbon emissions from land-use change are substantially enhanced by accounting for agricultural management, Environmental Research Letters, 10, 124008, 2015.

Pugh, T.A.M., Müller, C., Arneth, A., Haverd, V., Smith, B. Key knowledge and data gaps in modelling the influence of CO_2 concentration on the terrestrial carbon sink. J. Plant Physiol. 203, 3–15. doi:10.1016/j.jplph.2016.05.001, 2016.

Ramankutty, N., Evan, A. T., Monfreda, C., and Foley, J. A.: Farming the planet: 1. Geographic distribution of global agricultural lands in the year 2000, Global Biogeochem Cy, 22, n/a-n/a, 2008.

Ray, D. K., Mueller, N. D., West, P. C., and Foley, J. A.: Yield Trends Are Insufficient to Double Global Crop Production by 2050, PLoS ONE, 8, e66428, 2013.

Reich, P. F. and Eswaran, H.: Global resources. In: Lal, R. (ed.). Encyclopedia of Soil Science, pp. 607-611. Marcel Dekker, New York., 2002. 2002.

Rosenzweig, C., Elliott, J., Deryng, D., Ruane, A.C., Müller, C., Arneth, A., Boote, K.J., Folberth, C., Glotter, M., Khabarov, N., Neumann, K., Piontek, F., Pugh, T.A.M., Schmid, E., Stehfest, E., Yang, H., Jones, J.W..Assessing agricultural risks of climate change in the 21st century in a global gridded crop model intercomparison. Proc. Natl. Acad. Sci. U.S.A. 111, 3268–73. doi:10.1073/pnas.1222463110, 2014.

Running, S. W.: A regional look at HANPP: human consumption is increasing, NPP is not, Environmental Research Letters, 9, 111003, 2014.

Running, S. W., Nemani, R. R., Heinsch, F. A., Zhao, M., Reeves, M., and Hashimoto, H.: A Continuous Satellite-Derived Measure of Global Terrestrial Primary Production, BioScience, 54, 547-560, 2004.

Sallaba, F., Lehsten, D., Seaquist, J., and Sykes, M. T.: A rapid NPP meta-model for current and future climate and CO2 scenarios in Europe, Ecological Modelling, 302, 29-41, 2015.

Schwarz, G.: Estimating the Dimension of a Model, doi: 10.1214/aos/1176344136, 1978. 461-464, 1978.

Seaquist, J. W., Hickler, T., Eklundh, L., Ardo, J., and Heumann, B. W.: Disentangling the effects of climate and people on Sahel vegetation dynamics, Biogeosciences, 6, 469-477, 2009.

Sitch, S., Smith, B., Prentice, I. C., Arneth, A., Bondeau, A., Cramer, W., Kaplan, J. O., Levis, S., Lucht, W., Sykes, M. T., Thonicke, K., and Venevsky, S.: Evaluation of ecosystem dynamics, plant geography and terrestrial carbon cycling in the LPJ dynamic global vegetation model, Global Change Biology, 9, 161-185, 2003.

Smith, B., Prentice, I. C., and Sykes, M. T.: Representation of vegetation dynamics in the modelling of terrestrial ecosystems: comparing two contrasting approaches within European climate space, Global Ecology and Biogeography, 10, 621-637, 2001.

Smith, W.K., Reed, S.C., Cleveland, C.C., Ballantyne, A.P., Anderegg, W.R.L., Wieder, W.R., Liu, Y.Y. & Running, S.W. Large divergence of satellite and Earth system model estimates of global terrestrial CO2 fertilization. Nat. Clim. Chang., 6, 306–310, 2016..

Smith, B., Warlind, D., Arneth, A., Hickler, T., Leadley, P., Siltberg, J., and Zaehle, S.: Implications of incorporating N cycling and N limitations on primary production in an individual-based dynamic vegetation model, Biogeosciences, 11, 2027-2054, 2014.

Smith, J. U. and Smith, P.: Introduction to environmental modelling, Oxford University Press, Oxford ; New York, 2007.

Smith, P.: Delivering food security without increasing pressure on land, Glob Food Secur-Agr, 2, 18-23, 2013.

Smith, P., Smith, J. U., Powlson, D. S., McGill, W. B., Arah, J. R. M., Chertov, O. G., Coleman, K., Franko, U., Frolking, S., Jenkinson, D. S., Jensen, L. S., Kelly, R. H., Klein-Gunnewiek, H., Komarov, A. S., Li, C., Molina, J. A. E., Mueller, T., Parton, W. J., Thornley, J. H. M., and Whitmore, A. P.: A comparison of the performance of nine soil organic matter models using datasets from seven long-term experiments, Geoderma, 81, 153-225, 1997.

Tang, G. P., Beckage, B., Smith, B., and Miller, P. A.: Estimating potential forest NPP, biomass and their climatic sensitivity in New England using a dynamic ecosystem model, Ecosphere, 1, art18, 2010.

Tilman, D., Balzer, C., Hill, J., and Befort, B. L.: Global food demand and the sustainable intensification of agriculture, Proc Natl Acad Sci U S A, 108, 20260-20264, 2011.

Trenberth, K. E., Dai, A., van der Schrier, G., Jones, P.D., Barichivich, J., Briffa, K.R., and Sheffield, J. Global warming and changes in drought. Nature Clim. Change, 4:17-22, 2014.

Tschirley, D., Reardon, T., Dolislager, M., and Snyder, J.: The Rise of a Middle Class in East and Southern Africa: Implications for Food System Transformation, Journal of International Development, 27, 628-646, 2015.

UN: United Nations. Transforming our world: The 2030 Agenda for sustainable development. , 2016.

United Nations: Sahel Regional Strategy Mid-Year Review 2013, United Nations Office for the Coordination of Humanitarian Affairs, 2013.

van Vuuren, D. P., de Vries, B., Beusen, A., and Heuberger, P. S. C.: Conditional probabilistic estimates of 21st century greenhouse gas emissions based on the storylines of the IPCC-SRES scenarios, Global Environmental Change, 18, 635-654, 2008.

van Vuuren, D. P., Edmonds, J., Kainuma, M., Riahi, K., Thomson, A., Hibbard, K., Hurtt, G. C., Kram, T., Krey, V., Lamarque, J.-F., Masui, T., Meinshausen, M., Nakicenovic, N., Smith, S. J., and Rose, S. K.: The representative concentration pathways: an overview, Climatic Change, 109, 5-31, 2011.

van Vuuren, D. P., Kriegler, E., O'Neill, B. C., Ebi, K. L., Riahi, K., Carter, T. R., Edmonds, J., Hallegatte, S., Kram, T., Mathur, R., and Winkler, H.: A new scenario framework for Climate Change Research: scenario matrix architecture, Climatic Change, 122, 373-386, 2013.

Watanabe, M., Chikira, M., Imada, Y., and Kimoto, M.: Convective Control of ENSO Simulated in MIROC, Journal of Climate, 24, 543-562, 2011.

Wieder, W.R., Cleveland, C.C., Smith, W.K. & Todd-Brown, K. Future productivity and carbon storage limited by terrestrial nutrient availability. Nat. Geosci., 1–5, 2015.

Willmott, C. J., Robeson, S. M., and Matsuura, K.: A refined index of model performance, International Journal of Climatology, 32, 2088-2094, 2012.

Wirsenius, S.: Human use of land and organic materials: modeling the turnover of biomass in the global food system., Doctor of Philosophy, Department of Physical Resource Theory, Chalmers University of Technology, Gothenburg, 2000.

Yengoh, G. T. and Ardö, J.: Crop yield gaps in Cameroon, Ambio, 43, 175-190, 2014.

Figures

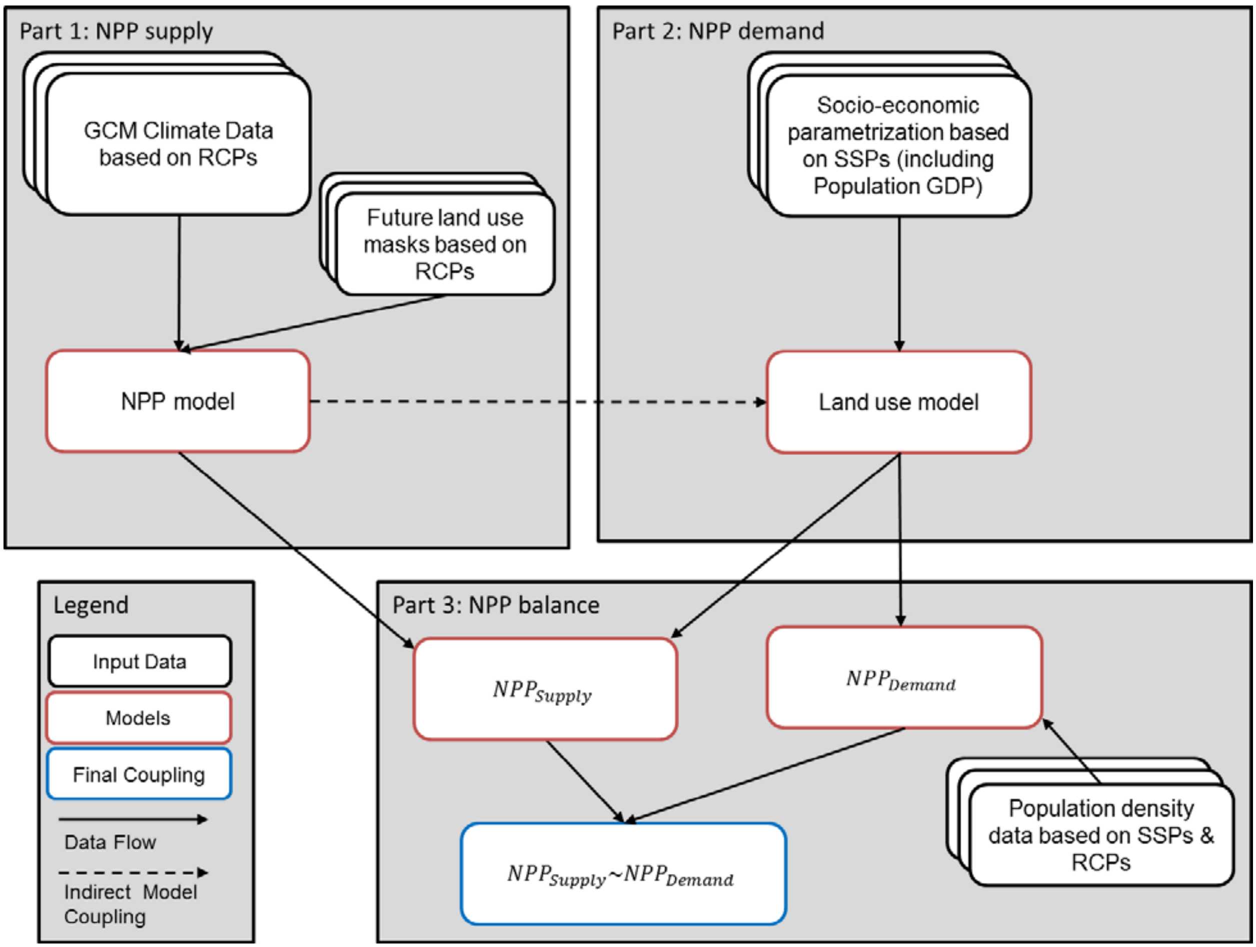

Fig. 1 Conceptual logic of the modelling framework. The framework is based on three components enclose by three grey boxes: (1) $\boldsymbol{NPP_{supply}}$, (2) $\boldsymbol{NPP_{demand}}$ and (3) $\boldsymbol{NPP_{balance}}$. The white boxes indicate data inputs originating from modelling studies (as referenced in section 2.2). The main models and equations are given in the boxes outlined in red, where solid arrows show the data flow. The dashed arrow between *NPP model* (section 2.1.1) and *Land use model* (section 2.1.2) represents an indirect model coupling for areas of cropland and pasture. The box outlined in blue indicates the final coupling allowing the assessment of $\boldsymbol{NPP_{supply}}$ and $\boldsymbol{NPP_{demand}}$.

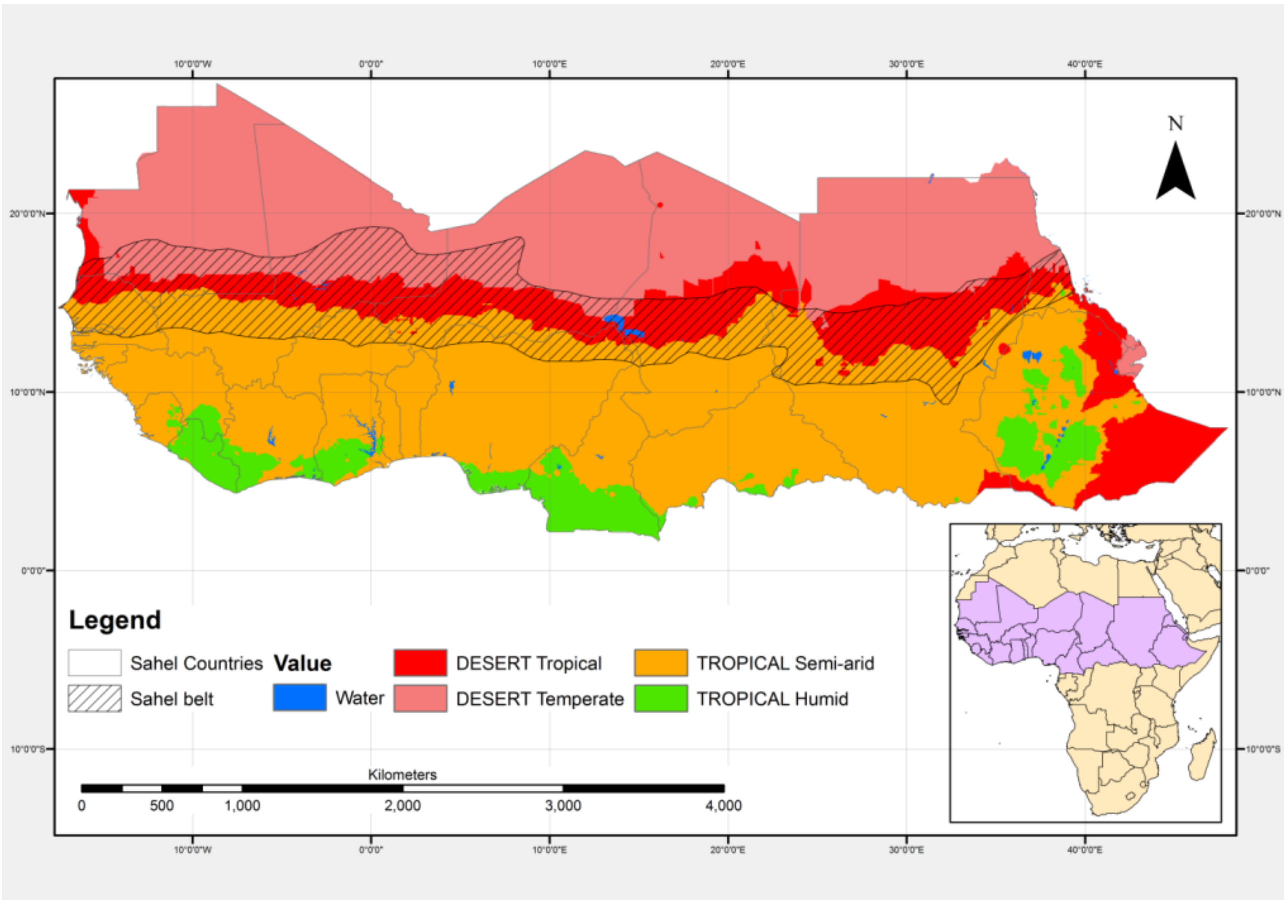

Fig. 2 Major Biome Map from year 2000 for greater Sahel region. The hatched area shows the traditionally-defined Sahel, where annual rainfall ranges from 100mm to 600mm. The Major Biome Map is based on Reich and Eswaran (2002).

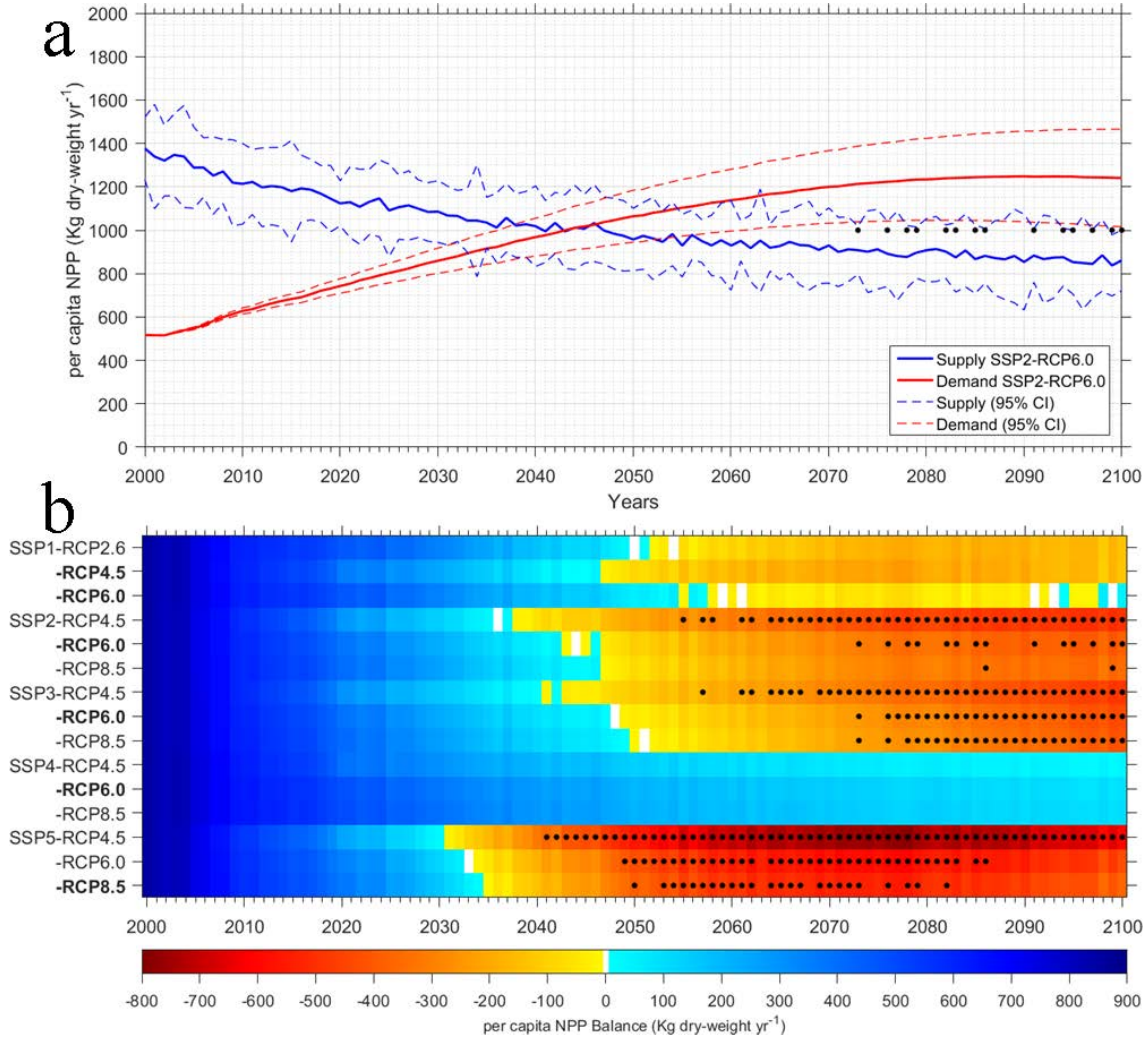

Fig. 3 The per capita NPP supply, demand and balance for the entire Sahel region over the time period. **3a)** shows NPP supply (red) and demand (blue). The solid curves illustrate the mean of the SSP2-RCP6.0 combination. The dashed blue curves show supply uncertainty (95% confidence interval around the mean) based on the five GCMs NPP results. The dashed red curves show demand uncertainty (95% confidence interval around the mean) based on the uncertainty related to the interpretation and quantification of SSP2. **3b)** shows the different magnitudes of the NPP balance and the varying onsets of shortage across all SSP-RCP combinations. Black dots illustrate years with a shortage outside of the 95% confidence intervals. The combinations are grouped according to the socio-economic scenarios (y-axis). The RCPs are ordered from low to high radiative forcing in each SSP group. The temporal trajectory is shown along the x-axis and the colouring indicates the sign of the annual NPP balance. Blues show a surplus of the NPP supply while yellow to red represent small to very large NPP shortages (i.e. the gap between supply and demand). SSP-RCP combinations in bold indicate the most likely SSP-RCP pairs based on Table 1.~~s 3 and 4 of Engström et al. (2016b).~~

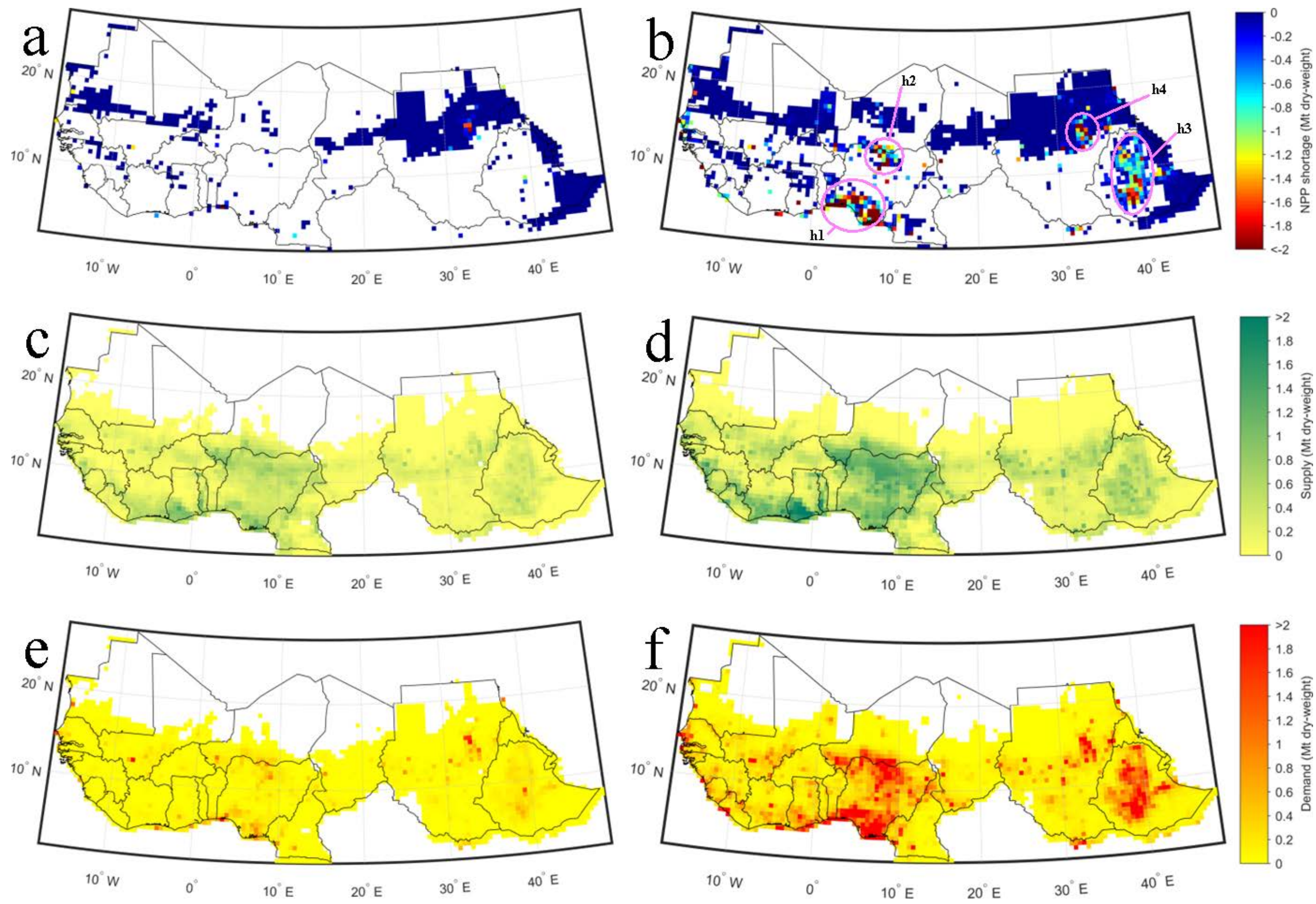

Fig 4 Maps of NPP shortage (**a,b**), NPP supply (**c,d**) and NPP demand (**e,f**) for the year 2000 (left panels) and SSP2-RCP6.0 year 2050 (right panels). The hotspots of large NPP shortage are marked with circles in 4b, where h1 is in the area around Lagos (Nigeria) and the Niger delta; h2 is in the Nigerian hinterlands (close to Kano); h3 is in the Ethiopian highlands (close to Addis Ababa); and h4 is in the area surrounding Khartoum (Sudan). In 4a we excluded all areas with a surplus in the NPP balance.

Tables

Table 1 Scenario matrix translated into quantitative probabilities (see also Engström et al. (2016b).

	RCP 2.6	RCP 4.5	RCP 6	RCP 8.5	Sum
SSP1	0.0909	0.4545	0.4545	0.0000	1
SSP2	0.0000	0.0909	0.6818	0.2273	1
SSP3	0.0000	0.1667	0.5000	0.3333	1
SSP4	0.0000	0.3704	0.5556	0.0741	1
SSP5	0.0000	0.0741	0.3704	0.5556	1

Table ~~1~~2 Rules of combining $NPP_{cereal\_balance}$ and $NPP_{grazing\_balance}$ to determine the final balance of NPP demand and supply.

Combination rule	$\boldsymbol{NPP_{cereal\_balance}}$	$\boldsymbol{NPP_{grazing\_balance}}$	$\boldsymbol{NPP_{balance}}$
1	<0	≥0	$NPP_{cereal\_balance}$
2	≥0	≥0	$NPP_{cereal\_balance}$
3	<0	<0	$NPP_{cereal\_balance}+ NPP_{grazing\_balance}$
4	≥0	<0	$NPP_{cereal\_balance}+ NPP_{grazing\_balance}$

Table 3~~2~~ Summary of the Shared Socio-economic Pathway key characteristics (population development, economic growth, consumption & diet, policy orientation and technological change) based on (Engström et al., 2016; O'Neill et al., 2017~~*in press*~~).

Pathway	Key characteristics
SSP1: **Sustainability - Taking the green road**	Relatively low population development Medium to high economic growth Low growth in material consumption, low-meat diets Towards sustainable development Rapid technology development and transfer
SSP2: **Middle of the road**	Medium population development Medium (but uneven) economic growth Material-intensive consumption, medium meat consumption Weak focus on sustainability Medium technology development and slow transfer
SSP3: **Regional rivalry - A rocky road**	High population development Slow economic growth Material-intensive consumption Oriented toward security Slow technology development and transfer
SSP4: **Inequality - A road divided**	Relatively high population development Low to medium economic growth Elites: high consumption, rest: low consumption Toward the benefit of the political and business elite Rapid technology transfer in high-tech sectors, but slow in other, little transfer within countries to poorer people
SSP5: **Fossil-fuel development - Taking the highway**	Relatively low population development High economic growth Materialisms, status consumption, meat-rich diets Toward development, free markets, human capital Rapid technology change and transfer

Table 4~~3~~ Per capita NPP balance, NPP supply, NPP demand and population for SSP2-RCP6 for 2000 and 2050. All NPP is given in dry-weight (DW).

Country	**Per capita NPP balance [kg DW yr^{-1}]**		**Per capita NPP supply [kg DW yr^{-1}]**		**Per capita NPP demand [kg DW yr^{-1}]**		**Total Population [millions]**	
	2000	2050	2000	2050	2000	2050	2000	2050
Benin	867	-267	1341	607	474	874	8	25
Burkina Faso	737	147	933	316	196	169	12	46
Cameroon	1740	456	2127	1173	387	717	16	40
Chad	1220	326	1878	1484	658	1157	8	26
Djibouti	-134	-119	0	0	134	120	1	2
Eritrea	218	91	333	221	124	130	4	12
Ethiopia	366	-660	825	779	459	1439	67	149
Gambia	431	-449	1137	632	706	1082	1	3
Ghana	1216	211	1490	1291	274	1080	19	48
Guinea	1371	631	1773	1697	402	1066	8	22
Guinea Bissau	1720	714	2319	1648	599	934	1	3
Ivory Coast	1513	737	1795	1549	282	811	17	41
Liberia	975	39	1186	1312	212	1273	3	10
Mali	818	-81	1929	1191	1111	1272	11	43
Mauritania	-401	-512	1129	1043	1530	1555	3	8
Niger	2163	-114	3437	1426	1274	1540	11	55
Nigeria	738	-204	1059	719	321	923	123	386
Senegal	369	-297	925	539	556	837	10	28
Sierra Leone	565	183	759	949	194	767	4	12
Sudan	986	-97	2517	1512	1530	1609	29	96
Togo	1900	838	2171	1491	271	653	5	11
Mean[1]	860	-107	1377	957	517	1064	361	1066

[1]Weighted mean using national population data as weight.

Future supply and demand of net primary production in the Sahel

Florian Sallaba[1], Stefan Olin[1], Kerstin Engström[1], Abdulhakim M. Abdi[1], Niklas Boke-Olén[1], Veiko Lehsten[1], Jonas Ardö[1], Jonathan W. Seaquist[1]

[1]Department of Physical Geography and Ecosystem Science, Lund University, Lund, 22362, Sweden

Correspondence to: J.W. Seaquist~~F. Sallaba~~ (jonathan.seaquist~~florian.sallaba~~@nateko.lu.se~~gmail.com~~)

Abstract

In the 21st century, climate change in combination with increasing demand, mainly from population growth, will exert greater pressure on the ecosystems of the Sahel to supply food and feed resources. The balance between supply and demand, defined as the ~~(~~annual biomass required for human consumption,~~)~~ serves as a key metric for quantifying basic resource shortfalls over broad regions.

Here we apply an exploratory modelling framework to analyze the variations in the timing and geography of different NPP (net primary production) supply-demand scenarios, ~~(~~with distinct assumptions determining supply and demand,~~)~~ for the 21st century Sahel. We achieve this by coupling a simple NPP supply model, ~~(~~forced with projections from four representative concentration pathways~~,)~~, with a global, reduced-complexity demand model ~~(~~driven by socio-economic data and assumptions derived from five shared socio-economic pathways~~)~~.

For the scenario that deviates least from current socio-economic and climate trends, we find that per capita NPP begins to outstrip~~s its~~ supply in the 204~~7~~0s, while by 2050, half the countries in the Sahel experience NPP shortfalls. We also find that despite variations in the timing of the onset of NPP shortfalls, demand cannot consistently be met across the majority of scenarios. Moreover, large between-country variations are shown across the scenarios where by the year 2050, some countries consistently experience shortage or~~, others~~ surplus, while~~ yet~~ others shift from surplus to shortage. At the local level (i.e. grid cell) hotspots of total NPP shortfall consistently occur in the same locations across all scenarios, but vary in size and magnitude. These hotspots are linked to population density and high demand. For all scenarios, total simulated NPP supply doubles by 2050 but is outpaced by increasing demand due to a combination of population growth and adoption of ~~a~~ diets rich in animal products. Finally, variations in the timing of onset and end of supply shortfalls stem from the assumptions that underpin the shared socio-economic pathways rather than the representative concentration pathways.

Our results suggest that the UN sustainable development goals for eradicating hunger are at high risk for failure. This emphasizes the importance of policy interventions such as the implementation of sustainable and healthy diets, family planning, reducing yield gaps, and encouraging transfer of resources to impoverished areas via trade relations.

1 Introduction

The global demand for food is projected to increase by up to double by 2050 (compared to the year 2005) due to rapid population growth and changes in dietary preferences (Hertel, 2015; Tilman et al., 2011). As a consequence, global agricultural supply needs to increase substantially in order to satisfy this demand (Ray et al., 2013). Agricultural practices can be intensified with technological investments (i.e. mechanization, irrigation and fertilization) to increase yields but these are costly and often lead to environmental degradation (Foley et al., 2005). As opposed to agricultural intensification, the amount of agricultural land can be expanded in order to meet future demand. This results in changing land use and land cover (LULCC), for example from natural vegetation to cropland. Approximately 35% of the total ice-free land surface is used for agriculture (Ramankutty et al., 2008). Agricultural land (grassland and cropland) expanded by 3% globally between 1985 and 2005 and is expected to further increase, especially in the tropics (Foley et al., 2011). The production of the most common crops (e.g. cereals, oil crops, and vegetables) increased by nearly 80% over the past four decades (FAOSTAT, 2015; Foley et al., 2011), mostly due to increases in yield (Kastner et al., 2012) and to a smaller extent by LULCC (Foley et al., 2011). Despite the large increase in agricultural production, global food security is~~cannot be~~ not ensured (due to access and distribution challenges~~ e.g.~~ (e.g. Brown, 2016; Pinstrup-Andersen, 2009)), as there are presently 792 million people chronically undernourished across the planet, a third of which are in Africa (FAOSTAT, 2015).

The Sahel region of sub-Saharan Africa is one of the most technologically underdeveloped regions in the world, where yield gaps are explained by low and variable rainfall combined with low soil fertility (Yengoh and Ardö, 2014). The population by-and-large relies on rain-fed farming practices including subsistence agriculture, cash crops, pastoralism and agro-pastoralism. The population has a high reliance on their own land, where 95% of food produce is for domestic consumption, (Abdi et al., 2014; Running, 2014). The vulnerability of the population to variations in agricultural supply due to frequent drought undermines wealth accumulation, which would otherwise provide a buffer in drought years (Barbier et al., 2009). Additionally, poor transportation infrastructure inhibit the trade and distribution of food resources (Olsson, 1993). Between the late-1960s to the early 1990s, the Sahel experienced a protracted dry period in which severe droughts caused fluctuating levels of food supply leading, in some cases, to severe humanitarian crises. The devastating droughts in 1972/73 and 1983/84 induced complete crop failure leading to the largest famines in the recent history of the Sahel (Ibrahim, 1988). The latest major drought to hit the region was in 2002. As of 2013, over 11 million people across the region were considered to be food insecure (United Nations, 2013).

NPP estimates from the MODIS (Moderate Resolution Imaging Spectroradiometer (MODIS) suggest that t~~T~~he Sahel region experienced a near-constant rate of crop productivity between 2000 and 2010, while population grew at a rate of 3.1% over the same period (Abdi et al., 2014). Abdi et al. (2014) also showed that 19% of the NPP supply in the Sahel was able to satisfy demand for the year 2000 but this increased to 41% in 2010 due to a 31% increase in the population. Since the NPP demand increased at an annual rate of 2.2% over the period while the supply was near constant, the near doubling in NPP demand implies, in relative terms, that there was less NPP supply to service the increase in population. This raises the question of whether demand could consistently outstrip supply in the future and underscores the importance for developing tools for analyzing potential future supply and demand that could be of use for policy makers. Indeed, the balance between supply and demand (annual biomass required for human consumption) serves as a key metric for quantifying basic resource shortfalls over broad regions (Abdi et al., 2014; Running, 2014).

Developing such tools requires coupling of specific models that address different sectors, such as a model for supply and a model for demand that can be run across multiple future climate, socio-economic and CO_2 concentration scenarios. However, the supply-demand system in the Sahel is complex and the future cannot be precisely evaluated. This is because there are many uncertainties associated with the assumptions that underpin the natural and socioeconomic drivers that lead to particular supply-demand balances. As such, an exploratory modelling approach is required, where an emphasis is placed on a structured analysis across a range of outcomes. This approach capitalizes on future indeterminacy for developing adaptive policy insights (e.g. Kwakkel and Pruyt (2013)). As the goal of exploratory frameworks is not prediction, they often employ parsimonious or simplified versions of more complex models (often referred to as meta-models in the latter case) that run across a range of scenarios (e.g. Harrison et al. (2016)). Another benefit of using such simplified models lies in the ease to which they can be coupled to other sectoral models (e.g. Kebede et al. (2015)).

In this study we couple a simple supply model (Biome-based Meta-model Ensemble - BME) with a demand model (Parsimonious Land Use Model - PLUM) to compute NPP supply-demand balance for a set of 21st century Sahel scenarios covering different climate, [CO_2] and socio-economic trajectories in an exploratory modelling framework. Our overall aim is to quantify variations in the timing and geography of NPP supply and demand in the Sahel in association with these trajectories. Three different aggregation levels are considered, including Sahel, the national~~country~~, and ~~the~~ local (cell level with a spatial resolution of $0.5^o \times 0.5^o$). Thereafter we discuss those natural and socio-economic factors that lead to changes in the balance between supply and demand throughout the 21st century, as accounted for by the coupled models. The Sahel-level analysis focuses on the total impact of the different future climatic and socio-economic pathways and its timing on supply and demand and asks the fundamental question of whether the Sahel as a whole, could potentially be self-sufficient. By contrast, the country-level analysis focusses on a level relevant for policy, international relations, and aid agencies. Finally, the local-level analysis identifies potential hotspots of supply shortage occurring at sub-national levels. We restrict our analyses to localized supply-demand only in order to flag those areas that would require the lateral transfer of supply from elsewhere via trade or aid. This would provide a first order boundary condition for further studies or for use by policy makers. As a consequence, specifically accounting for the myriad of political, social and cultural factors that affect lateral transfer, access to, and distribution of supply is beyond the scope of this study.

2 Materials and Methods

2.1 Modelling framework

In the current study, we couple two sectoral models to assess the future supply and demand trajectories for the Sahel region. We divided the modelling framework into three parts (Fig. 1), where the first part describes NPP supply; the second encapsulates NPP demand, while the third combines the two.

2.1.1 NPP supply

Supply is dependent on vegetation growth, and can be quantified as net primary production (NPP), which is defined as the difference in gross photosynthetic assimilation of carbon and carbon loss due to autotrophic respiration, per area per unit time (Foley, 1994). NPP is an established measure of ecosystem productivity indicating how much energy is available for all life on Earth. We estimated future plant productivity of the Sahel with the BME (Biome-based NPP meta-models). The BME is a rapid biome-based NPP meta-model that emulates the performance of the more complex model LPJ-GUESS (Lund-Potsdam-Jena General Ecosystem Simulator, Smith et al., 2014), but in a simplified, and more time-efficient manner. LPJ-GUESS is a state-of-the-art dynamic global potential natural vegetation model that incorporates carbon and nitrogen interactions (Smith et al., 2014). LPJ-GUESS (carbon cycling only) ~~that~~ shows good skill in predicting NPP at regional and global scales (Hickler et al., 2008; Tang et al., 2010). We developed the BME using LPJ-GUESS NPP simulations driven by several climate and CO_2 concentration perturbations (see Table A1). The biome definition in BME is taken from the Major Biome classification (MBC) (Reich and Eswaran, 2002), which stratifies the terrestrial biosphere into 13 biomes based on soil moisture and temperature regimes. We chose this biome definition because it represents a trade-off between global biosphere classifications that either have too many biomes or too few, compared to other stratifications (Kottek et al., 2006; Metzger et al., 2013; Olson et al., 2001). The trade-off also allowed for a reasonably accurate reproduction of vegetation dynamics, compared with LPJ-GUESS. For our study, we parameterized BME for the four major biomes of the Sahel: a) desert tropical, b) desert temperate, c) tropical semi-arid and d) tropical humid (~~see~~ Fig. 2). A recent study by Gonzalez et al. (2010) shows that climate change has the potential to shift biomes by the end 21st century. For simplicity, we therefore assumed static biomes that persist during climatic changes encountered during the modelling period (year 2000-2100). A detailed description of the BME implementation is provided in Appendix A.1.

We also evaluated LPJ-GUESS (e.g. Olin et al., 2015) and BME performance (magnitudes, trends and interannual variability) by first implementing a global biome-by-biome-level validation, where results from the Sahel are highlighted. We then ~~by~~ compare~~ing~~ BME estimates with LPJ-GUESS NPP simulations (including LPJ-GUESS managed land, in order to gauge the effect of agriculture on NPP, keeping in mind that BME is based on a model of potential natural vegetation) that were excluded from BME parameterization. Finally, we compare BME estimates against MODIS-derived NPP (2000-2006) (Running, 2004), as well as country-level censuses of crop yield trends from Rey et al. (2013). We also include a comparison with LPJ-GUESS C (carbon cycling only), a version that has been previously validated at the global scale (e.g. Hickler et al., 2008). The evaluation covered the entire Sahel region and was run from 1970 to 2006 (see Appendix A.2).

We forced BME with climate data (spatial resolution 0.5 x 0.5 degrees) from five GCMs (General Circulation Models, including HADLEY, GFDL, IPSL, MIROC and NorESM), and [CO_2] based on four RCPs (Representative Concentration Pathways, including 2.6, 4.5, 6.0 and 8.5) to estimate annual total NPP in kg dry-weight m^{-2} yr^{-1}~~.~~ (DW, dry-weight). We used climate data derived from runs across the 4 RCPs for each of the 5 models. We then calculated annual means of the five GCM NPP yields, resulting in four NPP time-series (covering each RCP) each spanning from 2000 to 2100. By averaging the GCM based NPP estimates we decreased the data amount while reducing spatial and temporal variability stemming from individual GCMs. In the next step, we summed ~~translated~~ the annual NPP estimates over the grid cell area~~to the total area of each grid cell~~ in m^2 using the latitude of each grid cell centre. Additionally, we used annual land use projections from Hurtt et al. (2011) to calculate the total area of pasture and cropland in each grid cell. This allowed us to estimate annual total NPP_{supply} (kg cell^{-1} yr^{-1}) for pasture and cropland separately. We estimated crop- and grassland scaling factors for each country by dividing the PLUM-predicted land-use area with the total land-use area provided by the Hurtt et al. (2011) dataset (Table C1). We then applied the scaling factors to the Hurtt et al. (2011) land-use data and multiplied the resulting crop- and grassland areas with the NPP estimates to obtain annual NPP_{cereal_supply} and $NPP_{grazing\_supply}$ (kg DW cell^{-1} yr^{-1}). We addressed potential developments in the wider use of existing agricultural technology that result in higher plant productivity with a technology improvement factor, where this factor is used to decrease~~close~~ the yield gap. The technology improvement factor is the aggregate result of parameterizing three technology related parameters (trends in technology, change in yield with GDP per capita, as well as how agricultural management practices are transferred both within and between countries) that are consistent with the scenario storyline of each SSP. Parameter ranges have been empirically determined based on analysis of data between the years 1995 and 2005. Yield gaps are not necessarily closed, but are decreased (see Engström eta al., 2016 for more detail). We then used country-wide yield gap fractions provided by PLUM spanning from 2000 to 2100 (Engström et al., 2016b; Licker et al., 2010). The yield gap fractions are country-specific and dependent on technological development in each scenario, and are thus consistent with the SSP storylines (Engström et al., 2016b). For example, a scenario with strong technological change has large decreasing yield gaps while a scenario with slow technological change has slowly, or stagnating (or even increasing) yield gaps. Here, we calculated yearly technology improvement factors by dividing the inverse yield gap fraction (i.e. 1-yield gap fraction) of the respective year with the inverse yield gap of the starting year (i.e. 2000). Thereafter, we applied the annual technology improvement factors to the NPP_{cereal_supply} (kg cell^{-1} yr^{-1}) of the respective year and country.

Finally, we used root-to-shoot ratio (R:S) to remove below ground biomass NPP of croplands (we exclude tubers and groundnuts) and pasture from our NPP estimates, since this component cannot generally be appropriated by humans or by the majority of animals. For croplands, we assumed common agricultural practice across the Sahel region and therefore applied a region-wide R:S=0.1 (Jackson et al., 1996). This a reasonable R:S since crops produce low root biomass compared to the above ground biomass. Moreover, we extracted the consumable parts of the above ground NPP by using a region-wide crop harvest index of 0.235, which is the average of reported harvest indices for maize, millet, sorghum and wheat (Haberl et al., 2007; Wirsenius, 2000). In contrast to crops, grasslands produce more below ground NPP in relation to above ground NPP (R:S >1) (Jackson et al., 1996). Therefore~~Furthermore~~ we considered the climatic limitations of individual biomes by extracting above ground NPP (for grasslands): a) desert tropical R:S=2.8; b) desert temperate R:S=1.1; c) tropical semi-arid R:S=2.8; and d) tropical humid R:S=1.6 (IPCC, 2006; Mokany et al., 2006).

2.1.2 NPP demand

For the calculation of NPP demand only, the parts of NPP that are available for direct consumption (excluding e.g. NPP preserved in e.g. national parks) are here considered. Future NPP demand can be projected applying a set of consistent assumptions for future societal and economic developments, described in socio-economic scenarios. We simulated future NPP demand for each country of the greater Sahel with PLUM, which is based on a conceptual model of socio-economic processes that determine global agricultural land-use change (Engström et al., 2016c). These processes include population and economic development, the consumption of cereal, milk and meat dependent on economic development and lifestyle/diet choice~~s~~ and the development of cereal yields dependent on technological change. PLUM is driven by country-level population and gross domestic product (GDP) data, and a range of parameters that characterize the development of the socio-economic processes mentioned above. PLUM was evaluated against historic (1991-2010) consumption and land-use data at the country scale and was shown to reproduce land-use change and consumption patterns at the global aggregated scale (Engström et al., 2016c). Due to the model's relative simplicity and the limited number of scenario parameters it is suited for scenario studies and was used to quantify uncertainty ranges for global cropland scenarios based on the Shared Socio-economic Pathways (SSPs) (Engström et al., 2016b). Mean cropland change for the five scenarios resulted in 963-2280 Mha cropland by 2100 compared to 1503 Mha cropland in 2000. The parameter-settings resulting in the uncertainty ranges for each scenario are described in Engström et al. (2016b) and the reported mean values were used in the current study. For more details see Engström et al. (2016b). In the version of PLUM applied in our study, we introduced an additional parameter which characterizes the increasing intensification of the livestock production systems in scenarios with strong increase in milk and meat consumption (Engström et al., 2016a). This process was previously not included in PLUM, but it was later identified to lead to an underestimation of land requirements for scenarios with strong increases in milk and meat consumption (Engström et al., 2016b).

We forced PLUM with the five socio-economic scenarios from 2000-2100 (see box outlined in red in Part 2 of Fig. 1~~2~~) taken from the SSPs, but it is important to remember that is it also coupled to the BME (see dashed arrow in Fig. 1~~2~~) through annual country-level total NPP estimates for cropland. Aggregation of BME NPP estimates was implemented as described in Engström et al. (2016b), except that cropland fractions in 2000 from MIRCA dataset were replaced with Hurtt et al. (2011) cropland fractions from 2000-2100.

Finally, we defined the demand of NPP as compounds that are necessary for human livelihood in the Sahel region, following the NPP_{demand} approach of Abdi et al. (2014). However, our approach differs from Abdi et al. (2014) by distinguishing between the demand of cereal- and pasture products~~ (see red box Fig. 2)~~. PLUM outputs were combined to determine NPP_{cereal_demand} as given in Eq. (1) and $NPP_{grazing\_demand}$ (see Eq. A9~~8~~ in the Appendix A.3).

$$NPP_{cereal\_demand} = NPP_{food} + NPP_{feed} \qquad (1)$$

where NPP_{cereal_demand} is the total amount of annual NPP needed for human appropriation via cropland; NPP_{food} (ton country^{-1}) is the NPP needed for consumed cereals; and NPP_{feed} (ton country^{-1}) is the amount of cereal based fodder to support the region's livestock population. $NPP_{grazing\_demand}$ is the NPP needed for sustaining the livestock by grazing (ton country^{-1}). Furthermore, we converted NPP_{cereal_demand} and $NPP_{grazing\_demand}$ to per capita demand (kg person^{-1}) using country population projections of the corresponding year in the SSP. A detailed methodology of the PLUM output combinations to satisfy Eq. (1) is given in Appendix A.

In the following step, we disaggregated the annual per capita NPP_{cereal_demand} and $NPP_{grazing\_demand}$ from country to 0.5 degree grid cell resolution in order to facilitate the spatial analysis of NPP supply and demand at the grid cell level. For that we multiplied annual per capita demands with gridded population data (0.5 x 0.5 degree resolution) of the corresponding years. The disaggregated annual NPP_{cereal_demand} and $NPP_{grazing\_demand}$ (kg cell^{-1} yr^{-1}) are therefore weighted by population density (i.e. population centers achieve high demand).

2.1.3 NPP Supply-Demand Balance

In the next step, we combined the NPP_{supply} (i.e. RCP based) with the NPP_{demand} (i.e. SSP driven) using a~~the~~ SSP-RCP likelihood matrix (Engström et al. (2016b), see Table 1~~4 therein~~) in order to facilitate the analysis of the NPP supply~~demand~~ and demand~~supply~~ balance. ~~The SSPs and RCPs were matched in a~~ To create the likelihood matrix, a~~likelihood matrix where a~~ qualitative probability was~~is~~ assigned to describe the likelihood of a SSP resulting in a RCP (Engström et al., 2016b). The qualitative likelihood estimates are based on experts' judgements, ranging from "very low" to "very high" and were translated to quantitative probabilities (Engström et al., 2016b). For the analysis, we considered SPP-RCP combinations with likelihoods above > 0.05 (> very low likelihood).

Next, we computed cereal-based (i.e. $NPP_{cereal\_balance}=NPP_{cereal\_supply}-NPP_{cereal\_demand}$) and grazing (i.e. $NPP_{grazing\_balance}=NPP_{grazing\_supply}-NPP_{grazing\_demand}$) balances. In order to combine the balances meaningfully we defined four rules as outlined in Table 2~~1~~. Rule no. 1 states that a deficit of cereal products ($NPP_{cereal\_balance}<0$) cannot be balanced with surplus of plant growth on grassland ($NPP_{grazing\_balance} \geq 0$) because grassland products are inappropriate for direct human consumption, resulting in all grazing surplus being disregarded. Rule no. 2 regulates the treatment of cereal and grazing surplus occurring simultaneously, where pasture NPP surplus ($NPP_{grazing\_balance} \geq 0$) is ignored but the cereal-based NPP surplus ($NPP_{cereal\_balance} \geq 0$) is retained. This surplus is of interest because it can potentially balance NPP shortages in adjacent grid cells as well as on the country level. Rule no. 3 permits the combination of cereal ($NPP_{cereal\_balance}<0$) and grazing ($NPP_{grazing\_balance}<0$) deficits in order to quantify the total NPP shortage of the grid cell. The last rule allows supplementation of grazing-based shortages ($NPP_{grazing\_balance}<0$) with cereal surplus ($NPP_{cereal\_balance} \geq 0$).

2.2 Scenarios

In the current study, we combine four Representative Concentration Pathways (RCPs) with five SSPs which are the latest future climate, [CO_2] and socio-economic projections (O'Neill et al., 2014; van Vuuren et al., 2011; van Vuuren et al., 2013) from the Intergovernmental Panel on Climate Change (IPCC) Fifth Assessment Report (AR5) framework. Each RCP represents a different cumulative measure of future human greenhouse gases (GHG) emissions and is defined by their radiative forcing targets for the year 2100, and which range from 2.6 to 8.5 W m^{-2} (van Vuuren et al., 2011). For each RCP, we obtained climate data from the Inter-Sectoral Impact Model Intercomparison project (ISI-MIP), containing climate simulations of five General Circulation Models (GCMs) for each RCP (Hempel et al., 2013). (GCMs : (Collins et al., 2013; Dufresne et al., 2013; Dunne et al., 2013; Iversen et al., 2013; Watanabe et al., 2011)). The climate data (0.5 x 0.5 degrees resolution) was bias corrected by the ISI-MIP approach that preserves trends in absolute changes in monthly temperature, and relative changes in monthly precipitation amounts (Hempel et al., 2013). For future socio-economic developments, the SSPs consider different narratives of future population levels, urbanization scenarios and economic development (O'Neill et al., 2017~~*in press*~~; van Vuuren et al., 2013) as summarized in Table 3 ~~2~~.

~~The SSPs and RCPs were matched in a likelihood matrix where a qualitative probability is assigned to describe the likelihood of a SSP resulting in a RCP (Engström et al., 2016b). The qualitative likelihood estimates are based on experts' judgements, ranging from "very low" to "very high" and were translated to quantitative probabilities (Engström et al., 2016b).~~ No mitigation strategies are assumed and resulting scenarios are thus reference scenarios. Furthermore, ~~we used~~ for each of the considered SSP and RCP combinations, we used a distributed population projection dataset at 1 km^2 from Boke-Olén et al. (~~*in review at Nature Scientific Data, submitted july*~~ *2017~~6~~*). The ~~used~~ population dataset was created by Boke-Olén et al. (~~*in review at Nature Scientific Data, submitted july*~~ *2017~~6~~*) to match both the RCP specific urban fractions from Hurtt et al. (2011) and SSP country urban and rural population counts. Hence, one population dataset exists for each SSP and RCP combination used in this study. We resampled (summed) the population dataset to the same spatial resolution as the climate data (0.5 x 0.5 degrees) and grid cells with population count below 3000 people per grid cell (~ one person per $1km^2$) were excluded following Abdi et al. (2014).

Additionally, variation in NPP supply estimates originating from the five GCMs was retained for an estimate of supply uncertainty to be included in the analysis. Uncertainty estimates for NPP demand associated with each SSP were derived from the results of Engström et al. (2016b) and applied here. In their study, conditional probability ranges were defined for twelve PLUM input parameters (reflecting uncertainties in SSP interpretation and quantification) in order to estimate uncertainty in a range of PLUM outputs.

2.3 Study area

The study area covers the African continent between roughly 5° and 25° northern latitude and stretches from the Red Sea to the Atlantic Ocean, hereafter referred to as the greater Sahel. Following Abdi et al. (2014), the area also includes the neighbouring countries of the Sahel belt (encompassing 21 countries see Table 4~~3~~). Note that this study uses the African country definition for the year 2000 where South Sudan was a part of Sudan. The actual Sahel belt is described by an annual rainfall range between 100mm and 600mm (hatched area in Fig. 2). The Sahel is an arid and semi-arid region that separates the Sahara desert from the humid and tropical regions to the south. The northern parts of the region border the Sahara Desert with low mean annual precipitation (<100mm) while the southern parts of the Sahel belt border the savannas of the tropical semi-arid biome, permitting increased plant productivity due to higher mean annual rainfall (~600mm). The southern parts of the study area cover the tropical semi-arid and tropical humid biomes with much higher mean annual precipitation amounts ranging from 600 to 1000 mm enabling larger vegetation growth. The study area is one of the poorest as well as most technologically underdeveloped regions on the African continent (Chidumayo and Gumbo, 2010).

3 Results

In the following the results are presented at Sahel, country and local (grid cell) level. Results for the different scenario combinations are reported, but emphasis is given to the SSP2-RCP6.0 scenario, as this scenario deviates least from current socio-economic and climate trends at the global level. Additionally, Fig. 3a also provides a basis for interpreting Fig. 3b.

3.1 Sahel

Per capita demand exceeds supply in the early 2040s for SSP2-RCP6.0 after which a very high likelihood for shortfalls begins in 2070 (see black dots in Fig. 3a showing non-overlapping 95% confidence limits). By 2050, per capita demand almost doubles while per capita supply drops by almost 30% for the same scenario. Across the scenarios, differences in the timing of the start of persistent supply shortfalls with high statistical certainty are observed (see black dots in Fig. 3b). Three of these high likelihood shortfalls begin at 2050 or before (SSP5 scenarios – see black dots in Fig. 3b) while an additional six display shortfalls with high certainty by the end of the 21st century (black dots in Fig. 3a, b). Out of these nine, two scenarios never achieve a sustained run of shortfalls (SSP2-RCP6.0, SPP2-RCP8.5). In total, there is better than an even chance for shortfalls before 2050 for 9 scenarios (exceptions are SSP1-RCP2.6, SSP1-RCP6.0, and all SSP4 scenarios.

Variations in the timing of onset and end of supply shortfalls are generally greater between the SSPs than between the RCPs (Fig. 3b). For SSP2 and SSP3 scenarios, onsets of high likelihood supply shortfall range from the early 2050s to the mid-2070s (even chance from late 2030s to early 2050s). The SSP5 family shows the largest deficits of high likelihood shortfalls beginning in the 2040s-2050s (even chance from the early 2030s), and after several decades of deepening begin to diminish in the 2080s. Shortfalls with high certainty never emerge for SSP1 (even chance from the early 2050s) while the SSP4 scenarios show sustained but diminishing surplus throughout.

~~Per capita demand exceeds supply in the 2070s for SSP2-RCP6.0 after which shortfalls occur discontinuously (Fig. 3a). By 2050, per capita demand almost doubles while per capita supply drops by almost 30% for the same scenario. Across the scenarios, differences in the timing of the start of persistent supply shortfalls are observed. Three of these show shortfalls at 2050 or before (SSP5 scenarios – see black dots in Fig. 3b) while an additional six display shortfalls by the end of the 21st century (black dots in Fig. 3a, b). Out of these nine, four scenarios never achieve a sustained run of shortfalls (SSP2-RCP6.0, SPP2-RCP8.5, SSP5-RCP6.0 and SSP5-RCP 8.5).~~

~~Variations in the timing of onset and end of supply shortfalls are generally greater between the SSPs than between the RCPs (Fig. 3b). For SSP2 and SSP3 scenarios, onsets of supply shortfall range from the early 2050s to the mid-2070s. The SSP5 family shows the largest deficits beginning in the 2040s-2050s, and after several decades of deepening begin to diminish in the 2080s. Shortfalls never emerge for the SSP1 and SSP4 scenario groups, with SSP4 scenarios showing diminishing surplus throughout.~~

3.2 Country-level

For scenario SSP2-RCP6.0, per capita NPP balances generally show a decrease for all countries. Eleven countries (out of twenty-two) experience per capita shortages by 2050, up from two countries (Djibouti and Mauritania) in 2000. Ethiopia shows the most extreme shortfall while Togo the greatest surplus. The largest change amongst all countries (is exemplified by Niger which starts with a surplus in 2000 but ends up with a deficit by 2050. Conversely, Djibouti shows a small decrease in deficit over the period (Table 4).

Large changes in per capita NPP balance are caused by contrasting development of NPP supply and demand, as analyzed in the following two paragraphs. Despite large total NPP increases between 2000 and 2050 (SSP2-RCP6.0), per capita NPP supply decreases for almost all countries, the largest decreases being for Niger and Sudan while an increase is noted for Liberia.

Since all countries double or even triple their population counts from 2000 to 2050 (Table 4~~3~~), large increases in demand occur over the 50 year period, while even per capita demand increases. By 2050, the largest increases in demand per capita are projected for Liberia, Ethiopia and Ghana by 2050 respectively (Table 4~~3~~).

Generally, the differences in NPP balances across scenarios are high, with the largest variations attributed to the SSPs as opposed to the RCPs (Table C2), with two~~three~~ countries (Sierra Leone and Liberia) showing considerable variation across the scenarios (coefficients of variation > 2.0).

3.3 Local level

For SSP2-RCP6.0, the localities experiencing negative NPP balance expand and become more connected between 2000 and 2050. By 2050, a semi continuous band of low magnitude NPP shortage emerges (generally > -0.2 Mt dry weight yr^{-1} per grid cell), stretching from the Atlantic Ocean to the Red Sea, between 15^{o} and 20^{o} N (Fig. 4b). In the east, this band extends down along the coast and wraps around the horn of Africa. A separate band of similar magnitude emerges toward the south, from just above 10^{o} N, and stretching toward the east-southeast into Cameroon. Additionally, four separate locations of large magnitude shortfalls (> 1.5 Mt dry weight yr^{-1} per grid cell) of varying extents emerge. The first hotspot (relatively small cluster of large magnitude shortfall) is located along the Nigerian coast, stretching from the metropolitan areas of Lagos to the densely populated area of the Niger delta (Fig. 4a, h1). The second hotspot is located in northern Nigeria, close to the city Kano (Fig. 4a, h2) while the third is located in the Ethiopian highlands of Eastern Africa (Fig. 4a, h3). Finally, the fourth covers the area of around Khartoum in the Sudan (Fig. 4a, h4). Elsewhere, very small pockets (e.g. 1 grid cell in size) of large magnitude NPP shortages (<-1.0 Mt DW yr^{-1} per grid cell) are distributed unevenly across the region.

Both supply and demand increase over most localities for the SSP2-6.0 scenario from 2000 to 2050 (Fig. 4 c-d). For supply, largest increases (up to, and exceeding 1 Mt dry weight yr^{-1} per grid cell) occur in those areas that already see large supply in 2000, including the southern parts of Ivory Coast and Ghana, and most of Nigeria and the southern part of Niger (Fig. 4c,d). Smaller increases occur throughout central Sudan and Ethiopia. Large magnitude increases (between 1 and > 2 Mt dry weight per year^{-1} per grid cell) in demand are seen for distinct geographic regions, the largest patches covering coastal Nigeria, northern Nigeria-southern Niger, north-central Sudan around Khartoum, and Ethiopia (Fig. 4f). By-and-large, these correspond to the hotspots of supply shortfall identified in Fig. 4b. Smaller areas, sometimes no larger than one grid cell, are seen scattered across Sudan, Chad, the west coast, and south Sudan.

The general geographical patterns of NPP shortage remain persistent across all scenarios, including the four hotspots identified for SSP2-RCP6.0. The largest magnitude shortages are indicated for SSP5-RCP8.5 (Fig. B1).

4 Discussion

4.1 Sahel-level

World-wide cereal production in 2010 amounted to 2400 Mt and current food aid shipments to countries in the Sahel are below 1 Mt yr^{-1} (FAOSTAT, 2016). At present about 260 million people are chronically undernourished in Africa (FAOSTAT, 2015) and this is despite the fact that we also estimate a per capita NPP surplus of 860 (±144) kg DW yr^{-1} (corresponding to 309 (±52) Mt DW yr^{-1}) in the Sahel for the year 2000. This implies that current challenges are associated with other determinants such as access to and distribution of resources (Brown, 2016; Olsson, 1993; Pinstrup-Andersen, 2009). These challenges are set to increase in the future, particularly for scenarios with high social and economic inequalities (SSP4). Furthermore, the majority of all other scenarios show that by mid-century, the NPP surplus will be much reduced compared to the year 2000. According to the sustainable development goals, hunger and all forms of malnutrition should be eradicated by the year 2030 (UN, 2016), but under the current trend given by the SSP2-RCP scenarios, there is a risk that 15-25% (160 to 270 million people) of the population would not be able to be supported with NPP supply (on the basis of assumed adoption of diets rich in animal products, consistent with the SSP2 storyline) and are therefore at high risk for malnutrition by 2050.

Presently, the Sahel has a high reliance on their own land by producing 90% of domestic food consumption resulting in very little import or export of crops (Abdi et al., 2014~~; Running, 2014~~). This implies that agricultural resources from global trade will need to increase considerably in order to reduce the future food shortages across the region. Participation in global markets and investments in infrastructure that enable trade of food commodities to ensure food security via trade will therefore be important (D'Odorico et al., 2014). However, it needs to be kept in mind that the simulated shortages partly occur due to steep increases in per capita consumption. For example, while reducing social inequities is clearly desirable (as embraced by the SSP5 RCP scenarios), from a sustainability perspective, it is questionable if this should mean that developing countries follow the development path of economically developed countries and adopt diets with very high consumption levels of animal products (O'Neill et al., 2017~~*in press*~~). The adoption of sustainable diets (i.e. reduced contribution of animal products to diets) has to be envisaged as a strategy consistent with efforts to reduce food demand to healthy and sustainable levels (Smith, 2013). This would be consistent with the SSP1 ('taking the green road' scenarios) where sustainable diets are adopted statistically significant shortages never develop (e.g. Fig. 3b).

4.2 Country-level

Beyond the import of agricultural products to the Sahel, inter-country trade of such resources will also need to become more important later in the 21st century. Trade relations between productive and high-demand countries should be encouraged (Ahmed et al., 2012). For instance, Cameroon, Ivory Coast, Chad and Togo produce NPP surplus for SSP2-RCP6.0 by 2050 which could be traded to neighbouring countries with NPP shortages (e.g. Nigeria). Across the scenarios, some countries showed continuous NPP shortfalls (e.g. Mauritania), while Ivory Coast and Guinea consistently produce NPP surplus (Table

C2). The large range of different climate conditions in the Sahel region implies that those countries within the tropical humid (and partly in tropical semi-arid) biome have larger potential NPP compared to countries in the desert temperate biome. We note that the closure of yield gaps by 2050 (for scenario SSP2-RCP6.0) would result in a change in mean per capita NPP balance from -107 kg DW yr-1 (see Table 3) to 9 kg DW yr^{-1}. Though the balance for many countries will still be negative, the shortfall magnitudes would be reduced. ~~Closing yield gaps is an important goal for all countries so strong efforts should be made to reduce these gaps~~. ~~As well as reducing yield gaps, d~~Decreased supply due to losses of food during harvest, transport and storage (i.e. household level) should be reduced through improvements of agricultural management, infrastructure and educational development (Godfray et al., 2010). For most countries however, the different socio-economic development pathways prescribed by the SSPs lead to high inter-scenario variability (having positive or negative balances depending on the scenario) and will determine if countries have the potential be a net exporter or importer of resources.

4.3 Local-level

At the local-level, robust NPP shortages across scenarios were found to be strongly linked to densely populated areas. For the example of SSP2-RCP6.0, by 2050, the number of grid cells with high population density (i.e. > 1 million population per 25 km x 25 km increased substantially compared to 2000 (see Fig. B4~~3~~))). For instance, > 1 million people per grid cell trigger NPP shortages in Ethiopia while > 2 million people per grid cell induce NPP shortfalls in Nigeria for SSP2-RCP6.0 by 2050. The NPP shortage hotspots in Nigeria and Ethiopia agree geographically with reported considerable NPP demand expansions in the 2000s (Abdi et al., 2014) indicating a combination of population growth and increased consumption as explanatory factors. Furthermore, the projected deepening and persistent shortages in urban areas underscore the hypothesis that the urban poor are especially at risk for food insecurity since they neither have the means to purchase food on the markets, nor the means to be self-sufficient due to limited land in densely populated areas (Lynch et al., 2001). Thus, connecting productive hinterlands with metropolitan areas will need to be achieved (Owuor, 2007).

That the locations of the hotspots and the overall patterning of NPP shortfalls remain consistent across all scenarios narrows the number of future policy choices in the region for alleviating environmental insecurity despite the very different assumptions and uncertainties embedded in the scenarios and models (Kwakkel and Pruyt, 2013).

4.4 Additional Perspectives

~~Our finding that supply increases for all SSP-RCP scenarios, partly due to increasing rainfall and CO_2 fertilization suggests that the current trend of Sahel greening identified from satellite sensor-based mapping studies (e.g. (Eklundh and Olsson, 2003; Hickler et al., 2005; Seaquist et al., 2009) may continue into the future. Livestock mobilization is one way local populations generally employ to manage risk (e.g. Herrmann et al. (2014). In a greening Sahel, this strategy may help regulate supply shortfalls locally, and over the short term. We also note that greener Sahel (increase in NPP supply) does not necessarily imply an increase in the amount of usable NPP or an enhancement in health and well-being. Recent studies in the Sahel show that much of the greening, at least in some regions, is due to undesirable shifts in species composition (e.g.~~

~~Herrmann et al. (2014)), reductions in biodiversity and an increases in woody biomass (e.g. Brandt et al. (2015)).~~ Livestock mobilization is one way local populations generally employ to manage risk (e.g. Herrmann et al. (2014). ~~In a greening Sahel, t~~This strategy may help regulate supply shortfalls locally, and over the short term. ~~We also note that greener Sahel~~Even if the Sahel were to continue to green up (increase in NPP supply) this would ~~does~~ not necessarily imply an increase in the amount of usable NPP or an enhancement in health and well-being. Recent studies in the Sahel show that much of the recent greening, at least in some regions, is due to undesirable shifts in species composition (e.g. Herrmann et al. (2014)), reductions in biodiversity and an increases in woody biomass (e.g. Brandt et al. (2015)).

Campbell et al. (2014) underscore the importance of family planning and education in the Sahel in order to curb population growth. Generating demand for various forms of birth control and gender empowerment would be two key interventions that would work towards slowing population growth, improving health and facilitating income generation. These interventions would act to curtail supply shortfalls in the future.

4.5 Mechanisms of changes in future NPP supply and demand

4.5.1 NPP supply

In order to isolate the CO_2 (rainfall) effect on NPP increase for RCP6.0, we compared a simulation where rainfall (CO_2) was held constant with a simulation where both were held constant for the period 2000-2050 for all GCMs. We found that supply increases mostly due to CO_2 fertilization (see Fig. B2), with very little attributed to rainfall. However, yield gap closure from SSP2 contributes most to the increase in simulated NPP supply (Fig. B2).

The CO_2 fertilization effect increases with the magnitude of climate change and explains the smaller shortages in SSP-RCP8.5 scenarios compared to SSP-RCP4.5 scenarios (Fig. 3b). ~~Generally, NPP supply increases for all SSP-RCP scenarios due to climate change-induced plant growth and due to decreasing yield gaps. Climate-change induced plant growth (mainly due to increases in rainfall combined with the CO_2 fertilization effect) was shown to increase with the magnitude of climate change, and explains the smaller shortages in SSP-RCP8.5 scenarios compared to SSP-RCP4.5 scenarios (Fig. 3b). Although uncertainty with respect to the total magnitude of simulated NPP supply exists (due to lack of ground truth for the region), greater confidence can be placed in the long-term trends in simulated vegetation growth (e.g. Seaquist et al. (2009) and Fig. A2).~~

The decreases in yield gap (applied to the NPP supply and demand balance through the technological improvement factor) are simulated with PLUM and are strongly dependent on scenario-driven assumptions for technological change. High rates of technological change explain the decreasing shortages at the end of the 21st century for SSP1-RCPs and SSP5-RCPs scenarios. For example, in the SSP1-RCP scenarios, the yield gap decreased from 0.55 in 2000 to 0.43 by 2050 in Nigeria and from 0.69 in 2000 to 0.56 by 2050 in Ethiopia. By contrast, slow technological change in SSP3-RCP scenarios leads to very small decreases in yield gaps, e.g. for Nigeria to 0.54 by 2050 while no improvement at all was simulated for Ethiopia. Uncertainties in yield improvements driven by technological development are very large and critically dependent on investments as well as on infrastructural and political development in developing countries (Engström et al., 2016b; Licker et al., 2010; Mueller et al., 2012). Reducing yield gaps to 0.5 in Sub-Saharan countries can be achieved by intensified nutrient management, while decreases down to 0.25 require increased irrigation and fertilization (Mueller et al., 2012). However, Elliott et al. (2014) underscore that freshwater limitations in the dryer regions of the globe could limit agricultural production, and even lead to the reversion of irrigated farmland to rainfed farmland, thereby negatively affecting food production. Conventional agricultural intensification, however, can result in environmental degradation, vulnerability to pests, and depletion of aquifers (Ceccato et al., 2007; Foley et al., 2005). Agricultural management should consider strategies of sustainable intensification while simultaneously considering adaptation of agriculture to changing climates (Dile et al., 2013; Pretty, 2008, 2011).

An additional driver of NPP supply is the simulated increase in agricultural land area provided by PLUM (i.e. grass- and cropland – Fig. B5). However, the simplified representation of grassland in PLUM potentially underestimates the expansion of agricultural land into naturally vegetated areas, and thus the magnitude of total NPP supply. As with agricultural intensification, the expansion of agricultural land into natural forests and grasslands has the potential to produce negative impacts on the environment and on climate (Canadell and Schulze, 2014; Foley et al., 2005; Pugh et al., 2015).

4.5.2 NPP demand

Despite increases in future NPP supply, according to our results, the Sahel is likely to~~will~~ experience NPP shortages for most NPP scenarios due to strong increases in demand. Generally, the increasing NPP demand in the Sahel region can be explained by doubling to tripling population in the period 2000-2050 across the scenarios (Fig. B3~~2~~a). However, changes in economy, lifestyle and consumption patterns as simulated with PLUM were shown to be the important drivers for large total NPP demand. For example, in the SSP5-RCP scenarios, per capita NPP demand almost triples (2000-2050, Fig. B3~~2~~b), driven by the adoption of meat- and milk-rich diets and processed food as previously pointed out by (Kearney, 2010; Tschirley et al., 2015). Increased per capita NPP demand coupled with the doubling in population (2000-2050) leads to almost seven-fold increases in total NPP demand during the period 2000-2100 for SSP5-RCP scenarios. By contrast, for SSP4-RCP scenarios population triples (2000-2050), but widening income gaps and no improvements in diets in the poor population lead to declining per capita NPP demand (Fig. B3~~2~~b) with a low increase (compared to other scenarios) in total NPP demand (doubling between 2000 and 2050, Fig. B3~~2~~b). The relatively weak increase of total NPP demand in the SSP4-RCP scenarios is the underlying reason for a sustained NPP surplus in the scenarios. The NPP surplus per se is not an indicator for achieved food security, as suggested by the decreasing per capita demand (described above). By contrast, food insecurity will be likely more wide-spread than today according to the SSP4-RCP scenarios, aggravated by strong inequalities within the population that are likely to worsen food distribution and food access for the poor (Pinstrup-Andersen, 2009).

The uneven projected changes in per capita NPP demand across countries (Table C1) are partly due to contrasts in the evolution of drivers (e.g. income) for different countries, but also due to differing initial conditions for the different countries. In countries with initially higher per capita demand (e.g. Sudan) the potential to increase per capita demand is limited, while for countries with lower initial per capita demands (e.g. Ethiopia) the potential to increase demands is comparatively higher. Finally, the NPP demand estimates are limited by the assumption of cereals, meat and milk being proxies for food supply, which for countries with high shares of pulses and tubers in their average diet in particular, underestimates the NPP demand.

4.6 Uncertainties

~~In this work we~~We show~~assume~~ that the deep uncertainties represented by the scenarios i.e. not knowing how drivers (e.g., population, technological change) will develop in the future (van Vuuren et al., 2008) are ~~the~~ major sources of uncertainty leading to variations in our results (Fig. 3b). T~~Additionally, t~~he variability in NPP supply and demand, originating from the five GCMs and uncertainties in SSP interpretation and quantification (see Engström et al. (2016b) and Table 1 and Table B1 ~~therein~~), respectively, allows us to ~~confidently~~ assess, with high statistical confidence, when the onset of supply shortfalls begin and are sustained.

Additional uncertainty exists with respect to the total magnitude and trends of simulated NPP supply, given the lack of ground truth for the region, and that differences in NPP trends between other models is very large (e.g. Friend et al., 2014; Körner et al., 2006; Pugh et al., 2016; Rosenzweig et al., 2014). Indeed, recent observational evidence suggests that the effect of CO_2 fertilization on plant growth may be constrained by counteracting feedbacks associated with increasing atmospheric moisture demand and nutrient availability (e.g. Smith et al., 2016; Wieder et al. 2015). For example, NPP is reduced under warmer and dryer conditions due to moisture stress, particularly in temperate and arid ecosystems. Future trends NPP trends in the Sahel could therefore be strongly determined by changes in the frequencies of wet years versus dry years, with the dry years counteracting the CO_2 fertilization effect. Furthermore, nutrient supply rates may not be able to keep up with extra demand associated with CO_2 fertilization, and leading to a depletion of soil nutrients, as current evidence suggests. This could also curtail the CO_2 fertilization effect, particularly in the more southerly parts of our study area, where nutrients tend to become a limiting factor. We performed a simple experiment negating the CO_2 fertilization effect in order to gauge its impact on supply-demand balance on all scenarios. For the SSP2-RCP6.0, per capita demand has an equal chance of exceeding per capita supply in 2036 for the SSP2-6.0 scenario as opposed to 2043 if CO_2 fertilization in included (Fig. B7), with a very high likelihood of continuous supply shortfall beginning in 2056, as opposed to 2073 with CO_2 fertilization. The effect on all other scenarios is an earlier shift to the onset of supply shortfalls, by about 10 years, compared to Fig. 3b (see Fig. B7). Supply shortfalls with high likelihood of occurrence (black dots showing non-overlapping 95% confidence intervals) are similarly shifted, and occur with greater consistency and frequency. All of this suggests that the NPP increases found in our current analysis are likely optimistic, due the potential overestimation of the CO_2 fertilization effect, as well as the fact that BME is based on potential natural vegetation.

Finally, we note that country-specific scaling factors used to convert PLUM output to per pixel changes using the Hurtt et al. (2011) data set for the year 2000 did not depart substantially from 1 (scaling factors for the larger countries were all within

10%, and the area weighted mean of the scaling factors was 0.95), but a few smaller countries in West Africa diverge by more than 25% (<0.80 or > 1.25) (see Table C1). We expect these to have only marginal influence on the results at the regional level, but could have a larger impact on localities along the West African coast (Fig. 4 and Fig. B1).

Other sources of uncertainty, such as model uncertainty stemming from the supply and demand models (Alexander et al., 2016) are not presently taken into account.

5 Conclusions

In the Sahel, population growth and climate change raise the question of whether the demand for NPP will outstrip supply during the 21st century. In order to address this question, we developed a reduced-complexity framework capable of generating a range of NPP supply-demand trajectories for different Sahel futures at the regional, country, and local levels of aggregation. These results are based on differing climate, [CO_2], and socio-economic scenarios supplied by different SSP and RCP combinations.

We conclude that the potential for NPP self-sufficiency in the Sahel will not likely be attainable later in the 21st century. The most likely consequence will be that hunger and malnutrition will become more widespread than it is currently, undermining the UN sustainable development goals. This highlights the importance of establishing strategies that address the reduction of NPP demand, increasing its supply as well as facilitating its access, particularly for the urban poor. The consistency of geographical shortfall patterns across all scenarios also suggests that, despite deep uncertainties associated with assumptions about how the future unfolds and uncertainties associated with NPP supply magnitudes and trends, a relatively narrow range of policy interventions can be crafted.

Finally, we advance previous research by showing how NPP supply-demand balance (a key metric for quantifying resource shortfalls over large regions, but applied retrospectively in previous studies) can also be used to explore the impact of changing socio-economic and climate assumptions in the Sahel to support policy.

Acknowledgements

FS acknowledges support from the Helge Ax:son Johnsons Stiftelse. SO, KE, and JWS acknowledge support from the FORMAS Strong Research Environment project Land use today and tomorrow (LUsTT; dnr: 211-2009-1682), while JWS also acknowledges partial support from LUCID (www.lucid.lu.se), a FORMAS-funded Linnaeus Centre of Excellence at Lund University (dnr: 259-2008-1718). AMA and JA acknowledge funding provided by Swedish National Space Board (Rymdstyrelsen). Finally, VL acknowledges support from the BIODIVERSA project CONNECT via FORMAS.

Appendices

Appendix A Methods

A.1 Biome based Meta-model Ensemble

In this section, we describe the development of the biome based meta-model ensemble (BME) for the Sahel region. BME consists of rapid NPP meta-models tailored for the desert temperate, desert tropical, tropical semi-arid and tropical humid biome. The BME is based on the dynamic vegetation model LPJ-GUESS (Smith et al., 2014) and NPP simulations following the methodology of Sallaba et al. (2015).

A.1.1 LPJ-GUESS

LPJ-GUESS (Smith et al., 2014) is a mechanistic model of plant physiological and biogeochemical processes that incorporate ecosystem carbon and nitrogen cycles as well as water fluxes. The model uses a detailed individual- and patch-based representation of vegetation structure where individual plants differ in growth form, phenology, life history strategy and photosynthetic pathway, demography and resource competition. LPJ-GUESS is forced by various climate (i.e. solar radiation, temperature and precipitation), atmospheric [CO_2], soil characteristics and nitrogen deposition. Vegetation is represented as plant functional types (PFTs) with different age cohorts interacting on patch level. Ten generalized trees and two generalized grass functional types (i.e. C3 and C4 grass) following Smith et al. (2014) were used for global potential natural vegetation (PNV). Several patches (here 25) are applied in parallel within a grid cell with distinguished establishment of vegetation, fire impacts, random disturbance and mortality rate of different age cohorts (Sitch et al., 2003; Smith et al., 2001; Smith et al., 2014). We applied the LPJ-GUESS in cohort mode which represents individual PFTs in different age classes competing for resources (light, water and space) in a patch. We defined disturbance events with an expected return interval of 100 years following Ahlström et al. (2015). We spun up each LPJ-GUESS simulations with a 500 years long phase of de-trended climate data and a particular [CO_2] (unique for each simulation as outlined in Input data) in order to run the model from bare soil to a vegetation equilibrium state.

A.1.2 Input Data

We collected our BME development dataset with a random stratified selection of climate data using the Major Biome classification (BMC) (Reich and Eswaran, 2002) on a 0.5°x0.5° spatial resolution. The BMC characterizes four biomes in the greater Sahel region based on soil moisture and soil temperature regimes (see Fig. 1). We chose randomly 2-5% of the total cells in each biome.

We overlaid the sampled cells with CRU TS. 3.0 climate data (Harris et al., 2014; Mitchell and Jones, 2005), which have the same spatial resolution. CRU data span from 1901 to 2006 providing monthly data of temperature, precipitation and cloudiness. Soil texture characteristics were taken from the FAO global soil dataset (FAO, 1991) as described in Sitch et al.

(2003). Historical monthly nitrogen deposition rates were achieved from the Atmospheric Chemistry and Climate Model Intercomparison Project (ACCMIP) database of Lamarque et al. (2010) and processed as described by Smith et al. (2014). We developed climate and [CO_2] scenarios based on a factorial approach where increasing monthly temperature, [CO_2] and changing monthly precipitation amounts are varied multiple variables -at-a-time (i.e. MAT) (Smith and Smith, 2007). We set maximum changes for each variable (see Table A1) in order to design reasonable climate and [CO_2] scenario limits as described by Sallaba et al. (2015). We used CRU TS 3.0 climate data as the baseline time-series and superimposed the climate and [CO_2] scenarios upon the baseline data while we held the nitrogen deposition rates according to the ACCMIP records. In total, we developed 100 scenarios (including baseline) for each CRU grid cell, which were then applied to simulate NPP in LPJ-GUESS. We assumed that grid cells maintain the biome membership even though the climate conditions change during the LPJ-GUESS simulations since we consider transitions of vegetation biomes to be long-termed, 100 years.

Table A1 Minimum and maximum stepwise changes of the climate variables and [CO_2]. The magnitudes of increases are related to how much a variable could be adjusted. Temperature was increased in four steps and the other variables in five steps resulting in 100 different climate change scenarios.

Change attributes	**Temperature change [°C]**	**Precipitation [% of baseline]**	**Atmospheric CO_2 [ppm]**
Minimum Value	0	50	350
Maximum Value	6	150	670
Magnitude of increase	2	25	80
No. of steps	4	5	5

A.1.3 Biome meta-models

We followed the assumption that plant growth is controlled by climate conditions (Sallaba et al., 2015) and defined biome specific assumptions of ecosystem-climate interactions. As Sallaba et al. (2015) we assume that vegetation growth is controlled synergistically by temperature and precipitation. Under optimal climate conditions maximum plant growth can be reached but decreases when temperature and/or precipitation are not at the optimum. In order to keep the meta-modelling framework as simple but efficient as possible, we limited the meta-model to three input climate surrogates that control plant growth: (1) annual precipitation (P_{cum}), (2) maximum temperature (T_{max}) and (3) minimum temperature (T_{min}) temperature. We followed the methodology of Sallaba et al. (2015) by defining functions of the climate surrogates that yield maximum NPP at baseline [CO_2], combining these in a synergistic function and then adding the CO_2 fertilization effect.

For the meta-model development at baseline [CO_2], we scaled the LPJ-GUESS NPP estimates between 0-1 (i.e. NPP_{min} =0 and NPP_{max} =1) using the highest NPP yield of each biome and combined them with the climate surrogates. The highest NPP yields of the biomes Max_{biome} at baseline [CO_2] are given in Table A3. We then extracted the climate surrogate - NPP value combinations that yield highest NPP, assuming that maximum NPP yields can only be reached under optimal climate conditions (Sallaba et al., 2015).

For NPP as a function of temperature we assumed a hump-shaped curve relationship, which is based on the temperature-photosynthesis relationship (Sallaba et al., 2015). For T_{max} we developed a function that is built upon the *beta*-distribution as given in Eq. (A1).

$$f(T_{max}) = \frac{\left(\frac{T-Lim_{min}}{Lim_{max}-Lim_{min}}\right)^{\partial-1}\left(1-\left(\frac{T-Lim_{min}}{Lim_{max}-Lim_{min}}\right)\right)^{\beta-1}}{\left(\frac{\Gamma(\partial)\Gamma(\partial\beta)}{\Gamma(\partial+\beta)}\right)}\, a \qquad \text{(A1)}$$

where $f(T_{max})$ calculates the NPP yield (relative) of the given temperature surrogate; T is the value (°C) of T_{max}; Lim_{min} and Lim_{max} are the minimum and maximum temperature limits of the biome normalizing T between 0 and 1; Γ is the gamma function ; ∂ and β describe the shape of the function and a stretches the function along the ordinate (the amplitude). For T_{min} we developed a function that is identical to T_{max} as given in Eq. (A2).

$$f(T_{min}) = \frac{\left(\frac{T-Lim_{min}}{Lim_{max}-Lim_{min}}\right)^{\partial-1}\left(1-\left(\frac{T-Lim_{min}}{Lim_{max}-Lim_{min}}\right)\right)^{\beta-1}}{\left(\frac{\Gamma(\partial)\Gamma(\partial\beta)}{\Gamma(\partial+\beta)}\right)}\, a \qquad \text{(A2)}$$

where$f(T_{min})$ estimates relative NPP and T is the value (°C) of T_{min}. The function parameters of Eq. (A1) and (A2) are provided in Table A2.

For NPP as a function of precipitation we applied two function types because the dataset shows saturation as well as linear NPP growth with increasing precipitation amounts in the Sahelian biomes. Both function types let NPP increase with increasing precipitation amounts until NPP_{max} is reached. Further increasing precipitation levels only yield NPP_{max} because precipitation surplus is assigned as run-off and percolation, following the treatment of high precipitation levels in LPJ-GUESS (Gerten et al., 2004; Smith et al., 2014).

Table A2 Parameter values for maximum temperature $\boldsymbol{f(T_{max})}$ in Eq. (A1) and minimum temperature $\boldsymbol{f(T_{min})}$ in Eq. (A2).

Biomes	**Temperature function in $\boldsymbol{f(T_{lim})}$**	$\boldsymbol{Lim_{min}}$	$\boldsymbol{Lim_{max}}$	$\boldsymbol{\partial}$	$\boldsymbol{\beta}$	$\boldsymbol{a}$
Desert tropical	$f(T_{min})$	9.00	33.00	2.12	1.22	0.46
Desert temperate	$f(T_{min})$	-14.00	28.00	2.06	1.33	0.52
Tropical semi-arid	$f(T_{min})$	4.00	33.00	2.27	1.57	0.52
Tropical humid	$f(T_{max})$	13.00	36	1.47	1.49	0.68

In the tropical humid and tropical semi-arid biomes, we applied a saturation function where NPP grows rapidly with increasing precipitation until NPP_{max} is reached, as given in Eq. (A3),

$$g(P_{cum}) = min\left(1, k - \frac{o}{P_{cum}{}^{l}}\right) \qquad \text{(A3)}$$

where $g(P_{cum})$ estimates the cumulative precipitation NPP (relative); P_{cum} is the annual cumulative precipitation; k is the maximum relative NPP (here NPP_{max}=1) that limits the growth of the function; o is a constant; l determines the slope of the function and min() limits the linear function to NPP_{max}=1. If P_{cum} is 0 mm than $g(P_{cum})$ is set to 0.

In the desert tropical and desert temperate biomes we defined NPP as a simple linear function of precipitation (see Eq. (A4)), which is limited to NPP_{max}=1 in order to consider the treatment of precipitation surplus in LPJ-GUESS (Gerten et al., 2004; Smith et al., 2014).

$$g(P_{cum}) = \min(1, mP_{cum}) \quad \text{(A4)}$$

where $g(P_{npp})$ calculates the cumulative precipitation NPP (relative); P is the annual cumulative precipitation; m is the slope of the linear function; and min() limits the linear function to NPP_{max}=1. All parameter values of Eq. (A3) and (A4) are presented in Table A3. For the parameter values determination of the temperature and precipitation functions we randomly halved the biome training subsets (at [CO_2] = 350 ppm) in analysis and validation parts, and then applied nonlinear least-squares model fit in MATLAB® (2015b). We chose the parameter values that yield the lowest root mean square error (RMSE) in the validation part following (Del Grosso et al., 2008).

Table A3 Parameter values for cumulative precipitation functions in Eq. (A2) for the tropical biomes and Eq. (A3) for the desert biomes.

Biomes	***k***	***o***	***l***	***m***
Desert tropical*	-	-	-	0.0009
Desert temperate*	-	-	-	0.0014
Tropical semi-arid	1.84	4.29	0.18	-
Tropical humid	1.24	19.69	0.51	-

* The asterisk indicates linear precipitation functions

We then combined the climate variable functions and investigated model complexity. We combined $f(T_{min}), f(T_{max})$ and $g(P_{cum})$ in seven groupings ranging from one function to multiplying all three climate functions to calculate NPP in each biome. We assessed model complexity with the Bayesian information criterion (BIC) (Burnham and Anderson, 2002; Schwarz, 1978) and model agreement with RMSE and the Wilmott index (DR) (Smith and Smith, 2007; Smith et al., 1997; Willmott et al., 2012). We chose the combinations with lowest BIC and best model agreement. In all biomes the best results were obtained by a combination of precipitation with either one temperature function (because T_{max} and T_{min} are potentially auto-correlated). The combination of $g(P_{cum})$ with $f(T_{max})$gave the best results in the tropical humid biome while $g(P_{cum})$ combined with $f(T_{min})$ yielded the best results in the remaining biomes (see applied temperature function in Table A2).

In the next step, we combined the selected functions, converted the synergistic function from relative to absolute NPP (kg C m^{-2} yr^{-1}) and rescaled the function to independent LPJ-GUESS NPP simulations in order to correct for differences in NPP magnitudes as given in Eq. (A4).

$$NPP_{base} = NPP_{scale}\left(\left(f(T_{lim})\, g(P_{cum})\right) Max_{biome}\right),\ f(T_{lim}) \in [f(T_{max}), f(T_{min})] \quad \text{(A4)}$$

where NPP_{base} is the estimate (kg C m^{-2} yr^{-1}) at baseline [CO_2]; $f(T_{lim})$ is the temperature function used for the specific biome (either $f(T_{max})$ or $f(T_{min})$ - see Table A2); Max_{biome} is maximum NPP yield of the biome at baseline [CO_2] for converting NPP from relative to absolute units; and NPP_{scale} is the scaling factor to minimize the magnitude difference between LPJ-GUESS and BME estimates. The scaling factor is a ratio based on the mean of LPJ-GUESS NPP and the mean of biome meta-model NPP estimates from 1985-2006. In the tropical humid biome $f(T_{min})$ is set to 1 and in the remaining biomes $f(T_{max})$ is set to 1 based on the model complexity analysis. The parameter values are given in Table A4.

Table A4 Parameter values of the synergistic function in Eq. (A4).

Biomes	$\boldsymbol{Max_{biome}}$	$\boldsymbol{NPP_{scale}}$
Desert tropical	1.25	1.46
Desert temperate	0.86	1.05
Tropical semi-arid	1.46	1.04
Tropical humid	1.56	0.97

We implemented the CO_2 fertilization effect on plant growth in the final meta-model function (see Eq. (A5)) by applying the same methodology as described in Sallaba et al. (2015) (assuming saturating NPP enhancement with increasing [CO_2]) but determined new parameters for each biome using linear fitting in MATLAB® (R2015b). We chose the parameters that yielded lowest RMSE are shown in Table A5.

$$NPP_{scenario} = \left(NPP_{baseline}\left(c\left(1 - \frac{CO_{2\_baseline}}{CO_{2\_scenario}}\right) + 1\right)\right) \qquad \text{(A5)}$$

Where $NPP_{scenario}$ is NPP (kg C m^{-2} yr^{-1}) under elevated [CO_2] (ppm); $NPP_{baseline}$ is modelled NPP at baseline [CO_2]; c is the slope; $CO_{2\_baseline}$ is the baseline [CO_2] of 350 ppm and $CO_{2\_scenario}$ is an [CO_2] > 350 ppm.

Table A5 Parameter values of the CO_2 function in Sallaba et al. (2015) Eq. (5) therein.

Biomes	$\boldsymbol{c}$
Desert tropical	-0.19
Desert temperate	-0.63
Tropical semi-arid	-0.70
Tropical humid	-1.03

For each biome, we determined CO_2 fertilization function parameter values with a nonlinear least-squares model fit in MATLAB® (R2015b) choosing values yielding the lowest root mean square error (RMSE).

A.2 Model Evaluation

A.2.1 Biome Level Model Validation

We validate biome-level LPJ-GUESS and BME performance for estimating NPP of natural vegetation with NPP field-measurements from Michaletz et al. (2016) and Luyssaert et al. (2009) (see Sallaba et al., 2015) for the Major Biome Classification of Reich and Eswaran (2002) including the biomes found in the Sahel (desert temperate, tropical semi-arid and tropical humid – no observations were available for desert tropical). Note that since only two observations were available for our study area (see Fig. A1) this evaluation demonstrates the ability of both LPJ-GUESS and BME to replicate NPP for Sahel biomes found elsewhere in the world.

Before we combined the Michaletz et al. (2016) and Luyssaert et al. (2009) datasets, we removed sites with no records of combined above- and below-ground NPP measurements. After we merged the data, we checked the final assembly of NPP measurements for duplicates and removed them. The final dataset consists of 1561 samples (i.e. 1247 samples from Michaletz et al. (2016) and 314 samples from Luyssaert et al. (2009)) representing total NPP measurements across the terrestrial biosphere (sample sizes are 18, 6, and 12 for Sahel biomes of desert temperate, tropical semi-arid and tropical humid, respectively) from 1959-2006. Both LPJ-GUESS and BME were driven with CRU TS 3.21 climate data (Harris et al. 2014, Trenberth et al. 2014) that has global coverage across the time period.

We calculated mean values of the NPP field-measurements and the modelled NPP estimates located in the respective biomes, following Smith et al. (2014b). We aggregated to the biome-level to account for the difference in scale between in situ NPP measurements and modelled grid cell NPP estimates (being grid cell averages).

Finally, we determined the overall model performance, biome-by-biome, with the coefficient of determination (R^2 value) and the root mean square error (RMSE). Additionally, we investigated model agreement with performance ratios (hereafter referred to as ‘Q’) by dividing mean biome NPP estimates (for both models) with mean biome NPP observations. Model overestimation in comparison to in situ NPP measurements is indicated by $Q > 1$ and underestimation by $Q < 1$. Good model performance is classified with a Q range between 0.9-1.1 assuming an error of ± 10% following Sallaba et al. (2015). However, we further defined an acceptable model performance error range of ±20% (i.e. Q = 0.8-1.25) given the limitations of using LPJ-GUESS standard modelling protocol, PNV and CRU climate observations, and especially the simplicity of BME.

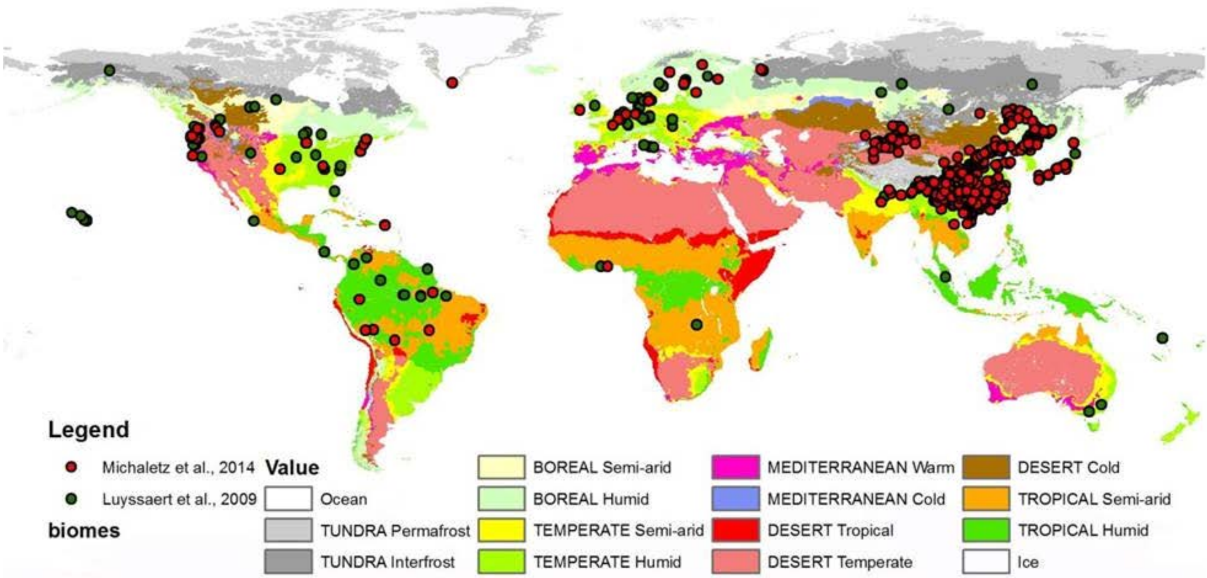

Fig. A1 Map of the Major Biome Classification based on Reich and Eswaran (2002). The red and green points are the locations of the NPP field-data from Michaletz et al. (2016) and Luyssaert et al. (2009).

LPJ-GUESS performs reasonably well in simulating NPP at the overall biome level ($R^2 = 0.71$ and RMSE = 0.16) but the model performance varies notably across the biomes (see Fig. A2 and Table A6). In general, LPJ-GUESS yields acceptable model agreement in seven (with good performance in four biomes) out of thirteen biomes. At the same time, the model underestimates NPP in three biomes while it overestimates NPP in two biomes (Fig. A2).

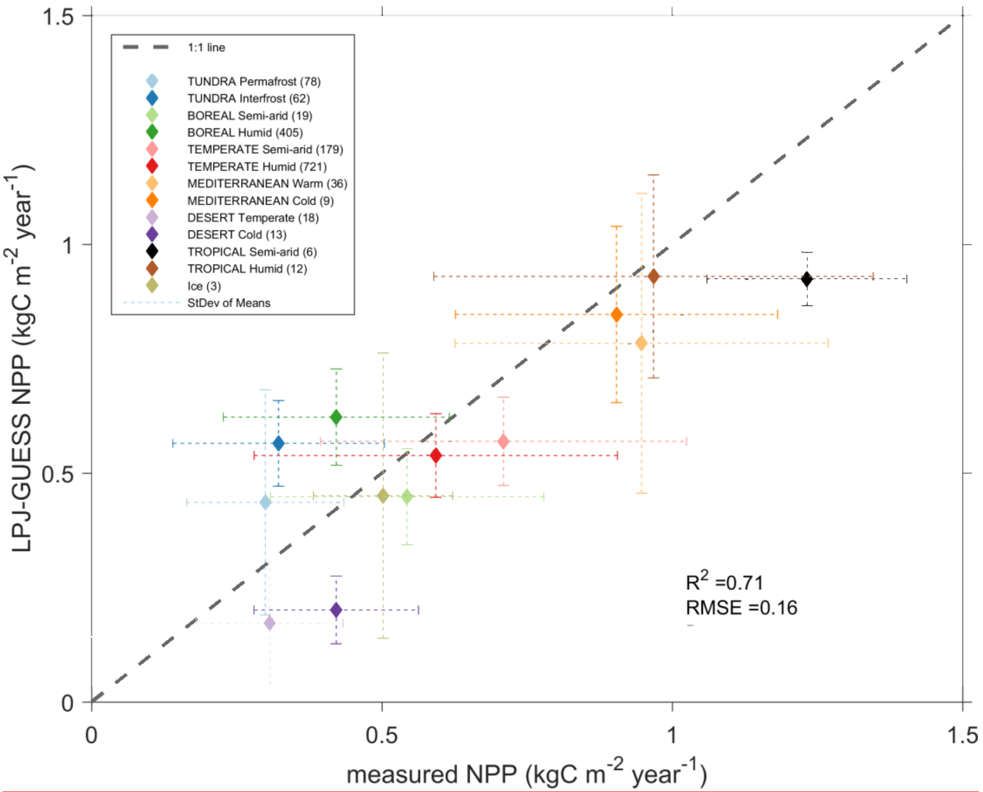

Fig. A2 Comparison of LPJ-GUESS through NPP estimates and NPP field-measurements at the biome level using biome mean NPP values and their standard deviation. The different colours represent MBC biomes based on (Reich and Eswaran 2002). The number of NPP observations in each biome is given in the legend. Note that Sahel biomes Desert temperate, Tropical Semi-arid, and Tropical Humid.

Table A6 Comparison between mean biome NPP field-measurements, LPJ-GUESS, BME NPP estimates; and their Q as model performance measure. Sahel biomes are underlined.

Biome (sample size)	Field-data mean NPP [kg C m^{-2} yr^{-1}]	LPJ-GUESS mean NPP [kgC m^{-2} yr^{-1}]	LPJ-GUESS Q	BME mean NPP [kgC m^{-2} yr^{-1}]	BME Q
TUNDRA Permafrost (78)	0.30	0.44	1.46	0.24	0.79
TUNDRA Interfrost (62)	0.32	0.56	1.75	0.44	1.36
BOREAL Semi-arid (19)	0.54	0.45	0.83	0.49	0.91
BOREAL Humid (405)	0.42	0.62	1.48	0.56	1.32
TEMPERATE Semi-arid (179)	0.71	0.57	0.80	0.45	0.63
TEMPERATE Humid (729)	0.59	0.54	0.91	0.56	0.95
MEDITERRANEAN Warm (36)	0.95	0.78	0.83	0.52	0.55
MEDITERRANEAN Cold (9)	0.90	0.85	0.94	0.41	0.45
DESERT Temperate (18)	0.31	0.17	0.56	0.09	0.28
DESERT Cold (13)	0.42	0.20	0.48	0.24	0.57
TROPICAL Semi-arid (6)	1.23	0.92	0.75	0.84	0.68
TROPICAL Humid (12)	0.97	0.93	0.96	0.81	0.84
Ice (3)	0.50	0.45	0.90	-	-

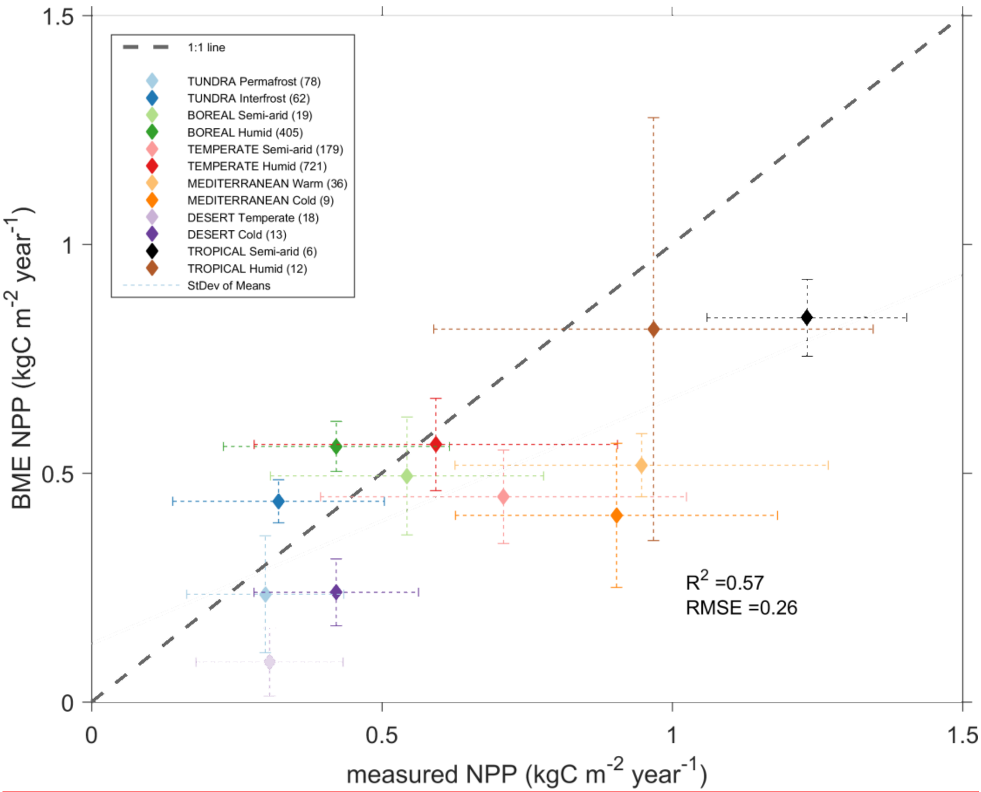

Fig. A3 Comparison of BME NPP estimates and NPP field-measurements on biome level using biome mean values as well as biome standard deviation of the means. The different colours represent MBC biomes based on (Reich and Eswaran 2002). The number of NPP observations in each biome is given in the legend. Note that Greter Sahel biomes Desert temperate, Tropical Semi-arid, and Tropical Humid.

For Greater Sahel biomes: LPJ-GUESS exhibits good skill in simulating NPP in the Tropical humid (Q = 0.96, see Table A6) where it also captures satisfactorily the variability of the NPP measurements. LPJ-GUESS underestimates NPP for the tropical semi-arid biome (Q = 0.75) showing reduced NPP variation compared to the observations. Performance is reduced for Desert temperate (Q =0.56).

BME performance is acceptable at the overall biome level (R^2 = 0.57 and RMSE = 0.26) but varies substantially for individual biomes (see Fig. A3). Overall, BME model agreement is reasonable in four biomes (with good performance in two biomes). At the same time, BME overestimates NPP in two biomes while it underestimates plant growth in six biomes. The variability in in- situ NPP measurements cannot be captured by BME in the majority of biomes except in the tropical humid and tundra permafrost biomes (see vertical and horizontal lines connected to the diamonds in Fig. A3).

For Greater Sahel biomes: BME yields acceptable agreement in estimating NPP in the tropical semi-arid and tropical humid biomes (Q = 0.84, 0.81 respectively) but accuracy drops more water limited biomes of desert temperate (Q = 0.28). Overall, BME mimics the behavior of LPJ-GUESS shown by a good model agreement of R^2 = 0.71 and moderate RMSE = 0.12 kg C m^{-2} yr^{-1} between the average biome NPP estimates of BME and LPJ-GUESS. Notable is that BME yields, on average, less NPP in the majority of biomes compared to the observations.

A.2.2 BME Performance in the Sahel

For the assessment of BME performance in the Sahel, we chose approximately 4000 CRU TS 3.0 grid cells that cover evenly distributed the Sahel region. We forced LPJ-GUESS with the CRU climate data and measured [CO_2] spanning from 1970-2006 and measured [CO_2] using the same modeling protocol as described in section A.1). The climate data were post-processed as in section A.1 and then applied to BME in order to estimate NPP. We employed several measures to gauge BME performance against LPJ-GUESS simulations. We calculated the BME's agreement (i.e. precision) with LPJ-GUESS simulations with the coefficient of determination (R^2 value) measuring the strength of linear association between the models; the root mean squared error (RMSE) gives the total difference between the models in NPP units (NPP kg C m^{-2} $year^{-1}$) and the Wilmott index (DR) determines how well the plot of LPJ-GUESS simulations and BME NPP fit to a perfect agreement line ranging from -1 to 1 (1 = optimal value) (Smith and Smith, 2007; Smith et al., 1997; Willmott et al., 2012).

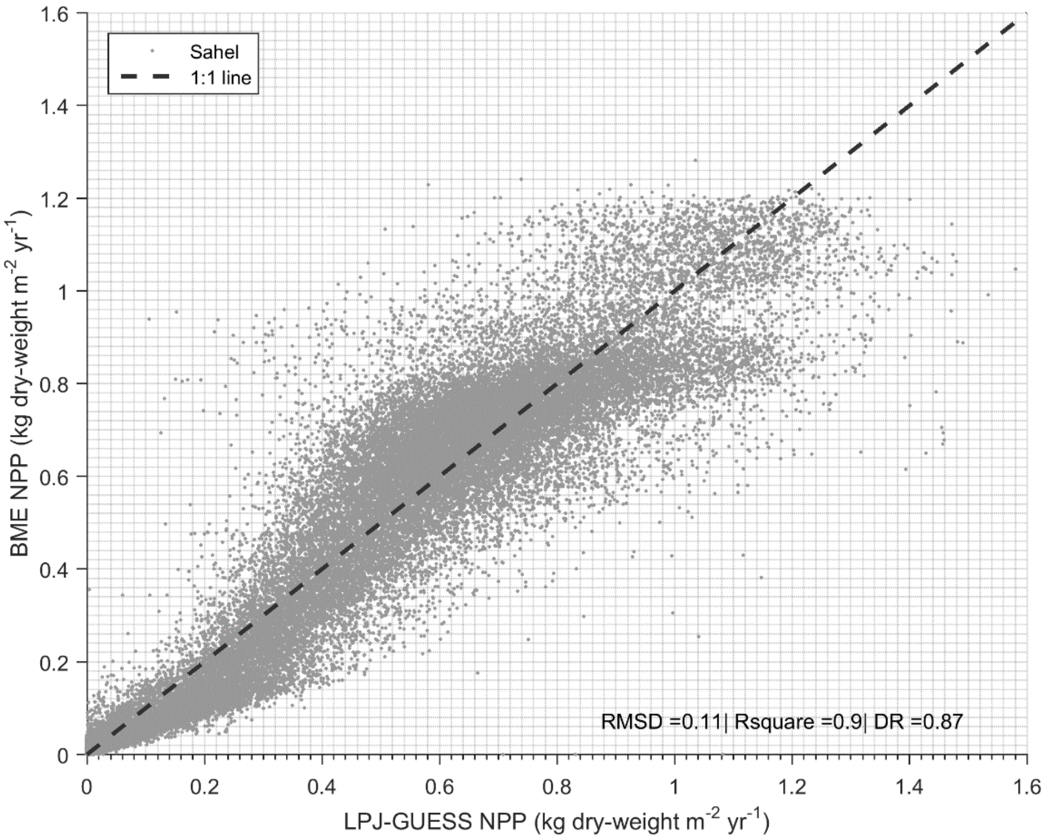

Fig A4~~1~~ Comparison between BME and LPJ-GUESS NPP estimates covering the Sahel region.

The comparison between BME and LPJ-GUESS NPP estimates (see Fig. A1) shows a good agreement R^2=0.9 and DR=0.87 while the RMSE=0.1 NPP kg DW m^{-2} $year^{-1}$ shows notable total differences between the models.

We then calculate annual means of BME and LPJ-GUESS NPP (i.e. aggregating the entire Sahel region) for the time period in order to investigate whether BME follows the inter-annual variation of LPJ-GUESS NPP. As shown in Fig A5~~2~~., BME NPP follows the inter-annual variation of LPJ-GUESS NPP. Both models yield depleted NPP in 1972/73 and 1983/84 showing the impact of devastating droughts that occurred in these years resulting in complete crop failure (Ibrahim, 1988). Furthermore, both models yield a dip in NPP in 2002 when the latest major drought befell the region (see Fig. A5~~2~~) (Balogun et al., 2013). In Fig. A5, we also include runs from LPJ-GUESS C (carbon cycling only), LPJ-GUESS ml (managed land) and MODIS derived NPP for comparison purposes.

In order to test how effectively the NPP of natural ecosystems can be can be used as a proxy for the NPP of agricultural ones we ran LPJ-GUESS managed land (Olin et al., 2015) for the period 1970 to 2006 and compared this to LPJ-GUESS (used to develop BME) for the entire Sahel region. The results (see Fig. A5) of this experiment show that mean NPP derived from LPJ-GUESS ml over the region underestimates mean NPP derived from BME by 0.7% (0.006 dry-weight m^{-2} yr^{-1}) and LPJ-

GUESS by 2.4% (0.020 kg dry-weight m^{-2} yr^{-1}), though all models show similar levels of interannual variability and trend (see Fig. A5). The implication of this experiment is that there is a demonstrable reduction in NPP when land management is taken into consideration, but the effect is relatively minor. Lindeskog et al. (2013) show that LPJ-GUESS managed land (C-version) overestimated actual yield derived from FAO country-level crop statistics and Smith et al. (2014b) also report that natural systems are more productive than agricultural systems in sub-Saharan Africa. We conclude with that possibility that our results are in the upper range for NPP found in the Sahel.

We also compare total yearly means of NPP from BME and LPJ-GUESS to NPP derived from the MOD17A3 processing stream (using MOD17A3 data obtained from the NASA Earth Observation System repository at the University of Montana at www.ntsg.umt.edu) for the period 2000 to 2006 for the greater Sahel region (Running, 2004). We averaged resampled MODIS NPP from 1km to the spatial resolution of the BME estimates (0.5 x 0.5 degrees) and excluded urban areas. We removed below-ground NPP and plant parts unable to be consumed by applying the same R:S and harvest index as described in Section 2.1.1. Lastly, we calculated mean values of MODIS NPP estimates from 2000 to 2010 for each grid cell covering the study area. Our results show that between 2000 and 2006 MODIS-derived NPP underestimate BME-derived NPP by 42% (difference of 0.38 kg dry-weight m^{-2} yr^{-1}), on average (Figure A5). Ardö (2015) also reports that that average annual MODIS NPP underestimates LPJ-GUESS (C version only, Fig. A5) for Africa for 2000-2010 and attributes this to the fact that autotrophic respiration is considerably higher for MODIS NPP compared to LPJ-GUESS, due to large temperature sensitivity in the MODIS algorithm, differences in the biome-specific parameterizations for MODIS as well as specification of plant functional types in LPJ-GUESS.

Country-level census yield trends (1989-2008) for 4 major crops from appendix Data S1 of Ray et al. (2013) for rice (Benin, Burkina Faso, Chad, Ghana, Guinea, Guinea-Bissau, Ivory Coast, Liberia, Mali, Nigeria, Senegal, Sierra Leone, Togo), maize (Benin, Burkina Faso, Cameroon, Chad, Ethiopia, Ghana, Guinea, Ivory Coast, Mali, Nigeria, Senegal, Togo), wheat (Cameroon, Chad, Eritrea, Ethiopia, Mali, Mauritania, Niger, Nigeria, Sudan) and soybean (Benin, Burkina Faso, and Nigeria) range from -5.98 to 2.80 (mean of -0.002), -0.94 to 4.08 (mean of 1.400), -2.58 to 3.1 (mean of 1.280) and 1.15 to 3.98 (mean of 2.280) respectively. Trends for BME, LPJ-GUESS, and MODIS NPP fall within most of the ranges for crop yield trends, showing yearly increases of 0.55% (BME), 0.58% (LPJ-GUESS), and 0.51% (MODIS) for the 7 year period of overlap. For the entire length of each series (1970-2006 for BME and LPJ-GUESS and 2000-2010 for MODIS), slopes indicate yearly increases of 0.40%, 0.40%, and 0.62% respectively. We note the number of uncertainties involved in this comparison (e.g. spatial/temporal sampling, and the fact that BME and MODIS represent natural vegetation and a mix of natural vegetation and crops, respectively).

A.2.3 Concluding Remarks for Model Validation and Evaluation

In sum, a validation involving ground measurements for the same biomes found in the Sahel (but observations mostly from other locations) show that LPJ-GUESS and BME underestimate NPP, while a comparison with MODIS shows that LPJ-GUESS (and BME) overestimate total mean annual NPP in the greater Sahel region (2000-2006). Yet is widely acknowledged, natural systems are likely more productive than agricultural systems. But we also show that trends for BME, LPJ-GUESS, and MODIS mostly fall within trend ranges for country-level yield statistics (though sample size is low). We acknowledge that the uncertainties are significant. Differences in estimates between methods are due to a combination of spatial aggregation/sampling issues (e.g. low sample sizes for biomes typically found in the Sahel, that CRU data do not necessarily represent site-level climate, and the uncertain assessment below-ground and short-lived above-ground plant matter at the site level) as well differing assumptions between the MODIS processing stream and LPJ-GUESS (particularly respiration). We therefore conclude that BME and LPJ-GUESS replicate ground observations of NPP at similar orders of magnitude at the biome level, but may be overestimated due to the fact that natural systems are usually more productive than agricultural ones. This underscores the fact that BME and LPJ-GUESS should be restricted to biome-level applications (or coarser) while applications on the grid cell level should be limited to explorations of patterns and trends, which is the reason why we emphasize an aggregated level of analysis.

~~This favors the application of BME since it mimics reasonably well the behavior of LPJ-GUESS, which exhibits good skills in reproducing vegetation dynamics of the Sahel region (Seaquist et al., 2009). Seaquist et al. (2009) demonstrate that LPJ-GUESS replicates reasonably well satellite-observed greening trend of the Sahel vegetation and its inter-annual variability from 1982 to 2002.~~

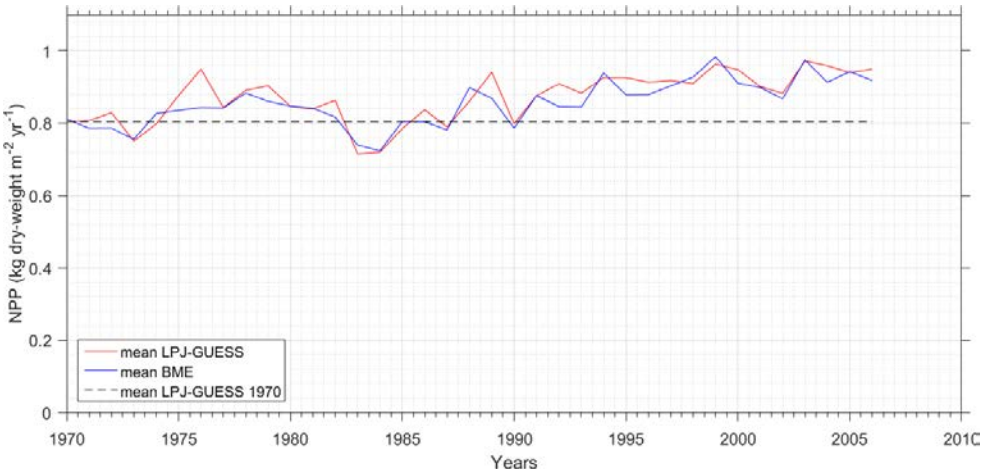

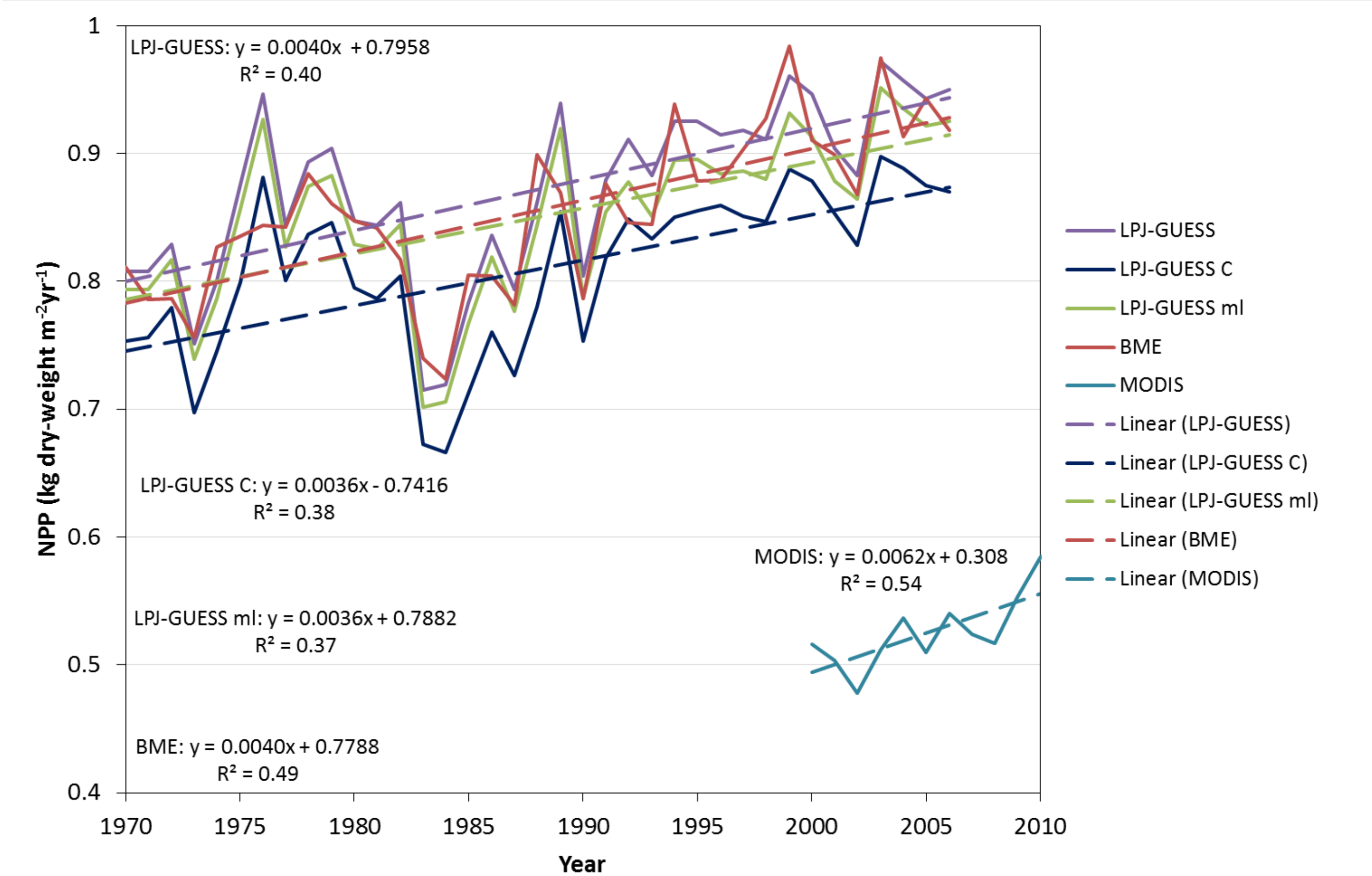

Fig A5~~2~~ Regional annual NPP Annual means of NPP for~~of~~ BME, ~~and~~ LPJ-GUESS, LPJ-GUESS C (carbon only) and LPJ-GUESS ml (managed land) (~~from~~ 1970 to 2006) and MODIS (2000-2010) for the greater Sahel region. ~~LPJ-GUESS NPP estimates are visualized in red and BME in blue.~~

A.3 Estimation of NPP supply and demand

In this modelling framework, we followed the NPP_{demand} definition Abdi et al. (2014) as given in Eq. (A6).

$$NPP_{demand} = NPP_{food} + NPP_{feed} + NPP_{residues} + NPP_{fuel} + NPP_{burned} \qquad \text{(A6)}$$

Where NPP_{demand} is the actual amount of annual NPP needed for human survival; NPP_{food} is the NPP needed for consumed cereals, meat and milk production; NPP_{feed} is the total amount of fodder to support the livestock population and $NPP_{residues}$ are agricultural by-products (after harvesting); NPP_{fuel} describes fuelwood and charcoal from the region's dry woodlands and NPP_{burned} represents the human-driven NPP loss from biomass burning of forest resources for land clearing due to land use change (Abdi et al., 2014).

We adapted Eq. (A6) to the current study's framework by dividing the demand into cereal (Eq. A7) and grazing (Eq. A8) based NPP, and PLUM outputs.

$$NPP_{cereal\_demand} = NPP_{food} + NPP_{feed} \qquad \text{(A7)}$$

where $NPP_{food} = cereal_{total} - cereal_{feed}$ (ton country^{-1}); $cereal_{total}$ (ton country^{-1}) is the total cereal consumption of human and livestock population provided by PLUM; $cereal_{feed}$ (ton country^{-1}) is the total cereal demand to sustain the livestock population (a direct PLUM ouput); NPP_{feed} (ton country^{-1}) is equal with $cereal_{feed}$; We then converted then NPP_{cereal_demand} to per capita (kg person^{-1}) using country population of the corresponding year in the SSP.

The amount of NPP needed to sustain the livestock by grazing that cannot be covered with $cereal_{feed}$ we applied Eq. (A7).

$$NPP_{grazing\_demand} = (1 - feed_{ratio}) * cereal_{feed}/feed_{ratio} \qquad \text{(A8)}$$

Where $NPP_{grazing\_demand}$ (ton country^{-1}) is the NPP obtained from grasslands for sustaining the livestock; $feed_{ratio}$ ranges between 0-1 (given by PLUM) and provides the proportion of how much $cereal_{feed}$ can meet the livestock demand of energy needed to sustain the livestock. Furthermore, we assumed that the Sahelian livestock is kept close to human populated areas and we therefore we converted $NPP_{grazing\_demand}$ to per capita (kg person^{-1}) using country population of the corresponding year in the SSP.

Furthermore, we eliminated NPP_{fuel} in Eq. (A6) because we assumed that fuelwood doesn't directly contribute to the availability of food resources. Fuelwood is a vital variable since it is a necessity for processing cereals and meat but it cannot provide information about food resource availability. Moreover, we eliminated NPP_{burned} in Eq. (A6) since it cannot be counted as an actual food resource in the particular year where the land-clearances occurs but it is an important indirect factor, determining how much food can be produced in the following years.

Appendix B Figures

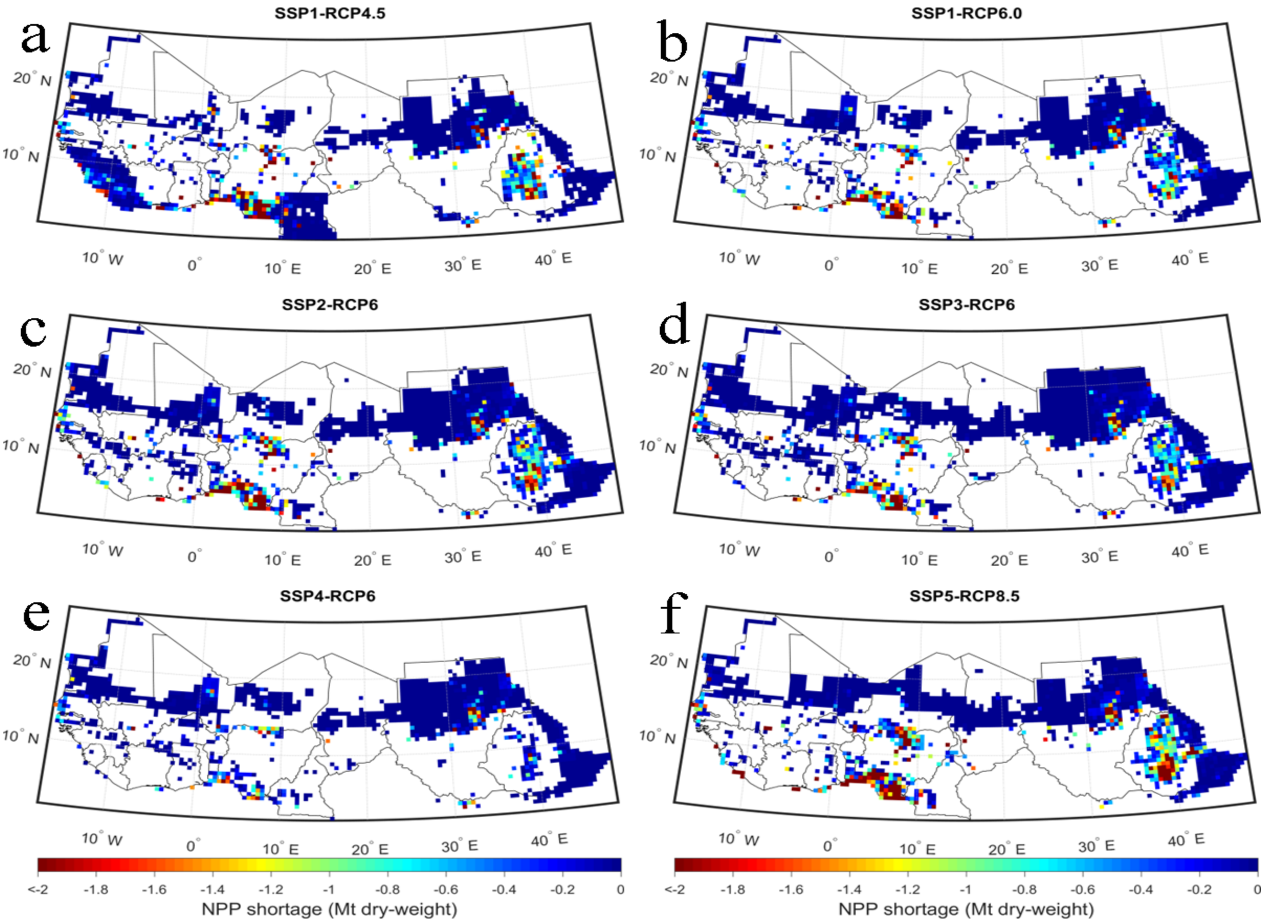

Fig. B1 Spatial distribution of NPP shortage in 2050 for the six most likely SSP-RCP combinations.

The future socio-economic and climatic scenarios are ordered in the panels as following: a) SSP1-RCP4.5, b) SSP1-RCP6.0, c) SSP2-RCP6.0, d) SSP3-RCP6.0, e) SSP4-RCP6.0 and f) SSP5-RCP8.5.

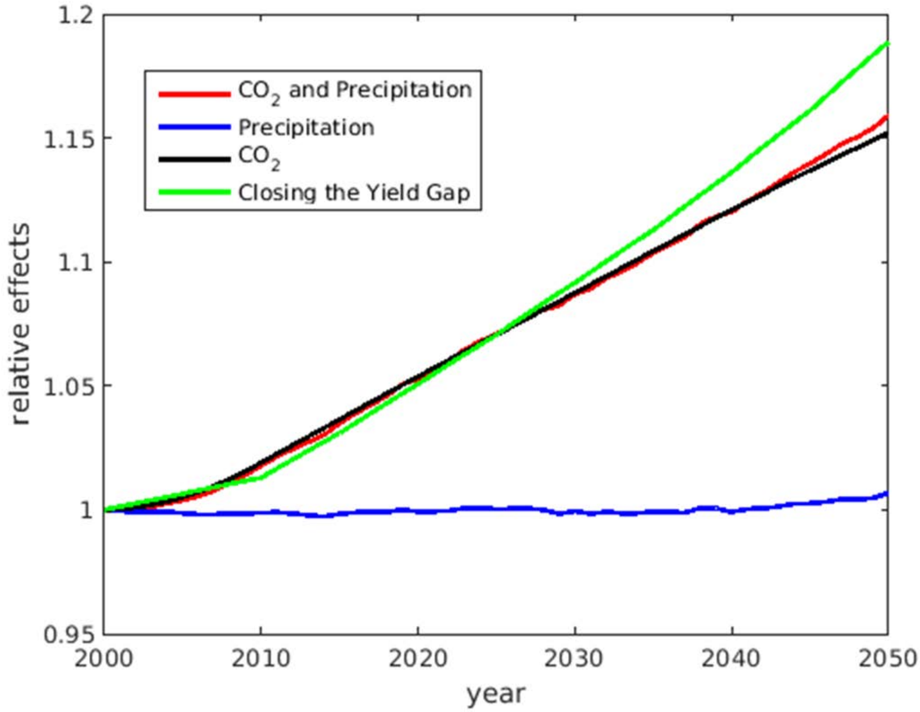

Fig. B2. The relative contributions of CO_2, precipitation and yield gap closure to the increase in NPP over the greater Sahel region, 2000-2050. Results for CO_2 and precipitation are from RCP 6.0 and yield gap is from SSP2. Simulated climate and CO_2 effects shown here are mean effects over the five GCMs (GFDL,MIROC,Hadley,NorESM, IPSL).

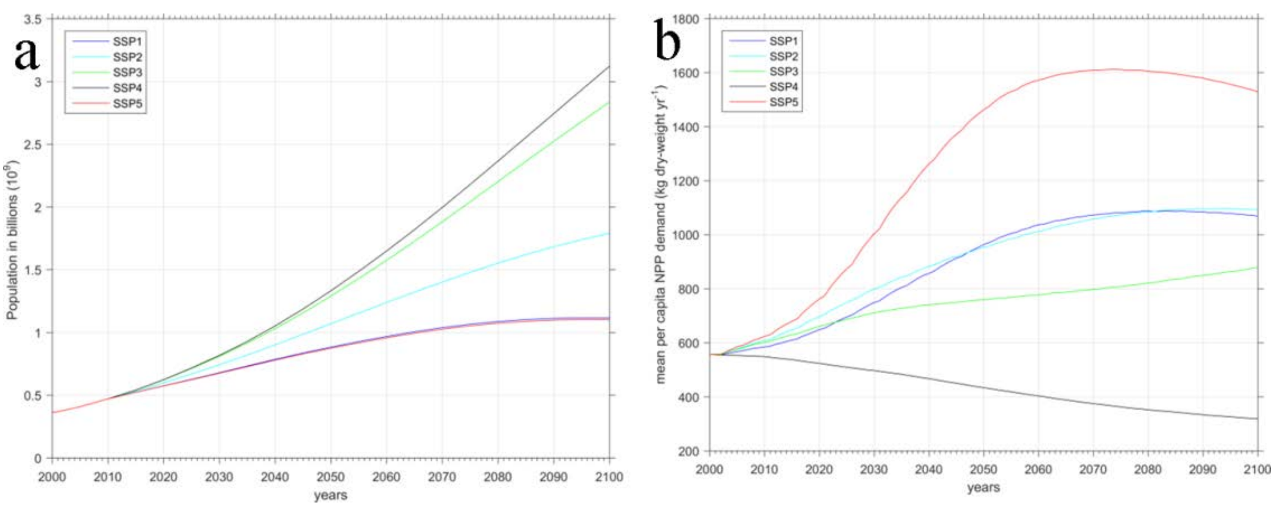

Fig. B3~~2~~ a) population growth scenarios of the greater Sahel region and b) mean per capita demand of Sahelian countries

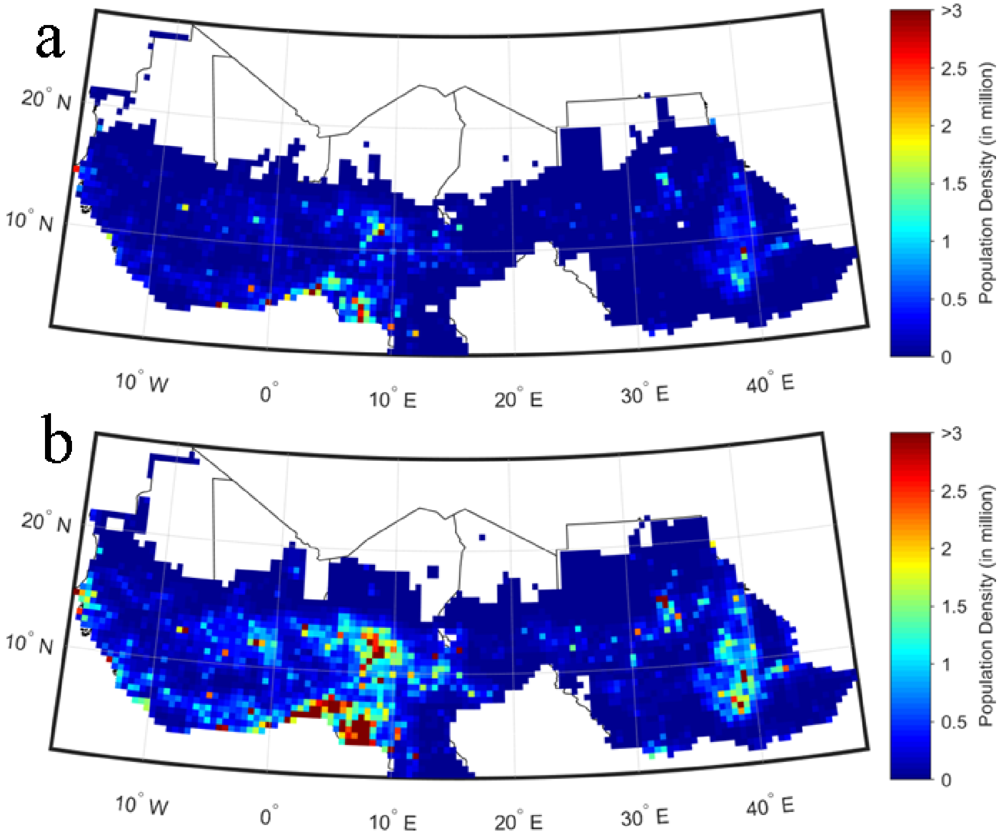

Fig. B4~~3~~ Distribution of population for SSP2-RCP6.0 for the years a) 2000 and b) 2050. Grid cells with less than one person per km^2 are excluded.

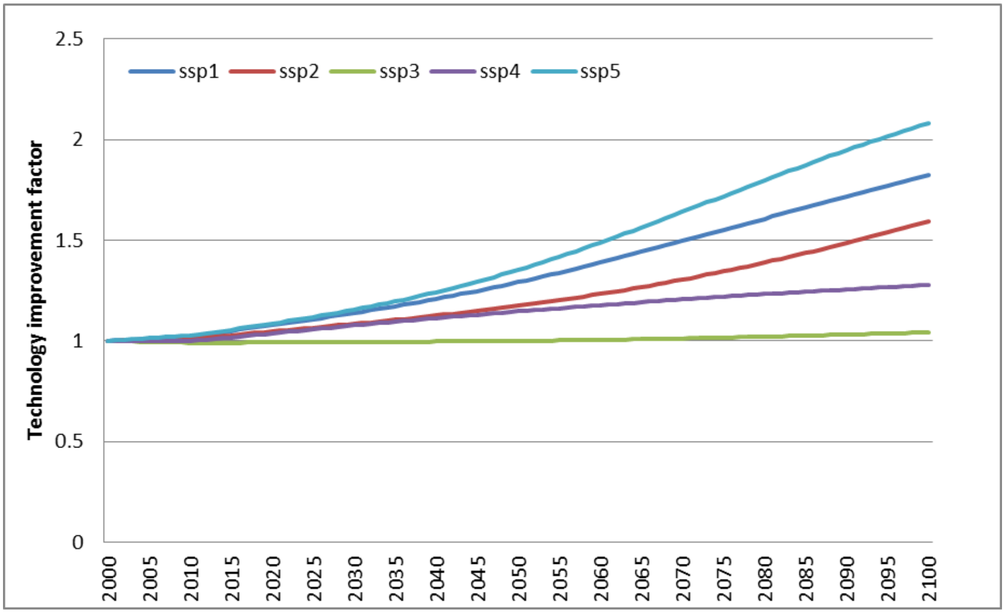

Fig. B5~~4~~ Development of mean technology improvement factor for all countries for the socio-economic pathways.

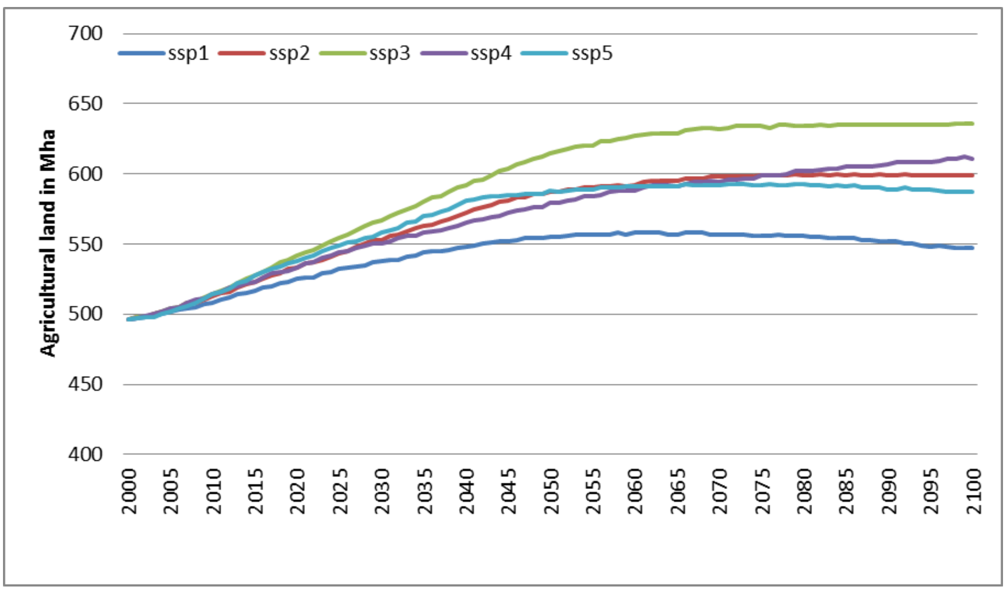

Fig. B6~~5~~ Expansion of total agricultural land, including grass- and cropland, in the Sahel for the socio-economic pathways

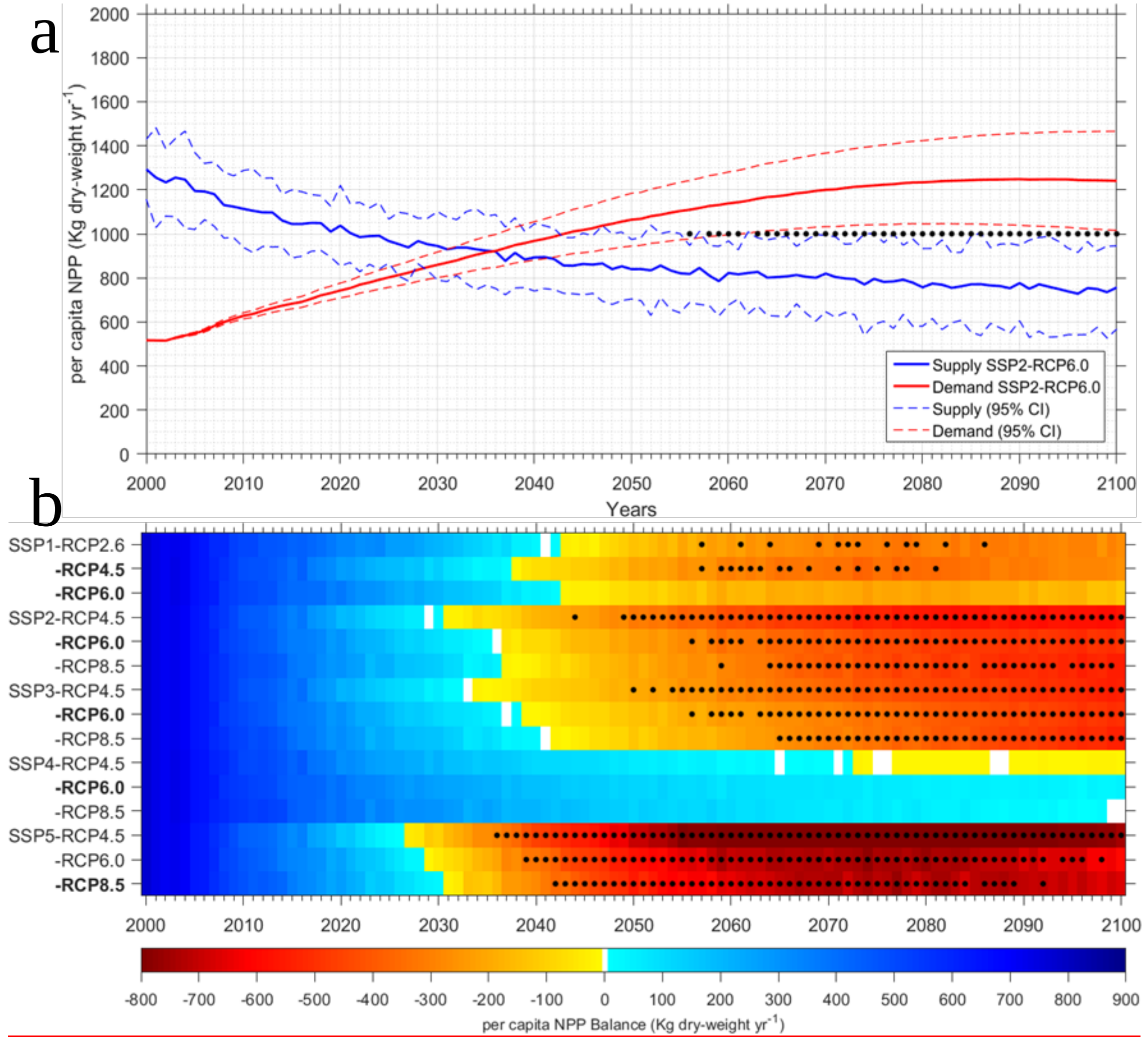

Fig. B7 Per capita NPP supply, demand and balance for the greater Sahel (2000-2100) without CO_2 fertilization. **B7a)** shows NPP supply (red) and demand (blue). The solid curves illustrate the mean of the SSP2-RCP6.0 combination. The dashed blue curves show supply uncertainty (95% confidence interval around the mean) based on the five GCMs NPP results. The dashed red curves show demand uncertainty (95% confidence interval around the mean) based on the uncertainty related to the interpretation and quantification of SSP2. **B7b)** shows the different magnitudes of the NPP balance and the varying onsets of shortage across all SSP-RCP combinations. Black dots illustrate years with a shortage outside of the 95% confidence intervals. Combinations are grouped according to the socio-economic scenarios (y-axis). The RCPs are ordered from low to high radiative forcing in each SSP group. The temporal trajectory is shown along the x-axis and the colouring indicates the sign of the annual NPP balance. Blues show a surplus of the NPP supply while yellow to red represent small to very large the gaps between supply and demand). SSP-RCP combinations in bold indicate the most likely SSP-RCP pairs based on Table 1.

Appendix C Tables

Table C1 Per capita NPP supply and demand of countries in the greater Sahel region for~~between~~ 2000 and 2050. Portions of food and feed (including grazing) in per capita NPP demand for SSP2-RCP6.0. All NPP is given in dry-weight (DW). Hurtt:PLUM scaling factors and land areas (from FAO) are also included.

Country	Per capita NPP supply [kg DW yr^{-1}]		Per capita NPP demand [kg DW yr^{-1}]		Food portions in per capita NPP demand [kg DW yr^{-1}]		Feed portions in per capita NPP demand[kg DW yr^{-1}]		Hurtt:PLUM scaling factors	Land Area from FAOSTAT
	2000	2050	2000	2050	2000	2050	2000	2050	2000	1000 ha
Benin	1341	607	474	874	99	92	375	782	0.89	11062
Burkina Faso	933	316	196	169	196	169	0	0	0.90	27360
Cameroon	2127	1173	387	717	90	82	297	635	1.04	47271
Chad	1878	1484	658	1157	120	116	538	1041	1.00	125920
Djibouti	0	0	134	120	134	120	0	0	0.00	2318
Eritrea	333	221	124	130	124	130	0	0	1.10	10100
Ethiopia	825	779	459	1439	135	157	323	1283	0.98	1000000
Gambia	1137	632	706	1082	168	142	539	940	1.58	1000
Ghana	1490	1291	274	1080	68	67	207	1013	1.03	22754
Guinea	1773	1697	402	1066	123	87	279	979	1.73	24572
Guinea Bissau	2319	1648	599	934	144	118	455	816	1.25	2812
Ivory Coast	1795	1549	282	811	95	75	188	736	0.98	31800
Liberia	1186	1312	212	1273	91	109	121	1164	0.91	9632
Mali	1929	1191	1111	1272	191	170	920	1102	0.97	122019
Mauritania	1129	1043	1530	1555	151	140	1379	1415	0.97	103070
Niger	3437	1426	1274	1540	210	202	1064	1338	1.01	126670
Nigeria	1059	719	321	923	139	139	182	784	1.04	91077
Senegal	925	539	556	837	155	137	401	699	0.74	19253
Sierra Leone	759	949	194	767	117	125	77	642	0.99	7162
Sudan	2517	1512	1530	1609	126	118	1404	1491	0.98	237600
Togo	2171	1491	271	653	127	124	144	529	1.10	5439
Mean[1]	1377	957	517	1064	-	-	-	-	-	-

[1] Weighted mean of per capita NPP measure using total population.

Table C2 Per capita NPP balances, mean, standard deviation and coefficient of variation for all SSP-RCP combinations for the year 2050. All values are given in Kg NPP dry-weight yr^{-1} except the dimensionless coefficient of variation.

2050	SSP1-RCP26	SSP1-RCP45	SSP1-RCP6	SSP2-RCP45	SSP2-RCP6	SSP2-RCP85	SSP3-RCP45	SSP3-RCP6	SSP3-RCP85	SSP4-RCP45	SSP4-RCP6	SSP4-RCP85	SSP5-RCP45	SSP5-RCP6	SSP5-RCP85	Mean	Standard deviation	Co-efficient of Variation
Benin	-288	-264	-290	-256	-267	-247	-95	-97	-84	148	118	150	-945	-968	-939	-288	364	1.3
Burkina Faso	261	257	258	147	147	152	78	78	82	93	95	98	244	244	251	166	75	0.5
Cameroon	604	134	627	47	456	526	91	439	500	258	621	679	-180	285	365	363	244	0.7
Chad	327	311	442	239	326	367	283	312	336	369	423	430	-13	205	314	311	108	0.3
Djibouti	-117	-117	-117	-120	-119	-120	-119	-119	-119	-101	-101	-101	-128	-128	-128	-117	9	0.1
Eritrea	113	142	138	94	91	87	69	67	64	75	73	69	121	117	111	95	26	0.3
Ethiopia	-498	-642	-444	-804	-660	-616	-560	-443	-410	-33	90	98	-1493	-1300	-1229	-596	455	0.8
Gambia	-464	-439	-424	-465	-449	-472	-328	-309	-328	-75	-57	-69	-842	-829	-851	-427	251	0.6
Ghana	289	362	437	151	211	226	253	297	302	488	513	506	-202	-122	-89	241	218	0.9
Guinea	915	675	968	403	631	644	395	603	611	584	808	754	347	633	646	641	170	0.3
Guinea Bissau	910	993	913	801	714	811	700	679	734	708	688	711	822	580	742	767	104	0.1
Ivory Coast	947	873	1044	586	737	773	513	645	680	700	780	785	546	734	780	742	138	0.2
Liberia	52	-1336	211	-1273	39	32	-686	292	290	-204	358	387	-2774	-934	-942	-433	859	2.0
Mali	-113	-123	-24	-147	-81	27	-103	-80	4	-48	12	83	-451	-305	-124	-98	129	1.3
Mauritania	-474	-475	-505	-502	-512	-527	-454	-449	-453	-382	-406	-424	-640	-663	-696	-504	90	0.2
Niger	117	183	247	-151	-114	-148	-290	-271	-303	-7	58	42	-315	-246	-265	-98	184	1.9
Nigeria	-95	-150	-77	-267	-204	-165	-132	-84	-52	135	162	184	-663	-581	-535	-168	248	1.5
Senegal	-119	-134	-202	-240	-297	-238	-205	-249	-193	-25	-51	-26	-421	-508	-429	-222	141	0.6
Sierra Leone	277	-728	334	-767	183	176	-493	217	215	-173	252	260	-1376	-115	-95	-122	487	4.0
Sudan	-44	-49	10	-144	-97	-91	-177	-139	-108	-30	14	-7	-281	-211	-227	-105	87	0.8
Togo	916	998	1022	827	838	842	794	788	789	870	887	894	547	568	581	811	139	0.2
Mean[1]	1	-84	47	-212	-107	-76	-119	-39	-12	131	200	213	-570	-428	-384	-96	217	2.3

[1]Weighted mean using national population data as weight.

References

Abdi, A. M., Seaquist, J., Tenenbaum, D. E., Eklundh, L., and Ardo, J.: The supply and demand of net primary production in the Sahel, Environmental Research Letters, 9, 094003, 2014.

Ahlström, A., Xia, J. Y., Arneth, A., Luo, Y., and Smith, B.: Importance of vegetation dynamics for future terrestrial carbon cycling, Environmental Research Letters, 10, 054019, 2015.

Ahmed, S. A., Diffenbaugh, N. S., Hertel, T. W., and Martin, W. J.: Agriculture and Trade Opportunities for Tanzania: Past Volatility and Future Climate Change, Review of Development Economics, 16, 429-447, 2012.

Alexander, P., Prestele, R., Verburg, P. H., Arneth, A., Baranzelli, C., Batista, E. S. F., Brown, C., Butler, A., Calvin, K., Dendoncker, N., Doelman, J. C., Dunford, R., Engstrom, K., Eitelberg, D., Fujimori, S., Harrison, P. A., Hasegawa, T., Havlik, P., Holzhauer, S., Humpenoder, F., Jacobs-Crisioni, C., Jain, A. K., Krisztin, T., Kyle, P., Lavalle, C., Lenton, T., Liu, J., Meiyappan, P., Popp, A., Powell, T., Sands, R. D., Schaldach, R., Stehfest, E., Steinbuks, J., Tabeau, A., van Meijl, H., Wise, M. A., and Rounsevell, M. D.: Assessing uncertainties in land cover projections, Glob Chang Biol, doi: 10.1111/gcb.13447, 2016. n/a-n/a, 2016.

Ardö, J. Comparison between remote sensing and a dynamic vegetation model for estimating terrestrial primary production of Africa. Carbon Balance and Management, 10(8), 2015.

Balogun, O., Yusuf, S., and Ayantoye, K.: The threats of climate change: implication for food crisis in sub-sahara Africa. In: Sustainable Food Security in the Era of Local and Global Environmental Change, Behnassi, M., Pollmann, O., and Kissinger, G. (Eds.), Springer, Dordrecht, 2013.

Barbier, B., Yacouba, H., Karambiri, H., Zoromé, M., and Somé, B.: Human Vulnerability to Climate Variability in the Sahel: Farmers' Adaptation Strategies in Northern Burkina Faso, Environmental Management, 43, 790-803, 2009.

Boke-Olén, N., Abdi, A. M., Hall, O., and Lehsten, V.: H~~A h~~igh resolution population projections ~~dataset for~~ ~~African future population developed with RCP and SSP scenarios for 2000 – 2100~~from radiative forcing and socio-economic models, 2000-2100,, ~~Nature~~ Scientific Data, ~~*in review at Nature Scientific Data, submitted july 2016. in review at Nature Scientific Data, submitted july 2016.*~~*4,160130, 2017.*

Brandt, M., Mbow, C., Diouf, A. A., Verger, A., Samimi, C., and Fensholt, R.: Ground- and satellite-based evidence of the biophysical mechanisms behind the greening Sahel, Global Change Biology, 21, 1610-1620, 2015.

Brown, M. E.: Remote sensing technology and land use analysis in food security assessment, Journal of Land Use Science, 11, 623-641, 2016.

Burnham, K. P. and Anderson, D. R.: Model Selection and Multimodal Inference. A Practical Information-Theoretic Approach, Springer, New York, 2002.

Campbell, M. M., Casterline, J., Castillo, F., Graves, A., Hall, T. L., May, J. F., Perlman, D., Potts, M., Speidel, J. J., Walsh, J., Wehner, M. F., and Zulu, E. M.: Population and climate change: who will the grand convergence leave behind?, The Lancet Global Health, 2, e253-e254, 2014.

Canadell, J. G. and Schulze, E. D.: Global potential of biospheric carbon management for climate mitigation, Nat Commun, 5, 5282, 2014.

Ceccato, P., Cressman, K., Giannini, A., and Trzaska, S.: The desert locust upsurge in West Africa (2003-2005): Information on the desert locust early warning system and the prospects for seasonal climate forecasting, International Journal of Pest Management, 53, 7-13, 2007.

Chidumayo, E. N. and Gumbo, D. J.: The dry forests and woodlands of Africa : managing for products and services, Routledge, London, 2010.

Collins, M., Knutti, R., Arblaster, J., Dufresne, J.-L., Fichefet, T., Friedlingstein, P., Gao, X., Gutowski, W. J., Johns, T., Krinner, G., Shongwe, M., Tebaldi, C., Weaver, A. J., and Wehner, M.: Long-term Climate Change: Projections, Commitments and Irreversibility. In: Climate Change 2013: The Physical Science Basis. Contribution of Working Group I to the Fifth Assessment Report of the Intergovernmental Panel on Climate Change, Stocker, T. F., Qin, D., Plattner, G.-K., Tignor, M., Allen, S. K., Boschung, J., Nauels, A., Xia, Y., Bex, V., and Midgley, P. M. (Eds.), Cambridge University Press, Cambridge, United Kingdom and New York, NY, USA, 2013.

D'Odorico, P., Carr, J. A., Laio, F., Ridolfi, L., and Vandoni, S.: Feeding humanity through global food trade, Earths Future, 2, 458-469, 2014.

Del Grosso, S., Parton, W., Stohlgren, T., Zheng, D., Bachelet, D., Prince, S., Hibbard, K., and Olson, R.: Global potential net primary production predicted from vegetation class, precipitation, and temperature, Ecology, 89, 2117-2126, 2008.

Dile, Y. T., Karlberg, L., Temesgen, M., and Rockstrom, J.: The role of water harvesting to achieve sustainable agricultural intensification and resilience against water related shocks in sub-Saharan Africa, Agr Ecosyst Environ, 181, 69-79, 2013.

Dufresne, J. L., Foujols, M. A., Denvil, S., Caubel, A., Marti, O., Aumont, O., Balkanski, Y., Bekki, S., Bellenger, H., Benshila, R., Bony, S., Bopp, L., Braconnot, P., Brockmann, P., Cadule, P., Cheruy, F., Codron, F., Cozic, A., Cugnet, D., de Noblet, N., Duvel, J. P., Ethe, C., Fairhead, L., Fichefet, T., Flavoni, S., Friedlingstein, P., Grandpeix, J. Y., Guez, L., Guilyardi, E., Hauglustaine, D., Hourdin, F., Idelkadi, A., Ghattas, J., Joussaume, S., Kageyama, M., Krinner, G., Labetoulle, S., Lahellec, A., Lefebvre, M. P., Lefevre, F., Levy, C., Li, Z. X., Lloyd, J., Lott, F., Madec, G., Mancip, M., Marchand, M., Masson, S., Meurdesoif, Y., Mignot, J., Musat, I., Parouty, S., Polcher, J., Rio, C., Schulz, M., Swingedouw, D., Szopa, S., Talandier, C., Terray, P., Viovy, N., and Vuichard, N.: Climate change projections using the IPSL-CM5 Earth System Model: from CMIP3 to CMIP5, Climate Dynamics, 40, 2123-2165, 2013.

Dunne, J. P., John, J. G., Shevliakova, E., Stouffer, R. J., Krasting, J. P., Malyshev, S. L., Milly, P. C. D., Sentman, L. T., Adcroft, A. J., Cooke, W., Dunne, K. A., Griffies, S. M., Hallberg, R. W., Harrison, M. J., Levy, H., Wittenberg, A. T., Phillips, P. J., and Zadeh, N.: GFDL's ESM2 Global Coupled Climate-Carbon Earth System Models. Part II: Carbon System Formulation and Baseline Simulation Characteristics, Journal of Climate, 26, 2247-2267, 2013.

Eklundh, L. and Olsson, L.: Vegetation index trends for the African Sahel 1982–1999, Geophysical Research Letters, 30, n/a-n/a, 2003.

Elliott, J., Deryng, D., Müller, C., Frieler, K., Konzmann, M., Gerten, D., Glotter, M., Flörke, M., Wada, Y., Best, N., Eisner, S., Fekete, B.M., Folberth, C., Foster, I., Gosling, S.N., Haddeland, I., Khabarov, N., Ludwig, F., Masaki, Y., Olin, S., Rosenzweig, C., Ruane, A.C., Satoh, Y., Schmid, E., Stacke, T., Tang, Q., Wisser, D. Constraints and potentials of future irrigation water availability on agricultural production under climate change. Proc. Natl. Acad. Sci. U.S.A. 111, 3239–44. doi:10.1073/pnas.1222474110, 2014

Engström, K., Lindeskog, M., Olin, S., Hassler, J., and Smith, B.: Impacts of climate mitigation strategies in the energy sector on global land use and carbon balance, Earth System Dynamics Discussions, 2016, 1-43, 2016a.

Engström, K., Olin, S., Rounsevell, M. D. A., Brogaard, S., van Vuuren, D. P., Alexander, P., Murray-Rust, D., and Arneth, A.: Assessing uncertainties in global cropland futures using a conditional probabilistic modelling framework, Earth System Dynamics Discussions, 2016, 1-33, 2016b.

Engström, K., Rounsevell, M. D. A., Murray-Rust, D., Hardacre, C., Alexander, P., Cui, X. F., Palmer, P. I., and Arneth, A.: Applying Occam's razor to global agricultural land use change, Environmental Modelling & Software, 75, 212-229, 2016c.

FAO: The Digitized Soil Map of the World (Release 1.0). World Soil Resources Report 67/1., Food and Agriculture Organization of the United Nations, Rome., 1991. 1991.

FAOSTAT: FAO Statistical Databases. Food and Agriculture Organization of the United Nations, Rome, Italy., 2015.

FAOSTAT: Food Aid Shipments (WFP), last access 2016/08/16. http://faostat3.fao.org/download/X/FA/E, 2016.

Foley, J. A.: Net Primary Productivity in the Terrestrial Biosphere - the Application of a Global-Model, J Geophys Res-Atmos, 99, 20773-20783, 1994.

Foley, J. A., Defries, R., Asner, G. P., Barford, C., Bonan, G., Carpenter, S. R., Chapin, F. S., Coe, M. T., Daily, G. C., Gibbs, H. K., Helkowski, J. H., Holloway, T., Howard, E. A., Kucharik, C. J., Monfreda, C., Patz, J. A., Prentice, I. C., Ramankutty, N., and Snyder, P. K.: Global consequences of land use, Science, 309, 570-574, 2005.

Foley, J. A., Ramankutty, N., Brauman, K. A., Cassidy, E. S., Gerber, J. S., Johnston, M., Mueller, N. D., O'Connell, C., Ray, D. K., West, P. C., Balzer, C., Bennett, E. M., Carpenter, S. R., Hill, J., Monfreda, C., Polasky, S., Rockstrom, J., Sheehan, J., Siebert, S., Tilman, D., and Zaks, D. P.: Solutions for a cultivated planet, Nature, 478, 337-342, 2011.

Friend, A.D., Lucht, W., Rademacher, T.T., Keribin, R., Betts, R., Cadule, P., Ciais, P., Clark, D.B., Dankers, R., Falloon, P.D., Ito, A., Kahana, R., Kleidon, A., Lomas, M.R., Nishina, K., Ostberg, S., Pavlick, R., Peylin, P., Schaphoff, S., Vuichard, N., Warszawski, L., Wiltshire, A., Woodward, F.I., 2014. Carbon residence time dominates uncertainty in terrestrial vegetation responses to future climate and atmospheric CO_2. Proc. Natl. Acad. Sci. U. S. A. 111, 3280–3285. doi:10.1073/pnas.1222477110

Gerten, D., Schaphoff, S., Haberlandt, U., Lucht, W., and Sitch, S.: Terrestrial vegetation and water balance - hydrological evaluation of a dynamic global vegetation model, J Hydrol, 286, 249-270, 2004.

Godfray, H. C., Beddington, J. R., Crute, I. R., Haddad, L., Lawrence, D., Muir, J. F., Pretty, J., Robinson, S., Thomas, S. M., and Toulmin, C.: Food security: the challenge of feeding 9 billion people, Science, 327, 812-818, 2010.

Gonzalez, P., Neilson, R. P., Lenihan, J. M., and Drapek, R. J.: Global patterns in the vulnerability of ecosystems to vegetation shifts due to climate change, Global Ecology and Biogeography, 19, 755-768, 2010.

Haberl, H., Erb, K. H., Krausmann, F., Gaube, V., Bondeau, A., Plutzar, C., Gingrich, S., Lucht, W., and Fischer-Kowalski, M.: Quantifying and mapping the human appropriation of net primary production in earth's terrestrial ecosystems, Proc Natl Acad Sci U S A, 104, 12942-12947, 2007.

Harris, I., Jones, P. D., Osborn, T. J., and Lister, D. H.: Updated high-resolution grids of monthly climatic observations - the CRU TS3.10 Dataset, International Journal of Climatology, 34, 623-642, 2014.

Harrison, P. A., Dunford, R. W., Holman, I. P., and Rounsevell, M. D. A.: Climate change impact modelling needs to include cross-sectoral interactions, Nature Clim. Change, advance online publication, 2016.

Hempel, S., Frieler, K., Warszawski, L., Schewe, J., and Piontek, F.: A trend-preserving bias correction; the ISI-MIP approach, Earth Syst. Dynam., 4, 219-236, 2013.

Herrmann, S. M., Sall, I., and Sy, O.: People and pixels in the Sahel: a study linking coarse-resolution remote sensing observations to land users' perceptions of their changing environment in Senegal, Ecology and Society, 19, 2014.

Hertel, T. W.: The challenges of sustainably feeding a growing planet, Food Security, 7, 185-198, 2015.

Hickler, T., Eklundh, L., Seaquist, J. W., Smith, B., Ardo, J., Olsson, L., Sykes, M. T., and Sjostrom, M.: Precipitation controls Sahel greening trend, Geophysical Research Letters, 32, L21415, 2005.

Hickler, T., Smith, B., Prentice, I. C., Mjöfors, K., Miller, P., Arneth, A., and Sykes, M. T.: CO_2fertilization in temperate FACE experiments not representative of boreal and tropical forests, Global Change Biology, 14, 1531-1542, 2008.

Hurtt, G. C., Chini, L. P., Frolking, S., Betts, R. A., Feddema, J., Fischer, G., Fisk, J. P., Hibbard, K., Houghton, R. A., Janetos, A., Jones, C. D., Kindermann, G., Kinoshita, T., Goldewijk, K. K., Riahi, K., Shevliakova, E., Smith, S., Stehfest, E., Thomson, A., Thornton, P., van Vuuren, D. P., and Wang, Y. P.: Harmonization of land-use scenarios for the period 1500-2100: 600 years of global gridded annual land-use transitions, wood harvest, and resulting secondary lands, Climatic Change, 109, 117-161, 2011.

Ibrahim, F. N.: Causes of the Famine among the Rural Population of the Sahelian Zone of the Sudan, GeoJournal, 17, 133-141, 1988.

IPCC: 2006 IPCC Guidelines for National Greenhouse Gas Inventories. Volume 4: Agriculture, Forestry, and Other Land Use., IGES, 2006.

Iversen, T., Bentsen, M., Bethke, I., Debernard, J. B., Kirkevåg, A., Seland, Ø., Drange, H., Kristjansson, J. E., Medhaug, I., Sand, M., and Seierstad, I. A.: The Norwegian Earth System Model, NorESM1-M – Part 2: Climate response and scenario projections, Geosci. Model Dev., 6, 389-415, 2013.

Jackson, R. B., Canadell, J., Ehleringer, J. R., Mooney, H. A., Sala, O. E., and Schulze, E. D.: A global analysis of root distributions for terrestrial biomes, Oecologia, 108, 389-411, 1996.

Kastner, T., Rivas, M. J., Koch, W., and Nonhebel, S.: Global changes in diets and the consequences for land requirements for food, Proc Natl Acad Sci U S A, 109, 6868-6872, 2012.

Kearney, J.: Food consumption trends and drivers, Philos Trans R Soc Lond B Biol Sci, 365, 2793-2807, 2010.

Kebede, A. S., Dunford, R., Mokrech, M., Audsley, E., Harrison, P. A., Holman, I. P., Nicholls, R. J., Rickebusch, S., Rounsevell, M. D. A., Sabaté, S., Sallaba, F., Sanchez, A., Savin, C., Trnka, M., and Wimmer, F.: Direct and indirect impacts of climate and socio-economic change in Europe: a sensitivity analysis for key land- and water-based sectors, Climatic Change, 128, 261-277, 2015.

Kottek, M., Grieser, J., Beck, C., Rudolf, B., and Rubel, F.: World map of the Koppen-Geiger climate classification updated, Meteorologische Zeitschrift, 15, 259-263, 2006.

Körner, C. Plant CO_2 responses: an issue of definition, time and resource supply. New Phytol. 172, 393–411. Pugh, T.A.M., Müller, C., Arneth, A., Haverd, V., Smith, B., 2016. Key knowledge and data gaps in modelling the influence of CO2 concentration on the terrestrial carbon sink. J. Plant Physiol. 203, 3–15. doi:10.1016/j.jplph.2016.05.001, 2006.

Kwakkel, J. H. and Pruyt, E.: Exploratory Modeling and Analysis, an approach for model-based foresight under deep uncertainty, Technological Forecasting and Social Change, 80, 419-431, 2013.

Lamarque, J. F., Bond, T. C., Eyring, V., Granier, C., Heil, A., Klimont, Z., Lee, D., Liousse, C., Mieville, A., Owen, B., Schultz, M. G., Shindell, D., Smith, S. J., Stehfest, E., Van Aardenne, J., Cooper, O. R., Kainuma, M., Mahowald, N., McConnell, J. R., Naik, V., Riahi, K., and van Vuuren, D. P.: Historical (1850-2000) gridded anthropogenic and biomass burning emissions of reactive gases and aerosols: methodology and application, Atmos Chem Phys, 10, 7017-7039, 2010.

Licker, R., Johnston, M., Foley, J. A., Barford, C., Kucharik, C. J., Monfreda, C., and Ramankutty, N.: Mind the gap: how do climate and agricultural management explain the 'yield gap' of croplands around the world?, Global Ecology and Biogeography, 19, 769-782, 2010.

Lindeskog, M., Arneth, A., Bondeau, A., Waha, K., Seaquist, J., Olin, S., and Smith, B.: Implications of accounting for land use in simulations of ecosystem carbon cycling in Africa, Earth Syst. Dynam., 4, 385-407, doi:10.5194/esd-4-385-2013, 2013.

Luyssaert, S., Inglima, I., and Jung, M. Global Forest Ecosystem Structure and Function Data for Carbon Balance Research. Global Forest Ecosystem Structure and Function Data for Carbon Balance Research. Data set. Available on-line [http://daac.ornl.gov/] from Oak Ridge National Laboratory Distributed Active Archive Center, Oak Ridge, Tennessee, U.S.A. doi:10.3334/ORNLDAAC/949, 2009.

Lynch, K., Binns, T., and Olofin, E.: Urban agriculture under threat - The land security question in Kano, Nigeria, Cities, 18, 159-171, 2001.

Metzger, M. J., Bunce, R. G. H., Jongman, R. H. G., Sayre, R., Trabucco, A., and Zomer, R.: A high-resolution bioclimate map of the world: a unifying framework for global biodiversity research and monitoring, Global Ecology and Biogeography, 22, 630-638, 2013.

Michaletz, S. T., Cheng, D., Kerkhoff, A.J., and Enquist, B.J.. Convergence of terrestrial plant production across global climate gradients. Nature 512:39-43, 2014.

Mitchell, T. D. and Jones, P. D.: An improved method of constructing a database of monthly climate observations and associated high-resolution grids, International Journal of Climatology, 25, 693-712, 2005.

Mokany, K., Raison, R. J., and Prokushkin, A. S.: Critical analysis of root : shoot ratios in terrestrial biomes, Global Change Biology, 12, 84-96, 2006.

Mueller, N. D., Gerber, J. S., Johnston, M., Ray, D. K., Ramankutty, N., and Foley, J. A.: Closing yield gaps through nutrient and water management, Nature, 490, 254-257, 2012.

Olin, S., Lindeskog, M., Pugh, T.A.M., Schurgers, G., Wårlind, D., Mishurov, M., Zaehle, S., Stocker, B.D., Smith, B., and Arneth, A..: Soil carbon management in large-scale Earth system modelling: implications for crop yields and nitrogen leaching, Earth System Dynamics, 6, 745-768, 2015.

O'Neill, B. C., Kriegler, E., Riahi, K., Ebi, K. L., Hallegatte, S., Carter, T. R., Mathur, R., and van Vuuren, D. P.: A new scenario framework for climate change research: the concept of shared socioeconomic pathways, Climatic Change, 122, 387-400, 2014.

O'Neill, B. C., Kriegler, E., Ebi, K. L., Kemp-Benedict, E., Riahi, K., Rothman, D. S., van Ruijven, B. J., van Vuuren, D. P., Birkmann, J., Kok, K., Levy, M., and Solecki, W.: The roads ahead: Narratives for shared socioeconomic pathways describing world futures in the 21st century, Global Environmental Change, ~~—~~42, 169-180, 2017.~~doi: 10.1016/j.gloenvcha.2015.01.004, *in press*. *in press*~~.

Olson, D. M., Dinerstein, E., Wikramanayake, E. D., Burgess, N. D., Powell, G. V. N., Underwood, E. C., D'amico, J. A., Itoua, I., Strand, H. E., Morrison, J. C., Loucks, C. J., Allnutt, T. F., Ricketts, T. H., Kura, Y., Lamoreux, J. F., Wettengel, W. W., Hedao, P., and Kassem, K. R.: Terrestrial Ecoregions of the World: A New Map of Life on Earth: A new global map of terrestrial ecoregions provides an innovative tool for conserving biodiversity, BioScience, 51, 933-938, 2001.

Olsson, L.: On the Causes of Famine Drought, Desertification and Market Failure in the Sudan, Ambio, 22, 395-403, 1993.

Owuor, S.: Migrants, urban poverty and the changing nature of urban-rural linkages in Kenya, Development Southern Africa, 24, 109-122, 2007.

Pinstrup-Andersen, P.: Food security: definition and measurement, Food Security, 1, 5-7, 2009.

Pretty, J.: Agricultural sustainability: concepts, principles and evidence, Philos Trans R Soc Lond B Biol Sci, 363, 447-465, 2008.

Pretty, J.: Sustainable intensification in Africa, International Journal of Agricultural Sustainability, 9, 3-4, 2011.

Pugh, T. A. M., Arneth, A., Olin, S., Ahlström, A., Bayer, A. D., Goldewijk, K. K., Lindeskog, M., and Schurgers, G.: Simulated carbon emissions from land-use change are substantially enhanced by accounting for agricultural management, Environmental Research Letters, 10, 124008, 2015.

Pugh, T.A.M., Müller, C., Arneth, A., Haverd, V., Smith, B. Key knowledge and data gaps in modelling the influence of CO_2 concentration on the terrestrial carbon sink. J. Plant Physiol. 203, 3–15. doi:10.1016/j.jplph.2016.05.001, 2016.

Ramankutty, N., Evan, A. T., Monfreda, C., and Foley, J. A.: Farming the planet: 1. Geographic distribution of global agricultural lands in the year 2000, Global Biogeochem Cy, 22, n/a-n/a, 2008.

Ray, D. K., Mueller, N. D., West, P. C., and Foley, J. A.: Yield Trends Are Insufficient to Double Global Crop Production by 2050, PLoS ONE, 8, e66428, 2013.

Reich, P. F. and Eswaran, H.: Global resources. In: Lal, R. (ed.). Encyclopedia of Soil Science, pp. 607-611. Marcel Dekker, New York., 2002. 2002.

Rosenzweig, C., Elliott, J., Deryng, D., Ruane, A.C., Müller, C., Arneth, A., Boote, K.J., Folberth, C., Glotter, M., Khabarov, N., Neumann, K., Piontek, F., Pugh, T.A.M., Schmid, E., Stehfest, E., Yang, H., Jones, J.W..Assessing agricultural risks of climate change in the 21st century in a global gridded crop model intercomparison. Proc. Natl. Acad. Sci. U.S.A. 111, 3268–73. doi:10.1073/pnas.1222463110, 2014.

Running, S. W.: A regional look at HANPP: human consumption is increasing, NPP is not, Environmental Research Letters, 9, 111003, 2014.

Running, S. W., Nemani, R. R., Heinsch, F. A., Zhao, M., Reeves, M., and Hashimoto, H.: A Continuous Satellite-Derived Measure of Global Terrestrial Primary Production, BioScience, 54, 547-560, 2004.

Sallaba, F., Lehsten, D., Seaquist, J., and Sykes, M. T.: A rapid NPP meta-model for current and future climate and CO2 scenarios in Europe, Ecological Modelling, 302, 29-41, 2015.

Schwarz, G.: Estimating the Dimension of a Model, doi: 10.1214/aos/1176344136, 1978. 461-464, 1978.

Seaquist, J. W., Hickler, T., Eklundh, L., Ardo, J., and Heumann, B. W.: Disentangling the effects of climate and people on Sahel vegetation dynamics, Biogeosciences, 6, 469-477, 2009.

Sitch, S., Smith, B., Prentice, I. C., Arneth, A., Bondeau, A., Cramer, W., Kaplan, J. O., Levis, S., Lucht, W., Sykes, M. T., Thonicke, K., and Venevsky, S.: Evaluation of ecosystem dynamics, plant geography and terrestrial carbon cycling in the LPJ dynamic global vegetation model, Global Change Biology, 9, 161-185, 2003.

Smith, B., Prentice, I. C., and Sykes, M. T.: Representation of vegetation dynamics in the modelling of terrestrial ecosystems: comparing two contrasting approaches within European climate space, Global Ecology and Biogeography, 10, 621-637, 2001.

Smith, W.K., Reed, S.C., Cleveland, C.C., Ballantyne, A.P., Anderegg, W.R.L., Wieder, W.R., Liu, Y.Y. & Running, S.W. Large divergence of satellite and Earth system model estimates of global terrestrial CO2 fertilization. Nat. Clim. Chang., 6, 306–310, 2016..

Smith, B., Warlind, D., Arneth, A., Hickler, T., Leadley, P., Siltberg, J., and Zaehle, S.: Implications of incorporating N cycling and N limitations on primary production in an individual-based dynamic vegetation model, Biogeosciences, 11, 2027-2054, 2014.

Smith, J. U. and Smith, P.: Introduction to environmental modelling, Oxford University Press, Oxford ; New York, 2007.

Smith, P.: Delivering food security without increasing pressure on land, Glob Food Secur-Agr, 2, 18-23, 2013.

Smith, P., Smith, J. U., Powlson, D. S., McGill, W. B., Arah, J. R. M., Chertov, O. G., Coleman, K., Franko, U., Frolking, S., Jenkinson, D. S., Jensen, L. S., Kelly, R. H., Klein-Gunnewiek, H., Komarov, A. S., Li, C., Molina, J. A. E., Mueller, T., Parton, W. J., Thornley, J. H. M., and Whitmore, A. P.: A comparison of the performance of nine soil organic matter models using datasets from seven long-term experiments, Geoderma, 81, 153-225, 1997.

Tang, G. P., Beckage, B., Smith, B., and Miller, P. A.: Estimating potential forest NPP, biomass and their climatic sensitivity in New England using a dynamic ecosystem model, Ecosphere, 1, art18, 2010.

Tilman, D., Balzer, C., Hill, J., and Befort, B. L.: Global food demand and the sustainable intensification of agriculture, Proc Natl Acad Sci U S A, 108, 20260-20264, 2011.

Trenberth, K. E., Dai, A., van der Schrier, G., Jones, P.D., Barichivich, J., Briffa, K.R., and Sheffield, J. Global warming and changes in drought. Nature Clim. Change, 4:17-22, 2014.

Tschirley, D., Reardon, T., Dolislager, M., and Snyder, J.: The Rise of a Middle Class in East and Southern Africa: Implications for Food System Transformation, Journal of International Development, 27, 628-646, 2015.

UN: United Nations. Transforming our world: The 2030 Agenda for sustainable development. , 2016.

United Nations: Sahel Regional Strategy Mid-Year Review 2013, United Nations Office for the Coordination of Humanitarian Affairs, 2013.

van Vuuren, D. P., de Vries, B., Beusen, A., and Heuberger, P. S. C.: Conditional probabilistic estimates of 21st century greenhouse gas emissions based on the storylines of the IPCC-SRES scenarios, Global Environmental Change, 18, 635-654, 2008.

van Vuuren, D. P., Edmonds, J., Kainuma, M., Riahi, K., Thomson, A., Hibbard, K., Hurtt, G. C., Kram, T., Krey, V., Lamarque, J.-F., Masui, T., Meinshausen, M., Nakicenovic, N., Smith, S. J., and Rose, S. K.: The representative concentration pathways: an overview, Climatic Change, 109, 5-31, 2011.

van Vuuren, D. P., Kriegler, E., O'Neill, B. C., Ebi, K. L., Riahi, K., Carter, T. R., Edmonds, J., Hallegatte, S., Kram, T., Mathur, R., and Winkler, H.: A new scenario framework for Climate Change Research: scenario matrix architecture, Climatic Change, 122, 373-386, 2013.

Watanabe, M., Chikira, M., Imada, Y., and Kimoto, M.: Convective Control of ENSO Simulated in MIROC, Journal of Climate, 24, 543-562, 2011.

Wieder, W.R., Cleveland, C.C., Smith, W.K. & Todd-Brown, K. Future productivity and carbon storage limited by terrestrial nutrient availability. Nat. Geosci., 1–5, 2015.

Willmott, C. J., Robeson, S. M., and Matsuura, K.: A refined index of model performance, International Journal of Climatology, 32, 2088-2094, 2012.

Wirsenius, S.: Human use of land and organic materials: modeling the turnover of biomass in the global food system., Doctor of Philosophy, Department of Physical Resource Theory, Chalmers University of Technology, Gothenburg, 2000.

Yengoh, G. T. and Ardö, J.: Crop yield gaps in Cameroon, Ambio, 43, 175-190, 2014.

Figures

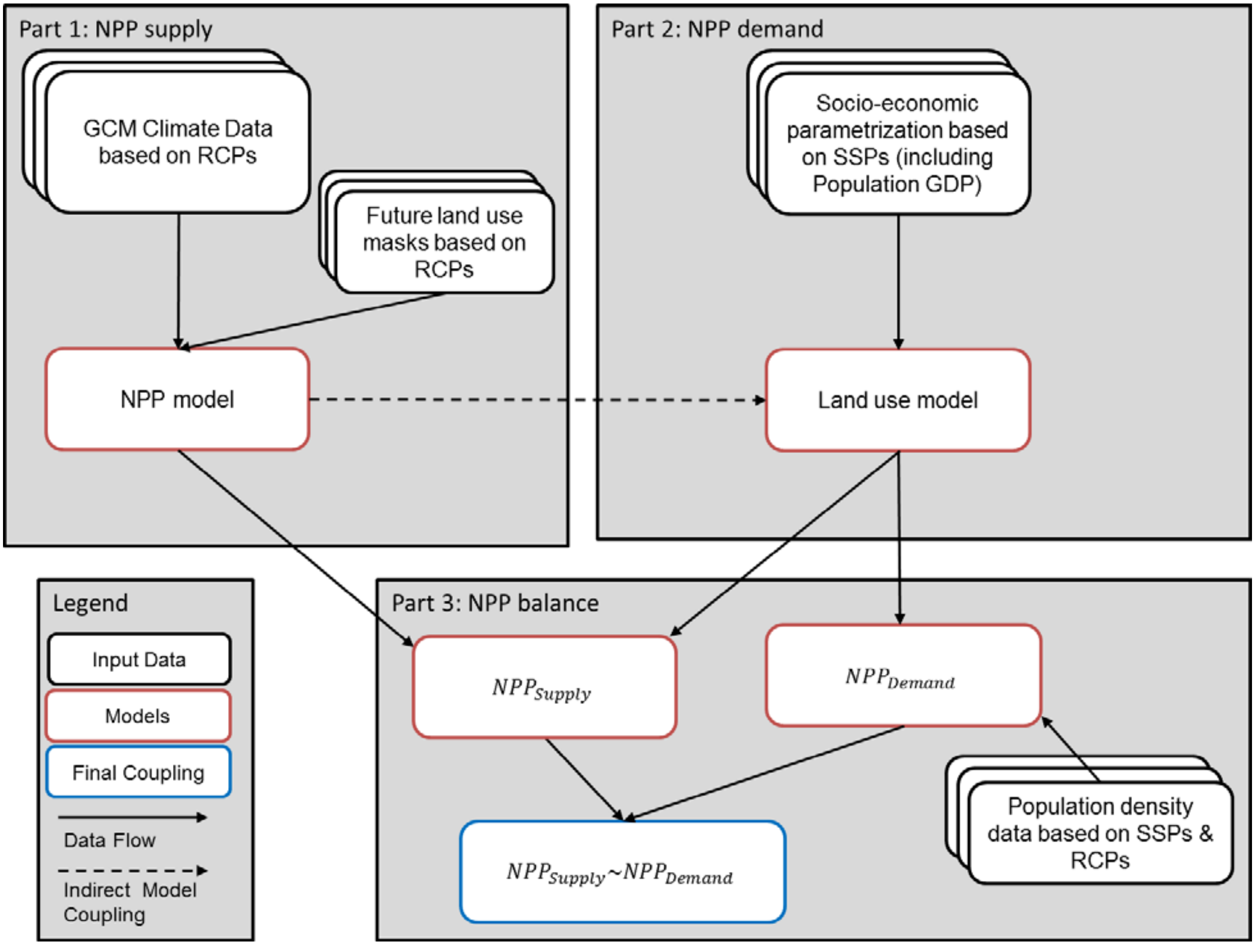

Fig. 1 Conceptual logic of the modelling framework. The framework is based on three components enclose by three grey boxes: (1) $\boldsymbol{NPP_{supply}}$, (2) $\boldsymbol{NPP_{demand}}$ and (3) $\boldsymbol{NPP_{balance}}$. The white boxes indicate data inputs originating from modelling studies (as referenced in section 2.2). The main models and equations are given in the boxes outlined in red, where solid arrows show the data flow. The dashed arrow between *NPP model* (section 2.1.1) and *Land use model* (section 2.1.2) represents an indirect model coupling for areas of cropland and pasture. The box outlined in blue indicates the final coupling allowing the assessment of $\boldsymbol{NPP_{supply}}$ and $\boldsymbol{NPP_{demand}}$.

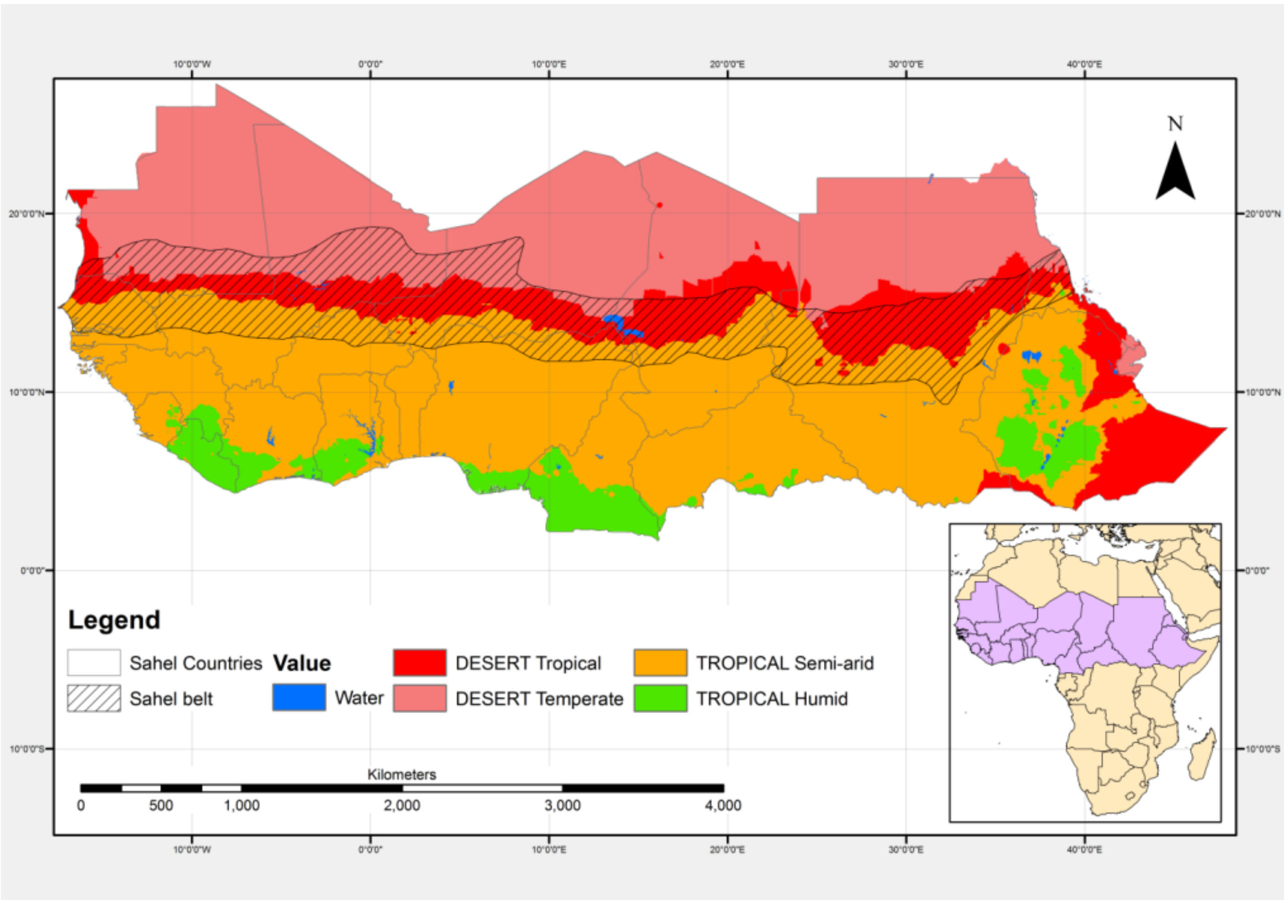

Fig. 2 Major Biome Map from year 2000 for greater Sahel region. The hatched area shows the traditionally-defined Sahel, where annual rainfall ranges from 100mm to 600mm. The Major Biome Map is based on Reich and Eswaran (2002).

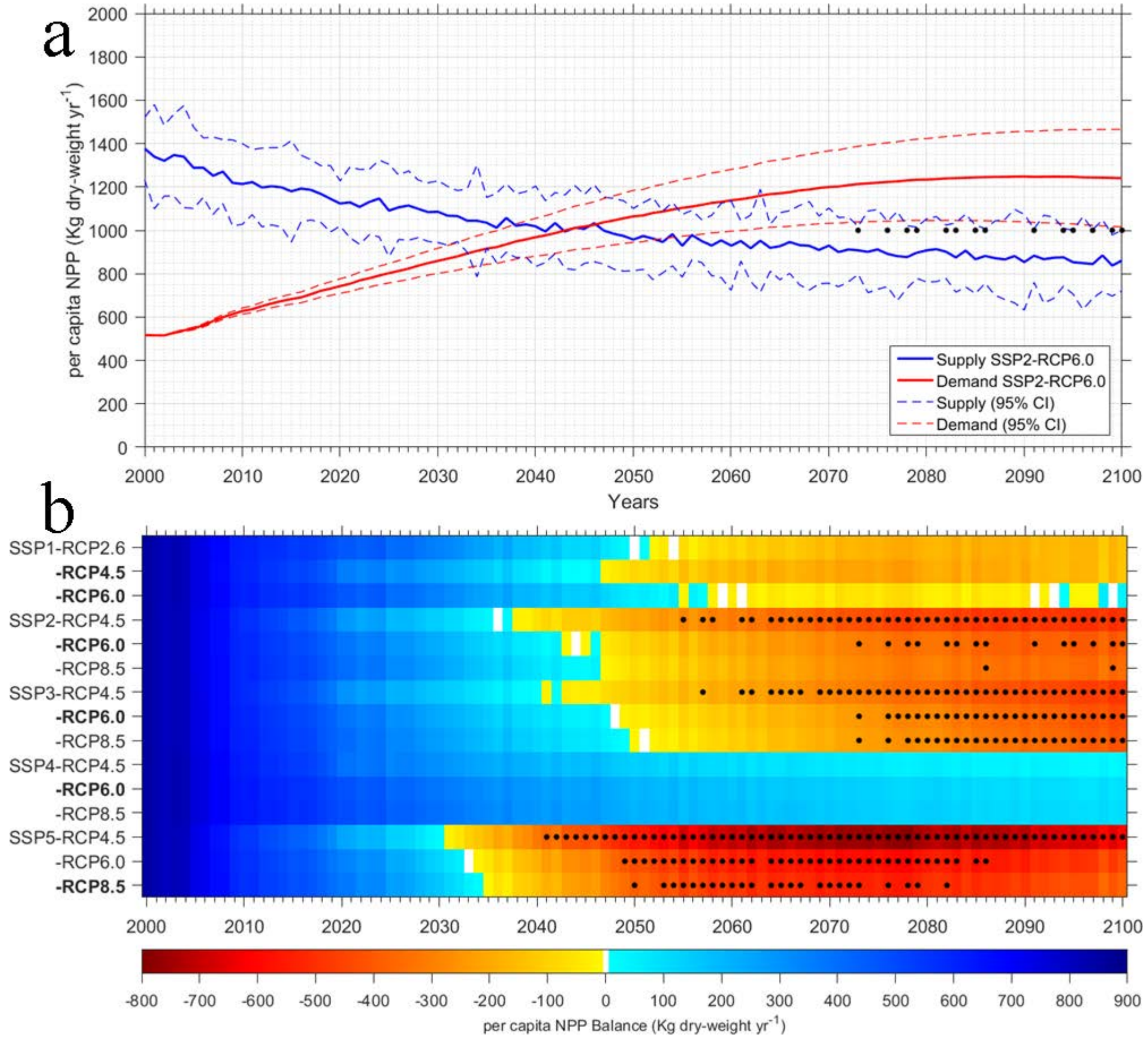

Fig. 3 The per capita NPP supply, demand and balance for the entire Sahel region over the time period. **3a)** shows NPP supply (red) and demand (blue). The solid curves illustrate the mean of the SSP2-RCP6.0 combination. The dashed blue curves show supply uncertainty (95% confidence interval around the mean) based on the five GCMs NPP results. The dashed red curves show demand uncertainty (95% confidence interval around the mean) based on the uncertainty related to the interpretation and quantification of SSP2. **3b)** shows the different magnitudes of the NPP balance and the varying onsets of shortage across all SSP-RCP combinations. Black dots illustrate years with a shortage outside of the 95% confidence intervals. The combinations are grouped according to the socio-economic scenarios (y-axis). The RCPs are ordered from low to high radiative forcing in each SSP group. The temporal trajectory is shown along the x-axis and the colouring indicates the sign of the annual NPP balance. Blues show a surplus of the NPP supply while yellow to red represent small to very large NPP shortages (i.e. the gap between supply and demand). SSP-RCP combinations in bold indicate the most likely SSP-RCP pairs based on Table 1.~~s 3 and 4 of Engström et al. (2016b).~~

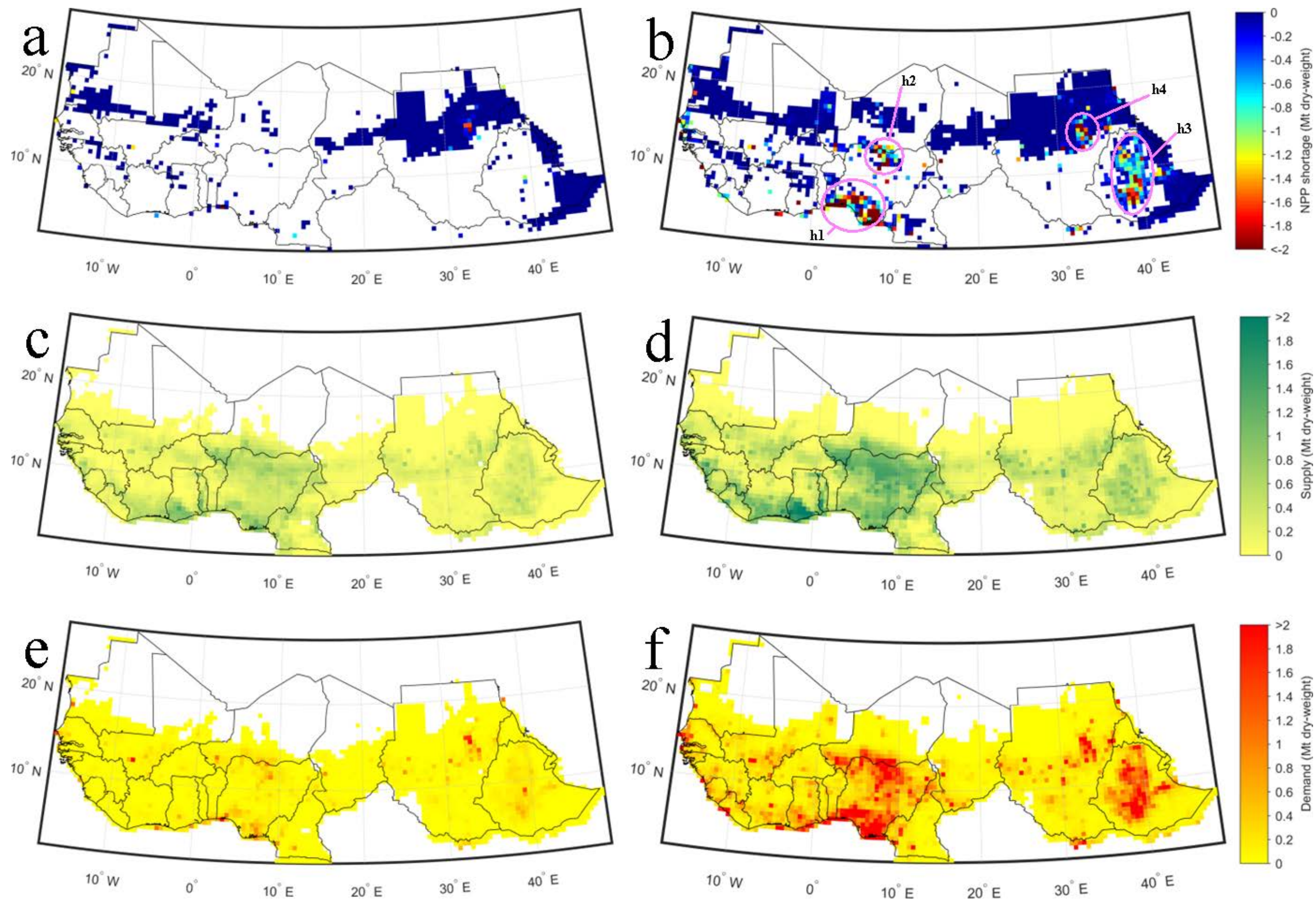

Fig 4 Maps of NPP shortage (**a,b**), NPP supply (**c,d**) and NPP demand (**e,f**) for the year 2000 (left panels) and SSP2-RCP6.0 year 2050 (right panels). The hotspots of large NPP shortage are marked with circles in 4b, where h1 is in the area around Lagos (Nigeria) and the Niger delta; h2 is in the Nigerian hinterlands (close to Kano); h3 is in the Ethiopian highlands (close to Addis Ababa); and h4 is in the area surrounding Khartoum (Sudan). In 4a we excluded all areas with a surplus in the NPP balance.

Tables

Table 1 Scenario matrix translated into quantitative probabilities (see also Engström et al. (2016b).

	RCP 2.6	RCP 4.5	RCP 6	RCP 8.5	Sum
SSP1	0.0909	0.4545	0.4545	0.0000	1
SSP2	0.0000	0.0909	0.6818	0.2273	1
SSP3	0.0000	0.1667	0.5000	0.3333	1
SSP4	0.0000	0.3704	0.5556	0.0741	1
SSP5	0.0000	0.0741	0.3704	0.5556	1

Table 2~~1~~ Rules of combining $NPP_{cereal\_balance}$ and $NPP_{grazing\_balance}$ to determine the final balance of NPP demand and supply.

Combination rule	$NPP_{cereal\_balance}$	$NPP_{grazing\_balance}$	$NPP_{balance}$
1	<0	≥0	$NPP_{cereal\_balance}$
2	≥0	≥0	$NPP_{cereal\_balance}$
3	<0	<0	$NPP_{cereal\_balance}+NPP_{grazing\_balance}$
4	≥0	<0	$NPP_{cereal\_balance}+NPP_{grazing\_balance}$

Table 3~~2~~ Summary of the Shared Socio-economic Pathway key characteristics (population development, economic growth, consumption & diet, policy orientation and technological change) based on (Engström et al., 2016; O'Neill et al., 2017~~*in press*~~).

Pathway	Key characteristics
SSP1: **Sustainability - Taking the green road**	Relatively low population development Medium to high economic growth Low growth in material consumption, low-meat diets Towards sustainable development Rapid technology development and transfer
SSP2: **Middle of the road**	Medium population development Medium (but uneven) economic growth Material-intensive consumption, medium meat consumption Weak focus on sustainability Medium technology development and slow transfer
SSP3: **Regional rivalry - A rocky road**	High population development Slow economic growth Material-intensive consumption Oriented toward security Slow technology development and transfer
SSP4: **Inequality - A road divided**	Relatively high population development Low to medium economic growth Elites: high consumption, rest: low consumption Toward the benefit of the political and business elite Rapid technology transfer in high-tech sectors, but slow in other, little transfer within countries to poorer people
SSP5: **Fossil-fuel development - Taking the highway**	Relatively low population development High economic growth Materialisms, status consumption, meat-rich diets Toward development, free markets, human capital Rapid technology change and transfer

Table 4~~3~~ Per capita NPP balance, NPP supply, NPP demand and population for SSP2-RCP6 for 2000 and 2050. All NPP is given in dry-weight (DW).

Country	**Per capita NPP balance [kg DW yr^{-1}]**		**Per capita NPP supply [kg DW yr^{-1}]**		**Per capita NPP demand [kg DW yr^{-1}]**		**Total Population [millions]**	
	2000	2050	2000	2050	2000	2050	2000	2050
Benin	867	-267	1341	607	474	874	8	25
Burkina Faso	737	147	933	316	196	169	12	46
Cameroon	1740	456	2127	1173	387	717	16	40
Chad	1220	326	1878	1484	658	1157	8	26
Djibouti	-134	-119	0	0	134	120	1	2
Eritrea	218	91	333	221	124	130	4	12
Ethiopia	366	-660	825	779	459	1439	67	149
Gambia	431	-449	1137	632	706	1082	1	3
Ghana	1216	211	1490	1291	274	1080	19	48
Guinea	1371	631	1773	1697	402	1066	8	22
Guinea Bissau	1720	714	2319	1648	599	934	1	3
Ivory Coast	1513	737	1795	1549	282	811	17	41
Liberia	975	39	1186	1312	212	1273	3	10
Mali	818	-81	1929	1191	1111	1272	11	43
Mauritania	-401	-512	1129	1043	1530	1555	3	8
Niger	2163	-114	3437	1426	1274	1540	11	55
Nigeria	738	-204	1059	719	321	923	123	386
Senegal	369	-297	925	539	556	837	10	28
Sierra Leone	565	183	759	949	194	767	4	12
Sudan	986	-97	2517	1512	1530	1609	29	96
Togo	1900	838	2171	1491	271	653	5	11
Mean[1]	860	-107	1377	957	517	1064	361	1066

[1]Weighted mean using national population data as weight.